# Performance-Based Optimisation of Friction Energy Dissipation Devices in RC Structures


THE UNIVERSITY OF SHEFFIELD

By:

**Neda Nabid**

A thesis submitted in partial fulfilment for the degree of

***Doctor of Philosophy***

in the

Faculty of Engineering

Department of Civil and Structural Engineering

October 2018

***T O***

***MY PARENTS***

***for their unconditional love and support***

***for being the light of my life***

# ABSTRACT

Energy dissipation devices are widely utilised as a viable cost-effective solution to enhance the seismic performance of existing/newly designed structures. Optimum design of control devices is a challenging task due to complexity and high nonlinearity of these systems under earthquake excitations. The existing optimisation techniques for non-linear problems are computationally expensive. This highlights the need for more efficient optimisation methods for the design of non-linear structures with supplemental damping devices.

In this study, a practical design method is proposed for more efficient design of friction dampers for different multi-storey buildings (3, 5, 10, 15 and 20-storey frames with 3 and 5 spans), friction damper designs (different slip load distribution patterns) and seismic design excitations (a set of twelve natural and synthetic earthquakes as well as twenty far- and near-field earthquakes). A low computational cost multi-criteria performance-based optimisation methodology is then developed for optimum design of friction dampers in RC structures (using a concept of Uniform Distribution of Deformation; UDD). In the proposed method, two or more predefined performance objectives are simultaneously satisfied under different earthquake levels. The reliability of the method is assessed through sensitivity analyses using different initial damper slip loads, convergence parameters and earthquake records. To accelerate the speed of the optimisation, a novel adaptive UDD optimisation method is also established for optimal arrangement of the friction dampers. The efficiency of the suggested approach is then evaluated against a Genetic Algorithm (GA) as a global evolutionary optimisation method. Using the same concept, a three-phase optimum design method is proposed for simultaneous discrete optimisation of bracing elements and continuous optimisation of friction devices in RC structures under strong earthquakes.

The results indicate that, irrespective of slip load distribution, the optimum range of slip loads leading to maximum energy dissipation efficiency is a function of the number of storeys and earthquake PGV level. The proposed performance-based UDD optimisation method can efficiently decrease the number of required friction dampers and additional imposed loads to the main structure while satisfying the predefined performance levels under the design earthquakes. The design solutions obtained from the adaptive UDD after a few nonlinear dynamic simulations are very close to those achieved from the GA approach after thousands of analyses. Compared to code-based design braced frames, using the proposed method leads to considerably lower number of bracing elements and reduced imposed loads to the structure, while satisfying multiple performance objectives under design earthquakes.

# RESEARCH CONTRIBUTION

Extensive analytical study was carried out on performance-based optimisation of friction-based energy dissipation devices in RC structures. As a result of the work presented here, the following journal and conference papers were either published or submitted for publication:

## Journal Papers

### Published

J1. Nabid, N., Hajirasouliha, I. and Petkovski, M. (2017), "A practical method for optimum seismic design of friction wall dampers." *Earthquake Spectra,* **33**(3): 1033–1052.

J2. Nabid, N., Hajirasouliha, I. and, Petkovski, M. (2018). "Performance-based optimisation of RC frames with friction wall dampers using a low-cost optimisation method." *Bulletin of Earthquake Engineering,* **16**(10): 5017–5040.

### Submitted

J3. Nabid, N., Hajirasouliha, I. and Petkovski, M. (2018), "Multi-criteria performance-based optimisation of friction energy dissipation devices in RC frames." *Journal of Structural Engineering (ASCE).*

J4. Nabid, N., Hajirasouliha, I. and Petkovski, M. (2018), "A simplified methodology for optimum design of friction dampers by considering near-field and far-field ground motions." *Journal of Earthquake Engineering.*

### Ready for Submission

J5. Nabid, N., Hajirasouliha, I. and Petkovski, M. (2018), "Adaptive low computational cost optimisation method for performance-based seismic design of friction dampers." *Journal of Engineering Structures*.

## Conference Papers

C1. Nabid, N., Hajirasouliha, I. and Petkovski, M. (2015). "Seismic investigation of multi-storey RC frames retrofitted using a friction panel with different slip load distributions." *The Annual Postgraduate Research Student Conference*. Sheffield, UK, 43–48.

C2. Nabid, N., Hajirasouliha, I. and Petkovski, M. (2016), "A practical design method for seismic strengthening of RC frames using friction-based passive energy dissipation devices*." 6th European Conference on Structural Control, EACS*, Sheffield, UK. Paper No. 120.

C3. Nabid, N., Hajirasouliha, I. and Petkovski, M. (2016), "Optimal seismic design of substandard RC frames using a friction-based passive wall damper." *11th fib International PhD Symposium in Civil Engineering*, Tokyo, Japan.

C4. Nabid, N., Hajirasouliha, I. and Petkovski, M. (2017), "A novel friction-based passive control wall damper for seismic strengthening of substandard RC frames." *16th World Conference on Earthquake Engineering, 16WCEE*, Santiago, Chile.

C5. Nabid, N., Hajirasouliha, I. and Petkovski, M. (2017), "A novel methodology for optimum seismic performance-based design of friction energy dissipation devices." *39th IABSE Symposium*, Vancouver, BC, Canada.

C6. Nabid, N., Hajirasouliha, I. and Petkovski, M. Escolano Margarit, D. (2018), "Optimum energy-based seismic design of energy dissipation devices in RC structures." *16th European Conference on Earthquake Engineering*, Thessaloniki, Greece.

# ACKNOWLEDGEMENTS

First and foremost, I would like to express my sincere acknowledgement to my research supervisors, Dr. Iman Hajirasouliha and Dr. Mihail Petkovski, whose fundamental advices led me to achieve the objectives of this research project.

My deepest gratitude and respect to Professor Kypros Pilakoutas and Dr. Maurizio Guadagnini whose constructive comments greatly contributed towards finding better solutions to my problems.

I would like to warmly thank all my friends in Sheffield for being supportive during the past years. I also like to express my greatest pleasure of having worked with the wonderful research members of Concrete and Earthquake Engineering group. A special thanks to my colleagues David and Mohammad for their time, generous help and advices. I would also like to thank my amazing friends, Mona, Nava and Farzaneh, for their sincere support throughout my years in the UK.

Finally, the unconditional love and encouragement of my parents and my brothers cannot be praised enough. I am incredibly grateful to my mom and dad for their continuous support and prayers, and for always being by my side through all tough times and for making me grow into a better person.

# TABLE OF CONTENTS

# LIST OF FIGURES

# LIST OF TABLES

# CHAPTER 1

# Introduction

## 1.1. RESEARCH MOTIVATION

Significant losses and damage caused by earthquakes in the last decade (e.g. China, 2008; Indonesia, 2009; Haiti, 2010; Nepal, 2015) highlighted the fact that the existing building structures in developing countries could be substandard and vulnerable in terms of failure in primary structural elements and even overall collapse. The main reasons for the vulnerability of these structures would be that they were designed to sustain gravity loads only; and constructed with little or no seismic detailing. The other possible reasons for the vulnerability of these structures could be changing the use of the structure (e.g. from residential to commercial use), using poor construction materials and deterioration of materials due to aging or aggressive environmental conditions. To protect these substandard structures against severe earthquakes, structural control systems can be considered as a viable alternative to increasing the strength of structural elements. This approach is based on increased dissipation of the input earthquake energy, leading to increased damping, reduced deformations and therefore, improved seismic performance of structures.

Structural control systems are categorised in four major groups in terms of their configurations and characteristics: (i) passive, (ii) active, (iii) semi-active, and (iv) hybrid control systems (Karnopp, 1995; Symans and Constantinou, 1999; Fisco and Adeli, 2011; Soong and Costantinou, 2014; Saaed et al., 2015). Passive control systems comprise simple energy dissipative devices that absorb the imparted seismic energy in the structure, with no need of external energy supply (e.g. Aiken et al., 1988; Zhang and Soong, 1992; Martinelli and Mulas, 2010; Zhang and Balendra, 2013). Active control systems are a smart evolution of the passive control systems comprised of sensors, controllers and actuators which are

powered by external energy supplies to produce control forces through real-time processing of information collected by sensors within the structure. These systems are extremely adaptable and flexible due to their capability of real-time modification of structure properties based on seismic excitation or structural response; however, they need a huge source of energy (Symans and Constantinou, 1999). Semi-active control systems require a small external power source (e.g. a battery) for regulator operation, and they utilise the structure motion for activation to generate the control forces. They have a higher adaptability as they can adjust to the structure's response continually, and therefore, they are more efficient in a wide range of earthquake frequencies but with more complex mechanism and expensive installations compared to the passive control systems (Symans and Constantinou, 1999; Fisco and Adeli, 2011). Hybrid control systems consist of combinations of the above-mentioned control systems with the goal of achieving improved performance (e.g. active mass damper) (Fisco and Adeli, 2011).

Passive energy dissipative devices have attracted a lot of attention due to their simplicity and low costs of manufacturing, implementation and maintenance, compared to the other structural controllers. These systems incorporate a variety of materials and devices to enhance damping, stiffness and strength for hazard mitigation of new structures and rehabilitation of aging or deficient structures (Soong and Dargush, 1997). Among different types of passive energy dissipation devices, friction-based dampers have the highest energy dissipation capacity for the same levels of force and deformation (Marsh, 2000; Pall and Pall, 2004). Moreover, friction devices are, in general, velocity and temperature-independent, tuneable to the characteristics of the structure, and capable to provide sustained performance under large number of cycles (Pall and Marsh, 1982; Aiken et al., 1993; Pall and Pall, 2004; Grigorian et al., 1993).

It should be noted that while using supplemental passive dampers can improve the overall seismic performance of controlled structures (e.g. reduced inter-storey drifts), some structural response parameters (e.g. axial load in columns) may be increased due to additional forces resulting from the new devices. In addition, using pre-defined characteristics and configurations for the supplemental dampers do not necessarily lead to the best seismic performance of the controlled structure. The key problem of the passive friction devices is their lack of adaptability and efficiency within a wide range of slip loads (the loads at which friction devices start slipping and dissipating energy). In other words, there is a specific range of slip loads in which the friction device can lead to a higher energy dissipation. Also, for the friction devices with very small and very large slip load values, the frame behaves like a bare frame and a frame with fixed brace/wall, respectively. This

highlights the importance of obtaining optimum ranges of slip loads leading to the optimum seismic performance of the controlled structure. In general, to increase the efficiency of the passive control systems, systematic optimisation design procedures can be employed by considering meaningful objective functions. However, the optimum design of passive control systems can be a challenging task due to the complexity and high non-linearity of the system resulting in high computational efforts.

A number of non-linear optimisation methodologies have been used to improve the efficiency of the passive energy dissipation devices, such as Genetic Algorithm (GA) (Holland, 1975; Golberg, 1989), Simulated Annealing (SA) (Kirkpatrick et al., 1983; Milman and Chu, 1994), Ant Colony Optimisation (ACO) (Dorigo and Stützle, 2004), Particle Swarm Optimisation (PSO) (Kennedy and Eberhart, 1995), Gradient-based Optimisation (Singh and Moreschi, 2001; Park et al., 2004; Lavan and Levy, 2006; Fujita et al., 2010) and Fully Stressed Design Optimisation (Levy and Lavan, 2006). It should be mentioned that most of the afore-mentioned optimisation methods are computationally expensive and/or require complex mathematical calculations, and therefore, may not be suitable for practical applications. Therefore, for simplification purposes, in most of the research the structure is assumed to remain linear-elastic, with energy dissipation devices as the only non-linear elements. In reality, the conventional structures are expected to exceed their elastic limits in severe earthquakes, so both the elements of the main structure and the supplemental devices are non-linear and dissipate energy. This study aims to develop a low computational cost, performance-based optimisation method for optimum seismic design of non-linear friction-based energy dissipation devices based on the concept of Uniform Distribution of Deformation (UDD).

## 1.2. BACKGROUND REVIEW

Structural control systems have been extensively researched as a way to reduce the responses of structures subjected to different kinds of dynamic loading. Among different types of control systems, passive supplemental dampers are the simplest and most cost-effective solution in terms of manufacturing, implementation and maintenance. Passive control of structures can be performed using non-structural elements at discrete zones (e.g. bracings, frames or beam-column connections) independent from any external energy suppliers (Reinhorn et al., 1995; Aiken, 1996; Moreschi, 2000). These control systems have been proved useful to control structural damage during strong earthquakes by dissipating seismic input energy and concentrating damage in non-structural elements (Soong and Constantinou, 1994; Aiken, 1996). Depending on the type of supplemental devices, they can

dissipate seismic energy through various mechanisms such as friction, yielding of metal, viscoelastic characteristic of the material, and shearing of viscous fluid (Reinhorn et al., 1995; Sadek et al., 1996; Aiken, 1996; Kasai et al., 1998; Symans and Constantinou, 1999).

Some of the advantages of the passive energy dissipation devices include: (1) reducing the response of the structure through adding damping and stiffness to the main building, (2) dissipating energy mainly by the supplemental devices and (3) concentrating damage in the non-structural elements which can be easily replaced after the earthquake (Sadek et al., 1996). The main disadvantage of these proposed systems is the lack of adaptability and flexibility which can restrict their efficiency to a limited range of frequencies (Quintana, 2013). However, if they are properly designed they can be as efficient as the other control systems with less cost, and that is the reason for the numerous (including ongoing) research studies on optimum design approaches to enhance the efficiency of these systems (e.g. Moreschi and Singh, 2003; Lee and Geem, 2004; Leung et al., 2008; Hejazi et al., 2013; Farshidianfar and Soheili, 2013; Liu et al., 2017). In general, passive control systems can be categorised in three major groups: (1) dynamic vibration absorbers, (2) viscous and viscoelastic dampers, and (3) hysteretic dampers.

### 1.2.1. Review of Passive Control Systems

#### *1.2.1.1. Dynamic vibration absorbers*

Dynamic vibration absorbers are moveable massive weights, which dissipate a considerable amount of input seismic energy through their large displacements. Tuned Mass Damper (TMD) and Tuned Liquid Dampers (TLD) are the most well-known representatives of this category of control systems (Moreschi, 2000; Marko, 2006). In general, TMD consist of a mass, spring and a viscous damper attached to a vibrating structure (Fraham, 1909; Ormondroyd and Den Hartog, 1928; Sadek et al., 1996; Fahim et al., 1997; Miranda, 2005; Bigdeli and Kim, 2016). The TMD moves relative to the structure and absorbs the kinetic energy transferred to it from the vibrating system (Marko, 2006). TLD comprises of rigid tanks filled with shallow liquid, and the energy is absorbed by the liquid-sloshing motion and dissipated through its viscous action (Sakai et al., 1989; Sadek et al., 1998; Dorothy, 1998; Novo et al., 2014; Bigdeli and Kim, 2016). As these types of dampers are not within the scope of this study, further information is not provided.

#### *1.2.1.2. Viscous and viscoelastic dampers*

The development of Viscous (VS) and Viscoelastic (VE) energy dissipation devices for earthquake engineering was initiated in the 1960s. These dampers are mostly used for wind-

induced vibrations of slender structures (Mahmoodi, 1969; Aiken et al., 1990; Constantinou and Symans, 1992; Marko, 2006; Symans et al., 2008; Saaed et al., 2015). VS and VE dampers can be activated at low deformations and they are velocity-dependent, which means that their energy dissipation performance is also dependent on the frequency of the response (Constantinou and Symans, 1992; Pekcan et al., 1999; Symans et al., 2008), and indirectly the frequency content of the input motion. While the efficiency of the VE dampers highly depends on the ambient temperature, the VS dampers are relatively insensitive to the temperature changes (Sadek et al., 1996; Symans et al., 2008).

Fig. 1.1 compares the idealised force-displacement responses of different passive energy dissipation devices (Constantinou and Symans, 1992; Aiken et al., 1993; Petkovski, 2001; Pall and Pall 2004; Symans et al., 2008). It is shown that VE dampers are less efficient in terms of energy dissipation compared to VS damped systems. This is due to the fact that VS dampers are more flexible to deform when they are subjected to the same deformation (Symans et al., 2008). In terms of reliability, there is a possibility of fluid seal leakage for the fluid VS dampers and debonding or tearing of VE dampers (Symans et al., 2008). Certain support members such as braces are usually required for installing VE or VS dampers into a frame (Fu and Kasai, 1998), and to fully utilise the efficiency of these dampers, they are usually attached to structures using stiff braces (Chen and Chai, 2011). As these types of dampers are not within the scope of this study, further information is not presented here.

#### *1.2.1.3. Hysteretic dampers*

Hysteretic devices, in general, are displacement-dependent devices categorised in two major types: 1) metallic yield dampers and 2) friction dampers, in which the input energy is dissipated through yielding of the metal, and generating heat due to dry friction, respectively. Unlike the other types of the passive dampers, these two energy dissipation devices are independent from load rate (velocity) and variation of temperature. Also, they have shown high fatigue resistance and performed well under a large number of load cycles (Grigorian et a., 1993; Reinhorn et al., 1995; Moreschi and Singh, 2003; Marko, 2006; Symans et al., 2008).

In general, yielding metallic dampers comprise of multiple parallel steel plates bolted together and installed between a chevron brace and the upper floor beam of a structure (Bergman et al., 1987; Whittaker et al., 1991; Tsai and Hong, 1993; Moreschi and Singh, 2003). Among all the yielding metallic devices, Added Damping and Stiffness (ADAS) (Scholl, 1984; Bergman et al., 1987) and Triangular Added Damping and Stiffness

(TADAS) (Tsai and Hong, 1993) are the most popular in seismic applications. It is worth mentioning that the energy dissipation depends on hysteretic behaviour of metals in the inelastic range, and only occurs when a certain level of force threshold is exceeded and steel plates start yielding. The non-linear behaviour of the system, the device damage and the need for replacement after the earthquake are some of the disadvantages of the yielding metallic dampers (Symans et al., 2008).

Friction dampers comprise of two or more plates with different materials bolted together and dissipate energy through their relative movements (Pall and Marsh, 1982; Fitzgerald et al., 1989; Grigorian et al., 1993; Aiken et al. 1993; Pall and Pall, 2004; Soong and Costantinou, 2014). Performance of the passive friction dampers is based on a pre-set slippage threshold, which can be tuned for each floor independently by controlling the clamping forces of the bolts. However, the optimum performance is limited to a narrow range of slip load (the load at which the friction device start slipping and dissipating energy) and the characteristics of the structure and the characteristics of the seismic input, which will be discussed in the following chapters. One of the possible drawbacks of the friction dampers is changing the condition of the interface with time that can be solved by choosing appropriate composition of the sliding interface (Housner et al., 1997; Symans et al., 2008). To insure the durability of the device operation, most friction devices use sliding interfaces comprising of steel on steel, brass on steel, or graphite impregnated bronze on stainless steel. It should be noted that there is moderate-to-severe additional corrosion of carbon and low alloy steel in contact with brass, copper or bronze (BSI, 1990). Only steels with high chromium content do not appear to suffer additional corrosion in contact with brass or steel (Housner et al., 1997). Grigorian et al. (1993) performed experimental tests and confirmed that the sliding interfaces consisting of brass and steel displayed a significantly more stable frictional characteristic compared to steel interfaces. Also, Pall and Marsh (1982) showed high durability when using heavy duty brake lining pads inserted between the sliding steel surfaces.

Depending on the characteristics of the sliding interface materials, friction-based dampers, can exhibit outstanding performance characteristics with almost constant force-displacement response independent of loading amplitude, frequency, number of loading cycles and temperature (Aiken et al., 1992). As illustrated by Fig. 1.1, they have shown almost rigid-plastic behaviour with rectangular hysteretic loops close to ideal dry coulomb friction behaviour, and hence, higher energy dissipation capacity compared to the other passive energy dissipative devices (Pall and Marsh, 1982; Aiken et al., 1993; Marsh, 2000; Pall and Pall, 2004).

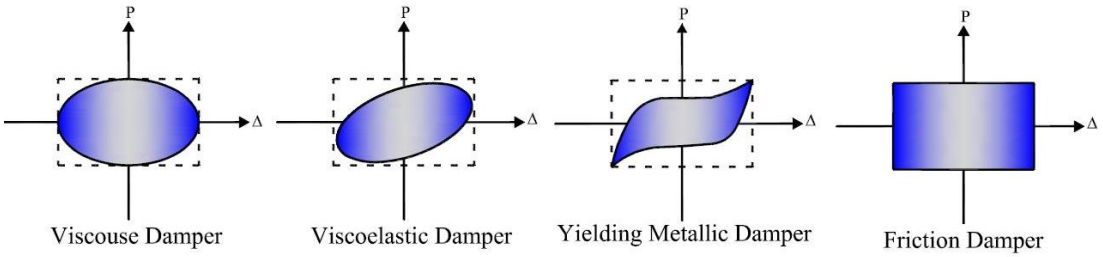


**Fig. 1.1.** Idealised force-displacement loops for different passive control devices

Fig. 1.2 shows the stiffness model of a structure equipped with fiction dampers when (a) the slip load of the damper ($f_p$) is higher than the yielding strength of the frame ($f_y$), and (b) the slip load of the damper is lower than the yielding strength of the frame. $\delta_{dy}$ and $\delta_{fy}$ represent yield deformation of the damper and the frame, respectively. Generally, by installing a friction damper in a structure, the stiffness of the combined system ($k_f + k_d$) is highly increased due to the high initial stiffness of the friction device ($k_d$) compared to that of the storey where the damper is installed ($k_f$). As a result, the inter-storey shear force of the combined system, which is represented by $F_v$, is increased due to the added stiffness. However, it is observed that for the slip load of the friction damper greater than the yield strength of the storey (i.e. Fig. 1.2 (a)), the shear force will be much higher compared to when the slip force is less than the storey yield strength (i.e. Fig. 1.2 (b)).

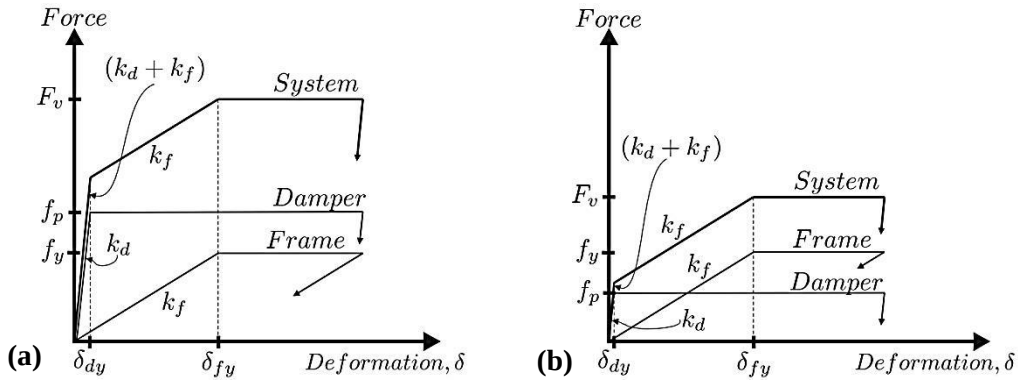


**Fig. 1.2.** Stiffness model of friction damper-structure system for (a) Slip load >frame's yield load, (b) slip load< frame's yield load (Quintana, 2013)

The mechanical behaviour of passive friction dampers can be modelled based on a Coulomb friction model as the following (Quintana, 2013):

$$f_{p,i} = \mu N_i sgn\left(\dot{\delta}_i(t)\right) \tag{1.1}$$

where $f_{p,i}$ represent the slip load of the $i^{th}$ friction damper, $\mu$ is defined as the friction coefficient of the sliding interface, and $N_i$ is the clamping force of the bolts. The direction of

the friction force (and motion in the damper) is determined by the sign function of the deformation rate across the damper (i.e. $sgn(\dot{\delta}_t(t))$). Some of the existing friction devices are presented in the following section.

## 1.2.2. Review of Friction-Based Passive Energy Dissipative Devices

### *1.2.2.1. Limited Slip Bolted (LSB) joints*

The first generation of dissipative friction devices was a system based on Limited Slip Bolted (LSB) joints, first suggested by Pall and Marsh (1979) for large panel structures to dissipate seismic energy through a limited slippage in the vertical joint of the panels. LSB joints incorporate steel inserts fastened to concrete panels and attached to slotted steel plates by high strength steel bolts. LSB joints are efficient for coupling adjacent units of a sectionalised concrete shear wall with one or more vertical joints (Pall and Marsh, 1981). Under a severe earthquake when the LSB joints are activated, they can increase the flexibility of the structure, and subsequently, reduce the response accelerations, dissipate large amounts of energy through friction in the slip joints, and delay or prevent the inelasticity of the walls. The study showed that, in general, they proved useful in reducing permanent deformation and damage in the main structural elements.

### *1.2.2.2. Pall friction dampers*

In a follow up study, inspired by the concept of friction brake in mid 1970's, Pall friction devices were proposed for the seismic control of braced steel frames (Pall and Marsh, 1982). Pall friction damper comprises a series of steel plates clamped together with high strength bolts and designed to slip under a predefined load to prevent compression buckling of the braces. Heavy duty brake lining pads are used in the friction interfaces. Pall and Marsh (1982) assumed that (1) during the slippage of the friction mechanism, the brace forces remain constant, and (2) the slippage of the device is large enough to straighten the buckled diagonal completely. Filiatrault and Cherry (1987) experimentally investigated the seismic behaviour of a 1/3 scale three storey friction damped braced frame on a shaking table. The results confirmed the high efficiency of the Pall friction dampers in enhancing the seismic performance of the controlled structure.

Pall friction devices are designed not to slip under wind loads, small earthquakes and service load conditions, and thus, the controlled frame performs as a braced frame. During a severe earthquake the joints slip with pre-set slip forces and the energy is dissipated in the controlled frame (Chandra et al., 2000). Pall and Pall (2004) showed that variations of up to $\pm 20\%$ of the optimum slip load (the load leading to minimum seismic response) do not

considerably affect the final results. The proposed system has been implemented in retrofit or design of several important buildings around the world: the Federal Electronic Research building (Sundararaj and Pall, 2004) in Canada, Boeing Commercial Airplane Factory at Everett (Vail et al., 2004) in USA, and La Gardenia residential complex of seven 18-storey towers in India (Chandra et al., 2000).

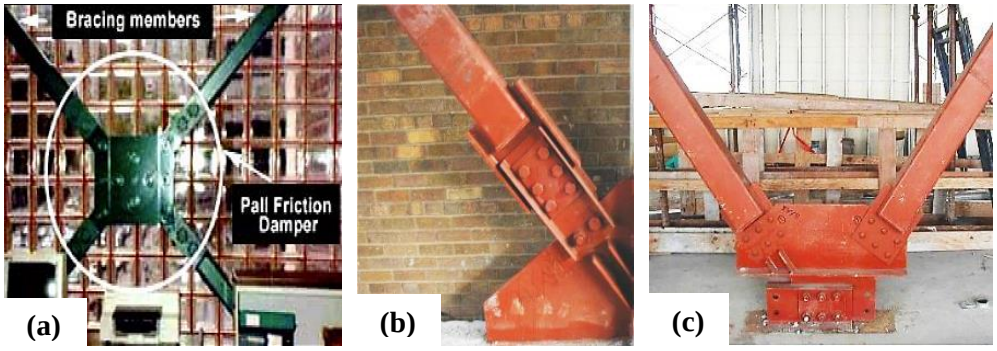


**Fig. 1.3.** Application of Pall friction damper in (a) x-bracing (Pall and Pall, 1996), (b) single diagonal bracing (Malhotra et al., 2004), and (c) chevron-bracing (Malhotra et al., 2004)

#### *1.2.2.3. Slotted Bolted Connections (SBCs)*

Slotted Bolted Connections (SBCs) are another type of friction-based damper proposed by Fitzgerald et al. (1989) to dissipate earthquake input energy and avoid buckling of brace elements in concentrically braced frames. Their proposed SBC assembly consists of a gusset plate and two back-to-back channel sections with the same position of slots, cover plates, and bolts with Belleville washers (see Fig. 1.4 (a)). The energy absorbing mechanism in SBCs is based on the friction between the gusset plates and the sliding channels. Constantinou et al. (1991) utilised graphite impregnated bronze plates to enhance the frictional behaviour of the slotted bolted connections (see Fig. 1.4 (b)). As a result, continuous lubrication of the rubbing elements along with extremely low wear rate, silent operation, and stable friction characteristics were observed.

In a follow-up study, Grigorian et al. (1993) improved the performance of the SBCs by using brass insert plates sandwiched between two outer steel plates to maintain a constant slip force (see Fig. 1.4 (c)). Extensive experimental tests were carried out on over 40 SBCs with and without shim like brass insert plates at the University of Berkeley. Better results and more stable friction characteristics were achieved for those connections with brass shim plates in the contact interface.

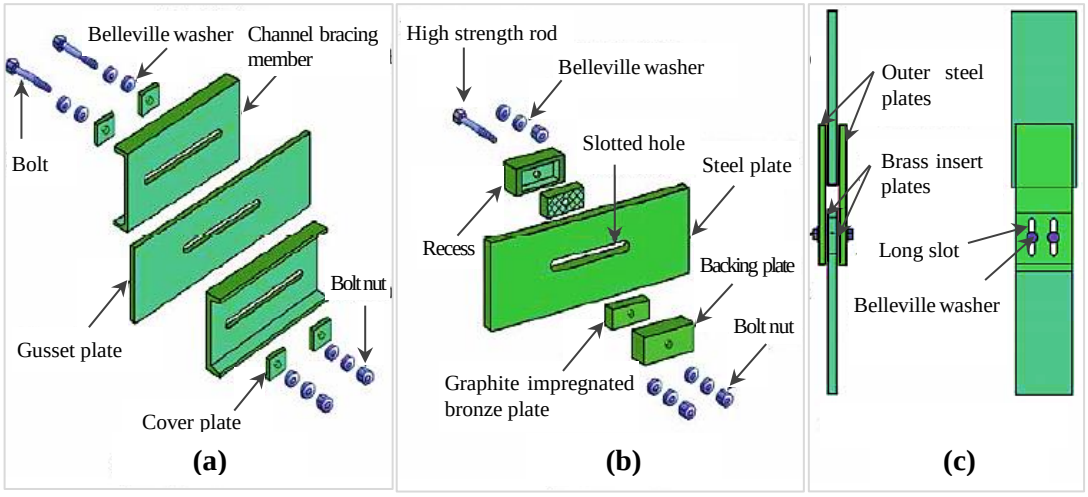


**Fig. 1.4.** Typical view of proposed SBCs assembly by (a) Fitzgerald et al. (1989), (b) Constantinou (1991), and (c) Grigorian et al. (1993) (adopted from Marko (2006))

### *1.2.2.4. Sumitomo dampers*

Sumitomo dampers are uniaxial friction dampers made of stainless steel casing with pre-compressed internal springs and friction pads developed by Sumitomo Metal Industries, Ltd, Japan (Aiken and Kelly, 1990; Aiken et al, 1993) (see Fig. 1.5). The force exerted by the pre-compressed internal spring is converted into a normal force on the friction pads through the action of inner and outer wedges. Dry lubrication is provided through the copper alloy friction pads containing graphite plug inserts to maintain a consistent coefficient of friction between the pads and the inner surface of the steel casing. Originally, the Sumitomo damper was developed as a shock absorber in railway rolling stock. In structural engineering applications, the device is attached to the upper floor beam and connected to a diagonal or chevron brace assemblage. The results of a test conducted on a ¼ scaled 9-storey building showed that Sumitomo dampers exhibited a consistent behaviour close to dry Coulomb friction behaviour with up to 60% reduction in drift responses.

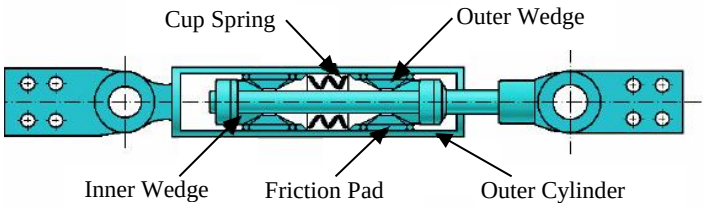


**Fig. 1.5.** Sectional view of uniaxial Sumitomo friction damper (after Aiken and Kelly (1990), in Marko (2006))

### *1.2.2.5. Rotational Friction Damper (RFD)*

A Rotational Friction Damper (RFD) was proposed by Mualla (Mualla, 2000), and developed by Damptech Ltd for an efficient seismic protection of a variety of structures with versatile applications. As shown in Fig. 1.6, RFD simply consists of a number of central and side steel plates (depends on the type and application) rotating relative to each other with circular friction pad discs in between. Dry friction lubrication is provided by the friction pads to ensure constant friction force, and to reduce the noise of the movements. In another study, the proposed RFD was extended to a friction-viscoelastic damper by using VE polymer pads in combination with friction pads for base isolation of structures (Nielsen et al., 2008).

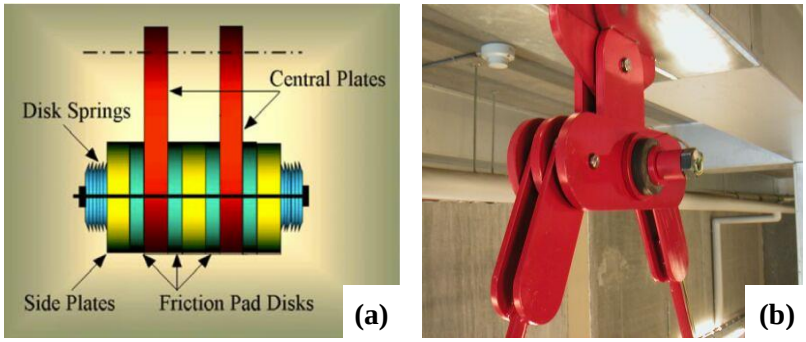


**Fig. 1.6.** Rotational Friction Damper: (a) front view, and (b) installation (www.damptech.com/articles-papers-and-more/)

The proposed friction device needs a bracing system or pre-stressed bar elements so that the shear loads can be transferred to the friction device. The experimental results of a full-scale 3-storey building subjected to two real excitation records showed, on average, 75% reduction in storey drifts. Over the last decade, different types of rotational friction dampers with various configurations were developed by Damptech Ltd for applications in buildings, bridges, highways and offshore structures against earthquakes, storms or waves (Mualla, 2000 ; Mualla and Belev, 2002; Nielsen et al., 2008; Barmo et al., 2015).

### *1.2.2.6. Wall-type friction dampers*

Most of the passive energy dissipation devices are attached to the main building structures using a bracing system which is not practical in reinforced concrete frames. In the past two decades, a number of wall-type friction dampers have been proposed. Sasani and Popov (1997; 2001) experimentally and analytically investigated the seismic behaviour of a friction-based wall-type passive damper designed by Nabih Youssef and Associates. The proposed system comprises of a non-structural lightweight reinforced concrete panel with

fixed support at the bottom and three friction energy dissipaters (i.e. SBCs) at the top. The concrete panel could dissipate energy through relative movement of the floors caused by seismic excitations and friction or gouging of sliding metal surfaces, resulting in a stable hysteresis loop. Sasani and Popov (1997; 2001) specifically investigated the behaviour of the connections when the impact of the bolts leads to extension of the concrete holes. They showed that the efficiency of their proposed system can be improved by using epoxy anchor bolts that provide adequate strength and stiffness at the base supports and, therefore, can minimise the rocking movement of the concrete panels during earthquakes. The results of their study indicated that their suggested passive concrete panels dissipated insignificant amount of energy at low amplitude motions, and therefore, were not very efficient under low to moderate earthquake motions.

Petkovski (2001) and Petkovski and Waldron (2003) investigated the effectiveness of another concrete wall panel (shown in Fig. 1.7) equipped with friction connections on reducing the seismic response of multi-storey RC structures. They also evaluated the effect of panel stiffness by considering various sizes of openings, and different thicknesses for the concrete panel design. Their results indicated that the stiffness of the thinnest panel is sufficiently larger than the stiffness of the frame, so that stiffer panels lead to very marginal improvement of the performance of the system. Also, the results of their study obtained for four real earthquake records confirmed that, in general, there is an optimum range of slip force to achieve the best seismic performance. Compared to the concrete panel system proposed by Sasani and Popov (1997), the system suggested by Petkovski (2001) could avoid transferring shear forces to the lower floor beam, and thus, could control the brittle shear failure of the beam elements.

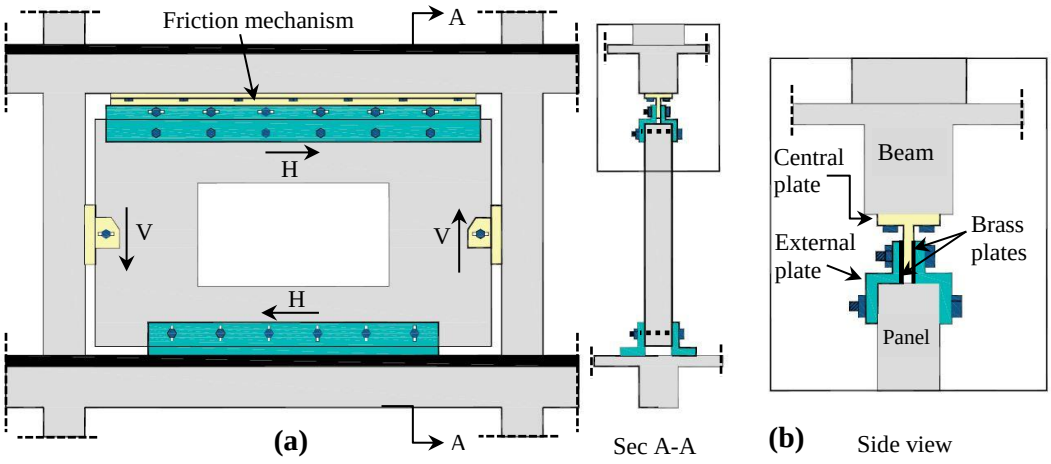


**Fig. 1.7.** Schematic model of a wall damper: (a) application in RC frame, and (b) friction connection detail (adopted from Petkovski, 2001)

While the proposed friction wall panel is designed to prevent additional shear forces to the adjacent beam and columns, it may still increase the total base shear and the axial load applied to the columns. This highlights the importance of using optimum height-wise distribution of slip force in passive friction dampers to minimise their adverse effects before it can be widely used in practice.

Another kind of wall-type friction damper was proposed by Cho and Kwon (2004) as a promising substitution for brace-type dampers to improve the performance of RC structures under seismic excitations. As illustrated in Fig. 1.8, the assembly consists of three main parts including a RC wall panel, U- and T-shape steel devices, and Teflon plates. Teflon sliding sheets are attached between steel devices to ensure more efficient friction mechanism. In this system, the clamping force on the Teflon slider is controlled by the load cell of an oil jack system which can be measured using a digital gauge attached to the load cell. Also, to avoid wearing the interface of the U- and T-shape steel plates, roller bearings are installed between these plates to allow horizontal slip during earthquake excitations. The friction between Teflon slider and the U- and T-shape steel devices due to relative horizontal movement provides the energy dissipation. The results of their study confirmed less stress concentration and damage in concrete elements along with considerable improvement of the seismic responses of the structure. However, compared to the friction panel proposed by Petkovski (2001), this type of panel would apply large shear to the lower floor beams due to the fixed connections at the bottom.

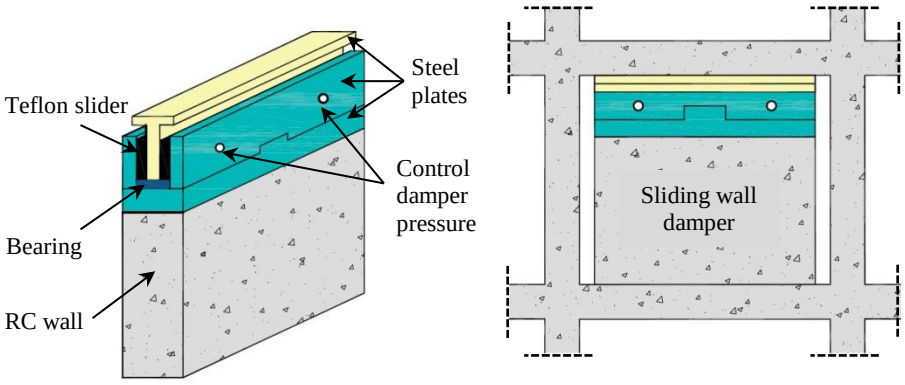


**Fig. 1.8.** Schematic model of wall friction damper (adopted from Cho and Kwon (2004))

Although friction-based passive control systems have been proved to be effective in seismic applications both analytically and experimentally, there are still some issues of concern in terms of their adaptability and efficiency within a wide range of control forces.

### 1.2.3. Review of Optimisation Methods Adopted for Passive Control Systems

Passive friction dampers are based on pre-set capacities (slip loads) which may lead to an inefficient design solution if they are not properly selected. For instance, if the control forces are designed to be too low or too high, the controlled structure may behave like a bare frame or a braced frame, respectively, for which the additional cost imposed by added dampers is not justified. Therefore, the main challenge of designing passive friction devices is to obtain the most appropriate slip load values to improve the seismic performance of the structure more efficiently. In this section, some of the possible optimisation strategies for optimum design of passive energy dissipation devices are discussed.

In the research literature there are numerous reports on studies focussed on finding the optimum control forces (either yield forces in yield devices or slip loads in friction devices) in passively controlled multi-storey buildings. Some of these studies use various optimisation techniques such as Genetic Algorithm (GA) and backtracking search optimization algorithm (BSA) (Moreschi and Singh, 2003; Apostolakis and Dargush, 2010; Honarparast and Mehmandoust, 2012; Miguel et al. 2016), or simply parametric studies with very limited variation of parameters. Often one building is analysed using several earthquake excitations or several buildings are studied with one or two seismic inputs (Filiatrault and Cherry, 1987; Xia and Hanson, 1992; Bhaskararao and Jangid, 2006; Kim and An, 2017). In most cases, the researchers vary the slip load at the base and use the same vertical (height-wise) distribution (Patro and Sinha, 2010). The performance is assessed by monitoring the changes in certain response parameter, such as maximum inter-storey drift or by introducing some ‘performance index’ that combines several parameters such as drift, energy and base shear (Austin and Pister, 1985; Filiatrault and Cherry, 1990; Lee et al., 2008; Patro and Sinha, 2010). The more elaborate optimisation is often carried out by using simplified, linear-elastic response simulations, often on equivalent single degree of freedom systems (e.g. Ciampi et al., 1995; Fu and Cherry, 2000; Bhaskararao and Jangid, 2006; Kim and An, 2017).

A number of advanced optimisation techniques have also been developed to tackle the complexity of large-scale problems with nonlinear objective functions. Evolutionary optimisation algorithms represent a robust optimisation category inspired by nature. They can be used to find the global optimum design solutions. Some of the methods from this category which have been adopted for optimisation of non-linear passive energy dissipation devices in the last two decades are: (1) Genetic Algorithm (GA) (Moreschi and Singh, 2003; Asahina et al., 2004; Lavan and Dargush, 2009; Honarparast and Mehmandoust, 2012; Hejazi et al., 2013), (2) Particle Swarm Optimisation (PSO) (Leung et al., 2008), (3) Ant

Colony Optimisation (ACO) (Farshidianfar and Soheili, 2013), (4) Simulated Annealing (SA) (Chen et al., 1991; Milman and Chu, 1994; Liu et al., 2017), and (5) Harmony search method (HS) (Lee and Geem, 2004). While the evolutionary algorithms are well suited for discrete optimisation problems, when applied to large non-linear systems, they lead to high computational cost and poor constraint handling abilities (Venter, 2010). Among all the evolutionary algorithms, the Genetic Algorithm (GA) (Holland, 1975) is the most established approach for the optimisation of passive energy dissipation devices.

#### *1.2.3.1. Genetic Algorithm (GA)*

Genetic algorithm (GA) (Holland, 1975; Goldberg, 1989) is a population-based random search, based on a biological evolution mechanism and Darwin's survival-of-the-fittest theory. It can be used for solving complex problems where the number of parameters is large and the analytical solutions are difficult to obtain. One of the major factors affecting the scalability and performance of genetic algorithms is the population size, which is usually a user-defined parameter. It is worth mentioning that small population sizes may lead to premature convergence and substandard solutions, while very large population sizes result in unnecessary computational cost (Sastry et al., 2005). GAs use random choice as a tool to guide a search toward regions of the search space by using genetic operators to find a new population. The old population is then substituted by the newly generated individuals using a fitness measure, and the evolution procedure proceeds until pre-defined termination criteria are satisfied. In general, a GA follows the following evolutionary steps:

1) *Initialisation:* The initial population of individuals is randomly created by incorporating domain-specific knowledge or other information. A set of binary strings (of 0s and 1s) is produced in which the string is referred to "chromosome" and the bits (0 or 1) in a string correspond to "genes" in natural genetics (Ghose, 2002; Rao and Savsani, 2012).

2) *Fitness Function:* In general, a fitness function is derived from the objective function and used in consecutive genetic operations. Once the population is initialised, the fitness values of the individuals are evaluated by the fitness function. GA is naturally suitable for solving maximisation problems in which the fitness function can be considered to be the same as the objective function. For minimisation problems, however, some suitable transformation is required on the objective function (Ghose, 2002; Sastry et al., 2005).

3) *GA Operators:* To improve the fitness of the individuals in each generation, three major operators are applied to the population including (i) Selection, (ii) Crossover and (iii) Mutation (Rao and Savsani, 2012) (Ghose, 2002)

(i) Selection: Selection operator imposes the survival-of-the-fittest rule on the individuals with higher fitness values by allocating more copies of the fittest solutions. The main idea of selection is to prefer stronger candidate solutions to weaker ones based on the objective function. Several selection methods have been proposed including stochastic uniform, uniform, roulette-wheel and tournament selection (Sastry et al., 2005). One of the commonly used selection schemes is the roulette-wheel selection in which an individual with the proportional probability to its fitness value is selected for the mating pool (Rao and Savsani, 2012).

(ii) Crossover: Crossover or recombination operator combines parts of two or more individuals called parents to create new, possibly better, solutions called children (i.e. offspring) with a crossover probability (Sastry et al., 2005; Rao and Savsani, 2012). In the crossover operator, new strings are created by exchanging information among strings of the mating pool. The offspring produced by recombination is not identical to any specific parent and instead is a novel combination of parental traits (Goldberg, 2002). There are many different crossover operators such as single-point, two-point and heuristic. For instance, for the two-point crossover operator, two strings are randomly picked from the mating pool and some portions of those are exchanged between the other strings (Ghose, 2002).

(iii) Mutation: Mutation operator locally modifies a solution by randomly changing 1 to 0 and vice versa in a bit position (i.e. a gene) using a small mutation probability which can be simulated by randomly choosing a number between 0 and 1. The randomly selected bit is modified if the random number is smaller than the mutation probability; otherwise, the bit is kept unchanged. The mutation is required to generate a new point in the neighbourhood of the current point to achieve a local search around the current solution, and also to maintain diversity in the population (Ghose, 2002; Sastry et al., 2005). Various mutation operators have been proposed such as adaptive feasible, uniform and Gaussian.

*4)* Replacement: The original parental population is substituted by the new offspring population produced by selection, crossover, and mutation replaces. Many replacement techniques are utilised in GAs such as elitist, generation-wise and steady-state replacement methods (Sastry et al., 2005).

During the GA optimisation process, steps 1 to 4 are repeated until a terminating condition is satisfied.

In the following chapters, a low computational cost performance-based optimisation method is developed using the concept of Uniform Distribution of Deformation (UDD) for optimum seismic design of non-linear passive energy dissipation devices, and its efficiency is compared to GA. It should be noted that the deformation demand in structures does not follow a height-wise uniform pattern during strong earthquakes. This implies that the deformation demand does not reach the allowable level of seismic capacity for some storeys, and therefore, the material is not fully exploited. However, if the strength of these strong parts decreases, the deformation is expected to increase. This can be continued until a status of uniform deformation is obtained, and the material capacity is fully exploited. This is considered as the concept of Uniform Distribution of Deformation (UDD) (Moghaddam and Hajirasouliha, 2006).

### 1.2.4. Conclusions on the current state of the art

The review of the reported research in the field passive control of the seismic response of multi-storey building shows that while there is a variety of practical solutions based on hysteretic damping (yield or friction based elements), the optimum distribution of control forces in the structure depends both on the type/size of the building and the characteristics of the seismic input. This means that the design of each passively controlled building needs to incorporate a lengthy parametric study, similar to the ones shown in the research; however, this is not practical for design purposes. Ideally, the designer should be able to choose the control force at the base (or the sum of the control forces at all storey levels), and the best distribution along the height, as a function of some selected characteristic of the building (e.g. number of storeys and bays; or first natural period), type of earthquake (e.g. near/far field, which is account for frequency content) and its intensity (low-moderate-high; represented by different levels of PGA). As this type of guidance is not available in the current design codes, a more detailed study is required on practical optimum design of control forces. The optimisation should be based on realistic dynamic response simulations that take into account the expected non-linear behaviour of the main structure (plastic hinges in main structural elements) as well as that of the control system. However, most of the previously studied optimisation techniques are highly computationally expensive due to non-linearity and complexity of these systems. The work presented in this study is an attempt to achieve optimum design solutions for structures with non-linear dampers under earthquake excitations.

## 1.3. SCOPE OF THE RESEARCH

This research is focused on optimum performance-based design of supplemental passive friction dampers which dissipate seismic input energy through friction between two or more sliding surfaces. Friction-based energy dissipation devices are installed in a main structure using (i) elastic concrete walls and (ii) inelastic chevron bracing elements. For more effective design of the selected dampers, different performance parameters are evaluated including maximum values of inter-storey drift, roof displacement, axial load in the columns, base shear and energy dissipation .For the development of a practical method for more efficient design of friction-based energy dissipation devices the following key parameters are considered: (i) size and geometry of RC frames (by using 3, 5, 10, 20-storey frames with 3 and 5 spans), (ii) dampers capacity (by using different height-wise slip load distribution patterns) and (iii) characteristics of seismic excitations (by using different synthetic and natural spectrum-compatible earthquakes and two sets of near and far-field ground motion records). The optimisation is carried out by single and multi-criteria performance-based approaches of the selected dampers, using the concept of Uniform Distribution of Deformation (UDD) and a comparison of this method with global optimisation techniques such as Genetic Algorithm (GA). At the end, a three-phase performance-based optimisation strategy is developed for simultaneous optimisation of the supporting brace elements and friction dampers while satisfying different performance targets under the representative design earthquakes.

## 1.4. AIMS AND OBJECTIVES

The aim of this research is to develop a low computational cost multi-criteria performance-based optimisation framework for optimal design of friction-based passive control systems. This was achieved by fulfilling the following objectives:

1. To define detailed non-linear FE models of different multi-storey RC buildings with wall-type friction-based passive energy dissipation devices.

2. To propose a simplified method for practical seismic design and strengthening of RC frames with passive friction dampers by considering a broad range of frame geometries, damper capacities and seismic excitations.

3. To develop a low computational cost method for multi-criteria performance-based optimisation of friction dampers.

4. To assess the efficiency of the new optimisation framework for simultaneous optimal design of friction dampers under different earthquake intensities.

5. To evaluate the effects of different parameters on the computational efficiency and convergence rate of the proposed optimisation methods.

6. To compare the efficiency of the proposed performance-based optimisation methodology with a global optimisation method such as GA.

7. To assess the efficiency of the proposed performance-based design methodology through several practical design examples.

## 1.1. TASKS AND METHODOLOGY

The following methodology is adopted to achieve the objectives.

1. Perform a comprehensive overall review of the state-of-the art of the research on passive control systems with a focus on friction-based energy dissipation devices and non-linear optimisation methods such as Genetic Algorithm (GA) [Objective 1, 2 and 3].

2. Design a series of prototype 2D frame buildings with different geometries (3, 5, 10, 15 and 20-storey frames with 3 and 5 bays) based on IBC-2015 (2015) and Eurocode 8 (EC8; CEN, 2004) response spectrum procedure. Develop detailed FE models of the prototype structures (with and without friction-based passive control dampers), using DRAIN-2DX and OPENSEES. Perform non-linear dynamic analyses to assess their seismic performance in terms of maximum inter-storey drifts, maximum column axial load, base shear and energy dissipation parameter (a ratio between the work of the friction device to the work of the beam and column elements) subjected to a set of synthetic and natural (far-field and near-field) ground motion records [Objective 1].

3. Perform a parametric study of seismic performance of the frames with friction dampers by considering a variety of frame geometries, damper mechanical properties and seismic excitation records to determine more efficient range and height-wise distribution of slip loads; and therefore, a more practical design method is developed for frames with friction-based dampers [Objective 2].

4. Establish a practical multi-criteria performance-based optimisation framework for optimum design of friction dampers based on the concept of Uniform Distribution of Deformation (UDD) to achieve desired performance levels under the design earthquakes [Objective 3].

5. Perform a parametric study on optimum design of friction dampers in RC structures by considering a variety of initial slip load distributions, earthquake excitations and convergence parameters to evaluate the computational efficiency and convergence speed of the proposed optimisation method [Objective 4, 5].

6. Propose a more efficient adaptive optimisation approach (Adaptive UDD; based on the standard UDD), and evaluate it for performance-based optimum design of 3, 5 and 10-storey frames. Its computational efficiency is then compared with a standard GA global optimisation method [Objective 6].

7. Extend the proposed multi-criteria optimisation method (UDD) to a three-phase optimisation strategy for simultaneous optimum design of chevron bracing elements and friction dampers in a 5-storey frame under a design earthquake to demonstrate the efficiency of the method for different design examples [Objective 7].

## 1.5. THESIS LAYOUT

This thesis is presented in an "alternative format" and consists of the following chapters, which were published (or submitted for publication) as journal papers:

### 1.1.1. Chapter 1

In this chapter is provided an overall introduction to the problem, research motivation, aims and objectives and the thesis layout. In addition, a general background review is briefly summarised. The literature review is presented on the following topics:

- Existing passive control systems including 1) Dynamic vibration absorbers 2) Viscous and viscoelastic dampers, and 3) Hysteretic dampers.

- Existing friction dampers including 1) Limited Slip Bolted (LSB) joints, 2) Pall friction dampers, 4) Sumitomo dampers, 5) Slotted Bolted Connections (SBCs), 6) Rotational friction damper and 7) Friction wall panels.

- Existing optimisation strategies for passive control systems and general information on Genetic algorithm (GA).

### 1.1.2. Chapter 2

**A practical method for optimum seismic design of friction wall dampers**

Chapter 2 addresses parts of the objectives 1 and 2 and is based on the following paper: Nabid, N., Hajirasouliha, I. and Petkovski, M. (2017), "A practical method for optimum seismic design of friction wall dampers." *Earthquake Spectra*, **33**(3): 1033–1052.

This chapter deals with proposing an empirical equation for practical optimum design of friction dampers by considering different frame geometries and earthquake excitations. A set of buildings with 3, 5, 10, 15 and 20 storeys and 5 spans equipped with friction wall dampers in their middle span is subjected to a set of natural and synthetic spectrum-compatible earthquakes. In this chapter, different height-wise distributions of slip loads are considered and their optimum ranges are determined based on the maximum energy dissipation efficiency for the spectrum-compatible earthquakes. Subsequently, a straightforward empirical equation is proposed for more efficient height-wise distribution of slip loads by considering the frame geometry.

### 1.1.3. Chapter 3

**A simplified methodology for optimum design of friction dampers by considering near-field and far-field ground motions**

In Chapter 3, seismic uncertainty is considered when addressing the objectives 1 and 2. This chapter is based on a recently submitted paper: Nabid, N., Hajirasouliha, I. and Petkovski, M. (2018), "A simplified methodology for optimum design of friction dampers by considering near-field and far-field ground motions." *Journal of Earthquake Engineering*.

To take into account the characteristic of the input earthquake, in this chapter, 3, 5, 10, 15 and 20-storey RC frames with 3 spans are subjected to two sets of near- and far-field ground excitations. The optimum ranges of the slip loads are obtained for the selected earthquakes with different Peak Ground Accelerations (PGA) and Peak Ground Velocities (PGV). It is observed that the optimum design solution depends more on the PGV of the earthquake rather than the PGA. Accordingly, to achieve an efficient and practical optimal design of the friction dampers, an empirical equation is proposed by considering the number of storeys and (PGV) of the earthquake.

### 1.1.4. Chapter 4

**Performance-based optimisation of RC frames with friction wall dampers using a low-cost optimisation method**

This chapter which addresses parts of the objectives 3 and 5 is based on the paper: Nabid, N., Hajirasouliha, I. and, Petkovski, M. (2018). "Performance-based optimisation of RC

frames with friction wall dampers using a low-cost optimisation method." *Bulletin of Earthquake Engineering*, **16**(10): 5017–5040.

In this chapter is presented the development of an efficient (low computational cost) optimisation method based on the theory of UDD for optimum design of friction dampers. In this method, the slip load at each storey level is modified, while the total slip load is constant (sum of the slip loads at all storeys), until a more uniform distribution of deformation (lateral inter-storey drift) is achieved. The efficiency of the method is evaluated through the optimum design of 3, 5, 10, 15 and 20-storey RC frames equipped with friction wall dampers under natural and synthetic spectrum-compatible earthquakes. In addition, the effects of different parameters such as different initial slip load distributions, convergence parameters and earthquake records are assessed on the computational efficiency and convergence rate of the proposed optimisation algorithm.

### 1.1.5. Chapter 5

**Multi-criteria performance-based optimisation of friction energy dissipation devices in RC frames**

Chapter 5 addresses the objectives 3 and 4 based on a submitted journal paper: Nabid, N., Hajirasouliha, I. and Petkovski, M. (2018), "Multi-criteria performance-based optimisation of friction energy dissipation devices in RC frames." *Journal of Structural Engineering (ASCE)*.

While the proposed empirical equation (in Chapter 2) may not necessarily satisfy a desired performance level, in this paper single and multi-criteria performance-based optimisation methods are proposed for optimum seismic design of friction-based energy dissipation devices. According to this method, the total value and the height-wise distribution of slip loads at the friction devices are modified until the predefined performance target levels are simultaneously satisfied under the representative earthquakes.

### 1.1.6. Chapter 6

**Performance-based optimisation of friction dampers using adaptive and genetic algorithm methods**

This chapter which addresses the objectives 5 and 6 is based on a ready for submission paper: Nabid, N., Hajirasouliha, I. and Petkovski, M. (2018), "Adaptive low computational cost optimisation method for performance-based seismic design of friction dampers." *Journal of Engineering Structures*.

In this paper, the effect of different convergence factors are investigated on the optimisation speed of the proposed UDD optimisation method, and subsequently, an efficient adaptive convergence parameter is proposed. The efficiency of the proposed adaptive optimisation method is then demonstrated through optimum design of 3, 5, and 10-storey RC frames with friction dampers and the results are compared with those obtained from a Genetic Algorithm (GA) as a global optimisation method. A combination method is also evaluated using the results of the adaptive UDD optimisation as the starting point of the GA optimisation that can lead to considerably higher convergence rate. In this chapter, the accuracy, computation efficiency and simplicity of the proposed UDD method is proved against the standard evolutionary optimisation method such as GA.

### 1.1.7. Chapter 7

**Application of UDD optimisation method in RC frames strengthened with friction dampers using chevron bracing system**

This chapter addresses the objective 7 by extending the UDD performance-based optimisation method to a three-phase algorithm capable of simultaneous optimum design of chevron bracing system and friction dampers to satisfy predefined performance objectives. At the first phase, a discrete optimisation algorithm is defined for size optimisation of the brace elements when the friction devices are fixed (i.e. very high slip load values) to satisfy Immediate Occupancy (IO) performance level under Design Basis Earthquake (DBE) record. In the second phase, slip load distribution of the friction devices is optimised in order to satisfy Life Safety (LS) performance level under a Maximum Considered Earthquake (MCE) record. In the last phase, the optimum design solution is checked under a DBE event and the slip loads are only allowed to increase for those storeys which violate the IO performance target and the final results are eventually obtained.

### 1.1.8. Chapter 8

This chapter contains a summary of the results, followed by recommendations for future work.

## REFERENCES

Aiken I. D., Kelly J. M., and Mahmoodi P. (1990). “The application of viscoelastic dampers to seismically resistant structures.” *In Proceedings: 4th US National Conference on Earthquake Engineering*, Palm Springs, CA, **3**: 459–468.

Aiken, I. (1996). "Passive energy dissipation - hardware and applications." *In Proceedings: Los Angeles County and Seaosc Symposium on Passive Energy Dissipation Systems for New and Existing Buildings*, Los Angeles, CA.

Aiken, I. D. and Kelly, J. M. (1990). "Earthquake simulator testing and analytical studies of two energy-absorbing systems for multi-storey structures." Report No. UCB/EERC-90/03, *Earthquake Engineering Research Centre*, University of California at Berkeley, Berkeley, CA.

Aiken, I. D. Nims, D. K., Whittaker, A. S. and Kelly, J. M. (1993). "Testing of passive energy dissipation systems." *Earthquake Spectra*, **9**(3): 335–370.

Aiken, I. D., Kelly, J. M. and Pall, A. S. (1988). "Seismic response of a nine-story steel frame with friction damped cross-bracing." *In Proceedings: 9th world Conference on Earthquake Engineering*, Tokyo, Japan.

Aiken, I. D., Nims, D. K. and Kelly, J. M. (1992). "Comparative study of four passive energy dissipation systems." *Bulletin of the New Zealand National Society for Earthquake Engineering*, **25**: 175–192.

Asahina, D., Bolander, J. E. and Berton, S. (2004). "Design optimisation of passive devices in multi-degree of freedom structures." *In Proceedings: 13th World Conference on Earthquake Engineering*, Vancouver, B.C., Canada.

Barmo, A., Mualla, I. H. and Hasan, H. T. (2015). "The behavior of multi-story buildings seismically isolated system hybrid isolation (friction, rubber and with the addition of rotational friction dampers)." *Open Journal of Earthquake Research*, **4**: 1–13.

Bergman, D. M. and Goel, S. C., (1987). "Evaluation of Cyclic Testing of Steel-Plate Devices for Added Damping and Stiffness," *Report No. UMCE 87-10*, University of Michigan, Ann Harbor, MI.

Bigdeli, Y. and Kim, D. (2016). "Damping effects of the passive control devices on structural vibration control: TMD, TLC and TLCD for varying total masses." *KSCE Journal of Civil Engineering*, **20**(1): 301–308.

British Standards Institution (1990). "Steel, concrete and composite bridges." Part 9. section 9.1, Bridge bearings, *code of practice for design of bridge bearings*, BS5400, London, UK.

CEN (Comité Européen de Normalization) (2004a). "Eurocode 8: Design of structures for earthquake resistance-Part 1: General rules, seismic actions and rules for buildings," EN 1998-1-1, Brussels.

Chandra, R. eta l. (2000). "Friction-dampers for seismic control of la gardenia towers." *In Proceedings: 12th World Conference on Earthquake Engineering*. Auckland, New Zealand, 1–8.

Chen, G. S., Bruno, R. J., Salama, M. (1991). "Optimal placement of active/passive elements in truss structures using simulated annealing." *AIAA Journal*, **29**: 1327–1334.

Chen, Y. T. and Chai, Y. H. (2011). "Effects of brace stiffness on performance of structures with supplemental Maxwell model-based brace-damper systems." *Earthquake Engineering and Structural Dynamics*, **40**: 75–92.

Cho, C. G. and Kwon, M. (2004). "Development and modeling of a frictional wall damper and its applications in reinforced concrete frame structures." *Earthquake Engineering and Structural Dynamics*, **33**: 821–838.

Ciampi, V., De Angelis, M. and Paolacci, F. (1995). "Design of yielding or friction-based dissipative bracings for seismic protection of buildings." *Engineering Structures*, **17**(5): 381–391.

Constantinou, M. C. and Symans, M. D. (1992). "Experimental and Analytical Investigation of Seismic Response of Structures with Supplemental Fluid Viscous Dampers." Report No. NCEER-92-0032, *National Center for Earthquake Engineering Research*, Buffalo, NY.

Constantinou, M. C., Reihorn, A. M., Mokha, A. and Watson, R. (1991). "Displacement control device for base isolated bridges." *Earthquake Spectra*, **7**(2): 179–200.

Dorigo, M. and Stützle, T. (2004). "Ant colony optimisation." *A Bradford Book, the Massachusetts Institute of Technology (MIT) Press,* Scituate, MA,

Dorothy, R., (1998). "Investigation of tuned liquid dampers under large amplitude excitation." *Journal of Engineering Mechanics*, **124**(4): 405–413.

Fahim, S., Mohraz, B., Taylor, A. W. and Chung, R. M. (1997). "A method of estimating the parameters of tuned mass dampers for seismic applications." *Earthquake Engineering and Structural Dynamics*, **26**: 617–635.

Farshidianfar, A. and Soheili, S. (2013). "Ant colony optimisation of tuned mass dampers for earthquake oscillations of high-rise structures including soil-structure interaction." *Soil Dynamics and Earthquake Engineering*, **51**: 14–22.

Filiatrault, A. and Cherry, S. (1987). "Performance evaluation of friction damped braced steel frames under simulated earthquake loads." *Earthquake Spectra*, **3**(1): 57–78.

Fisco, N. and Adeli, H. (2011). "Smart structures: Part II - Hybrid control systems and control strategies." *Scientia Iranica, **18**, 285–295.*

FitzGerald, T. F., Anagnos, T., Goodson, M. and Zsutty, T. (1989). "Slotted bolted connections in aseismic design for concentrically braced connections." *Earthquake Spectra*, **5**: 383–391.

Frahm, H. (1909). "Device for damping vibrations of bodies." US Patent 989,958.

Fu, Y. and Cherry, S. (2000). "Design of friction damped structures using lateral force procedure." *Earthquake Engineering and Structural Dynamics*, **29**:989–1010.

Fu, Y. and Kasai, K. (1998). "Comparative study of frames using viscoelastic." *Journal of Structural Engineering*, **124**(5): 513–522.

Fujita, K., Yamamoto, K. and Takewaki, I. (2010). "An evolutionary algorithm for optimal damper placement to minimize interstorey-drift transfer function in shear building." *Earthquakes and Structures*, **1**(3): 289–306

Ghose, T. (2002). "Optimisation technique and an introduction to genetic algorithms and simulated annealing", *In Proceedings: International workshop on Soft Computing and Systems*, Birla Institute of Technology (BIT), Mesra, Ranchi, India, 1–19.

Goldberg, D. E. (1989). "Genetic algorithms in search, optimisation and machine learning." *Addison-Wesley*: Reading, MA.

Goldberg, D. E. (2002). "The design of innovation: lessons from and for competent Genetic Algorithms", *Kluwer Academic Publishers*, Boston, MA.

Grigorian, C. E., Yang, T. S. and Popov, E. P. (1993). "Slotted bolted connection energy dissipators." *Earthquake Spectra*, **9**(3): 491–504.

Hejazi, F., Toloue, I. and Jaafar, M. S. (2013). "Optimisation of earthquake energy dissipation system by genetic algorithm." *Computer-Aided Civil and Infrastructure Engineering*, **28**: 796–810.

Holland, J. H. (1975). "Adaptation in natural and artificial systems." *Ann Arbor: The University of Michigan Press*.

Honarparast, S., Mehmandoust, S. (2012). "Optimum distribution of slip load of friction dampers using multi- objective genetic algorithm." *In Proceedings: 15th World Conference on Earthquake Engineering*, Lisbon, Portugal.

Housner, G. W., Bergman, L. A., Caughey, T. K., Chassiakos, A. G. et al. (1997). "Structural control : past , present , and future." *Journal of Engineering Mechanics*, **123**(9): 897–971.

International Building Code (IBC). (2015). *International Code Council*, Country Club Hills, USA.

Karnopp, D. (1995). "Active and semi-active vibration isolation." *Journal of Vibration and Acoustics*, **117**: 177–185.

Kasai, K., Fu, Y. and Watanabe, A. (1998). "Passive control systems for seismic damage mitigation." *Journal of Structural Engineering*, **124**(5): 501–512.

Kennedy, J. and Eberhart, R. (1995). "Particle swarm optimisation." *In Proceedings*: *IEEE International Conference on Neural Networks*, **4**: 1942–1948.

Kim, J. and An, S. (2017). "Optimal distribution of friction dampers for seismic retrofit of a reinforced concrete moment frame." *Advances in Structural Engineering*, **20**(10): 1523–1539.

Kirkpatrick, S., Gelatt, C. D. and Vecchi, M. P. (1983). "Optimisation by simulated annealing." *Science*, **220**: 671–680.

Lavan, O. and Levy, R. (2006). "Optimal peripheral drift control of 3D supplemental viscous dampers." *Journal of Earthquake Engineering*, **10**(6): 903–923.

Lavan, O., Dargush, G. F. (2009). "Multi-objective evolutionary seismic design with passive energy dissipation systems." *Journal of Earthquake Engineering*, **13**: 758–790.

Lee, K. S., Geem, Z. W. (2004). "A new structural optimisation method based on the harmony search algorithm." *Computers and Structures*, **82**: 781–798.

Lee, S., Park, J., Moon, B., Min, K. et al. (2008). "Design of a bracing-friction damper system for seismic retrofitting." *Smart Structures and Systems*, **4**(5): 685–696.

Leung, A. Y. T., Zhang, H., Cheng, C. C. and Lee, Y. Y. (2008). "Particle swarm optimisation of TMD by non-stationary base excitation during earthquake." *Earthquake Engineering and Structural Dynamics,* **37**: 223–1246.

Levy, R. and Lavan, O. (2006). "Fully stressed design of passive controllers in framed structures for seismic loadings." *Structural and Multidisciplinary Optimisation,* **32**(6): 485–498.

Liu, M., Liang, W. and Lin, Y. (2017). "Simulated annealing optimisation of tuned mass dampers for vibration control of seismic-excited buildings." *In Proceedings: 9th International Conference on Applied Operational Research (ICAOR),* Taoyuan, Taiwan.

Mahmoodi, P. (1969). "Structural Dampers." *Journal of Structural Division. ASCE,* 95(ST8), New York.

Malhotra, A. Carson, D., Gopal, P., Braimah, A. et al. (2004). "Friction dampers for seismic upgrade of St. Vincent Hospital, Ottawa." *In Proceedings: 13th World Conference on Earthquake Engineering*, Paper No. 1952.

Marko, J. (2006). "Influence of Damping Systems on Building Structures Subject to Seismic Effects." *PhD Thesis*, Queensland University of Technology, Brisbane, Australia.

Marsh, C. (2000). "The control of building motion by friction dampers." *In Proceedings: 12th world Conference on Earthquake Engineering*, Auckland, New Zealand.

Martinelli, P. and Mulas, M. G. (2010). "An innovative passive control technique for industrial precast frames." *Engineering Structures*, **32**(4): 1123–1132.

Miguel, L. F. F., Miguel, L. F. F. and Lopez, R. H. (2016). "Simultaneous optimization of force and placement of friction dampers under seismic loading." *Engineering Optimization,* **48**: 586–602.

Milman, M. H. and Chu, C. C. (1994). "Optimisation methods for passive damper placement and tuning." J*ournal of guidance, control and dynamics*, **17**(4): 848–856.

Miranda, J. C. (2005). "On tuned mass dampers for reducing the seismic response of structures." *Earthquake Engineering and Structural Dynamics*, **34**: 847–865.

Moghaddam, H. and Hajirasouliha, I. (2006). "Toward more rational criteria for determination of design earthquake forces." *International Journal of Solids and Structures,* **43**(9), 2631–2645

Moreschi, L. M. (2000). "Seismic design of energy dissipation systems for optimal structural performance." *PhD Thesis*, Virginia Polytechnic Institute and State University, Virginia.

Moreschi, L. M. and Singh, M. P. (2003). "Design of yielding metallic and friction dampers for optimal seismic performance." *Earthquake Engineering and Structural Dynamics*, **32**: 1291–1311.

Mualla, I. H. (2000). "Parameters influencing the behavior of a new friction damper device." *In Proceedings: 7th International Symposium on Smart Structures and Materials (SPIE)*, Newport Beach, **3988**: 64–74.

Mualla, I. H. and Belev, B. (2002). "Performance of steel frames with a new friction damper device under earthquake excitation." *Engineering Structures*, **24**: 365–371.

Nielsen, L. O., Mualla, I. H., Iwai, Y. and Nagase, T. (2008). "Seismic isolation systems based on friction-fractional viscoelastic dampers." *In Proceedings: 14th World Conference on Earthquake Engineering*. Beijing, China.

Novo, T., Varum, H., Teixeira-Dias, F., Rodrigues, H. et al. (2014). "Tuned liquid dampers simulation for earthquake response control of buildings." *Bulletin of Earthquake Engineering*, **12**: 1007–1024.

Ormondroyd, J. and Den Hartog, J. P. (1928). "The theory of the dynamic vibration absorber." *Transactions of the ASME, Applied Mechanics*, **50**: 9–22.

Pall, A. S. and Marsh, C. (1981). "Friction-damped concrete shearwalls." *ACI Journal Proctedings*, **3**(78): 187–193.

Pall, A. S. and Marsh, C. (1982). "Response of friction damped braced frames." *Journal of the Structural Division*, **108**(6): 1313–1323.

Pall, A. S. and Pall, R. T. (2004). "Performance-based design using pall friction dampers - an economical design solution." *In Proceedings: 13th world Conference on Earthquake Engineering*, Vancouver, B.C., Canada: Paper No. 1955.

Pall, A. S. and Pall, R., (1996). "Friction dampers for seismic control of buildings: A Canadian experience." *In Proceedings: 11th World Conference on Earthquake Engineering*, Acapulco, Mexico, Paper No. 497.

Pall, A. S., and Marsh, C. (1979). "Seismic response of large panel structures using limited slip bolted joints." *In Proceedings: 3rd Canadian Conference on Earthquake Engineering*, Montreal, Canada, 899–916.

Park, J. H., Kim, J. and Min, K. W. (2004). "Optimal design of added viscoelastic dampers and supporting braces." *Earthquake Engineering and Structural Dynamics*, **33**(4): 465–484.

Patro, S. K. and Sinha, R. (2010). "Seismic performance of dry-friction devices in shear-frame buildings." *Journal of Civil Engineering and Architecture* **4**(12).

Pekcan, G., Mander, J. B. and Chen, S. S. (1999). "Non-linear viscous dampers." *Earthquake Engineering and Structural Dynamics*, **28**: 1405–1425.

Petkovski, M. (2001). "Friction based passive control of the seismic response of multi-storey reinforced concrete frames." *PhD Thesis*, The University of Sheffield, UK.

Petkovski, M. and Waldron, P. (2003). "Optimum friction forces for passive control of the seismic response of multi-storey Buildings." *In Proceedings: 40 years of European Earthquake Engineering, SE40EEE,* Ohrid, Macedonia.

Quintana, H. C. (2013). "Semiactive friction connections for seismic control of multi-storey buildings." *PhD Thesis*, The University of Sheffield, UK.

Rao, R. V. and Savsani, V. J. (2012). "Mechanical design optimisation using advanced optimisation techniques." *Springer Series in Advanced Manufacturing*, London, UK.

Reinhorn, A. M., Constantinou, M. C. AND Li, C. (1995). "Use of supplemental damping devices for seismic strengthening of lightly reinforced concrete frames." *NIST Workshop.*

Rotational friction damper, Damptech earthquake protection. Available at: http://www.damptech.com/articles-papers-and-more/ [last accessed: 15/11/2015]

Saaed, T. E. Nikolakopoulos, G., Jonasson, J. and Hedlund, H. (2015). "A state-of-the-art review of structural control systems." *Journal of Vibration and Control*, **21**(5): 919–937.

Sadek, F., Mohraz, B., Taylor, A. W. and Chung, R. M. (1996). "Passive energy dissipation devices for seismic applications." *National Institute of Standards and technology (NIST)*, Maryland, USA, NISTIR 5923.

Sadek, F., Mohraz, B. and Lew, H. S. (1998). "Single and multiple tuned liquid column dampers for seismic applications." *Earthquake Engineering and Structural Dynamics*, **27**: 439–463.

Sakai, F., Takeda, S., and Tamaki, T. (1989). "Tuned liquid column damper-new type device for suppression of building vibrations." *In Proceedings: International Conference on High-rise Buildings*, Nanjing, China, 926–931.

Sasani, M. and Popov, E. P. (1997). "Experimental and analythical studies on the seismic behavior of lightweight concrete panels with friction energy dissipators." *Earthquake Engineering Research Centre*, University of California, Berkely, CA, UBC/EERC-97/17.

Sasani, M. and Popov, E. P. (2001). "Seismic energy dissipators for RC panels; Analytical studies." *Journal of Engineering Mechanics*, **127**(8), 835–843.

Sastry, K., Goldberg, D., and Kendall, G. (2005). "Genetic algorithms." *In Book: Search methodologies*, New York, Springer, 93–117.

Scholl, R. E. (1984). "Brace dampers: an alternative structural system for improving the earthquake performance of buildings." *In Proceedings: 8th World Conference on Earthquake Engineering*, San Francisco, CA, 1015–1022.

Singh, M. P, Moreschi, L. M. (2001). "Optimal seismic response control with dampers." *Earthquake Engineering and Structural Dynamics*, **30**: 553–572.

Soong, T. T. and Constantinou, M. C. (1994). "Passive and active structural vibration." State University of New York, Buffalo, NY.

Soong, T. T. and Costantinou, M. C. (2014). "Passive and active structural vibration control in civil engineering." Springer.

Soong, T. T. and Dargush, G. F. (1997). "Passive energy dissipation systems in structural engineering." *John Wiley & Sons*, Chichester, England, UK.

Sundararaj, P. R. and Pall, R. T. (2004). "Seismic control of federal electronics research building." *In Proceeding, 13th World Conference on Earthquake Engineering*, Vancouver, B.C., Canada, Paper No. 2016.

Symans, M. D. and Constantinou, M. C. (1999). "Semi-active control systems for seismic protection of structures: a state-of-the-art review." *Engineering Structures*, **21**: 469–487.

Symans, M. D., Charney, F. A., Whittaker, A. S., Constantinou, M. C. et al. (2008). "Energy dissipation systems for seismic applications: current practice and recent developments." *Journal of Structural Engineering*, **134**(1): 3–21.

Tsai, K. C., Chen, H. W., Hong, C. P. and Su, Y. F. (1993). "Design of steel triangular plate energy absorbers for seismic-resistant construction." *Earthquake Spectra*, **9**(3): 505–528.

Vail, C. Hubbell, J., O'connor, B., King, J. et al. (2004). "Seismic upgrade of the boeing commercial airplane factory at Everett, WA, USA." *In Proceeding, 13th World Conference on Earthquake Engineering,* Vancouver, B.C., Canada, Paper No. 3207.

Venter, G., (2010). "Review of optimisation techniques." *Encyclopaedia of Aerospace Engineering, John Wiley & Sons*, New York, NY.

Whittaker, A. S., Bertero, V. V., Thompson, C. L. and Alonso, L. J. (1991). "Seismic testing of steel plate energy dissipation devices." *Earthquake Spectra*, **7**(4): 563–604.

Zhang, R. and Soong, T. T. (1992). "Seismic design of viscoelastic dampers for structural applications." *Journal of Structural Engineering*, 118: 1375–1392.

Zhang, Z. and Balendra, T. (2013). "Passive control of bilinear hysteretic structures by tuned mass damper for narrow band seismic motions." *Engineering Structures,* **54**: 103–111.

# CHAPTER 2

# A Practical Method for Optimum Seismic Design of Friction Wall Dampers

## 2.1. ABSTRACT

Friction control systems have been widely used as one of the efficient and cost effective solutions to control structural damage during strong earthquakes. However, the height-wise distribution of slip loads can significantly affect the seismic performance of the strengthened frames. In this study, a practical design methodology is developed for more efficient design of friction wall dampers by performing extensive nonlinear dynamic analyses on 3, 5, 10, 15, and 20-storey RC frames subjected to eleven spectrum-compatible design earthquakes and five different slip load distribution patterns. The results show that a uniform cumulative distribution can provide considerably higher energy dissipation capacity than the commonly used uniform slip load pattern. It is also proved that for a set of design earthquakes, there is an optimum range for slip loads that is a function of number of storeys. Based on the results of this study, an empirical equation is proposed to calculate a more efficient slip load distribution of friction wall dampers for practical applications. The efficiency of the proposed method is demonstrated through several design examples.

## 2.2. INTRODUCTION

Much of the existing building structures in developing countries are designed primarily to sustain gravity loads with little or no seismic detailing. Many catastrophic failures in RC buildings during recent major earthquakes (e.g. Kashmir, 2005; China, 2008; Indonesia, 2009; Haiti, 2010; Turkey, 2011; Nepal, 2015) have highlighted the urgent need to improve

*Earthquake Spectra, Volume 33, Issue 3, August 2017, Pages 1033–1052*

the seismic performance of these substandard buildings. Passive energy dissipation devices have been proven as one of the most efficient and cost effective solutions in terms of controlling structural damage during strong earthquakes by dissipating the imparted seismic energy and reducing damage in structural elements (Symans et al., 2008; Soong and Costantinou, 2014). Among the different types of passive energy dissipation devices, friction-based dampers usually have the highest energy dissipation capacity for the same levels of force and deformation (Pall and Pall, 2004). Moreover, friction devices are in general velocity and temperature-independent, can be easily tuned to the characteristics of the structure, and provide sustained performance under large number of cycles (Grigorian et al., 1993; Aiken et al., 1993; Pall and Pall, 2004).

Pall and Marsh (1982) introduced the first generation of friction dampers for braced steel frames, which were designed to slip under a predetermined load before the buckling of the braces occurred. Wu et al. (2005) developed an improved model of Pall friction dampers using a T-shaped core plate, which was easier to manufacture and assembly. Slotted Bolted Connections (SBC) were initially used by Fitzgerald (1989) to dissipate earthquake input energy and prevent buckling of brace elements in steel braced frames. The energy absorbing mechanism in SBCs is based on the friction between the gusset plates and the sliding channels. More recently, shear slotted bolted connections (SSBC) were proposed to extend the application of SBC in members with shear-dominated behaviour (Nikoukalam et al., 2015).

While most of existing friction-based dampers were developed for steel bracing systems, using brace elements in RC frames can lead to high stress concentration and damage in the connection zones. This problem can be addressed by using wall-type systems that provide enough space to transfer lateral forces to the adjacent elements. Sasani and Popov (1997) experimentally and analytically investigated the performance of a wall-type friction damper using lightweight concrete panels. Their proposed system consisted of a precast concrete wall which was connected to the lower floor beam by bolted supports and to the upper floor beam by friction energy dissipating connectors. In a follow up study, they increased the efficiency of their proposed system by using epoxy-anchored bolts to provide adequate strength and stiffness at the base supports to minimise the rocking movement of the wall panels during strong earthquakes (Sasani and Popov, 2001). Petkovski and Waldron (2003) studied the effectiveness of friction-based concrete wall dampers (with and without opening) to improve the seismic performance of 6, 8 and 10-storey RC structures subjected to four real earthquake records. They concluded that, irrespective of the stiffness of the wall panels, there was an optimum range for the slip force in the friction connections that led to the best

seismic performance. Although their proposed friction wall dampers were designed not to transfer additional shear forces to the adjacent columns, the results of their study showed that they still considerably increase the base shear and the axial loads of the columns. However, these adverse effects can be controlled by limiting the slip forces in the friction dampers as it will be discussed in this study. A similar wall friction damper was proposed by Cho and Kwon (2004), incorporated an RC wall connected to the upper floor beam using a T-shape steel device with Teflon sliding sheets. In their system, the clamping force could be easily adjusted based on the expected earthquake magnitude using an oil jack loading system.

While several research studies have covered the optimum design of viscous and viscoelastic dampers (e.g. Park et al., 2004; Levy and Lavan, 2006; Takewaki, 2011; Whittle et al., 2012; Adachi et al., 2013, Sonmez et al., 2013), very limited studies are focused on the optimisation of friction-based dampers subjected to seismic actions. In one of the early attempts, Filiatrault and Cherry (1990) proposed a simplified seismic design procedure to obtain the optimum slip load values by minimizing an energy derivation parameter denoted as relative performance index (RPI). It was shown that the optimum slip load values depend more on the amplitude and frequency of the design earthquake rather than the structural characteristics. Subsequently, Moreschi and Singh (2003) used Genetic Algorithm (GA) to determine the optimum height-wise placement of yielding metallic and friction dampers in braced steel frames. Patro and Sinha (2010) investigated the seismic performance of shear-frame building structures with dry-friction devices, using uniform height-wise slip load distribution. They showed that, in general, a suitable slip load range can be determined such that the seismic response of the structure is nearly optimal for a wide range of ground motion characteristics. Fallah and Honarparast (2013) optimised the slip load distribution and placement of Pall friction dampers in multi-storey shear braced frame using a non-dominated sorting genetic algorithm (NSGA-II). In a more recent study, Miguel et al. (2016) adopted a backtracking search optimisation algorithm to simultaneously optimise the location and slip load distribution of friction dampers subjected to seismic loading.

It should be noted that most of the above mentioned optimisation techniques may not be suitable for practical design purposes due to the high computational efforts required to analyse a large number of non-linear dynamic systems. This study aims to develop, for the first time, a practical method for more efficient design of friction-based wall dampers under earthquake loads without using complex optimisation techniques. To obtain the best slip load distribution along the height of the building, extensive nonlinear dynamic analyses are conducted on 3, 5, 10, 15, and 20-storey RC frames subjected to a set of earthquake records

representing a design spectrum. The results are then used to develop an empirical design equation, which leads to design solutions with maximum energy dissipation in the friction wall dampers. The efficiency of the proposed equation is demonstrated through several design examples.

## 2.3. MODELING AND ASSUMPTIONS

### 2.3.1. Reference Frames

In this study 3, 5, 10, 15 and 20-storey RC frames were selected with the typical geometry shown in Fig. 2.1. The frames were assumed to be located on a soil type D of the IBC (2015) category, with the design spectral response acceleration at short periods and 1-sec period equal to 0.40g and 0.64g, respectively. To represent substandard RC structures, the frames were designed based on the low-to-medium seismicity regions using a design earthquake with PGA of 0.2g. The uniformly distributed dead and live loads were assumed as 6 kN/m$^2$ and 2 kN/m$^2$ for interior storeys, and 5 kN/m$^2$ and 1.5 kN/m$^2$ for the roof level. The frames were designed to support the seismic loads based on IBC (2015) and ASCE/SEI 7-10 (2010) and in accordance with the minimum requirements of ACI 318 (2014) for RC frames with intermediate ductility. The concrete compressive strength ($f_c'$) and the yield strength of steel reinforcement bars ($f_y$) were assumed to be 35 and 400 Mpa, respectively. Square and rectangular sections were used for column and beam elements as shown in Fig. 2.1 for the 10-storey frame.

To predict the seismic response of the RC frames, nonlinear time-history analyses were carried out using computer program DRAIN-2DX (Prakash et al. 1993). Rayleigh damping model with a constant damping ratio of 0.05 was assigned to the first mode and to any mode at which the cumulative mass participation exceeded 95%. Nonlinear moment-rotation (M-θ) and axial-moment (P-M) plastic hinges were assigned at both ends of RC beam and column elements, respectively, using element Type 2 in DRAIN-2DX. The friction mechanism at the top edge of the panel was modelled by means of an inelastic link element (element Type 4 in DRAIN-2DX) to provide an ideal Coulomb friction hysteretic behaviour. In this study, it was assumed that the strength of the concrete wall panel is always greater than the effects of the maximum slip load of the friction device. Therefore, the wall panels were modelled with elastic panel elements (15 cm thickness) using element Type 6 in DRAIN-2DX. To consider rigid diaphragms in the analytical models, the frames nodes were constrained to each other in horizontal direction.

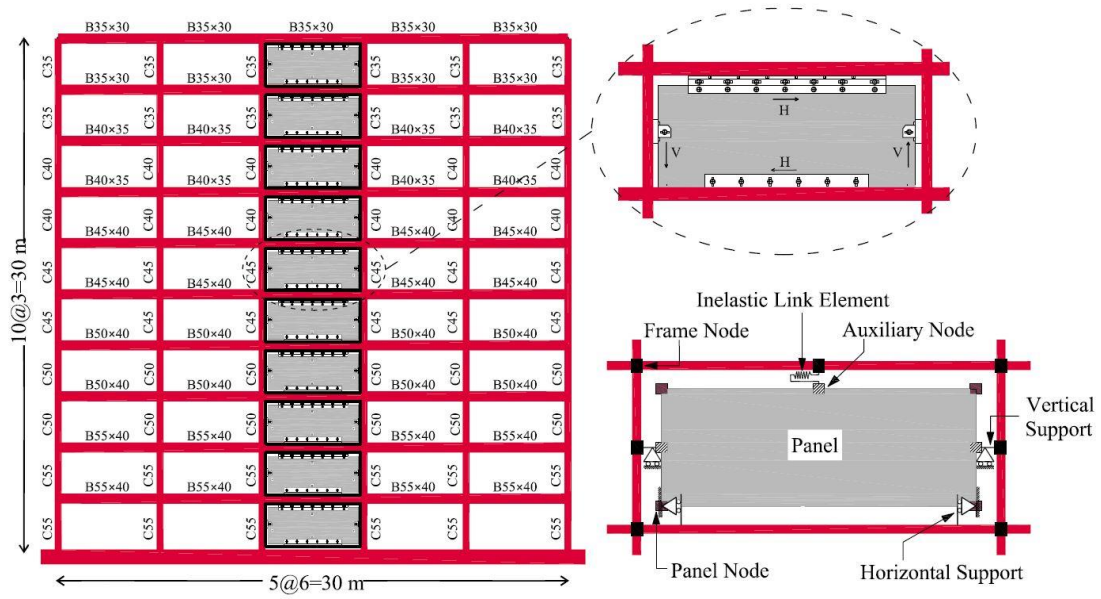


**Fig. 2.1.** Schematic geometry of the reference RC frames and the analytical model of the studied friction-based wall dampers

### 2.3.2. Proposed Friction-Based Wall Damper

The friction-based wall damper used in this study consists of a structural concrete panel that is connected to the frame by using two vertical supports in the sides, one horizontal connection at the bottom, and a friction device at the top. Fig. 2.2 illustrates the details of the proposed friction panel. The vertical support for the concrete panel is provided by using panel-to-column connections with horizontal slots, which prevent transfer of shear forces to the columns. The panel is connected to the lower floor by horizontally fixed connections with vertical slots to avoid transferring shear forces to the beams. This arrangement will ensure that the displacement of the friction device at the top of the panel is equal to the inter-storey drift at each level. The proposed friction device is a simple panel-to-frame Slotted Bolted Connection, which consists of two steel plates bolted at the top of the panel (external plates) clamped together over a slotted stainless steel plate anchored to the top beam (central plate). The friction mechanism is obtained through friction between the central stainless steel plate and the two brass plates (see Fig. 2.2 (b)). Extensive experimental tests conducted by Grigorian et al. (1993) demonstrated the reliable hysteretic behaviour of this type of friction device under sinusoidal and simulated seismic imposed displacements.

By using over-sized holes in the central steel plate (as shown in Fig. 2.2), the largest friction forces will occur between the central and the brass plates. The size of these holes in the horizontal and vertical directions can be calculated to accommodate the expected maximum lateral drift and vertical deformations of the beam, which would prevent transfer of large

stresses on the central plate around the slotted holes. The concentrated moments applied to the columns at the location of the connections should be considered in the design process of the proposed friction wall system. The results of this study indicate that these additional loads are relatively low compared to the maximum bending moments in the corresponding bare frame.

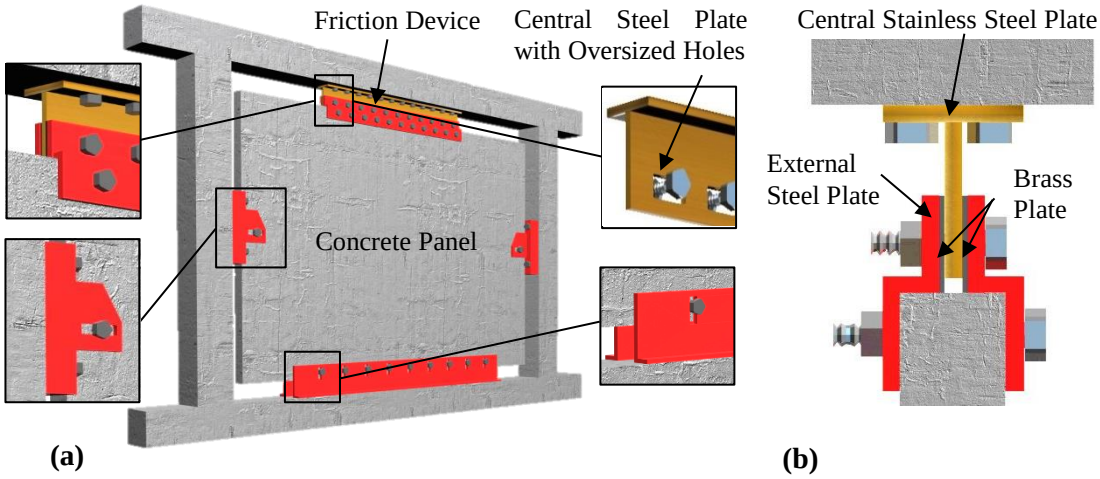


**Fig. 2.2.** Schematic view of the (a) proposed friction wall damper, (b) friction device

### 2.3.3. Slip Load Distribution Patterns

The slip force in the friction connections of the proposed wall damper can be adjusted and tuned independently for each storey by controlling the clamping forces of the bolts. Such capability provides the possibility of using the same connection with different (optimised) slip loads. Wall dampers with very low slip loads (i.e. $F_s \cong 0$) do not have any lateral load resistance and, therefore, are not considered as structural elements. On the contrary, using large slip load values may lead to a connection lock-up under design earthquakes, which implies the passive control system behaves as a fixed wall panel with negligible energy dissipation capacity. In practical applications, a uniform height-wise slip load distribution is usually employed for design of passive friction dampers. However, this may not necessarily lead to an optimum design solution for a range of structures and design earthquakes.

To identify more efficient slip load distributions, five different distribution patterns are considered: (1) uniform, (2) uniform cumulative, (3) triangular cumulative, (4) inverted triangular cumulative and (5) a distribution proportional to the storey shear strengths. Fig. 2.3 shows the different slip load distribution patterns, scaled to produce the same base shear in first mode response (i.e. $\Sigma F_s$=constant). The shear strength of each storey ($F_{y,i}$) can be calculated from a non-linear pushover analysis (Hajirasouliha and Doostan, 2010).

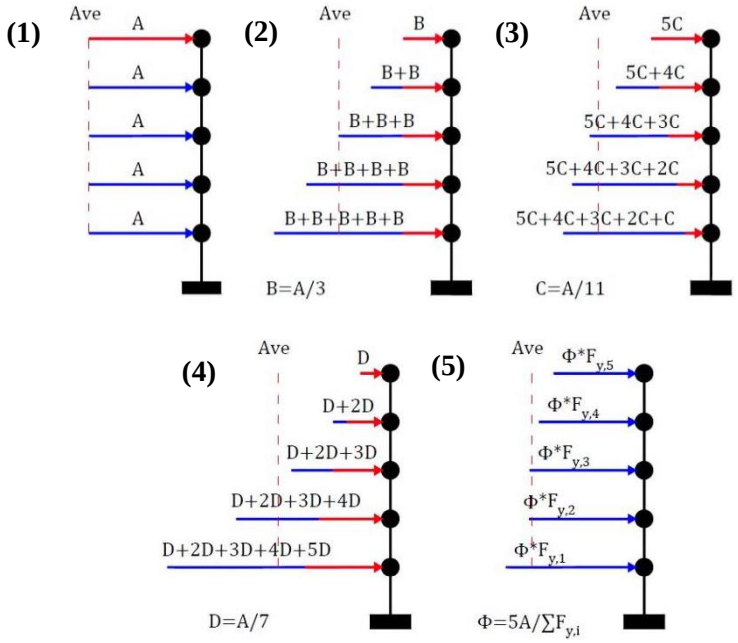


**Fig. 2.3.** Typical patterns of the selected slip load distributions with the same average value

### 2.3.4. Selected Seismic Excitations

The reference structures are subjected to six real strong ground motions selected from the Pacific Earthquake Engineering Research Center online database (PEER, 2016) including: Cape Mendocino 1992, Duzce 1999, Superstition Hills 1987, Imperial Valley 1979, Loma Prieta 1989, and Northridge 1994. The characteristics of the selected records are listed in Table 2.1. All of these ground motions correspond to soil class D of IBC-2015 and are recorded in low to moderate distances from the epicentre (less than 45 km) with high local magnitudes (i.e. M>6.5). Fig. 2.4 illustrates the 5% damped elastic acceleration response spectra of the six natural earthquake records in Table 2.1. It is shown that, on average, the selected ground motions provide a close approximation to the design response spectra of IBC-2015 for the site class D in high seismic zones (i.e. PGA=0.4g). This is particularly evident at the first mode periods of the bare frames denoted as Tb3 to Tb20. Therefore, in this study these earthquake records are used directly without being normalised. A set of five synthetic earthquake records with a PGA of 0.4 g is also generated using SIMQKE program (Vanmarke, 1976) to be compatible with the soil type D of IBC (2015) elastic design spectrum.

**Table 2.1.** Characteristics of the selected seismic excitation records

| *No.* | *Earthquake Name* | *M* | *Record* | *Duration (s)* | *PGA (g)* | *PGV (Cm/s)* | *PGD (Cm)* |
|---|---|---|---|---|---|---|---|
| 1 | 1992 Cape Mendocino | 6.9 | CAPEMEND/PET000 | 36 | 0.590 | 48.4 | 21.74 |
| 2 | 1999 Duzce, Turkey | 7.2 | DUZCE/DZC270 | 26 | 0.535 | 83.5 | 51.59 |
| 3 | 1987 Superstition Hills | 6.7 | SUPERST/B-ICC000 | 60 | 0.358 | 46.4 | 17.50 |
| 4 | 1979 Imperial Valley | 6.5 | IMPVALL/H-E04140 | 39 | 0.485 | 37.4 | 20.23 |
| 5 | 1989 Loma Prieta | 6.9 | LOMAP/G03000 | 40 | 0.555 | 35.7 | 8.21 |
| 6 | 1994 Northridge | 6.7 | NORTHR/NWH360 | 40 | 0.590 | 97.2 | 38.05 |

To simulate non-stationary spatially variable ground motions, a trapezoidal intensity envelope function with the rise time, level time and total duration of 2.5, 12 and 35 sec, respectively, was applied. Fig. 2.4 demonstrates a good compatibility between the average spectrum of the synthetic earthquakes and the IBC (2015) design spectrum. Therefore, these synthetic earthquakes can be considered to be good representatives of the design response spectrum.

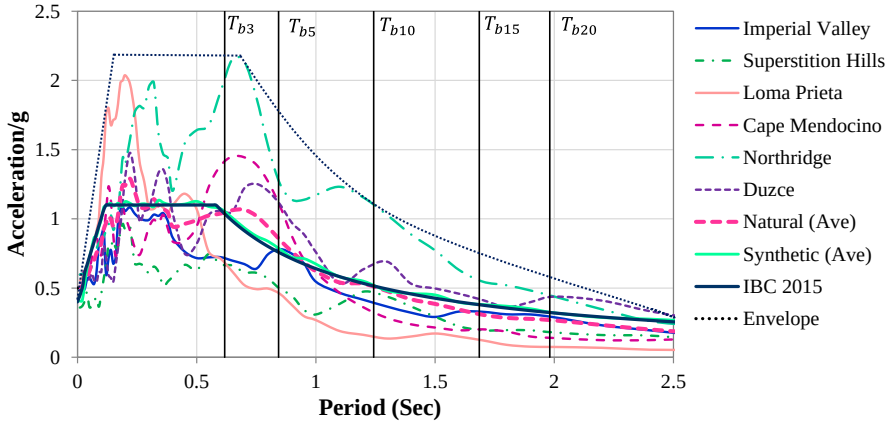


**Fig. 2.4.** Comparison between elastic spectral acceleration of the six selected earthquakes, average of five synthetic earthquakes and IBC-2015 design spectrum for soil type D, 5% damping ratio. $Tb_3$ to $Tb_{20}$ are first mode periods of the bare frames

## 2.4. RC FRAMES WITH FRICTION-BASED WALL DAMPERS

To investigate the efficiency of the proposed passive-control system, a wide range of slip load values and height-wise distribution patterns are considered, aiming to cover all practical design solutions. Different structural performance parameters such as maximum inter-storey drift, roof displacement, maximum axial load in columns, base shear, and cumulative energy dissipation are calculated. For comparison purposes, the slip load ratio $F_{SR}$ is defined as:

$$F_{SR} = \frac{\sum_{i=1}^{n} F_{s,i}}{\sum_{i=1}^{n} F_{y,i}} \tag{2.1}$$

where $n$ is number of storeys, $F_{s,i}$ is slip force at $i^{th}$ storey, and $F_{y,i}$ is storey shear strength of the $i^{th}$ storey. Using this parameter helps to compare the effects of using different slip load distributions, while the base shear force remains constant.

### 2.4.1. Maximum Inter-storey Drift

Maximum inter-storey drift is widely used to evaluate the level of damage to both structural and non-structural elements in RC structures (Hajirasouliha et al., 2012). Fig. 2.5 shows the variation of maximum inter-storey drift ratios (normalised to the bare frames) for 5, 10, 15 and 20-storey frames using five different slip load distribution patterns with a wide range of slip load ratios $F_{SR}$. The results are the average of the displacement demands obtained in the six selected earthquakes listed in Table 2.1. The energy dissipation capacity of wall panels with very small $F_{SR}$ values is negligible, and therefore, their response is close to that of bare frames (normalised response parameters are close to 1.0). Fig. 2.5 demonstrates a similar trend for different slip load patterns, where the maximum drift ratios generally reduce by increasing the friction slip load ratios up to a certain limit. This is followed by a constant trend in 3 and 5-storey and an ascending trend in 10, 15 and 20-storey frames.

The results in Fig. 2.5 indicate that there is an optimum range for slip load ratios that, on average, leads to lower inter-storey drifts. Similar conclusions have been reported by Petkovski and Waldron (2003) and Fallah and Honarparast (2013) for other types of friction dampers. Fig. 2.5 shows that by using friction wall dampers with more efficient slip load distributions, the maximum inter-storey drift of 3, 5, 10, 15, and 20-storey frames reduced by up to 85%, 75%, 38%, 40%, and 30%, respectively. This implies that the reduction in maximum drift ratio is more prominent in low rise buildings. While the inverted triangular cumulative slip load distribution (Type 4 in Fig. 2.3) seems to be less effective in reducing maximum inter-storey drifts, other distribution patterns lead to similar levels of reduction.

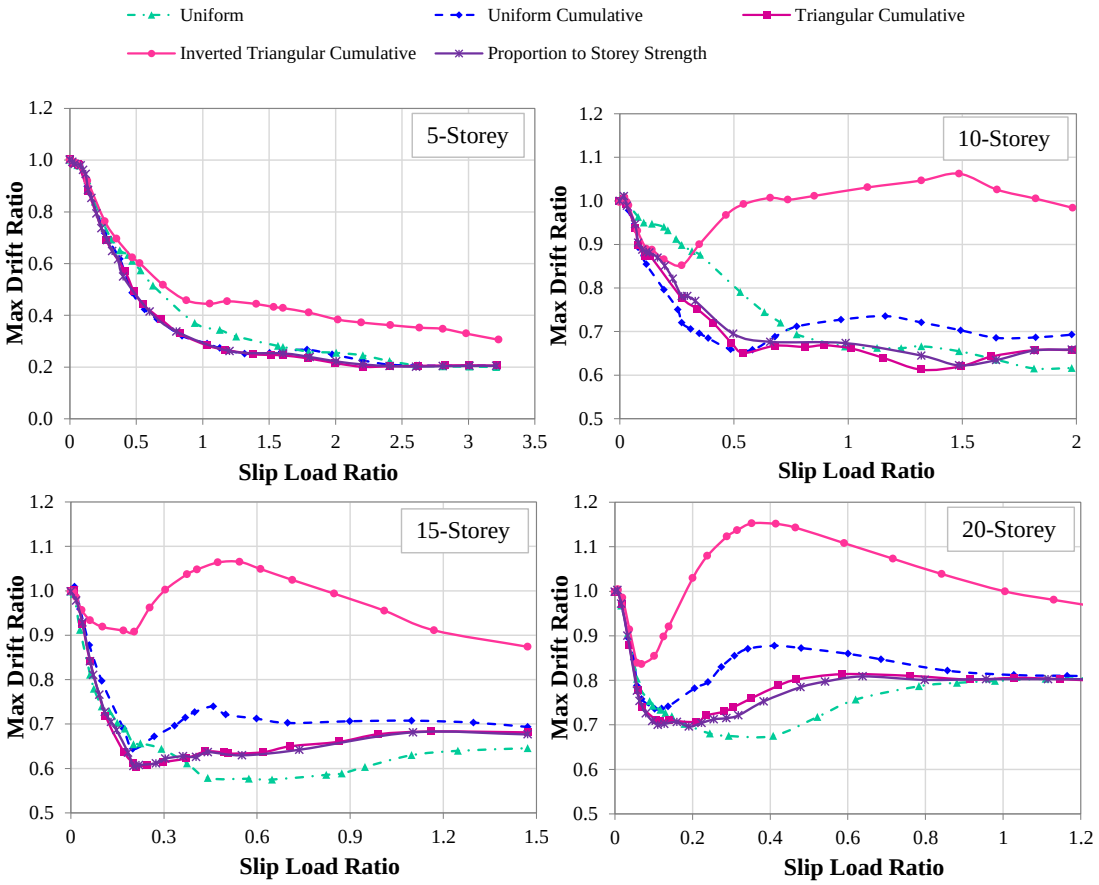


**Fig. 2.5.** Variation of maximum inter-storey drift for 5, 10, 15 and 20-storey RC frames using different slip load distributions, average of the six selected earthquakes

### 2.4.2. Column Axial Load

Figs. 2.6 (a and b) display the maximum axial load ratios (normalised to the bare frames) of the columns connected to the friction wall dampers in 10 and 20-storey frames using different slip load ratios. The results show that, regardless of the selected slip load distribution pattern, the maximum axial load in the columns increases by increasing the slip load ratios up to a steady-state level (see Fig. 2.6 (b)). At this stage, the wall dampers are locked at all storey levels, which is referred to as "fixed-wall" in this study. As expected, increasing slip load ratios beyond this limit does not affect the seismic performance of the frames. It is shown that, for the same slip load ratio, using uniform distribution (Type 1 in Fig. 2.3) results in lower axial loads compared to other slip load distributions. However, for practical design purposes, it is important to obtain slip load ratios that control the lateral displacement demands of the structure without imposing high axial loads to the columns and foundations. Fig. 2.7 (a and b) compare the maximum column axial load ratio for different slip load distributions as a function of maximum inter-storey drift. The results in general indicate that, for a specific inter-storey drift, using a uniform cumulative distribution (Type 2

in Fig. 2.3) leads to minimum axial loads compared to other slip load distributions. A similar trend was observed for the other frames with different number of storeys.

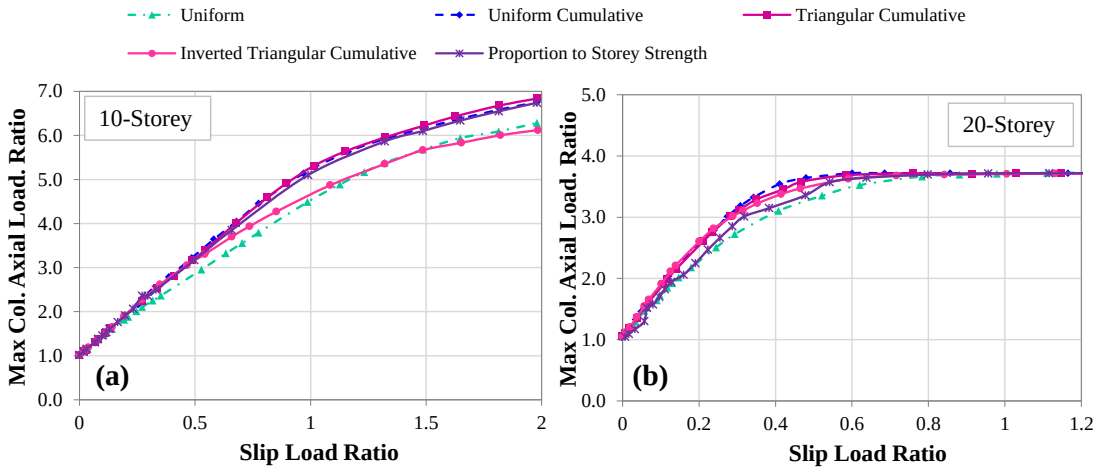


**Fig. 2.6.** Variation of maximum column axial load ratio as a function of slip load ratio for (a) 10- and (b) 20-storey frame, average of the six selected earthquakes

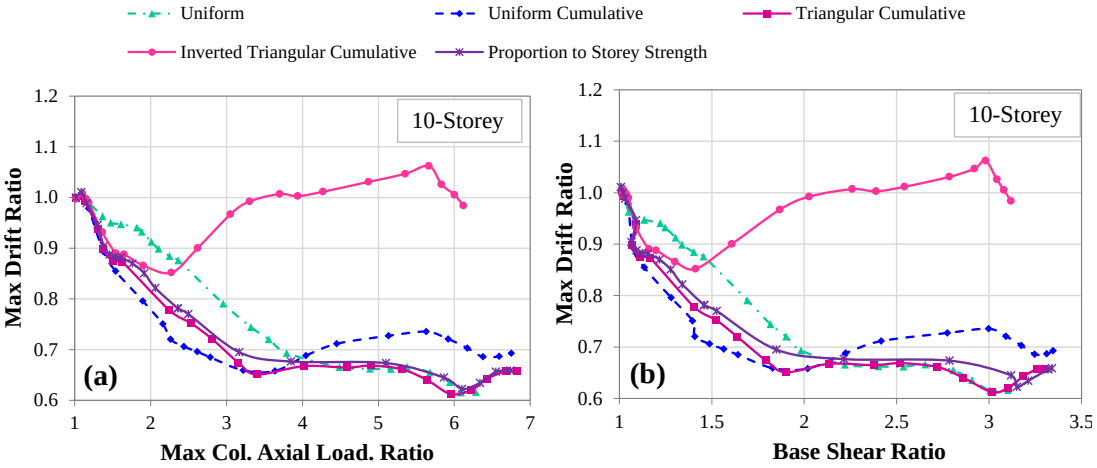


**Fig. 2.7.** Variation of maximum drift ratio as a function of (a) column axial load and (b) base shear ratio for 10-storey frame, average of the six selected earthquakes

### 2.4.3. Base Shear

Increasing the base shear demand is one of the main barriers to the use of passive control systems such as shear walls and bracings. Although the proposed friction wall damper increases the base shear demand of the bare frame, this increase can be efficiently controlled by using appropriate slip loads in friction devices. For example, Figs. 2.8 (a) and (b) compare the maximum column shear force and the base shear ratios of 10-storey frames with different slip load distributions as a function of the slip load ratio, respectively. The results show that increasing the slip loads is always accompanied by an increase of the base shear until a maximum level is reached. For similar slip load ratios, using uniform slip load

distribution leads to lower base shear when compared with other distribution patterns. However, for the same inter-storey drift ratios, uniform cumulative slip load distribution in general leads to lower base shear values compared to the other distribution patterns (see Fig. 2.7 (b)).

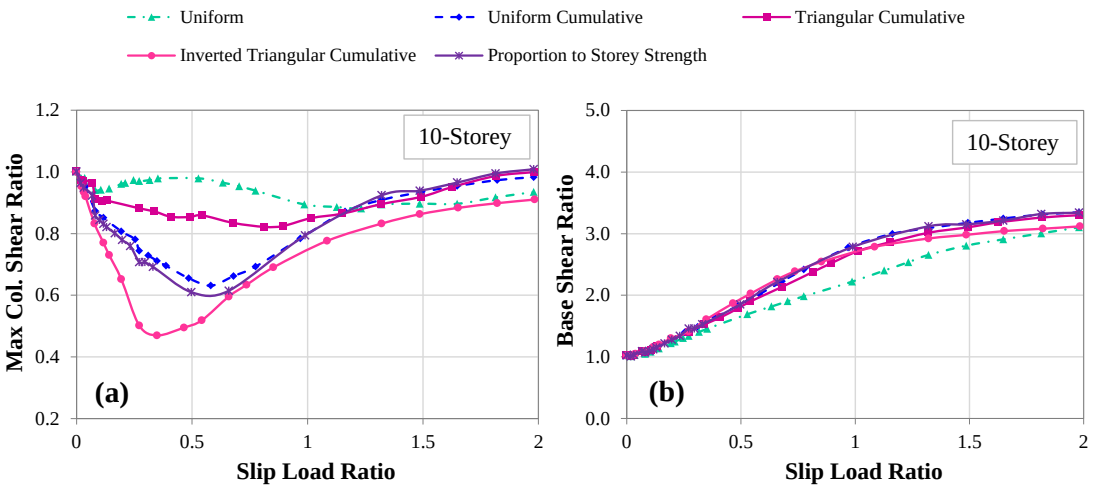


**Fig. 2.8.** Variation of: (a) maximum column shear force ratio, and (b) base shear ratio as functions of slip load ratio, 10-storey frame, average of the six selected earthquakes

It should be noted that the proposed friction wall damper is capable of transferring some of the base shear forces directly to the foundation at the ground floor. Therefore, despite increasing the total base shear, the proposed wall dampers can generally reduce the maximum shear forces in the columns at the base of the structure. For instance, the results in Fig. 2.8 (a) indicates that unlike the base shear, increasing the slip load ratio is usually accompanied by a decrease in the maximum column shear forces until a minimum value is reached.

The most reduction in the maximum column shear forces was observed in the frame with the inverted triangular cumulative pattern (Type 4 in Fig. 2.3). The main reason is that, for the same average slip load, the inverted triangular pattern has larger slip load values at the ground floor. This implies that the friction wall system can transfer higher shear forces directly to the foundation, which reduces the maximum shear forces at the columns.

### 2.4.4. Energy Dissipation Capacity

In this study, $R_{w1}$ is defined as the ratio of the deformation work of structural elements in the structure with friction wall dampers ($W_{cs}$) to that in the corresponding bare frame ($W_{bf}$):

$$R_{w1} = \frac{W_{cs}}{W_{bf}} = \frac{(W_{sb} + W_{sc})_{cs}}{(W_{sb} + W_{sc})_{bf}} \tag{2.2}$$

where $W_{sb}$ and $W_{sc}$ denote the static work of the beam and column elements, respectively. $R_{w1}$ decreases by increasing the efficiency of the friction wall dampers in dissipating the earthquake input energy. Fig. 2.9 (a) shows the $R_{w1}$ as a function of the slip load ratio for 5, 10, 15 and 20-storey frames using different slip load distribution patterns. In general, $R_{w1}$ reaches a minimum value at a slip load ratio which is almost independent of the selected slip load distribution pattern. This implies that there is an optimum range for the slip load ratios that leads to the lowest deformation work (or structural damage) in the structural elements. The reduction in $R_{w1}$ is more evident in low- to medium-rise buildings. The results also indicate that the optimum slip force ratios decrease by increasing the number of storeys (from $F_{SR}$=1 in 3-storey to $F_{SR}$=0.15 in 20-storey frames). Also it can be noted that, in general, the optimum range narrows by increasing the number of storeys.

The amount of energy dissipated in the friction device under a design earthquake can be evaluated by calculating the ratio of the friction work in the wall dampers ($W_{sf}$) to the deformation work of the main structural elements ($W_{cs}$):

$$R_{w2} = \frac{(W_{sf})_{cs}}{(W_{sb} + W_{sc})_{cs}} \tag{2.3}$$

While $R_{w1}$ gives a measure of the efficiency of the dampers in reducing the energy dissipation demand of the structural elements, $R_{w2}$ represents the energy dissipation capacity of the dampers. The variation of $R_{w2}$ as a function of the slip load ratio is illustrated in Fig. 2.9 (b) for 3, 5, 10, 15 and 20-storey frames. The $R_{w2}$ parameter tends to zero for very low and very high slip forces. The reason is that the energy dissipated in the dampers with very low slip forces is negligible, while the dampers with very high slip forces are locked and hence do not dissipate any energy. The results indicate that the overall trend of $R_{w2}$ is similar for all the reference frames irrespective to the number of storeys. However, on average, by increasing the number of storeys the maximum $R_{w2}$ values are reached at lower slip load ratios.

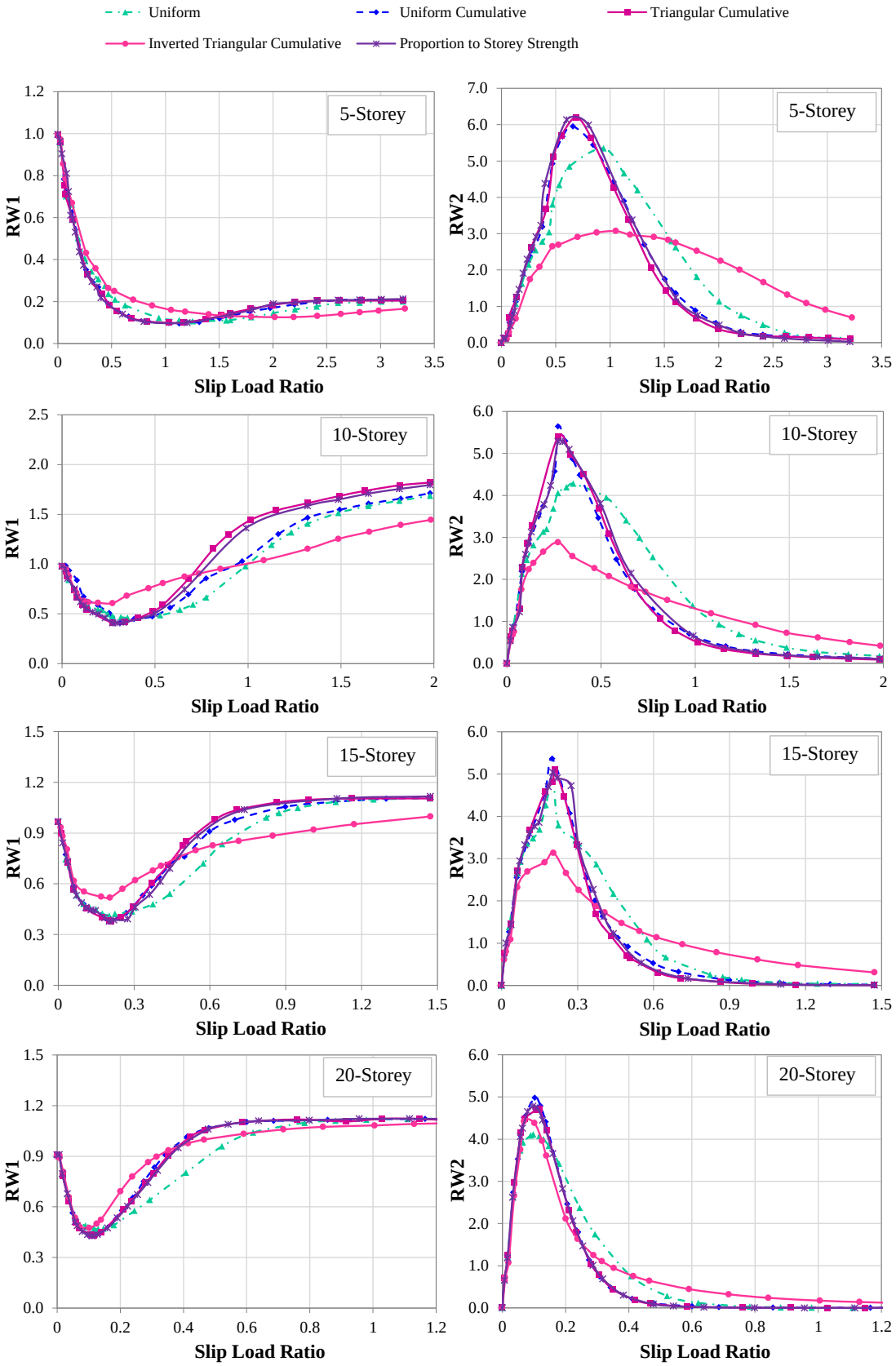


**Fig. 2.9.** Envelope of energy dissipation parameters (a) $R_{w1}$ and (b) $R_{w2}$ as a function of the slip load ratio, average of the six selected real earthquakes

It is evident that the uniform cumulative slip load pattern is usually the most effective pattern in terms of increasing the energy dissipation capacity of the friction-based wall dampers (except for the 3-storey frame), while the inverted triangular cumulative pattern is the least efficient. Based on the results in Fig. 2.9, the optimum range of the slip load ratios for 3, 5, 10, 15, and 20-storey frames with uniform cumulative slip load distribution is within 0.65-0.95, 0.55-0.85, 0.25-0.45, 0.10-0.30, and 0.05-0.15, respectively.

Fig. 2.10 shows the variation of energy dissipation parameter $R_{w2}$ as a function of the slip load ratio for the 10-storey and 20-storey frames subjected to the six selected real excitation records. It is evident that the amount of energy dissipated in the wall dampers is highly dependent on the input earthquake and the slip load ratio. However, the results show that the range in which the slip load ratio $R_{w2}$ reaches maximum (i.e. the best damper performance) is not significantly affected by the selected design earthquake. This conclusion was confirmed by the results for all the reference frames.

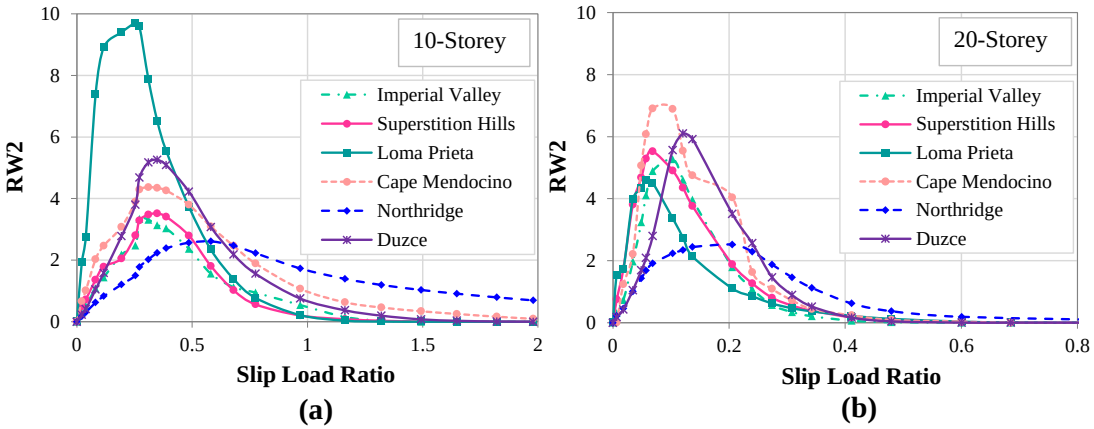


**Fig. 2.10.** Envelope of $R_{w2}$ energy dissipation parameter for (a) 10-storey frame, (b) 20-storey frame as a function of the slip load ratio, selected real earthquakes

## 2.5. A PRACTICAL DESIGN METHOD FOR FRICTION DAMPERS

Fig. 2.11 shows the optimum range of the slip load ratios obtained in the previous section as a function of number of storeys. The optimum design solutions for low rise buildings tend to a fixed wall system, while for high-rise buildings the best design solutions have lower average slip load ratios. The results of this study indicate that the optimum range of slip load ratio for RC frames with friction wall dampers is mainly a function of the number of storeys, and it is not considerably affected by the selected earthquake records if they match a similar design spectrum. Using the median values of the optimum slip load ranges and a regression

analysis, it is shown in Fig. 2.11 that the average value of the optimum slip load ratios can be represented by the following exponential function:

$$R = 1.12e^{-0.11n} \tag{2.4}$$

where $R$ is the most appropriate slip load ratio and $n$ is the number of storeys which is indirectly representative of the fundamental period of the structure. The slip load ratio $R$ calculated from Equation 2.4 is the ratio between the average of the slip loads with uniform cumulative distribution and the average of the storey shear strengths. Therefore, the following equation can be used to acquire the more efficient slip load values at each storey:

$$F_{s,i} = \frac{\sum F_{y,i} \times R}{n(n+1)/2} \times (n+1-i) = \frac{\sum F_{y,i} \times 1.12e^{-0.11n}}{n(n+1)/2} \times (n+1-i) \tag{2.5}$$

where $n$ is the number of storeys; and $F_{s,i}$ and $F_{y,i}$ are the slip load and the storey shear. It should be noted that Equation 2.4 is based on the models considered in this study, and the optimum range might change for structures with other dynamic characteristics or very different geometries (e.g. different storey heights).

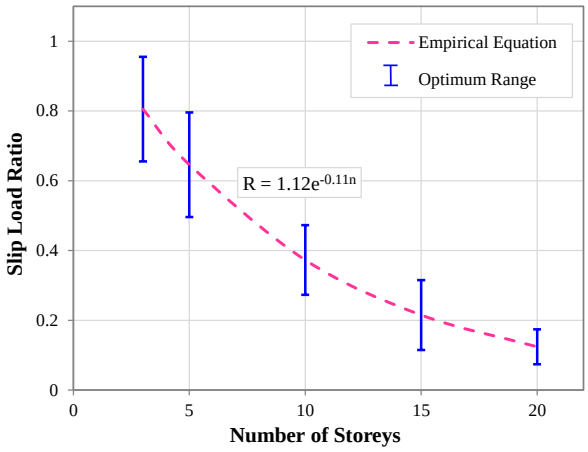


**Fig. 2.11.** Comparison between the empirical equation and the best analytical slip load range for frames with different number of storeys

## 2.6. EFFICIENCY OF THE PROPOSED DESIGN METHOD

The efficiency of the proposed equation to obtain more efficient design solutions is investigated for 3, 5, 10, 15, and 20-storey frames under a set of five design spectrum compatible synthetic earthquakes (see Fig. 2.4). For comparison purposes, the seismic performances of the frames with friction wall dampers designed using Equation 2.4 are

compared with those designed based on the uniform slip load distribution (i.e. conventional design) as well as the frames with fixed panel-to-frame connections. The more efficient slip load values at different storeys are calculated by using Equation 2.5. For a better comparison, the slip load values are scaled in the frames with uniform slip load distribution (without changing the distribution pattern) to have a similar average value in all design solutions.

Fig. 2.12 shows that, in general, the friction-based wall dampers designed with the proposed slip load distribution pattern provide better design solutions with lower maximum drift and roof displacement ratios compared to the conventionally designed wall dampers with uniform slip load distributions. This is especially evident for medium to high-rise buildings. As illustrated in Fig. 2.12, in some cases, using a fixed-wall system can lead to lower inter-storey drift and roof displacement demands compared to the frames with friction-based wall dampers. However, fixed-wall systems considerably increase the total base shear and also transfer excessive additional axial loads to the columns and foundation (Fig. 2.12 c and d).

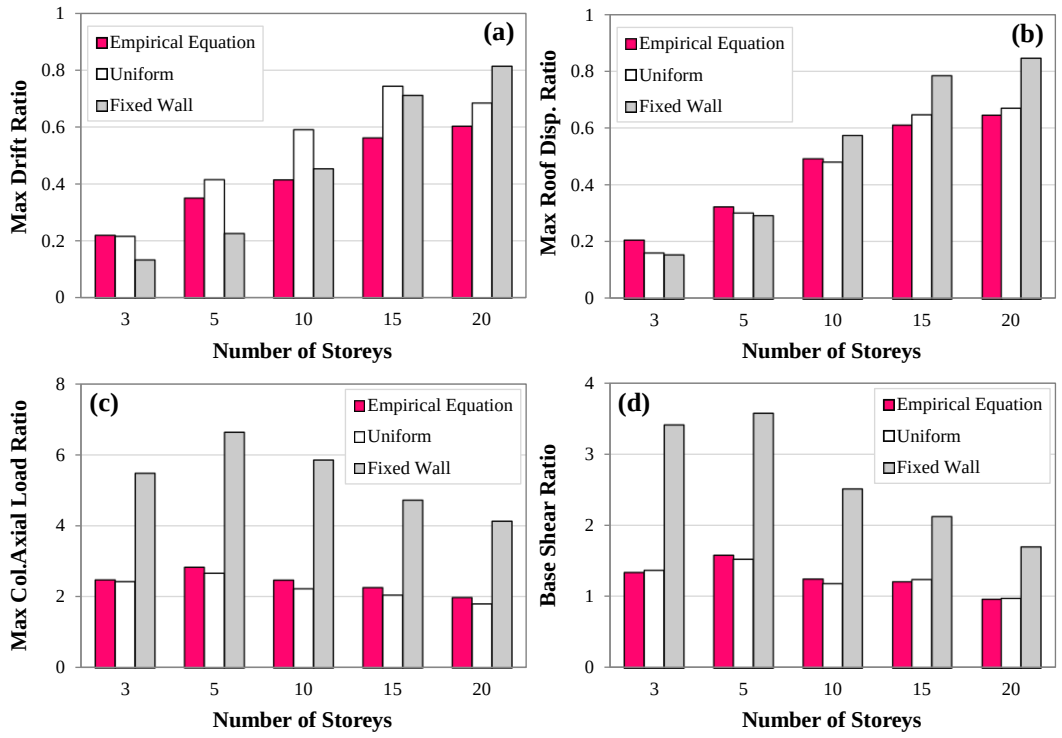


**Fig. 2.12.** The ratio of (a) maximum drift; (b) maximum roof displacement; (c) maximum column axial load; (d) maximum base shear to the bare frames, average of five synthetic earthquakes

To ensure that these added axial force demands are within the load bearing capacity of the columns, the moment-axial load interaction curves of the column sections are investigated. The example in Fig. 2.13 shows that the critical moment-axial load combinations (at the first

storey) in the 10 and 15-storey frames with fixed walls are generally beyond the load bearing capacity of the sections under the set of five synthetic spectrum-compatible earthquakes, while the friction wall dampers designed with the proposed methodology lead to acceptable design solutions. It can also be noted that fixed wall systems under seismic load will produce large tensile forces in the columns that can significantly reduce their moment resistance capacity.

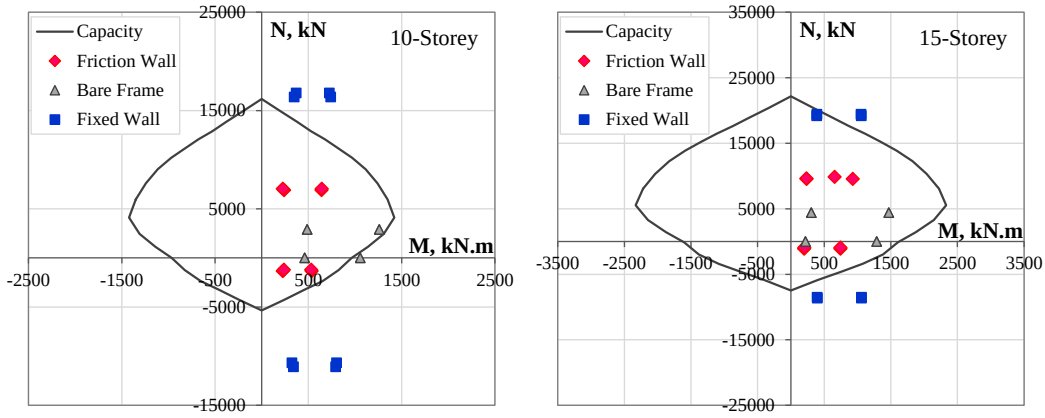


**Fig. 2.13.** Comparison of the 1st floor column axial load-moment interaction for the bare frames and the frames designed with the empirical equation and fixed wall, average of five synthetic earthquakes

In the case of friction walls designed using the proposed empirical equation the moment-axial load demands on the columns are all within the acceptable range. This is a result of the limits to the storey shear introduced by the friction connections. The results also indicate that the performance of the columns of the frames with more efficient design of friction walls can be better than those in the bare frames. The reason is that the increase in axial load of the columns in these frames is accompanied by a decrease in the maximum bending moments due to reduction of inter-storey drifts. Fig. 2.14 shows that the proposed slip load distributions in this study can lead to up to 61% higher energy dissipation capacity in the friction devices (i.e. higher $R_{w2}$ factor) and up to 40% lower energy dissipation demand in the structural elements (i.e. lower $R_{w1}$ factor) compared to the conventional solutions.

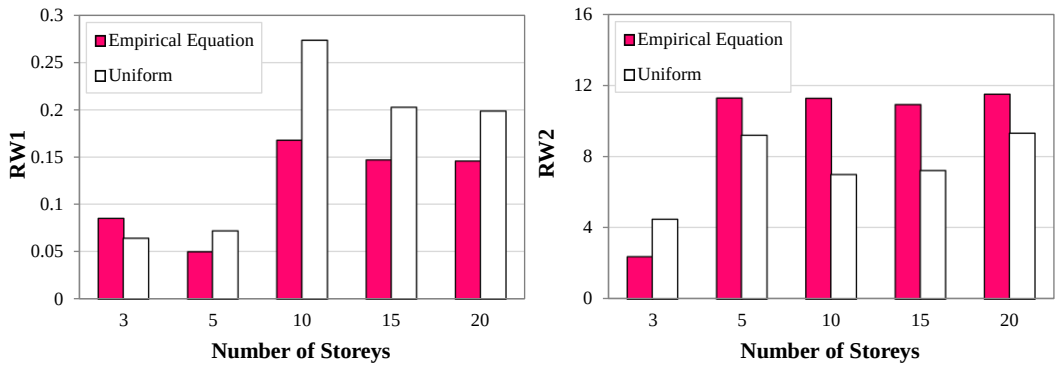


**Fig. 2.14.** Energy dissipation parameters $R_{w1}$ and $R_{w2}$ as a function of number of storeys, average of five synthetic earthquakes

## 2.7. GLOBAL DAMAGE INDEX

A linear cumulative damage model is used to calculate the overall damage index of the structure during seismic excitations by taking into account the changes in the energy dissipation capacity of the structure as a function of displacement demands (Miner, 1945; Teran-Gilmore and Jirsa, 2004). In this model it is assumed that the damage caused by plastic excursions are independent, while excursions are identified by using the Rainbow Counting Method suggested by Powell and Allahabadi (1987). In this study the inter-storey inelastic deformation is chosen as the basic damage quantity, and the cumulative damage index after N excursions of plastic deformation is calculated using the following equation:

$$DI_i = \sum_{j=1}^{N} \left(\frac{\delta_{pj}}{\delta_y}\right)^C \tag{2.6}$$

where $DI_i$ is the cumulative damage index at $i^{th}$ storey, ranging from 0 for undamaged to 1 for severely damaged storeys, $N$ is the total number of plastic excursions, $\delta_{pj}$ is the plastic displacement of the $j^{th}$ excursion, $\delta_y$ is the nominal yield deformation, and $c$ is a structural parameter which accounts for the stability of the hysteretic behaviour. In this study, $c$ is considered to be 1.5, as suggested by Cosenza and Manfredi (1996) for damage analysis of reinforced concrete structures.

The global damage index ($DI_g$) evaluates the damage of the whole structure by considering the weighted average of the storey damage indices. The following equation is used to calculate the global damage index of the structures:

$$DI_g = \frac{\sum_{i=1}^{n} DI_i W_{pi}}{\sum_{i=1}^{n} W_{pi}} \tag{2.7}$$

where $n$ is the number of storeys, $W_{pi}$ and $DI_i$ are the dissipated energy and the damage index of the $i^{th}$ storey, respectively.

In Fig. 2.15, the global damage indices of the bare frames under the set of five synthetic spectrum compatible earthquakes are compared with the frames with friction-based wall dampers designed using the proposed equation (Equation 2.5) and the uniform slip load distribution. In general the results indicate that friction-based dampers could significantly improve the seismic performance of the bare frames, especially for low to medium-rise buildings where the global damage index was reduced by up to 91%. Fig. 2.15 (a) shows that friction dampers designed with the proposed equation could reduce the global damage index of the 3, 5, 10, 15 and 20-storey frames by 45%, 19%, 43%, 50% and 26%, respectively, compared to conventionally designed dampers.

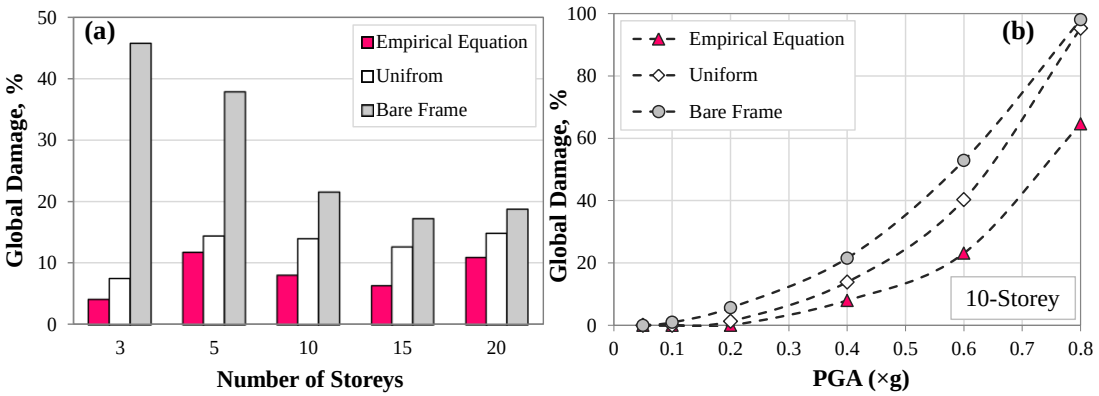


**Fig. 2.15.** Global damage index of (a) the bare frames compared to the frames with friction-based wall dampers designed using the proposed equation and uniform distribution and (b) the 10-storey frame under different earthquake PGA scale factor, average of five synthetic earthquakes

The efficiency of the proposed optimisation method is also investigated for different earthquake intensity levels. Fig. 2.15 (b) compares the global damage index ($DI_g$) of the 10-storey bare frame with the frames with friction wall dampers designed using Equation 2.5 and uniform slip load distributions subjected to the set of five synthetic earthquakes with PGA levels ranging from 0.05 to 0.8 g. It is shown that on average the friction wall dampers with the slip load distribution suggested in this study always exhibit less global damage compared to the frames with conventional friction walls at all PGA levels. The results in Fig. 2.15 (b) imply that the effectiveness of the wall dampers with a uniform slip load

distribution was considerably reduced at higher earthquake intensity levels (e.g. PGA> 0.6 g). This is because using equal slip loads at all storey levels led to a non-uniform distribution of lateral displacement demands and consequently high local damage concentrated at some of the storeys (i.e. soft storey failure), while the proposed slip load distribution resulted in a more uniform distribution of storey damage.

Although in general the seismic performance of friction wall dampers depends on the frequency content of the input earthquake, number of storeys and the earthquake intensity, the outcomes of this study demonstrate that the dampers designed with the proposed method consistently outperform those designed with uniform distribution of slip forces.

## 2.8. SUMMARY AND CONCLUSIONS

In this study, the efficiency of a friction-based wall system was investigated by extensive nonlinear dynamic analyses on 3, 5, 10, 15, and 20-storey RC frames subjected to six real and a set of five synthetic design spectrum-compatible earthquakes. To obtain the most efficient height-wise slip load distribution, five different distribution patterns were investigated, including uniform, uniform cumulative, triangular cumulative, inverted triangular cumulative and a distribution proportional to the storey shear strengths. Based on the results presented in this paper, the following conclusions can be drawn:

- Uniform cumulative slip load distribution is usually the most effective pattern in terms of increasing the energy dissipation capacity of the friction-based wall dampers. However, irrespective to the slip load distributions, there is always an optimum range for the slip load ratios (normalised to the storey shear strength) that leads to minimum displacement demands under design compatible earthquakes. For slip load ratios lower than the optimum value, the effectiveness of the dampers can be limited due to the small energy dissipation in the friction devices. Larger slip force ratios, however, may lead to connection lock-ups resulting in a linear elastic response with large dynamic magnification and low energy dissipation. The results show that the optimum range of the slip loads exponentially decreases with the increase of the number of storeys.

- Based on the results of this study, an empirical equation was proposed to calculate a more efficient slip load distribution for seismic strengthening/design of RC structures with different number of storeys. The friction wall systems designed based on the proposed equation was shown to result in lower displacement demands (by up to 30%)

and higher energy dissipation capacities (by up to 61%), compared to the conventional systems with a uniform slip load distribution.

- It was shown that friction wall dampers designed with the proposed equation can significantly reduce the displacement demands of the bare frames without large increase in base shear. Although friction wall dampers impose additional axial loads to the adjacent columns, it was shown that by using the proposed design method the axial loads generally remain within the capacity of the column sections. However, if fixed panels are added to the bare frame (as a retrofit measure) the maximum axial loads can be well beyond the maximum capacity of the columns.

- The results of nonlinear incremental dynamic analyses show that the friction dampers designed with the proposed empirical equation can reduce the global damage index of the RC frames with conventionally designed dampers by up to 43%. While the efficiency of the wall dampers with a uniform slip load distribution was considerably reduced at higher earthquake intensity levels, the suggested design solutions were efficient at all PGA levels.

## REFERENCES

ACI 318-14 (2014). "Building Code Requirements for Structural Concrete and Commentary on Building Code Requirements for Structural Concrete (ACI 318R-14)." *American Concrete Institute*, Farmington Hills, MI.

Adachi, F., Yoshitomi, S., Tsuji, M. and Takewaki, I. (2013). "Nonlinear optimal oil damper design in seismically controlled multi-storey building frame." *Soil Dynamics and Earthquake Engineering*, **44**: 1–13.

Aiken, I. D. Nims, D. K., Whittaker, A. S. and Kelly, J. M. (1993). "Testing of passive energy dissipation systems." *Earthquake Spectra* **9**(3): 335–370.

ASCE/SEI Standard 7-10 (2010), "Minimum Design Loads for Buildings and Other Structures." *American Society of Civil Engineers*, Reston, Virginia.

Cho, C. G. and Kwon, M. (2004). "Development and modelling of a frictional wall damper and its applications in reinforced concrete frame structures." *Earthquake Engineering and Structural Dynamic,s* **33**, 821–838.

Cosenza, E. and Manfredi, G. (1996). "Seismic design based on low cycle fatigue criteria." *In Proceedings: 11th World Conference on Earthquake Engineering,* Acapulco, Mexico. Paper No. 1141.

Fallah, N. and Honarparast, S. (2013). "NSGA-II based multi-objective optimisation in design of Pall friction dampers." *Journal of Constructional Steel Research,* **89**, 75–85.

Filiatrault, A. and Cherry, S. (1990). "Seismic design spectra for friction-damped structures." *Journal of Structural Engineering*, **116(**5): 1334–1355.

FitzGerald, T. F., Anagnos, T. and Goodson, M., Zsutty, T. (1989). "Slotted bolted connections in aseismic design for concentrically braced connections." *Earthquake Spectra,* **5**: 383–391.

Grigorian, C.E., Yang, T.S. and Popov, E. P. (1993). "Slotted bolted connection energy dissipators." *Earthquake Spectra,* **9**(3): 491–504.

Hajirasouliha, I. and Doostan, A. (2010). "A simplified model for seismic response prediction of concentrically braced frames." *Advances in Engineering Software*, **41**(3): 497–505.

Hajirasouliha, I., Asadi, P. and Pilakoutas, K. (2012). "An efficient performance-based seismic design method for reinforced concrete frames." *Earthquake Engineering and Structural Dynamics*, **41**(4): 663–679.

International Building Code (IBC) (2015). International Code Council, Country Club Hills, USA.

Levy, R. and Lavan, O. (2006). "Fully stressed design of passive controllers in framed structures for seismic loadings." *Structural and Multidisciplinary Optimisation,* **32**(6): 485–498.

Miguel, L. F. F., Miguel, L. F. F. and Lopez, R. H. (2016). "Simultaneous optimisation of force and placement of friction dampers under seismic loading." *Engineering Optimisation*, **1**: 1-21.

Miner, M. A. (1945). "Cumulative damage in fatigue." *Journal of Application Mechanics,* **12** (3): 59–164.

Moreschi, L .M. and Singh, M. P. (2003). "Design of yielding metallic and friction dampers for optimal seismic performance." *Earthquake Engineering and Structural Dynamics,* **32**: 1291–1311.

Nikoukalam, M. T., Mirghaderi, S. R. and Dolatshahi, K. M. (2015). "Analytical study of moment-resisting frames retrofitted with shear slotted bolted connection." *Journal of Structural Engineering(ASCE),* **141**(11): 4015–4019.

Pall, A. S. and Marsh, C. (1982). "Response of friction damped braced frames." *Journal of Structural Division (ASCE),* **108**, 1313–1323.

Pall, A. S. and Pall, R. T. (2004). "Performance-based design using pall friction dampers; an economical design solution." I*n Proceedings, 13th World Conference on Earthquake Engineering*, Vancouver, Canada, Paper No. 1955,

Park, J. H., Kim, J. and Min, K.W. (2004). "Optimal design of added viscoelastic dampers and supporting braces." *Earthquake Engineering and Structural Dynamics,* **33**(4): 465–484.

Patro, S. K. and Sinha, R. (2010). "Seismic performance of dry-friction devices in shear-frame buildings." *Journal of Civil Engineering and Architecture* **4**(12).

PEER NGA. Online database. Available from: <http://peer.berkeley.edu/nga/search.html> (23 Feb 2016).

Petkovski, M. and Waldron, P. (2003). "Optimum friction forces for passive control of the seismic response of multi-storey Buildings." *In Proceedings: 40 years of European Earthquake Engineering SE40EEE,* Ohrid, Macedonia.

Powell, G. H., and Allahabadi, R. (1987). "Seismic damage prediction by deterministic methods: concepts and procedures." *Earthquake Engineering and Structural Dynamics,* **16**: 719–734.

Prakash, V., Powell, G. H. and Campbell, S. (1993). "DRAIN-2DX base program description and user guide." Version 1.10. University of California, Berkeley, California.

Sasani, M. and Popov, E. P. (1997). "Experimental and analytical studies on the seismic behaviour of lightweight concrete panels with friction energy dissipaters." *Earthquake Engineering Research Centre*, Report No. UBC/EERC-97/17, Berkeley, California.

Sasani, M. and Popov, E. P. (2001). "Seismic energy dissipaters for RC panels; analytical studies." *Journal of Engineering Mechanics,* **127**(8), 835–843.

Sonmez, M., E. Aydin, and T. Karabork. (2013). "Using an artificial bee colony algorithm for the optimal placement of viscous dampers in planar building frames." *Structural and Multidisciplinary Optimisation*, **48**: 395–409.

Soong, T. T. and Costantinou, M. C. (2014). "Passive and active structural vibration control in civil engineering." *Springer* 345.

Symans, M. D., Charney, F. A., Whittaker, A. S., Constantinou, M. C. et al. (2008). "Energy dissipation systems for seismic applications: current practice and recent developments." *Journal of Structural Engineering*, **134**(1): 3–21.

Takewaki, I. (2011). "Building control with passive dampers: optimal performance-based design for earthquakes." *John Wiley and Sons (Asia) Books*, Singapore, 51–75.

Teran-Gilmore, A. and Jirsa, J. O. (2004). "The concept of cumulative ductility strength spectra and its use within performance-based seismic design." *ISET Journal of Earthquake Technology*, **41**(1): 183–200.

Vanmarke, E. H. (1976). SIMQKE: A program for artificial motion generation, user's manual and documentation. Department of Civil Engineering, Massachusetts Institute of Technology.

Whittle, J.K., Williams, M.S., Karavasilis, T.L. and Blakeborough, A. (2012). "A comparison of viscous damper placement methods for improving seismic building design." *Journal of Earthquake Engineering*, **16**(4): 540–560.

Wu, B., Zhang, J., Williams, M. S., Ou, J. (2005). "Hysteretic behaviour of improved pall-typed frictional dampers." *Engineering Structures*, **27**: 1258–1267.

# CHAPTER 3

# A Simplified Methodology for Optimum Design of Friction Dampers by Considering Near-Field and Far-Field Ground Motions

## 3.1. ABSTRACT

A simplified method is proposed for optimum design of friction dampers by considering the characteristics of design earthquakes. Optimum slip loads for 3, 5, 10, 15 and 20-storey RC frames with friction wall-dampers are obtained for a set of 20 near and far-field earthquakes as well as artificial spectrum-compatible records scaled to different acceleration levels. Optimum solutions are shown to be more sensitive to Peak Ground Velocity (PGV) than Peak Ground Acceleration (PGA), especially for near-field earthquakes with high velocity pulses. For identical PGA levels, far-field earthquakes on average result in 1.5 times lower optimum slip loads compared to near-field records, while they lead to 118% higher energy dissipation and 24% lower maximum inter-storey drifts. Empirical equations are proposed to predict optimum slip loads (as a function of number of storeys and PGA/PGV of design earthquakes) and their efficiency is demonstrated through selected examples.

*Keywords: Near- and far-field earthquakes; Optimum design; Friction damper; Slip load distribution; Energy dissipation*.

## 3.2. INTRODUCTION

Friction-based passive energy dissipation devices have been successfully used in practice to enhance seismic performance of both newly designed and existing structures subjected to

earthquake excitations (Vezina and Pall, 2004; Pasquin et al., 2004). The design of a friction energy dissipation system is essentially a problem of finding the optimum values of slip loads in the friction devices (the loads at which the friction devices start slipping and hence dissipating energy). These values can be sensitive to the characteristics of the seismic excitation.

Several research studies have been carried out on optimum design of friction dampers under earthquake excitations using different optimisation techniques such as Genetic Algorithm (GA) (Moreschi and Singh, 2003; Mohammadi et al., 2018), backtracking search optimisation algorithm (BSA) (Miguel et al., 2016) and Uniform Distribution of Deformation (UDD) (Nabid et al., 2018), or used iterative methods to find the optimum range of slip load values. However, the aforementioned optimisation approaches are computationally expensive and/or require complex mathematical calculations, and therefore, may not be directly used in practical applications. On the other hand, most of the existing research studies on optimum design of friction dampers have been either based on a code-based design spectrum, a set of spectrum-compatible natural/synthetic earthquakes or a single natural earthquake (Petkovski and Waldron, 2003; Pall and Pall, 2004; Lee et al., 2008; Shirkhani et al., 2015; Nabid et al., 2017), where the effects of different types of earthquakes have been neglected. For more accurate design, however, the earthquake uncertainties should be taken into account in terms of fault type, earthquake intensity, peak acceleration and velocity, frequency content, duration, earthquake magnitude and distance.

In an early attempt, a design slip load spectrum was developed by Filiatrault and Cherry (1990) to obtain the best slip load distribution for friction dampers by minimising an energy performance index while considering the properties of the structure and the ground motion anticipated at the construction site. They concluded that the optimum slip load is not only a structural property but also depends on the frequency and amplitude of the ground motion. The values of the optimum slip loads in their study were shown to be linearly proportional to the peak ground acceleration of the input earthquake. In a more recent study, Kiris and Boduroglu (2013) investigated the correlation between the peak displacement demand of a RC structure with friction damper and different parameters used to measure the severity of ground motions. It was demonstrated that depending on the fundamental period of the frame, the strength ratio of the system at slip displacement and the soil profile, different ground motion parameters can play a dominant role in the seismic response of the structure.

In general, the distance of the structure from the fault rupture is one of the dominant factors influencing the imposed peak displacement demand. The near-field zones are typically

considered to be within 12 km from the fault rupture, while far-field regions are those with epicentral distances of the recording stations ranging from 12 to 64 km (Chopra and Chintanapakdee, 2001). Some researchers have classified near-field zones as those within 20-60 km from the fault rupture (Stewart et al., 2002). In general, in a near-field zone and at a particular site, the earthquake characteristics are significantly influenced by three factors: the rupture mechanism, slip direction relative to the site and the residual ground displacement at the site due to the tectonic movement. Forward-directivity pulses usually occur when the rupture propagation velocity is close to the shear-wave velocity and the direction of slip on the fault is aligned with the site (mainly oriented in the fault-normal direction due to the radiation pattern of the fault) (Somerville and Smith, 1996; Bray and Rodriguez-Marek, 2004; Davoodi and Sadjadi, 2015). Due to forward-directivity effect, large-amplitude pulses of motion are generated with long period (1–1.5 s) and short duration while having a high ratio of Peak Ground Velocity (PGV) to Peak Ground Acceleration (PGA) (Somerville et al., 1997). Therefore, in near-field areas high velocity pulses, which are extremely destructive in nature, are one of the main factors to define the severity of the seismic input rather than the PGA value. Regarding the last factor, the tectonic deformation associated with the fault rupture may contain a significant permanent static displacement termed fling-step effect (Bray and Rodriguez-Marek, 2004). It produces a high amplitude velocity pulse and a monotonic step in the displacement time history (Somerville, 2002). Additionally, hanging wall and footwall effects can be observed in dipping fault earthquakes. The fault plane has generally closer proximity to the sites on the hanging wall than the sites on the footwall at the same distance. The hanging wall sites have larger amplitude and slower attenuation in ground motion parameters than the footwall sites with the same distance. These effects have higher influence on the acceleration spectra in short periods. The aforementioned fling-step effect is the relative slip between the hanging wall and footwall (Abrahamson and Somerville, 1996).

Near-field earthquakes transfer a major portion of fault energy in the form of pulses, which can be frequently seen in displacement, velocity, and acceleration time histories. These pulses tend to have high Fourier spectrum in limited periods, while in far-field earthquakes the high Fourier spectrum generally occurs in broad range of periods (Iwan, 1994; Bhandari et al., 2017). In the frequency domain, depending on the fault-normal or fault-parallel components of the forward-directivity ground motions in near-field region, near-field earthquakes can have either higher or lower frequency contents compared to the far-field earthquakes (Davoodi and Sadjadi, 2015). Davoodi and Sadjadi (2015) also showed that the maximum Fourier amplitudes of far-field earthquakes and fault-parallel component of

forward-directivity ground motions are distributed at higher frequencies (mostly beyond 1Hz) compared to the maximum Fourier amplitudes of near-field earthquakes with fling-step and fault-normal component of forward-directivity records which generally occurs at frequencies less than 1Hz. It was demonstrated by Malhotra (1999) that, for the same PGA and duration of shaking, ground motions containing directivity pulses can result in much higher base shear, inter-storey drift, and roof displacement in high-rise structures as compared to those without pulses.

Previous studies show that structures designed using older seismic design provisions, based on far-field earthquakes, may experience extensive damage or failure in case of near-field earthquakes (Alavi and Krawinkler, 2001). The main reason is that large displacement demands can be imposed to the structures by severe pulses of near-field ground motions compared to the far-field earthquakes. In pulse-like ground motions, the amplitude and period of the pulse in the velocity time history are the key parameters to control the performance of the structures, and therefore, they should be taken into account for both design and retrofit of structures in the near-field zones (Alavi and Krawinkler, 2001). There is also displacement amplification in the long-period structures caused by the large amplitudes in the long period range of displacement response spectra (Anderson and Bertero, 1987). The results of Alavi ansd Krawinkler (2001) study indicated that conventional retrofit techniques accompanied by increasing the stiffness and/or strength of the system are not efficient for long-period structures subjected to severe pulse-like earthquakes. This is due to moving the structure into a range of higher spectral accelerations by increasing the stiffness (or decreasing the period) of the system. Unlike the cumulative effects of far-field ground motions, the structure dissipates the earthquake input energy in few large displacement excursions under near-field records, where most of the seismic input energy arrives in a single long-period velocity pulse associated with forward directivity or fling step displacements and response amplification of the long-period structures (Somerville, 1998).

Tirca et al. (2003) investigated the response of middle-rise steel moment-resisting frames with and without shear link (SL) devices subjected to near-field ground motions. Based on their results, the near-field earthquakes expose the structure to higher ductility demands than the far or intermediate-field ground motions. Also, they showed that for the stiffer structures, the shear forces were generally higher at the upper storeys. In a study performed by Xu et al. (2007), the performance of yielding and viscous passive energy dissipation systems were investigated subjected to near-field ground motions by using an analytical ground velocity pulse model. They concluded that the performance of different passive energy dissipation

systems depends significantly on the period of the pulse excitation, and therefore, to achieve the best performance, the pulse periods must be taken into account when designing passive energy dissipation systems. Lin et al. (2010) evaluated the efficiency of using initially accelerated passive tuned mass damper (PTMD) to reduce the dynamic responses of structures under near-fault ground motion records. They showed that an appropriate PTMD initial velocity used to accelerate the motion can efficiently reduce the local peak seismic responses of the system under near-fault earthquakes. In another relevant study, Hatzigeorgiou and Pnevmatikos (2014) developed a straightforward method for the evaluation of effective velocities and damping forces for single-degree-of-freedom (SDOF) structures with supplemental viscous dampers under near-source earthquakes. Using their proposed method, it was observed that the inelastic velocity ratio is strongly affected by the period of vibration, the effective viscous damping ratio, the force reduction factors and the type of seismic fault mechanism. In a more recent study, Bhandari et al. (2017) investigated the behaviour of a base-isolated building structure subjected to far-field and near-field earthquakes with directivity and fling-step effects. According to their results, under the near-field earthquakes with fling-step effect, the base isolation proved to be ineffective in terms of reducing base shear, top storey absolute acceleration and maximum inter-storey drift.

The research on the effects of near and far-field earthquakes is mainly focussed on the efficiency of base-isolated systems, viscous dampers and semi-active control devices, with few efforts in the design of friction-based passive control systems subjected to the near and far-field records. This study aims to evaluate the effects of near-field and far-field ground motions on optimum design of friction wall dampers leading to a maximum amount of energy dissipation efficiency in friction devices. To achieve this, at first, a comprehensive parametric study is performed on 3, 5, 10, 15 and 20-storey RC frames equipped with friction wall dampers (using a wide range of slip load values) under spectrum compatible earthquakes scaled to different PGA levels as well as a set of 20 near and far-field earthquake records. Based on the results, empirical equations are proposed to obtain the optimum slip load values by considering the effects of number of storeys and earthquake PGA and PGV levels. The efficiency of the proposed design method is then demonstrated through several design examples.

## 3.3. NUMERICAL MODELLING

In this study 3, 5, 10, 15, and 20-storey RC frames were selected with the typical geometry shown in Fig. 3.1 (a). The utilised friction damper (schematic view shown in Fig. 3.1 (b))

comprises a reinforced concrete wall panel connected to the frame through a friction device at the top, a horizontal connection at the bottom, and two vertical supports in the sides. The connections are designed to transfer the loads to the beam-column connection, thus avoiding extra shear forces in the middle of the adjacent columns and beams. The friction device is a Slotted Bolted Connection (SBC) using two steel plates over a central T-shape slotted steel plate anchored to the top floor beam (see Fig. 3.1 (b)). It should be noted that the bottom of the concrete panels at ground level is fixed to the base to transfer the imposed loads directly to the foundation, and therefore, reduce the maximum axial loads in the columns at the ground level. More detailed information about the adopted friction wall damper can be found in Nabid et al. (2017).

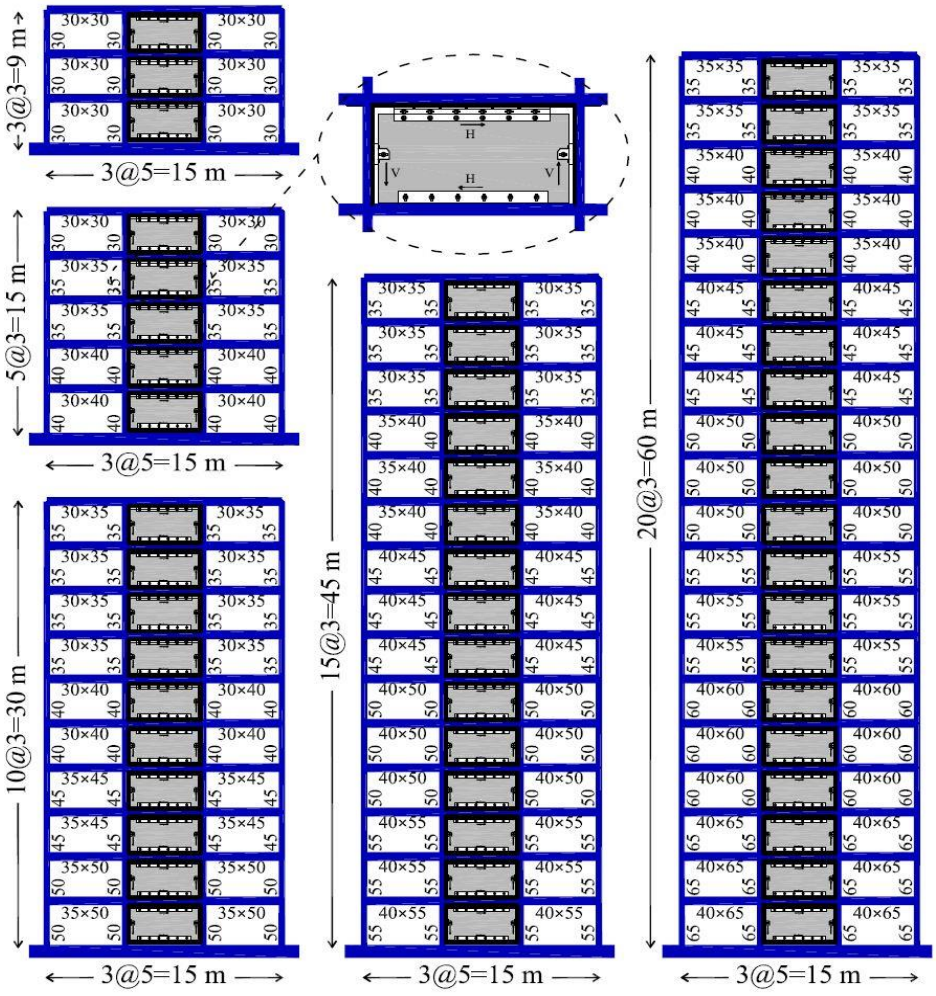


**Fig. 3.1.** (a) Geometry of the reference RC frames equipped with friction wall dampers, (b) schematic view of the friction wall damper (adopted from Nabid et al. (2017))

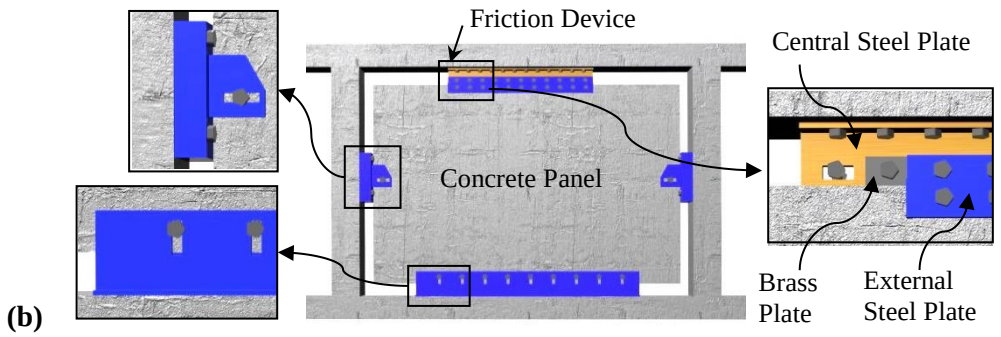


**Fig. 3.1. (Continued)** (a) Geometry of the reference RC frames equipped with friction wall dampers, (b) schematic view of the friction wall damper (adopted from Nabid et al. (2017))

The frames were assumed to be located on a soil type C of Eurocode 8 (EC8; CEN, 2004a) category and were designed for low-to-medium seismicity regions, using PGA of 0.2 g. The uniformly distributed permanent and non-permanent loads were considered to be 5.5 kN⁄m2 and 2.5 kN⁄m2 for interior floors, and 5.3 kN⁄m2 and 1.0 kN⁄m2 for the roof, respectively. The reference frames were initially designed to resist the seismic loads based on EC8 (CEN, 2004a) and in accordance with the minimum requirements of Eurocode 2 (EC2; CEN, 2004b) for moment-resisting RC frames with medium ductility (DCM). The concrete compressive strength ($f_c'$) and the yield strength of steel reinforcement bars ($f_y$) were assumed to be 35 MPa and 400 MPa, respectively.

Pushover and nonlinear time-history analyses were conducted using the OpenSees software (McKenna and Fenves, 2000). Concrete and reinforcing steel bars were modelled using a uniaxial constitutive material with linear tension softening (Concrete02) and a Giuffre–Menegotto–Pinto model (Steel02) with 1% isotropic strain hardening, respectively. Beam and column members were divided into three elements and modelled using displacement-based nonlinear beam-column elements with fibre sections while four Gauss–Lobatto integration points were considered for each element. P-Delta effects were taken into account and the Rayleigh damping model with a constant damping ratio of 0.05 was assigned to the first mode and to the modes at which the cumulative mass participation exceeds 95%.

In this study, it was assumed that the strength of the concrete wall panels (15 cm thickness) is always higher than the maximum loads transferred from the friction device, and therefore, they were modelled using equivalent elastic elements. A nonlinear spring with an elastic-perfectly plastic uniaxial material, representing an ideal Coulomb friction hysteretic behaviour, was used to model the friction device. The beam-to-column connections were assumed to be fully rigid with no shear failure in the panel zones. A computer code in MATLAB (2014) was developed and linked to the OpenSees (McKenna et al., 2000)

program to calculate the energy dissipation in the beam and column elements and friction devices under earthquake loads.

## 3.4. GROUND MOTION DATASETS

### 3.4.1. Natural Near-field and Far-field Earthquake records

Two sets of 10 near-field and 10 far-field ground motions were selected from the Pacific Earthquake Engineering Research Center online database (PEER, 2017) to evaluate the seismic performance of the 3, 5, 10, 15 and 20-storey frame structures with friction wall dampers. All the selected ground motions correspond to soil class C of EC8 with surface magnitudes ranging from 6.5 to 7.4. Tables 3.1 and 3.2 list the designations and characteristics of the selected unscaled near-field and far-field ground motions, respectively. The rupture distances (R: distance from the fault rupture plane to the site) are within 10 km for the near-field records and between 12 and 30 km for the selected far-field ground motions. The fault rupture mechanisms are strike slip and reverse for all the records. It should be noted that the forward directivity effect of the near-field ground motions generally leads to more intense fault-normal component compared to the fault-parallel component (Somerville, 1998). In this study, the fault-normal components with higher intensities were selected for the nonlinear time history analyses.

Fig. 3.2 (a) and (b) compare the 5% damped elastic acceleration and velocity response spectra of the studied unscaled near-field and far-field earthquakes, respectively. The acceleration response spectra show that the mean spectrum of the near-field earthquakes is well above whereas the far-field mean spectrum is well below the EC8 design spectrum. This implies that, with the same range of surface magnitudes, the intensity of near-field records is much higher than those recorded far away from the earthquake epicentre. Although the elastic acceleration response spectrum provides the basis to identify the characteristics of the design earthquakes, in case of near-field ground motions, the acceleration response spectrum does not adequately characterise the design earthquake. This is because near-field earthquakes are mainly characterised by a relatively long period pulse of strong motion with fairly short duration, while the far-field motions have relatively long duration (Somerville, 1998). Therefore, to better show the characteristics of the selected earthquakes, the elastic velocity response spectra of the selected near-field and far-field earthquakes with their mean spectra are also shown in Fig. 3.2.

**Table 3.1.** Properties of the selected near-field ground motions

| *No.* | *Earthquake* | *Ms* | *Station* | *Abr.* | *R (km)* | *PGA (g)* | *PGV (cm/s)* | *PGV/PGA (s)* |
|---|---|---|---|---|---|---|---|---|
| **1** | 1999 Duzce | 7.14 | Duzce | DUZ | 6.58 | 0.515 | 84 | 0.166 |
| **2** | 1992 Erzincan | 6.69 | Erzincan | ERZ | 4.38 | 0.387 | 107 | 0.282 |
| **3** | 1994 Northridge | 6.69 | Rinaldi Receiving Sta | RIN | 6.50 | 0.874 | 148 | 0.173 |
| **4** | 1994 Northridge | 6.69 | Newhall - Fire Sta | NEW | 5.92 | 0.590 | 97 | 0.168 |
| **5** | 1994 Northridge | 6.69 | LA-Sepulveda Hospital | SEP | 8.44 | 0.932 | 76 | 0.083 |
| **6** | 1995 Kobe | 6.9 | KJMA | JMA | 0.96 | 0.630 | 76 | 0.123 |
| **7** | 1995 Kobe | 6.9 | Takatori | TAK | 1.47 | 0.671 | 123 | 0.187 |
| **8** | 1995 Kobe | 6.9 | Port Island | POR | 3.31 | 0.290 | 51 | 0.179 |
| **9** | 1979 Imperial Valley | 6.53 | Meloland Geot. Array | MEL | 0.07 | 0.298 | 93 | 0.168 |
| **10** | 1979 Imperial Valley | 6.53 | El Centro Array #4 | ARR4 | 7.05 | 0.484 | 40 | 0.084 |

**Table 3.2.** Properties of the selected far-field ground motions

| *No.* | *Earthquake* | *Ms* | *Station* | *Abr.* | *R (km)* | *PGA (g)* | *PGV (cm/s)* | *PGV/PGA (s)* |
|---|---|---|---|---|---|---|---|---|
| **1** | 1994 Northridge | 6.69 | Canoga Park-Topanga | CAN | 14.70 | 0.358 | 34 | 0.097 |
| **2** | 1994 Northridge | 6.69 | Northridge-Saticoy St | SAT | 12.09 | 0.459 | 60 | 0.133 |
| **3** | 1994 Northridge | 6.93 | Capitola | CAPIT | 15.23 | 0.511 | 38 | 0.076 |
| **4** | 1989 Loma Prieta | 6.93 | Sunnyvale-Colton Ave. | SUN | 24.23 | 0.207 | 37 | 0.182 |
| **5** | 1989 Loma Prieta | 6.93 | Gilroy Array #3 | GIL3 | 12.82 | 0.559 | 36 | 0.066 |
| **6** | 1987 Superstition hills | 6.54 | El Centro Imp. Co. Cent | COC | 18.20 | 0.357 | 48 | 0.137 |
| **7** | 1987 Superstition hills | 6.54 | Westmorland Fire St. | WES | 13.03 | 0.211 | 32 | 0.155 |
| **8** | 1971 San Fernado | 6.61 | LA-Hollywood Stor Lot | HOLL | 22.77 | 0.225 | 22 | 0.100 |
| **9** | 1992 Landers | 7.28 | Desert Hot Springs | LAN | 21.78 | 0.171 | 19 | 0.113 |
| **10** | 1978 Tabas | 7.35 | Boshrooyeh | TAB | 28.79 | 0.106 | 13 | 0.125 |

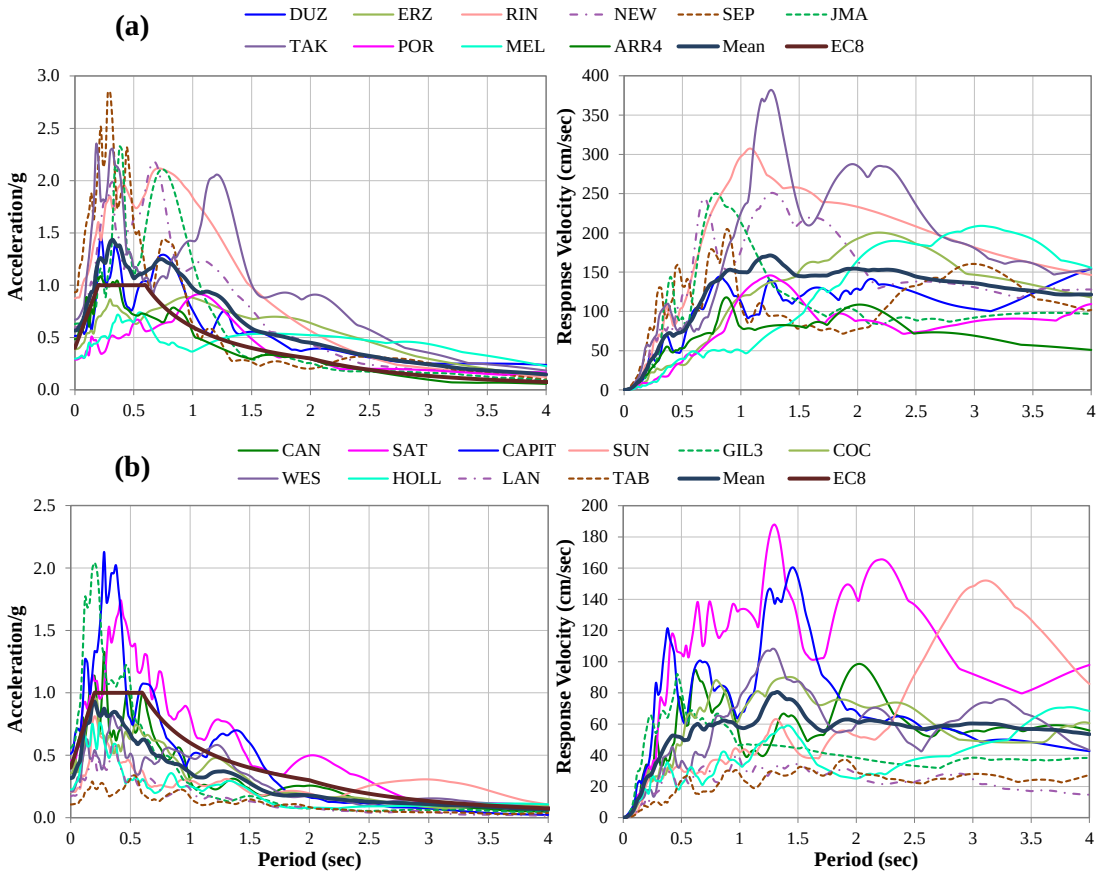


**Fig. 3.2.** Elastic acceleration and velocity response spectra of the selected (a) near-field and (b) far-field earthquakes and the EC8 design spectrum, 5% damping ratio

Figs. 3.2 (a) and (b) show that while the near-field ground motions have a narrower velocity-sensitive region at longer periods, they have wider acceleration-sensitive region compared to the far-field excitation records (except SUN). These results are in agreement with those obtained from the research carried out by Chopra and Chintanapakdee (2001) and Hall et al. (1995). Fig. 3.3 compares the mean velocity response spectra of the selected near and far-field ground motions showing significantly higher velocity for the near-field records.

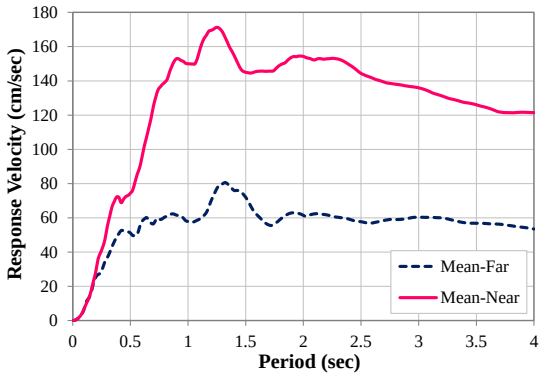


**Fig. 3.3.** Mean velocity response spectra of the selected near-field and far-field earthquakes, 5% damping ratio

### 3.4.2. Synthetic Earthquake Record

The previous research by Nabid et al. (2017, 2018) implied that the earthquake uncertainty, in terms of acceleration response spectra, can be efficiently managed by using synthetic earthquakes representing the average spectrum of a selected set of natural earthquakes. Therefore, a synthetic earthquake is generated using the TARSCTHS (Papageorgiou et al., 2002) program to be compatible with EC8 design response spectrum for high seismicity regions (i.e. PGA=0.4g) and soil class C. Fig. 3.4 shows the good agreement between the elastic acceleration response spectrum of the simulated earthquake record and the corresponding EC8 design spectrum.

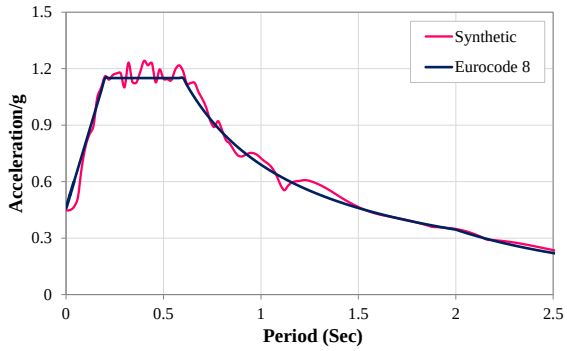


**Fig. 3.4.** Elastic acceleration response spectra of the synthetic earthquake record and the EC8 design spectrum, 5% damping ratio

## 3.5. EFFECT OF EARTHQUAKE INTENSITY LEVEL ON ENERGY DISSIPATION EFFICIENCY

The synthetic earthquake (compatible with the EC8 spectrum) was utilised to investigate the effect of the peak ground acceleration (PGA) used as a measure of earthquake intensity level on the maximum energy dissipation efficiency of the selected frames with friction wall dampers. The energy dissipation parameter, RW, which is the ratio between the work of the friction devices to the work of the beam and column elements (introduced in (Nabid et al., 2017)), is considered as an effective factor for assessing the efficiency of the proposed friction wall dampers. Fig. 3.5 shows the relationships between the slip load ratio (ratio between the average of slip loads and the average of storey shear strengths at all storey levels) and the energy dissipation parameter, RW, for the 3, 5, 10, 15 and 20-storey frames, subjected to the selected synthetic earthquake with a range of different PGA values (ranging from 0.1g to 1.2g). The optimum value of the slip load ratio is considered to be the one at which the RW factor reaches its peak. The results in Fig. 3.5 show that for stronger earthquakes (higher PGA levels) the optimum slip load ratios are higher and distributed over

a wider range. It is also shown that the energy dissipation efficiency (RW) is generally increased for lower earthquake intensity levels. This can be attributed to the fact that most structural elements remain in the elastic (or near elastic) range under low intensity earthquakes. The results also show a clear difference between the optimum ranges of slip load values for structures with different number of storeys as will be taken into consideration in the empirical equations proposed in the following sections.

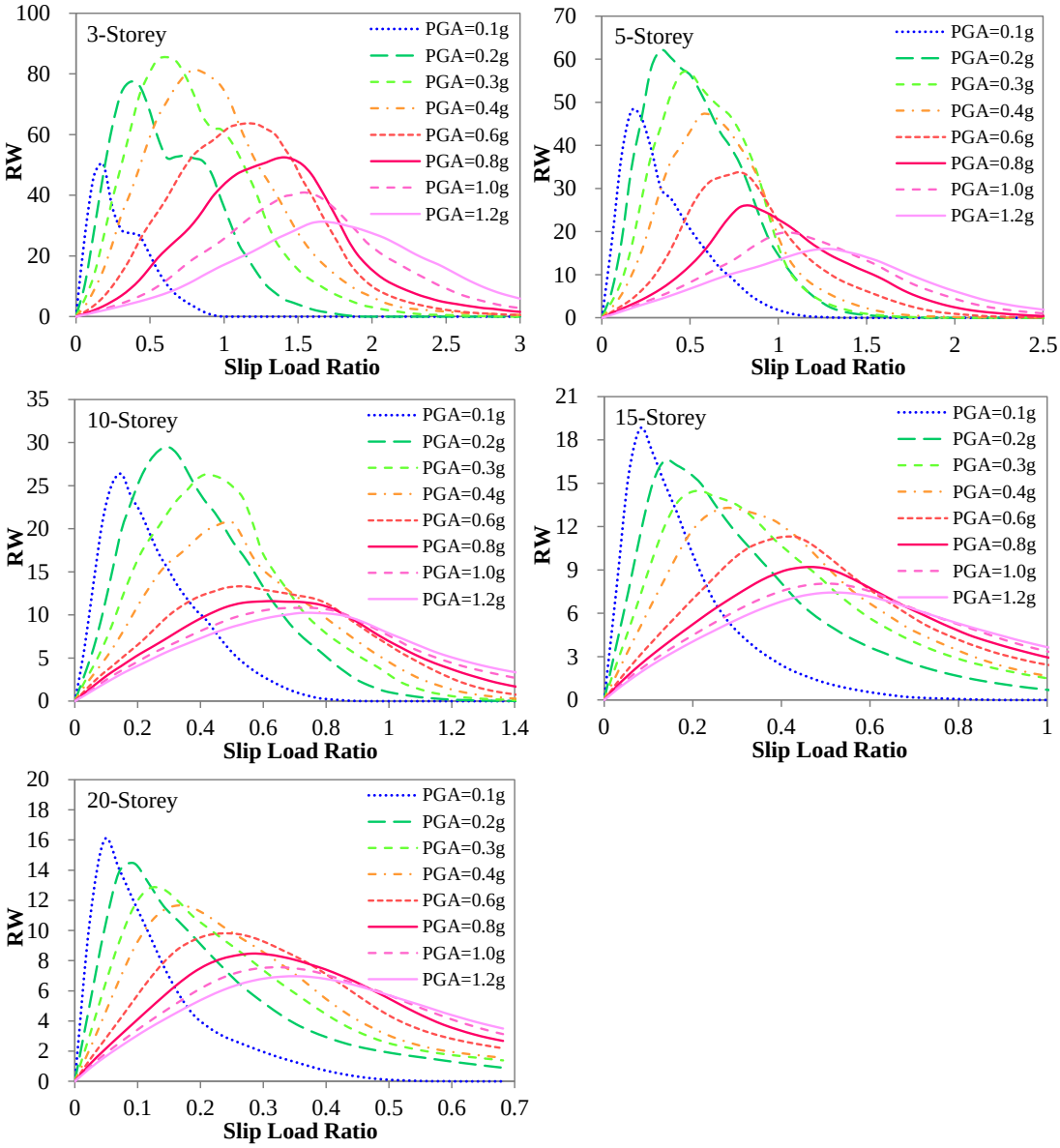


**Fig. 3.5.** Variation of energy dissipation parameter, RW, of the 3, 5, 10, 15 and 20-storey frames as function of slip load ratio under a synthetic earthquake record with different PGA levels

The results of a previous study (Pall and Pall, 2004) suggested that variations up to ±20% of the optimum slip load do not significantly affect the response; however, the range of these

variations depends on the earthquake intensity. The results in Fig. 3.5 imply that this is true for high PGA levels but not for low PGA levels, where the optimum response is significantly affected by small variations in the optimum slip load ratio. The energy dissipation effectiveness of the friction wall dampers in low to medium-rise structures initially increases with the increase of earthquake intensity up to a certain level. For the high-rise structures (15 and 20-storey); however, RW decreases monotonically by increasing the PGA. This can be mainly caused by the high stiffness of the low-rise building that in turn leads to smaller deformation demands under low PGA level earthquakes, and therefore, less energy dissipation through the work of the friction devices. This is more highlighted for the 3-storey frames with almost 70% higher RW for the 0.3g input compared with that for 0.1g. Fig. 3.6 illustrates the variation of the energy dissipated through the work of the friction devices in the 3, 5, 10, 15 and 20-storey frames under the selected synthetic spectrum compatible earthquake with different PGAs. As can be observed, a negligible amount of energy is dissipated by the friction dampers in the 3 and 5-storey frames under the 0.1g earthquake compared to the other earthquake PGA levels.

The results of the initial study conducted by Nabid et al. (2017) indicated that the optimum range of slip force ratio for RC frames with friction wall dampers is not considerably affected by the selected earthquake records if they match a similar design spectrum. While Nabid et al.'s (2017) equation may not be directly applicable for the buildings under earthquakes with different PGA intensity levels, a parametric study was performed on the selected low to high-rise structures under a range of PGA levels and their energy dissipation parameter, RW, was obtained. Then, the slip load ratios for which the RW parameter is greater than 90% of the its maximum value (i.e. less than 10% reduction), are considered as the optimum practical design range. The median (middle point) of the optimum slip load ratio ranges for the selected frames is then calculated under the synthetic spectrum-compatible earthquake using different PGA levels. Based on regression analysis using the median points, the following equation is suggested to calculate the optimum slip load ratio as a function of the earthquake PGA and number of storeys:

$$R_{Syn} = 1.16 \times e^{-0.09n} \times (a_g)^{0.75} \tag{3.1}$$

where $R_{Syn}$ is the optimum slip load ratio obtained for the selected spectrum-compatible synthetic earthquake (see Fig. 3.4) and defined as the ratio between the average of slip loads and the average of storey shear strengths at all storey levels; $n$ is the number of storeys and $a_g$ is the PGA of the design earthquake (given as proportion of g). The constant values are

selected so as the discrepancy between the equation and the results is minimised. The proposed equation, on average, leads to relatively small errors (9.8%) compared to the results obtained from the parametric study on 3, 5, 10, 15 and 20-storey frames with friction wall dampers. Fig. 3.7 shows the slip load design curves obtained from Equation 3.1 and the corresponding optimum slip load ranges as a function of earthquake intensity (PGA). While Filiatrault and Cherry (1990) suggested that the value of the optimum slip load is linearly proportional to the PGA level, the results of this study show a non-linear relationship between the PGA and optimum slip load values.

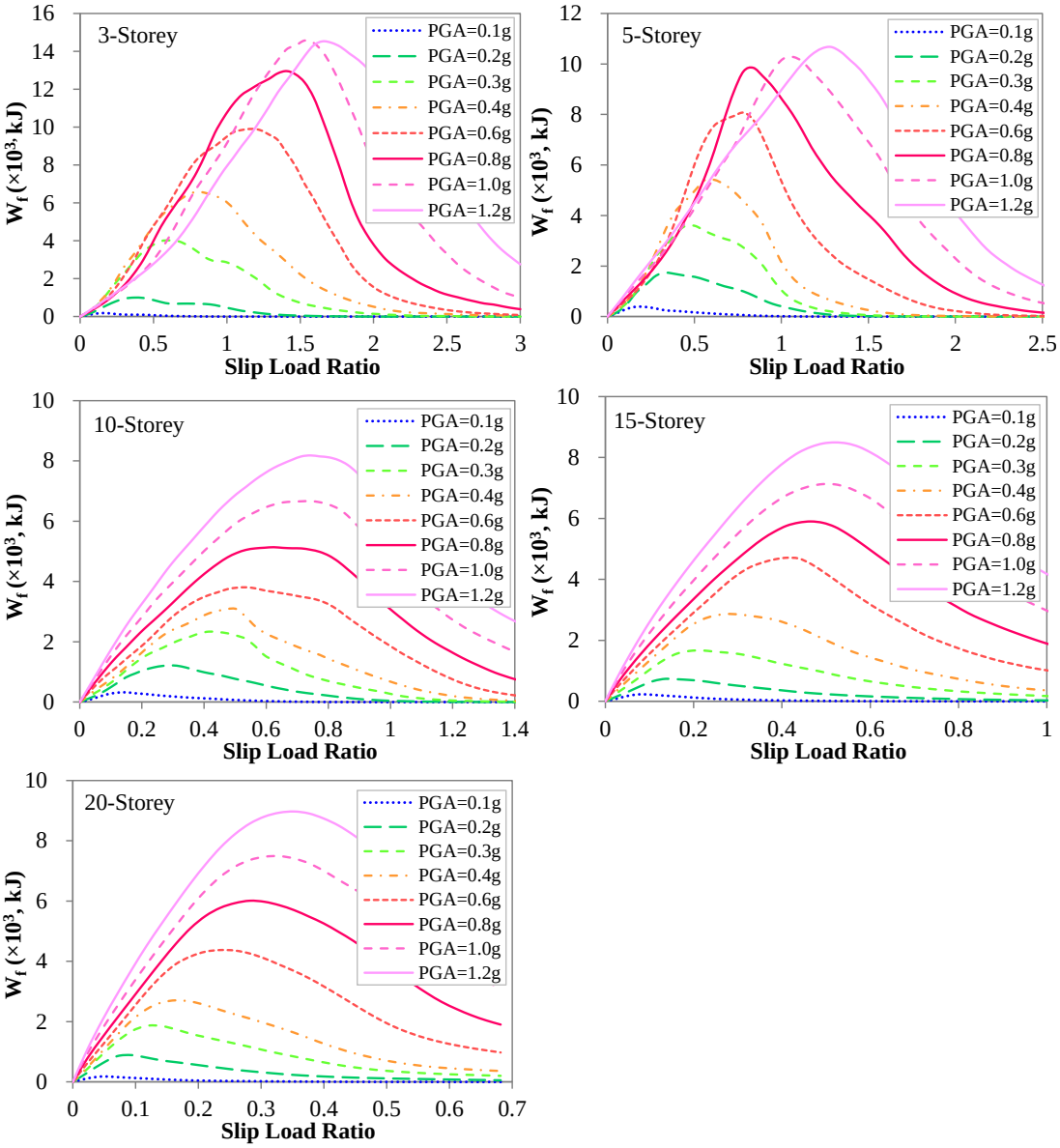


**Fig. 3.6.** Variation of work of the friction devices for the 3, 5, 10, 15 and 20-storey frames as function of slip load ratio under a synthetic earthquake record with different PGA levels

While PGA is the parameter most commonly used to identify earthquake intensity, it has also been reported that it is not a totally reliable parameter to assess the seismic performance of structures. For instance, according to Housner and Jennings (1982), peak ground velocity (PGV) can be a better parameter due to its direct connection to energy demand. On the other hand, near-fault impulsive ground motions are often characterised by PGV (Malhotra, 1999; Bray and Rodriguez-Marek, 2004). For this reason, in the following sections the effect of near-field and far-field earthquake ground motions with variable ranges of both PGA and PGV is investigated in the optimum design of friction dampers.

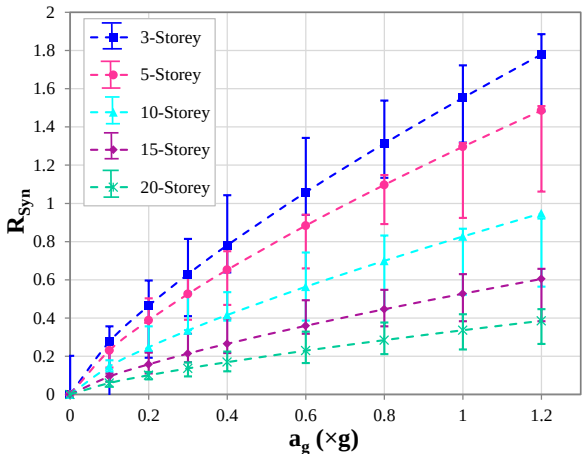


**Fig. 3.7.** Design slip load ratios for 3, 5, 10, 15 and 20-storey frames as a function of earthquake PGA

## 3.6. EFFECT OF NEAR AND FAR-FIELD EARTHQUAKES ON OPTIMUM DESIGN OF FRICTION DAMPERS

To evaluate the effect of near-field and far-field ground motions on optimum design solutions, the 3, 5, 10, 15 and 20-storey frames with friction wall dampers are subjected to the natural records listed in Tables 3.1 and 3.2. Figs. 3.8 (a) and (b) present the energy dissipation parameter RW, as a function of slip load ratio for the frames under the selected near-field and far-field earthquakes, respectively. The comparison of peaks of the mean-value curves shows about twice higher energy dissipation efficiency of the friction dampers for far-field earthquakes (i.e. 2.02, 1.81, 2.13, 2.18 and 2.09 for the 3, 5, 10, 15 and 20-storey frames, respectively). By considering the acceleration and velocity response spectra of the earthquakes (see Fig. 3.2), those records with more intense velocity pulse and/or higher response acceleration (such as SEP, TAK, RIN and JMA from the near-field set, and CAPIT, SAT and GIL3 from the far-field set of earthquakes), in general, result in maximum energy dissipation efficiency at higher slip load ratios. The earthquakes with relatively high

velocities at longer periods (e.g. MEL and SUN) led to higher optimum ranges of slip load ratios for taller buildings, compared to their corresponding mean curves; whereas for the low to medium-rise structures their optimum ranges are close to those of the mean curves. On the contrary, for the low to medium-rise frames, the earthquakes with the maximum velocity at lower periods (e.g. RIN) resulted in very high optimum slip load ratios. This is due to the earthquake high velocity occurring at the periods close to the natural period of the structure, and therefore, due to dynamic magnification effects, higher friction forces are required for optimum performance of the structure.

By considering no more than 10% reduction in the maximum of the mean RW curves, the range of optimum slip load ratios for the selected near-field earthquakes can be defined as 0.89-1.51, 0.56-0.95, 0.34-0.54, 0.25-0.44 and 0.17-0.28 for the 3, 5, 10, 15 and 20-storey frames, respectively. The corresponding optimum slip load ratio ranges obtained for the far-field earthquakes are 0.31-0.67, 0.33-0.73, 0.16-0.27, 0.09-0.16 and 0.06-0.12. The results indicate that the near-field earthquakes with higher velocity levels generally lead to higher and wider optimum ranges of slip load ratios for the supplemental friction-based energy dissipation devices compared to the far-field ground motions.

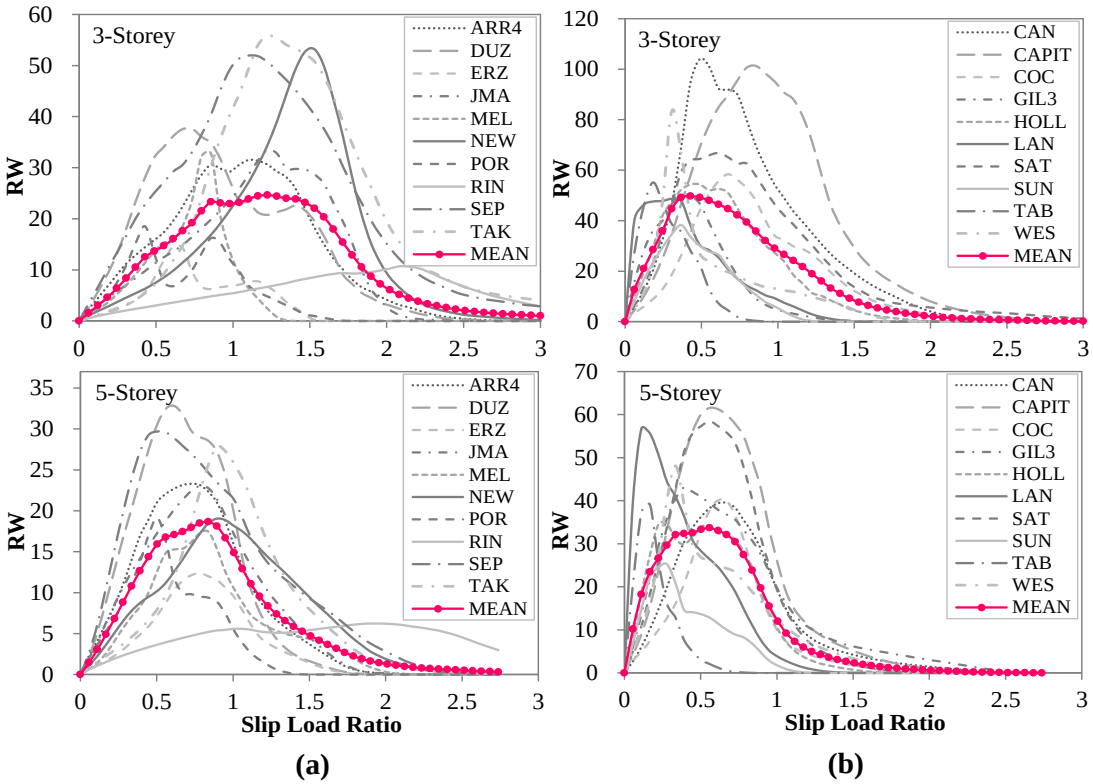


**Fig. 3.8.** Variation of energy dissipation parameter, RW, of the 3, 5, 10, 15 and 20-storey frames as function of slip load ratio under (a) near-field and (b) far-field ground motions

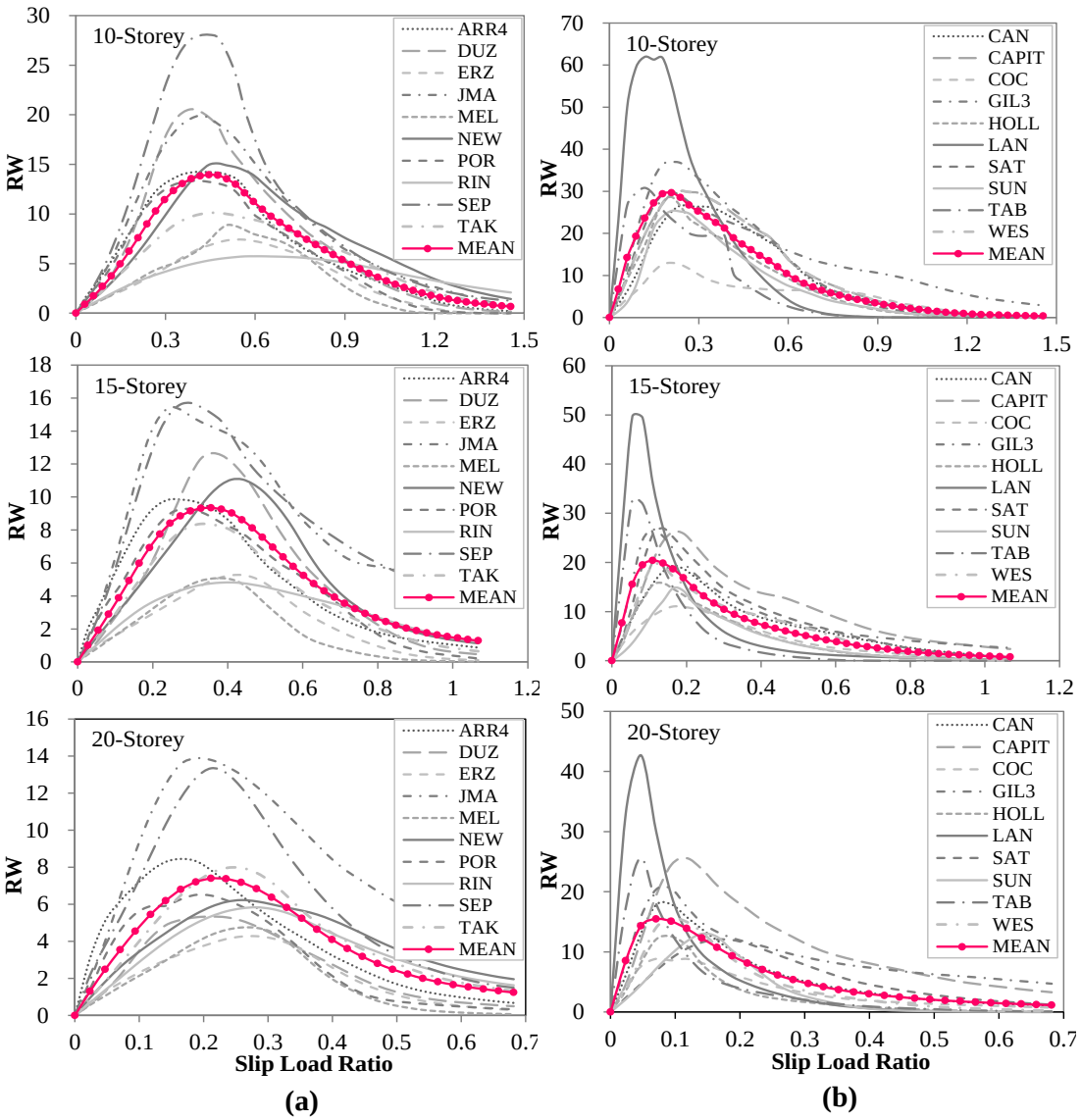


**Fig. 3.8. (Continued)** Variation of energy dissipation parameter, RW, of the 3, 5, 10, 15 and 20-storey frames as function of slip load ratio under (a) near-field and (b) far-field ground motions

Fig. 3.9 shows the variation of maximum inter-storey drift ratio of the 3, 5, 10, 15 and 20-storey frames as function of slip load ratio under the selected near-field and far-field earthquakes. It should be noted that, for better comparison, the results in Fig. 3.9 are scaled to the maximum inter-storey drifts of the corresponding bare frames. It is shown that the optimum slip load ratio ranges, defined earlier as those leading to the maximum energy dissipation efficiency, also result in minimum drift ratios. The maximum inter-storey drift ratios were, on average, attenuated by 94%, 80%, 55%, 44% and 34% for the 3, 5, 10, 15 and 20-storey frames under the near-field earthquakes, respectively; and by 92%, 85%, 63%, 54% and 42% for the 3, 5, 10, 15 and 20-storey frames under the far-field earthquakes, respectively. In general, the reduction in drift ratios was more noticeable in far-field

earthquakes, with the difference between near and far-field increasing with the increase in height of the buildings (i.e. by maximum 24% reduction in 20-storey frame).

While Equation 3.1 may not be directly applicable for the buildings under far-field and near-field earthquakes with different PGA intensity levels, new constant coefficients were calculated based on regression analysis for near and far-field earthquakes separately. The constants were obtained using the results of a comprehensive parametric study on 3 to 20-storey structures so that the discrepancies between the proposed equations and the results are minimised. Using individual optimum slip load ratios corresponding to the maximum energy dissipation efficiency obtained for each near-field and far-field earthquake with specific PGA, Equation 3.1 can be modified to the following equations:

$$R_{near} = (1.29 \times e^{-0.09n} \times (a_g)^{0.75}) / 100 \tag{3.2}$$

$$R_{far} = (0.86 \times e^{-0.09n} \times (a_g)^{0.75}) / 100 \tag{3.3}$$

where $R_{near}$ and $R_{far}$ are the optimum slip load ratios estimated for near-field and far-field earthquakes, respectively.

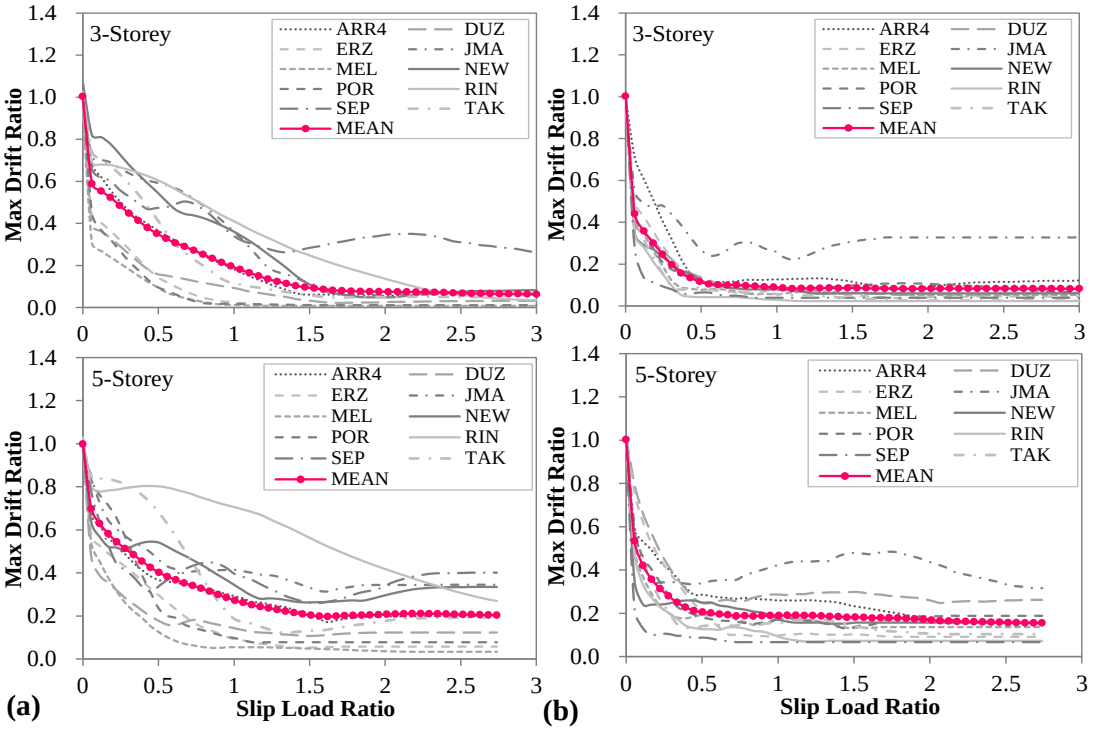


**Fig. 3.9.** Variation of maximum inter-storey drift ratio (scaled to the bare frame) of the 3, 5, 10, 15 and 20-storey frames as function of slip load ratio under (a) near-field and (b) far-field ground motions

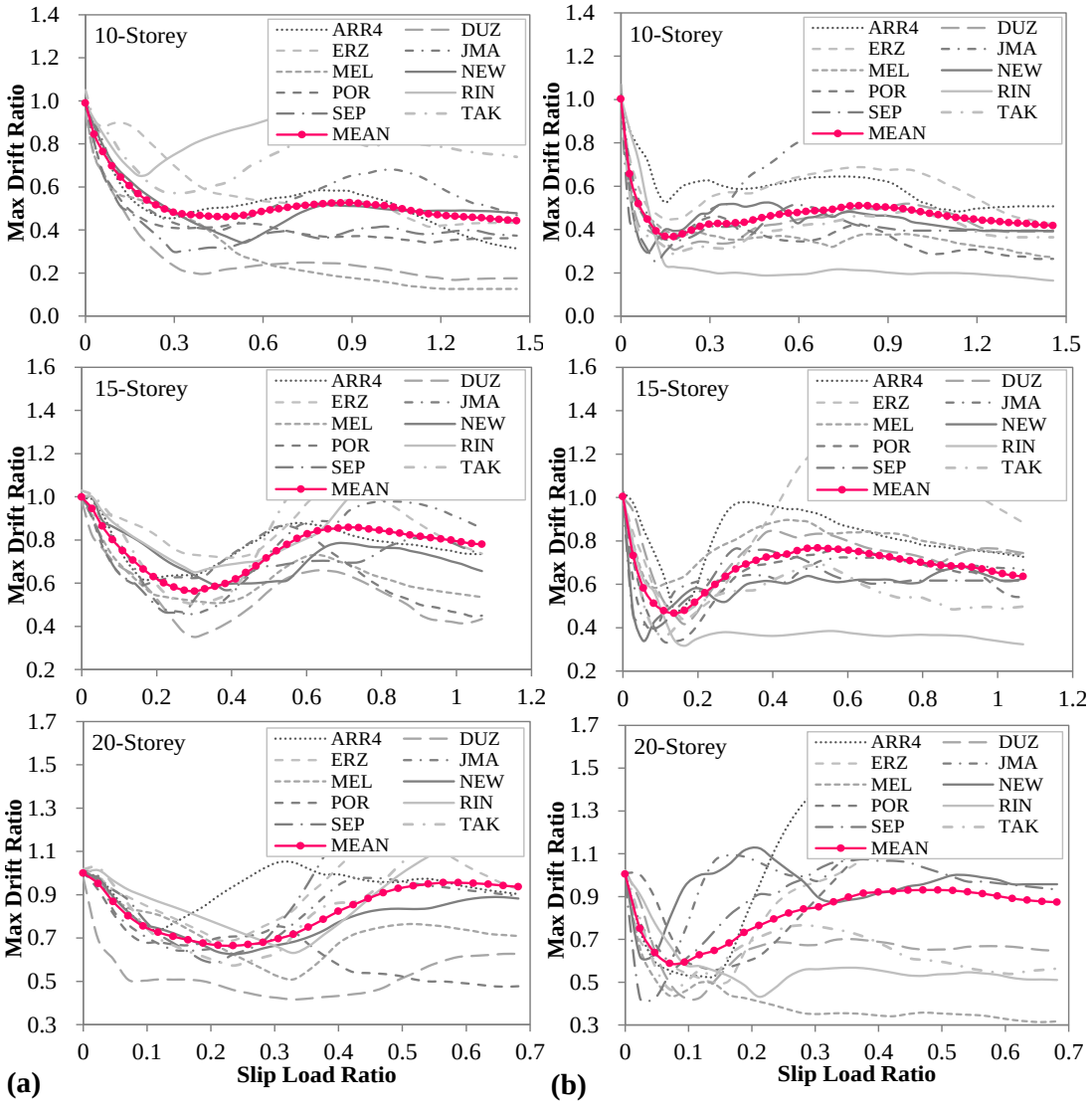


**Fig. 3.9. (Continued)** Variation of maximum inter-storey drift ratio (scaled to the bare frame) of the 3, 5, 10, 15 and 20-storey frames as function of slip load ratio under (a) near-field and (b) far-field ground motions

Fig. 3.10 shows the variation of optimum slip load ratios of the 3, 5, 10, 15 and 20-storey frames as function of earthquake PGA for the near and far-field earthquakes overlaid with their corresponding design curves (Equations 3.2 and 3.3). Equations 3.2 and 3.3 are proposed to have, on average, minimum errors (i.e. 27% and 23%) to the optimum results obtained for the near and far-field earthquakes, respectively. However, there are still high dispersions of the results around the proposed equations especially for the 10 and 15-storey frames.

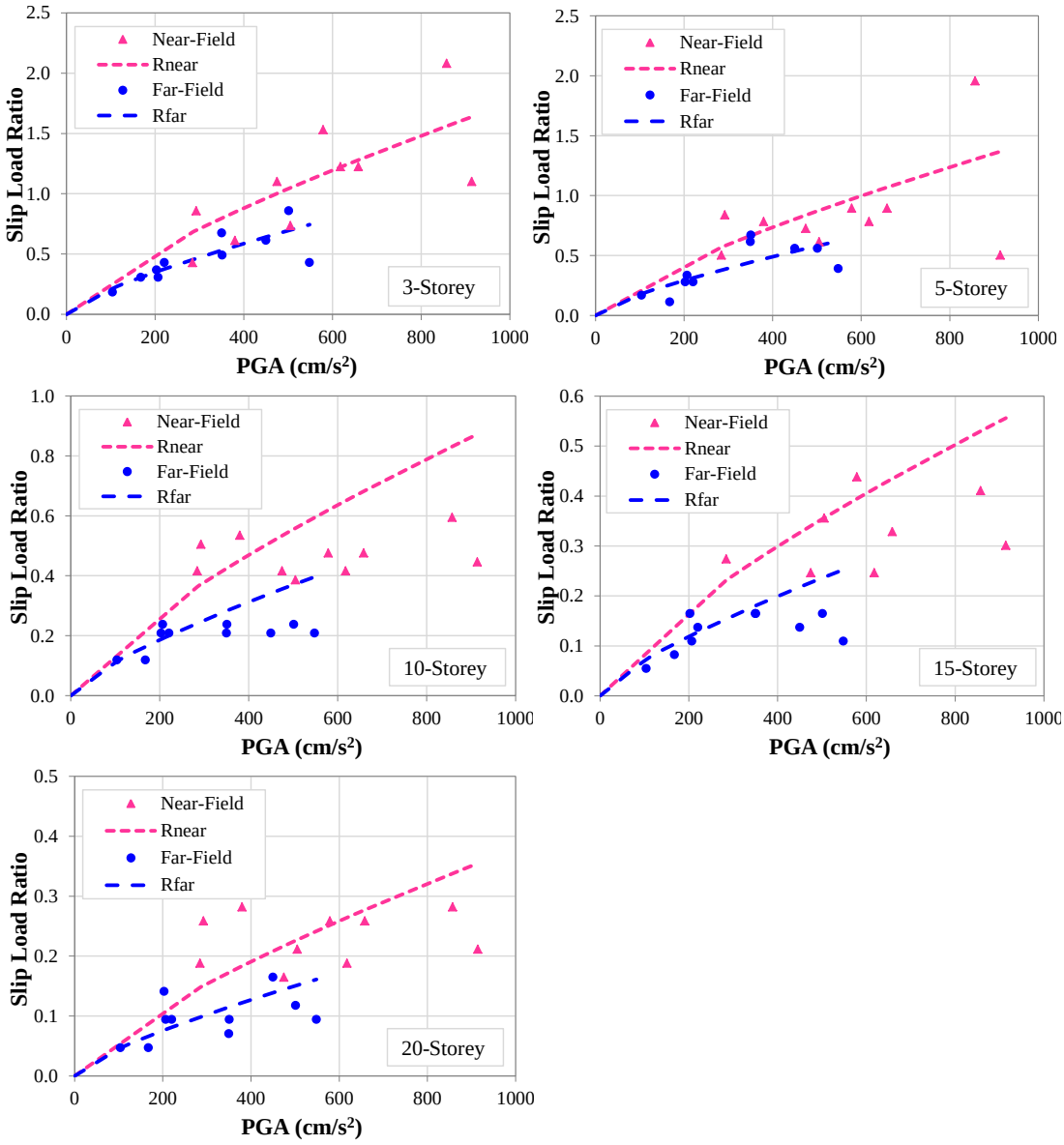


**Fig. 3.10.** Variation of optimum slip load ratio of the 3, 5, 10, 15 and 20-storey frames as function of earthquake PGA level for the near-field and far-field earthquakes with their corresponding design equation curves (Equations 3.2 and 3.3)

Based on Equations 3.2 and 3.3, for the same earthquake PGA, on average, near-field earthquakes result in 1.5 times higher optimum slip loads than those for far-field earthquakes. The reason for this is the higher PGV levels of the near-field earthquakes compared to the far-field records. For example, DUZ from the near-field set of earthquake versus GIL3 from the far-field (Table 3.1) have PGAs of 0.515g and 0.559g, and PGV of 84m/s and 36m/s, respectively. As outlined in Zhu et al. (1988) and Pavel and Lungu (2013), the PGV/PGA ratio can be used as an indicator of both frequency content of strong ground motions and potential structural damage. They revealed that low PGV/PGA ratios generally correspond to ground motions with a high frequency content in the strong-motion phase (e.g.

SEP, CAPIT and GIL3), whereas high PGV/PGA ratios, in general, are associated with the ground motions with intense, long-duration acceleration pulses (e.g. TAK and NEW). In pulse-like ground motions, the coherent long-period pulses may lead to the PGV/PGA ratio of ground motions become larger (e.g. ERZ and TAK). Therefore, the ground motions with higher PGV/PGA values generally have larger damage potential (Meskouris at al., 1992). Ground motions at moderate distances from the energy source normally have a broad range of significant frequency content, resulting in intermediate PGV/PGA ratios (e.g. TAB and LAN).

Fig. 3.11 shows the optimum slip load ratios of the 3, 5, 10, 15 and 20-storey frames under the selected near and far-field earthquakes as function of the earthquake PGV/PGA ratios. For similar PGV/PGA ratios, the earthquakes with higher values of PGA and PGV result in higher optimum slip load ratios (e.g. RIN compared to NEW, DUZ, POR and TAK). While the earthquake response velocity can affect the optimum design solution, the optimum results were also depicted as a function of earthquake PGV level (see Fig. 3.12). According to the result, one single equation can be suggested for both near and far-field earthquakes to capture the relationship between the optimum slip load ratio and the PGV of the near and far-field earthquakes. The constants were obtained so that the discrepancies between the proposed equations and the results are minimised. The following equation calculates the optimum slip load ratios for all types of earthquakes, giving an average error of 18% (better than both Equations 3.2 and 3.3) when compared with the results obtained for near and far-field natural earthquakes. This implies that the PGV factor can be a better parameter to estimate the optimum slip load values.

$$R_{EQ} = \left(4.75 \times e^{-0.09n} \times (a_v)^{0.75}\right) / 100 \tag{3.4}$$

where $R_{EQ}$ is the optimum slip load ratio for both near-field and far- field earthquakes and $a_v$ is the PGV of the earthquake. Equations 3.1 to 3.4 are based on the models considered in this study, and the optimum range might change for different structural systems or for the structures with very different geometries (e.g. very different slenderness ratio or storey height).

Finally, by using a previously defined uniform cumulative pattern (Nabid et al., 2017) for the height-wise distribution of slip loads, the equation below can be used to find the slip load values at each storey level:

$$F_{s,i} = \frac{\sum_{1}^{n} F_{y,i} \times 4.75 \times e^{-0.09n} \times (a_v)^{0.75}}{100 \times n(n+1)/2} \times (n+1-i) \tag{3.5}$$

where $F_{s,i}$ and $F_{y,i}$ are the slip load and the storey shear strength of the $i^{th}$ storey, respectively.

The accuracy of the proposed empirical equation (Equation 3.4) can be assessed from Fig. 3.12, showing the individual optimum slip load ratios obtained for the selected natural near-field and far-field earthquakes and the curves resulting from Equation 3.4 (as functions of earthquake PGV level). The proposed equation curve is the best fit to the series of optimum slip load ratios obtained for the selected earthquakes.

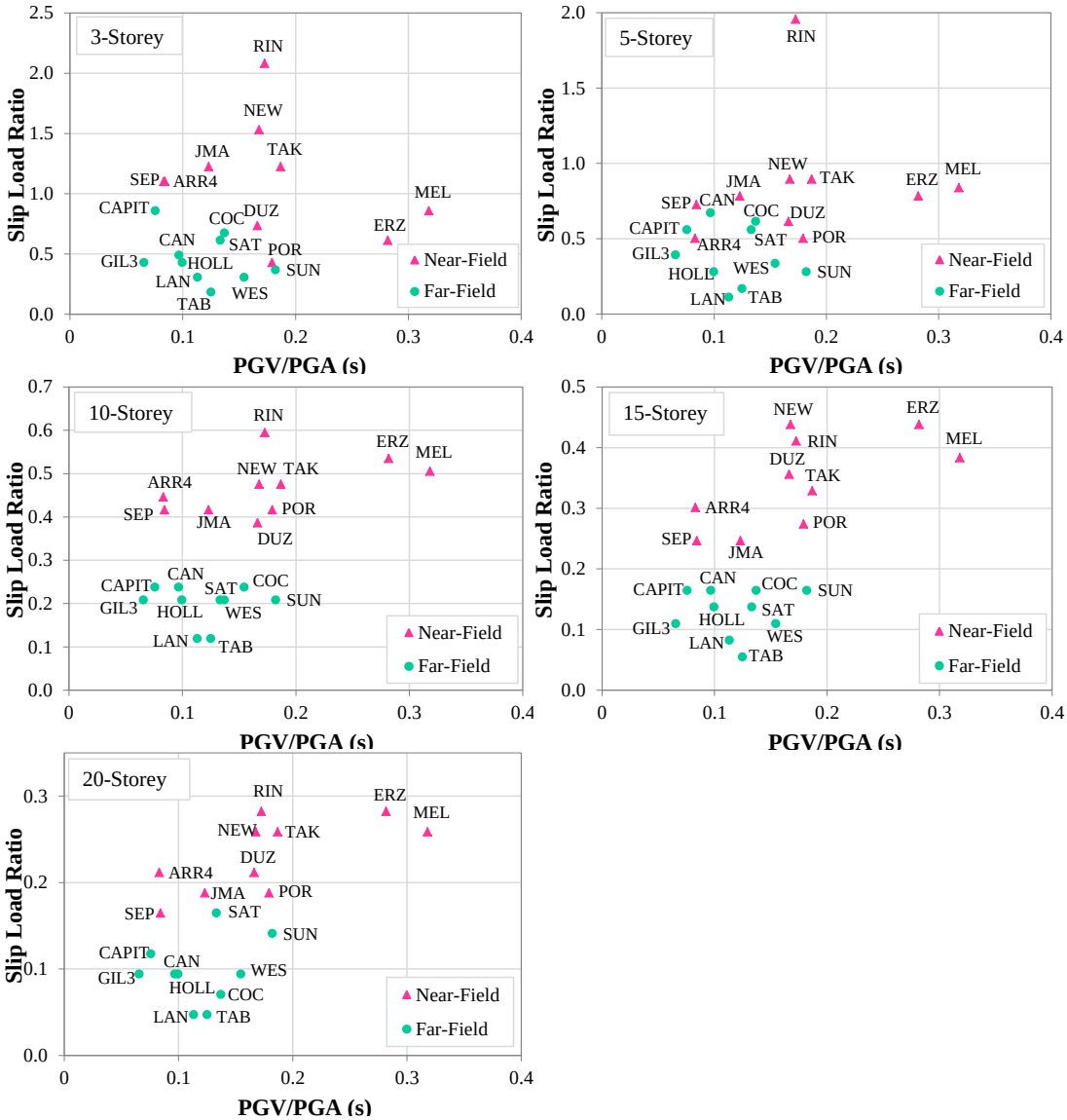


**Fig. 3.11.** Comparison of optimum slip load ratios of the 3, 5, 10, 15 and 20-storey frames under the selected near and far-field earthquakes as function of earthquake PGV/PGA ratio

The comparison with the results obtained from Equations 3.2 and 3.3, where PGA is the optimisation parameter (Fig. 3.10), shows that PGV is a more reliable parameter to determine the optimum design solutions for the frames subjected to both near and far-field earthquakes. It can be observed from Fig. 3.12 that the upper parts of the data sets with higher optimum slip load ratios are associated with the results of the near-field earthquakes, whereas the lower parts correspond to those of the far-field records. The dispersion of the results and discrepancy between the data sets and the proposed equation curve can be caused by different pulse periods and frequency contents of the design earthquakes.

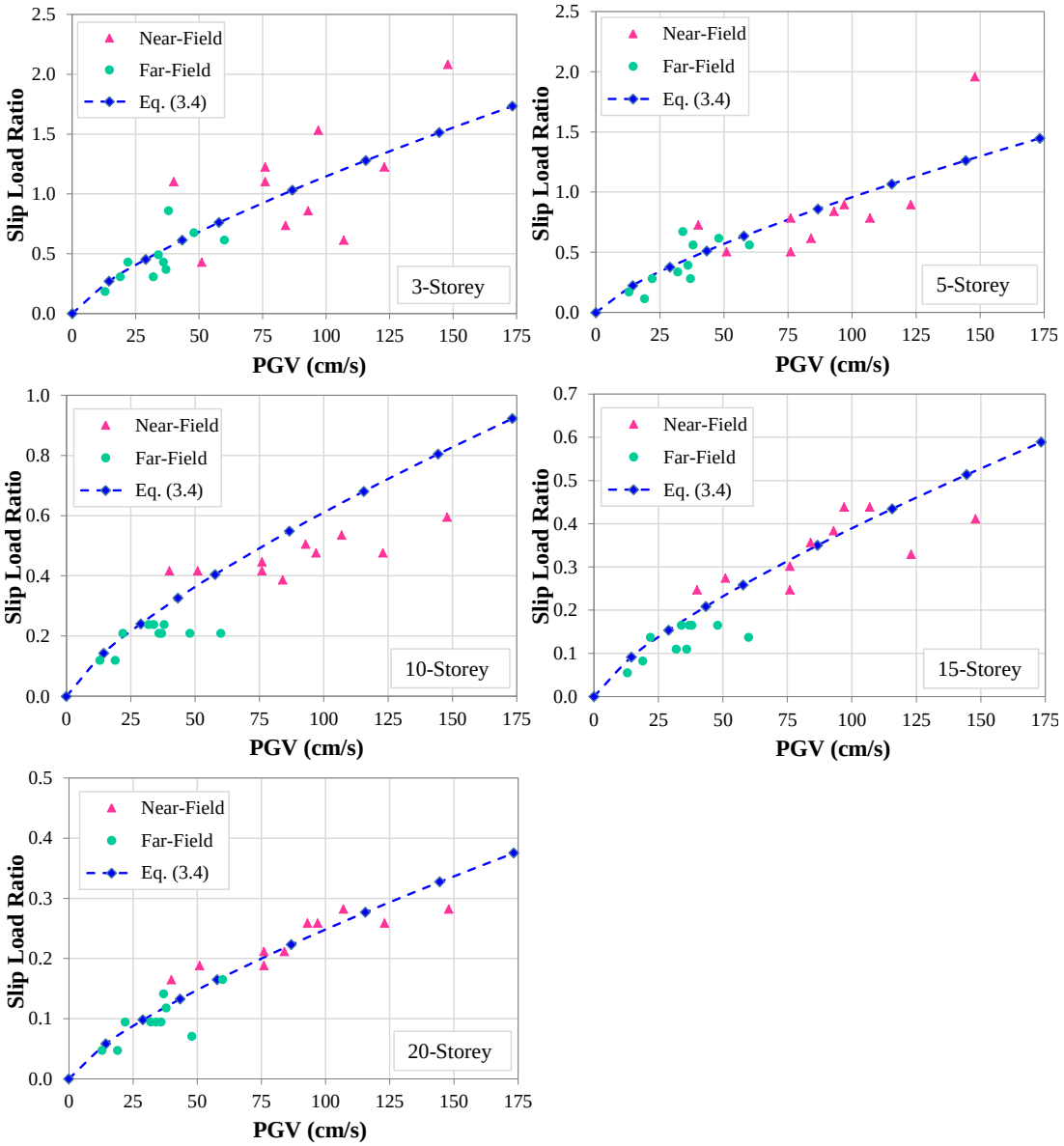


**Fig. 3.12.** Comparison of optimum slip load ratios for the selected near and far-field earthquakes with the proposed empirical equation (Equation 3.4) as functions of earthquake PGV level

## 3.7. EFFICIENCY OF THE PROPOSED DESIGN METHOD

To assess the efficiency of the proposed design equation, the selected frames were designed using the slip load values obtained from Equation 3.5 and the following design equation suggested by Nabid et al. (2017):

$$F_{s,i} = \frac{\sum_{1}^{n} F_{y,i} \times 1.12 \times e^{-0.11n}}{n(n+1)/2} \times (n+1-i) \tag{3.6}$$

The designed frames were then subjected to the selected near-field and far-field earthquakes. It should be noted that, unlike the equation proposed in this study, Equation 3.6 does not take into account the characteristics of the design earthquake (i.e. far-field and near-field effects). Fig. 3.13 compares the average ratios between structural responses (i.e. energy dissipation parameters RW and maximum inter-storey drift) obtained by using Equations 3.5 and 3.6 for the 3, 5, 10, 15 and 20-storey frames subjected to the selected sets of near and far-field earthquakes. In general, the results indicate that the new design equation (Equation 3.5) increases the energy dissipation efficiency of the friction devices (i.e. average ratios above 1) and slightly decreases the maximum inter-storey drifts (i.e. average ratios below 1) of the studied frames. Based on the results, on average, the proposed design method could increase the energy dissipation efficiency parameters (RW) of the 3, 5, 10, 15 and 20-storey frames by 17%, 13%, 5%, 21% and 38%, for the selected near-field records and by 62%, 44%, 41%, 54% and 35%, for the far-field earthquakes, respectively. The maximum drift ratios (Equation 3.5 to Equation 3.6) are decreased by 20% and 11.4% for the near-field and far-field earthquakes, respectively. While the general design methodology proposed in this study can be easily adopted for any set of design earthquakes, the proposed equation should prove useful in more efficient design of friction dampers in practical applications.

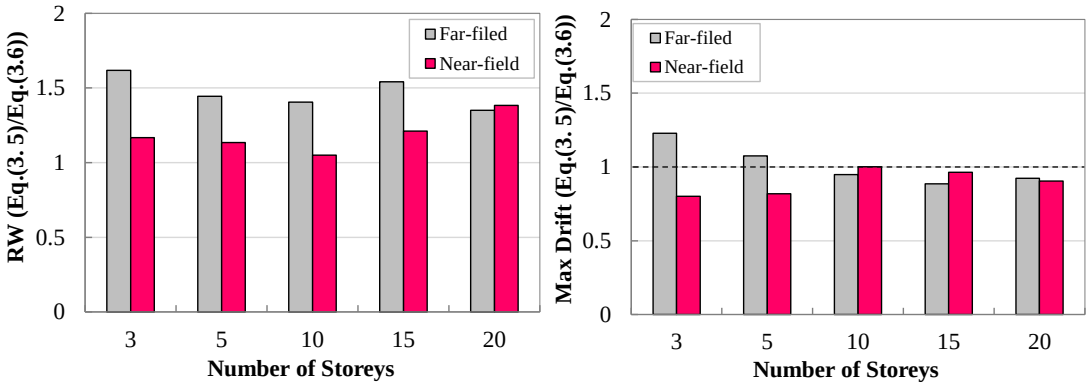


**Fig. 3.13.** Average ratios (this study to Nabid et al.'s (2017) study) of the (a) energy dissipation parameter (RW) and (b) maximum inter-storey drift for the 3, 5, 10, 15 and 20-storey frames under 20 near and far-field earthquakes

## 3.8. SUMMARY AND CONCLUSIONS

An efficient simplified model was proposed for optimum seismic design of friction-based dampers by considering the effects of near-field and far-field ground motions. To obtain the optimum slip load ranges, a comprehensive parametric study was performed on 3, 5, 10, 15, and 20-storey RC frames with friction wall dampers under spectrum compatible earthquakes scaled to different PGA levels as well as a set of 20 near and far-field earthquake records. Subsequently, empirical equations were proposed to obtain the optimum slip loads based on the number of storeys and PGA (or PGV) of the design earthquake. The efficacy of the proposed method was demonstrated through the optimum design of the selected frames to achieve maximum energy dissipation efficiency. Based on the results of this study, the following conclusions can be drawn:

- By using synthetic spectrum-compatible earthquakes scaled to different PGA levels, it was shown that higher PGA (or PGV) levels generally lead to lower energy dissipation efficiency with higher and wider range of optimum slip load ratios. However, the relationship between the PGA and optimum slip load values is not linear and depends on the number of storeys.

- Friction wall dampers were found to be more efficient under far-field earthquakes. It was shown that, on average, 118% higher energy dissipation efficiency and 24% lower maximum inter-storey drifts were attained for the far-field earthquakes compared to the near-field records. In general, the optimum ranges of slip load ratios obtained for the frames under the near-field earthquakes were noticeably wider and higher compared to those achieved under the far-field ground motions. By considering the same PGA level, near-field earthquakes led to about 1.5 times higher optimum slip loads than far-field earthquakes.

- It was shown that for the same PGV/PGA level (or similar frequency content), the earthquakes with higher PGA and PGV values resulted in higher optimum slip load ratios. In addition, the earthquakes with relatively high velocities occurring at the periods close to the period of the corresponding bare frames result in higher range of optimum slip load values.

- The optimum response of the structures was more sensitive to the PGV than PGA. The proposed design equation for (optimum) slip load ratio R as a function of PGV resulted in better curve fitting (lower dispersions of the results) than the equations using PGA as

a design variable. In general, the upper parts of the equation curve based on PGV were compatible with the results obtained for the near-field ground motions while the lower parts were corresponding to those of the far-field earthquakes.

- Compared to the previous equation suggested by Nabid et al. (2017) (without consideration of far-field/ near-field effects), the design method proposed here is considerably more efficient in increasing the energy dissipation efficiency of the friction devices (up to 62%) and decreasing the maximum inter-storey drift of the studied frames (up to 20%) subjected to both near-field and far-field earthquakes.

## REFERENCES

Abrahamson, N. and Somerville, P. (1996). "Effects of the hanging wall and footwall on ground motions recorded during the Northridge earthquake," *Bulletin of the Seismological Society of America*, **86**(1B): S93–S99.

Alavi, B. and Krawinkler, H. (2001). "Effects of near fault ground motions on frame structures." *The John A. Blume Earthquake Engineering Center*, Report No. 138, Stanford University, CA.

Anderson, J. C. and Bertero, V. V. (1987). "Uncertainties in establishing design earthquakes," *Journal of Structural Engineering*, **113**(8): 1709–1724.

Bhandari, M., Bharti, S. D., Shrimali, M. K. and Datta, T. K. (2017). "The numerical study of base-isolated buildings under near-field and far-field earthquakes." *Journal of Earthquake Engineering*, **22**(6): 989–1007.

Bray, J.D. and Rodriguez-Marek, A. (2004). "Characterization of forward-directivity ground motions in the near-fault region." *Soil Dynamics and Earthquake Engineering*, **24**(11), 815–828.

CEN (Comité Européen de Normalization) (2004a). "Eurocode 8: Design of structures for earthquake resistance-Part 1: General rules, seismic actions and rules for buildings." EN 1998–1–1, Brussels.

CEN (Comité Européen de Normalization) (2004b). "Eurocode 2: Design of concrete structures -Part 1-1: General rules and rules for buildings," EN 1992–1–2, Brussels.

Chopra, A.K. and Chintanapakdee, C. (2001). "Comparing response of SDF systems to near-fault and far-fault earthquake motions in the context of spectral regions," *Earthquake Engineering and Structural Dynamics*, **30**(12): 1769–1789.

Davoodi, M. and Sadjadi, M. (2015) "Assessment of near-field and far-field strong ground motion effects on soil- structure SDOF system," *International Journal of Civil Engineering*, **13**: 153–166.

Filiatrault, A. and Cherry, S. (1990) "Seismic design spectra for friction-damped structures," *Journal of Structural Engineering*, **116**(5), 1334–1355.

Hall, J. F., Heaton, T. H., Halling, M. W. and Wald, D. J. (1995). "Near-source ground motion and its effects on flexible buildings." *Earthquake Spectra*, **11**(4), 569–605.

Hatzigeorgiou, G. D. and Pnevmatikos, N. G. (2014). "Maximum damping forces for structures with viscous dampers under near-source earthquakes." *Engineering Structures*, **68**: 1–13.

Housner, G. W. and Jennings, P. C. (1982). "Earthquake design criteria." *EERI Monograph Series*, Berkeley, CA.

Iwan, W. D. (1994) "Near-field considerations in specification of seismic design motions for structures." *In Proceedings: 10th European Conference on Earthquake Engineering*, Vienna, Austria.

Kiris, S. S. and Boduroglu, M. H. (2013). "Earthquake parameters affecting the performance of an RC frame with friction damper." *Soil Dynamics and Earthquake Engineering*, **55**: 148–160.

Lee, S. H., Park, J. H., Lee, S. K. and Min, K. W. (2008) "Allocation and slip load of friction dampers for a seismically excited building structure based on storey shear force distribution." *Engineering Structures*, **30**: 930–940.

Lin, C. C., Chen, C. L. and Wang, J. F. (2010) "Vibration control of structures with initially accelerated passive tuned mass dampers under near-fault earthquake excitation," *Computer-Aided Civil and Infrastructure Engineering*, **25**(1): 69–75.

Malhotra, P. K. (1999) "Response of buildings to near-field pulse-like ground motions." Earthquake Engineering and Structural Dynamics, **28**(11): 1309–1326.

MATLAB (2014). The MathWorks, Inc.: Natick, Massachusetts, USA.

McKenna, F., Fenves, G. L., Scott, M. H. (2000). "Open system for earthquake engineering simulation," University of California, Berkeley, California, <http://opensees.berkeley. Edu> (1 August 2016).

Meskouris K., Kratzig W. B. and Hanskotter U. (1992) "Seismic motion damage potential for R/C wall-stiffened buildings In: Fajfar P. and Krawinkler H. (eds) Nonlinear seismic analysis and design of reinforced concrete buildings." Oxford: Elsevier Applied Science, 125–136.

Miguel, L. F. F., Miguel, L. F. F. and Lopez, R. H. (2016). "Simultaneous optimization of force and placement of friction dampers under seismic loading," *Engineering Optimization*, **48**: 586–602.

Mohammadi, R. K. Mirjalaly, M., Mirtaheri, M., and Nazeryan, M., (2018). "Comparison between uniform deformation method and Genetic Algorithm for optimizing mechanical properties of dampers," *Earthquakes and Structures*, **1**(14): 1–10.

Moreschi, L. M., Singh, M. P. (2003). "Design of yielding metallic and friction dampers for optimal seismic performance." *Earthquake Engineering and Structural Dynamics*, **32**: 1291–1311.

Nabid, N., Hajirasouliha, I. and Petkovski, M. (2017) "A practical method for optimum seismic design of friction wall dampers." *Earthquake Spectra*, **33**(3): 1033–1052.

Nabid, N., Hajirasouliha, I., and Petkovski, M. (2018) "Performance-based optimisation of RC frames with friction wall dampers using a low-cost optimisation method." *Bulletin of Earthquake Engineering*, **16(**10): 5017–5040.

Pall, A. S. and Pall, R. T. (2004) "performance-based design using pall friction dampers - an economical design solution," *In Proceedings: 13th World Conference on Earthquake Engineering*, Vancouver, B.C., Canada, Paper No. 1955.

Papageorgiou, A., Halldorsson, B., and Dong, G. (2002) "TARSCTH (Target Acceleration Spectra Compatible Time Histories)," Engineering Seismology Laboratory (ESL) at the State University of New York at Buffalo.

Pasquin, C., Leboeuf, N., Pall, R. T. and Pall, A. (2004) "Friction dampers for seismic rehabilitation of Eaton's building, Montreal," *In Proceedings: 13th World Conference on Earthquake Engineering*, Vancouver, B.C., Canada.

Pavel, F. and Lungu, D. (2013) "Correlations between frequency content indicators of strong ground motions and PGV." *Journal of Earthquake Engineering*, **17**(4): 543–559.

PEER NGA. Online database. Available from: <http://peer.berkeley.edu/nga/search.html> (20 September 2017).

Petkovski, M. and Waldron, P. (2003) "Optimum friction forces for passive control of the seismic response of multi-storey Buildings," *In Proceedings: 40 years of European Earthquake Engineering SE40EEE*. Ohrid, Macedonia.

Shirkhani, A., Mualla, I. H., Shabakhty, N. and Mousavi, S. R. (2015). "Behavior of steel frames with rotational friction dampers by endurance time method." *Journal of Constructional Steel Research*, **107**: 211–222.

Somerville, P. and Smith, N. F. (1996) "Accounting for near-fault rupture directivity effects in the development of design ground motions," *In Proceedings: 11th World Conference on Earthquake Engineering*, Acapulco, Mexico, Paper No. 711.

Somerville, P., Smith, N. F. and Graves R. W. (1997). "Norman A. Abrahamson; Modification of Empirical Strong Ground Motion Attenuation Relations to Include the Amplitude and Duration Effects of Rupture Directivity." *Seismological Research Letters*, **68** (1): 199-222.

Somerville, P. (1998) "Development of an improved representation of near-fault ground motions," SMIP98 Seminar on Utilization of Strong-Motion Data, 1–20.

Somerville, P. G. (2002) "Characterizing near fault ground motion for the design and evaluation of bridges," *In Proceedings: 3rd National Seismic Conference and Workshop on Bridges and Highways*, Portland, Oregon, 137–148.

Stewart, J. P. Chiou, S. J., Bray, J. D., Graves, R. W. et al. (2002). "Ground motion evaluation procedures for performance-based design." *Soil Dynamics and Earthquake Engineering* **22**(9): 765–772.

Tirca, L. D., Foti, D. and Diaferio, M. (2003). "Response of middle-rise steel frames with and without passive dampers to near-field ground motions." *Engineering Structures*, **25**(2), 169–179.

Vezina, S. and Pall, R. T. (2004). "Seismic retrofit of MUCTC building using friction dampers." Palais des Congres, Montreal. *In Proceedings:* 13th *World Conference on Earthquake Engineering*, Vancouver, B.C., Canada, Paper No. 1964.

Xu, Z., Agrawal, A. K., He, W. L., and Tan, P. (2007) "Performance of passive energy dissipation systems during near-field ground motion type pulses." *Engineering Structures* **29**(2): 224–236.

Zhu, T. J., Tso, W., and Heidebrecht, A. (1988). "Effect of peak ground A/V ratio on structural damage." *Journal of Structural Engineering* **114**, 1019–1037.

# CHAPTER 4

# Performance-based Optimisation of RC Frames with Friction Wall Dampers Using a Low Computational Cost Optimisation Algorithm

## 4.1. ABSTRACT

Friction-based dampers have been extensively used for seismic strengthening and rehabilitation of existing substandard structures. The main issues in the design of the system are the magnitude of the maximum slip force and the distribution of slip forces along the height of the building. In this study, a practical performance-based optimisation methodology is developed for seismic design of RC frame buildings with friction energy dissipation devices, which allows for an accurate solution at low computational cost. The proposed method aims at distributing the slip loads of the friction dampers to achieve a uniform distribution of damage along the height of the building. The efficiency of the method is evaluated through the optimum design of five different low to high-rise RC frames equipped with friction wall dampers under six natural and six synthetic spectrum-compatible earthquakes. Sensitivity analyses are performed to assess the reliability of the method using different initial height-wise slip load distributions, convergence parameters and earthquake records. The results indicate that optimum frames exhibit less maximum inter-storey drift (up to 43%) and global damage index (up to 75%), compared to uniform slip load distribution. The method is then developed to obtain the optimum design solution for a set of earthquakes representing a design spectrum. It is shown that the proposed

*Bulletin of Earthquake Engineering, Volume 16, Issue 10, 3 May 2018, Pages 5017-5040*

method can provide an efficient tool for optimum seismic design of RC structures with friction energy dissipation devices for practical purposes.

## 4.2. INTRODUCTION

Passive energy dissipation devices have been widely used for improving the seismic performance of new buildings or strengthening of existing substandard structures. Friction-based dampers are among the most popular passive energy dissipative devices due to their high energy dissipation capacity resulting from Coulomb dry friction (Pall and Pall, 1995; Aiken, 1996; Sadek et al., 1996; Marsh, 2000). The first generation of friction dampers was introduced by Pall and Marsh (1982) for braced steel frames using series of steel plates clamped together designed to slip at a predetermined load. Fitzgerald (1989) utilised Slotted Bolted Connections (SBC) in steel braced frames to dissipate earthquake input energy and control the axial loads in braced elements to avoid buckling. Subsequently, several other friction-based dampers were introduced mainly combined with steel bracing systems such as Rotational Friction Damper (RFD) (Mualla, 2000; Shirkhani et al., 2015). Improved Pall Friction Damper (Wu et al., 2005) and Shear Slotted Bolted Connection (SSBC) (Nikoukalam et al., 2015). However, using brace-type control devices in RC frames may be accompanied by the risk of damaging the concrete at the connection zones due to high stress concentrations. To address this issue, wall-type systems can be used to provide adequate space to transfer forces to the surrounding elements. In one of the early attempts, Sasani and Popov (1997, 2001) studied the behaviour of friction energy dissipators combined with a lightweight concrete panel for different input displacements. The friction-based damper they proposed incorporates a precast concrete wall fixed to the lower floor beam using anchor bolts and to the upper floor beam using SBC friction energy dissipators. The results of their study indicated that this type of damper can provide a stable hysteresis loop through friction mechanism between the sliding metal surfaces of the connectors. In another relevant study, Petkovski and Waldron (2003) showed the efficiency of SBC devices attached to concrete wall panels (with and without openings to enhance the seismic performance of multi-storey RC structures subjected to a set of natural earthquake records. More recently, Nabid et al. (2017) investigated the efficiency of friction-based wall dampers designed with different slip load distribution patterns in improving the seismic performance of substandard RC structures. Based on the results of their extensive analytical study, an empirical formula was proposed to obtain more efficient height-wise distribution of slip loads by considering different seismic performance parameters. However, they did not use any optimisation method to obtain the best design solutions.

Obtaining the optimum design solutions of energy dissipation devices can be a challenging task due to complexity and high nonlinearity of these systems under earthquake excitations (Whittle et al., 2012 and 2013). Over the past two decades, a number of different optimisation methods have been used for optimum design of energy dissipation devices, including Simulated Annealing (SA) (Milman and Chu, 1994), Linear Quadratic Regulator (LQR) (Gluck et al., 1996; Agrawal and Yang, 1999) Gradient-based Optimisation (Singh and Moreschi, 2001; Park et al. 2004; Lavan and Levy, 2006; Fujita et al., 2010), Fully Stressed Design Optimisation (Levy and Lavan, 2006), Genetic Algorithm (GA) techniques (Moreschi and Singh, 2003; Asahina et al., 2004; Lavan and Dargush, 2009; Honarparast and Mehmandoust, 2012; Hejazi et al., 2013) and a successive procedure using Sensitivity Analysis and Redesign (Takewaki, 2011; Adachi et al., 2013). While conventional structures are expected to exceed their elastic limits in severe earthquakes, for simplification purposes, most of these studies assumed a linear behaviour for the structural systems equipped with the supplemental energy dissipation devices. Moreover, the above optimisation methodologies were mainly developed for viscous and viscoelastic dampers.

The efficiency of friction-based dampers is strongly associated with the location of the dampers and the height-wise distribution of slip loads, which can be then tuned to obtain the required performance objectives. While most optimisation techniques developed for hysteretic dampers (e.g. Uetani et al., 2003; Murakami et al., 2013; Martinez et al. 2014) can be also adopted for friction-based devices, there are limited studies available on the optimum design of friction-based dampers. In one of the early attempts, an optimisation algorithm was developed by Filiatrault and Cherry (1990) which was capable to achieve the optimum slip load values while minimizing an energy performance index (RPI). Based on the results of their study, a design slip load spectrum was proposed to obtain the optimum distribution of the slip loads. It was also shown that the optimum slip load values are more affected by the amplitude and frequency of the input earthquakes (e.g. peak ground acceleration) rather than the characteristics of the structure. Patro and Sinha (2010) evaluated the seismic performance of shear building structures with dry-friction devices using a constant slip load distribution pattern subjected to a set of earthquake ground motions. They concluded that while the optimum slip load values can be considerably affected by the characteristics of the selected input earthquake, a suitable range of slip loads can be obtained which generally leads to a better seismic performance under a wide range of design earthquake ground motions. In another relevant study, the Genetic Algorithm (GA) optimisation method was used by Moreschi and Singh (2003) for optimum placement of friction and yielding metallic dampers in multi-storey steel braced frames to satisfy a prescribed performance objective.

Using a similar approach, Miguel et al. (2014) adopted a GA methodology for multi-objective optimisation of friction dampers in shear building structures subjected to earthquake ground motions. In more recent studies, a Backtracking Search Algorithm (BSA) was adopted by Miguel et al. (2016a, 2016b) to optimise simultaneously the location and the slip force values of the friction devices in shear buildings subjected to seismic loads. It should be mentioned that most of the aforementioned optimisation methods are computationally expensive and/or require complex mathematical calculations, and therefore, may not be suitable for practical applications.

This study aims to develop a low-cost performance-based optimisation method for seismic design of non-linear friction-based wall dampers based on the concept of Uniform Damage Distribution. The proposed optimisation method can considerably improve the seismic behaviour of the structures in only a few steps by controlling performance indices such as maximum inter-storey drift and maximum energy dissipation capacity. The efficiency of the method in improving the seismic behaviour of RC frames with friction wall dampers is demonstrated through several design examples under a set of natural and synthetic spectrum compatible earthquakes.

## 4.3. MODELLING AND ASSUMPTIONS

### 4.3.1. Reference Frames

Friction energy dissipative devices are commonly used in practice to reduce earthquake-induced response of structures for both new building designs and strengthening purposes. In this study, five different substandard moment-resisting RC frames with 3, 5, 10, 15 and 20 storeys are strengthened with wall-type friction energy dissipation devices in their middle span as shown in Fig. 4.1. To represent substandard structures in high-seismic regions, the reference frames were designed using the IBC-2015 (and ASCE/SEI 7-10 (2010)) proposed design spectrum with 0.2g peak ground acceleration (PGA), and 0.20g and 0.32g spectral response accelerations at short and 1-sec periods, respectively. The site soil profile was assumed to be type D of IBC (2015) soil category. The dead and live loads for interior storeys were considered to be 6 kN/m$^2$ and 2 kN/m$^2$, respectively, while the corresponding loads were reduced to 5 kN/m$^2$ and 1.5 kN/m$^2$ for the roof level. The RC frames were primarily designed to satisfy the minimum requirements of ACI 318-14 (2014) for intermediate ductility level. The yield strength of steel reinforcement ($f_y$) and the compressive strength of concrete ($f'_c$) were selected to be 400 and 35 MPa, respectively.

Nonlinear time-history and pushover analyses were performed using DRAIN-2DX computer program (Parkash and Powel, 1993). The Rayleigh damping ratio of 0.05 was assigned to the first mode of vibration and to the mode at which the cumulative mass participation exceeds 95%. Nonlinear beam and column elements were respectively modelled using moment rotation (M-ϑ) and axial-moment interaction (P-M) plastic hinges at their both ends.

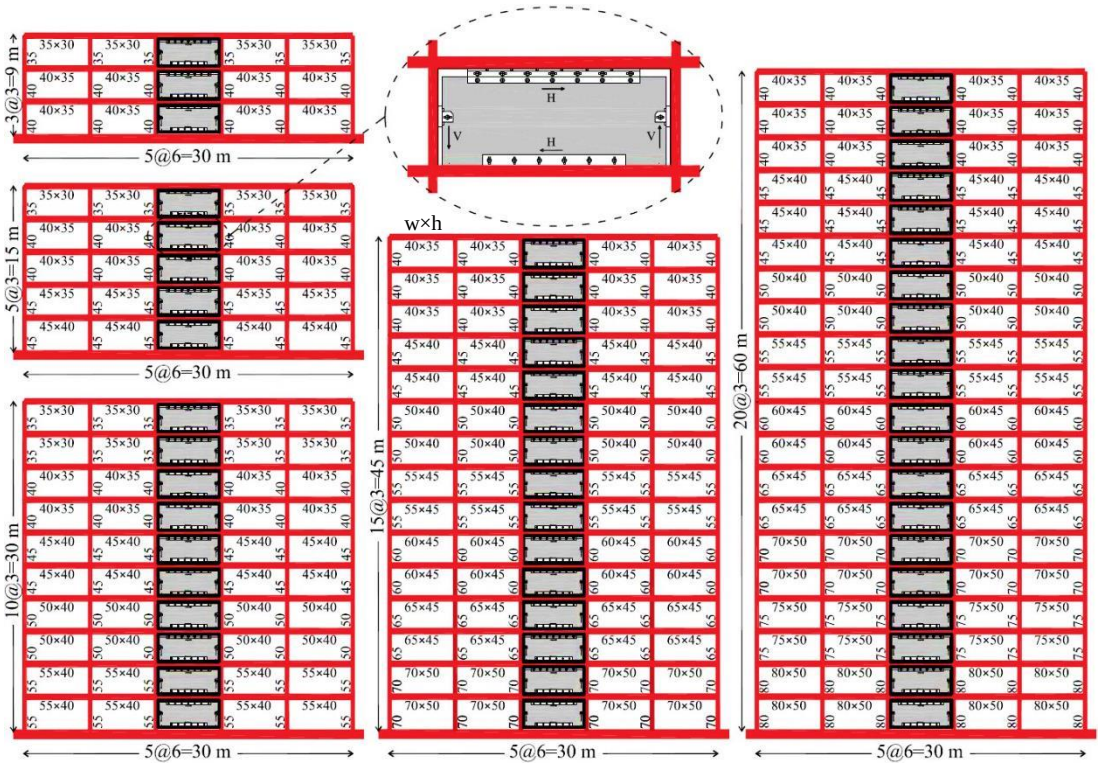


**Fig. 4.1.** Geometry of the reference RC frames equipped with friction wall dampers

### 4.3.2. Friction Wall Dampers

Fig. 4.2 shows the schematic view of the friction wall damper used in this study, which consists of a concrete wall panel attached to the surrounded beam and column elements by using a horizontal support at the bottom, two vertical supports in the lateral sides and a friction connection at the top. Panel-to-column connections with horizontal slots are used in the vertical supports to prevent transferring shear forces to the adjacent columns. The support between the wall panel and the lower floor beam is also fixed horizontally by using vertical slots to avoid transferring additional shear forces to the floor beam. By using this configuration, the lateral movement of the friction device connected to the top of each wall panel would be equal to the inter-storey drift at that level. The friction device is a typical Slotted Bolted Connection (SBC) with two external steel plates fixed to the top edge of the wall panel and a central T-shape slotted stainless steel plate sandwiched between the two external plates and anchored to the top floor beam. The over-sized holes located at the

central stainless steel plate ensure the dry friction between the central plate and the two external brass plates (see Fig. 4.2).

The reliability of the hysteretic behaviour of the slotted bolted connection was proved by Grigorian et al. (1993) through extensive experimental tests under sinusoidal and simulated seismic excitations. In the analytical models developed in this study, an inelastic link element was used to simulate the ideal Coulomb friction hysteretic behaviour of the friction device. An elastic panel element with 15 cm thickness was also utilised to model the wall panel. The concrete wall panels were designed based on the maximum loads that could be transferred from the friction devices and therefore were assumed to remain in the elastic range.

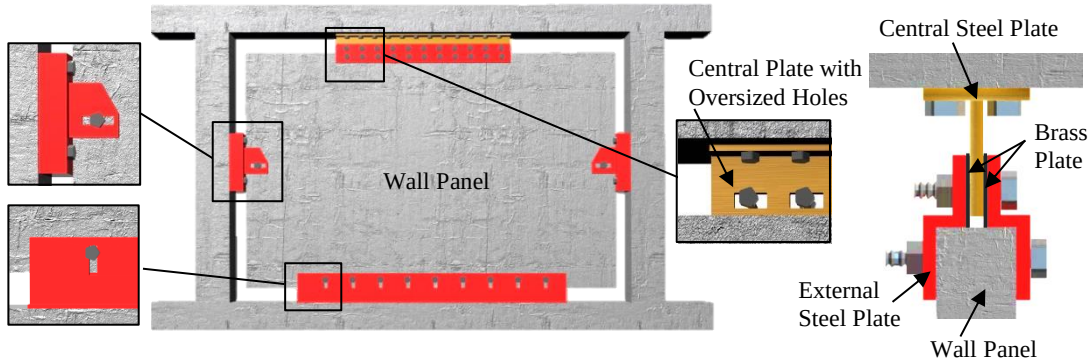


**Fig. 4.2.** Schematic view of the adopted friction-based wall damper and the utilised slotted bolted connection

### 4.3.3. Selected Excitation Records

To demonstrate the efficiency of the proposed optimisation framework, six medium-to-strong ground motions obtained from the Pacific Earthquake Engineering Research Center online database (PEER, 2016) were selected including: Imperial Valley 1979, Superstition Hills 1987, Loma Prieta 1989, Cape Mendocino 1992, Northridge 1994 and Duzce 1999 (see Table 4.1 for more details). These ground motions have high local magnitudes (i.e. Ms>6.5) and were recorded on IBC-2015 soil class D profiles with less than 45 km distance from the epicentre. A set of six synthetic earthquakes were also generated using SIMQKE program (Vanmarke, 1976) to be well-matched with the IBC (2015) design response spectrum for the high seismicity regions (i.e. PGA=0.4g) with site class D. Fig. 4.3 illustrates the elastic acceleration response spectra of the six selected natural earthquakes, the IBC-2015 design spectrum and the average spectrum of the generated synthetic earthquakes. It is shown that both the average spectrum of the natural ground motions and the average spectrum of the synthetic earthquakes provide a close approximation to the IBC response spectrum. This

implies that on average these earthquake records can be used as good representatives of the selected design spectrum.

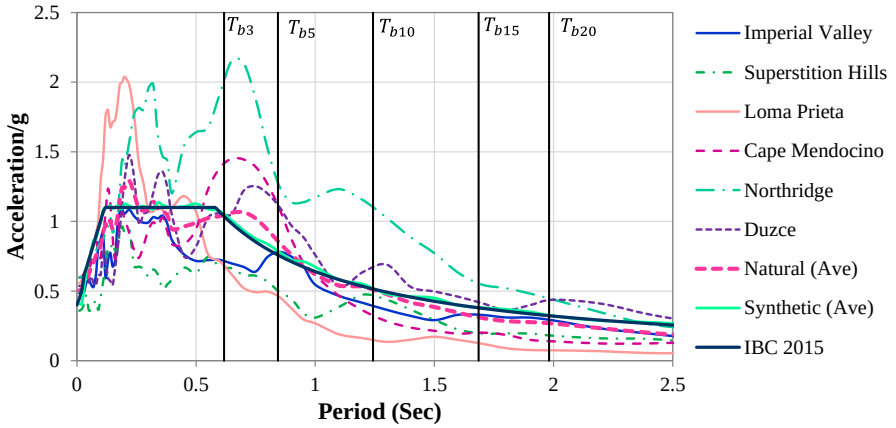


**Fig. 4.3.** Elastic spectral acceleration of natural and synthetic earthquakes and the IBC design spectrum for soil type D, 5% damping ratio

**Table 4.1.** Selected natural earthquake ground motion records

| *No.* | *Earthquake* | *Ms* | *Station/Component* | *Duration (s)* | *PGA (g)* | *PGV (Cm/s)* | *PGD (Cm)* |
|---|---|---|---|---|---|---|---|
| 1 | 1979 Imperial Valley | 6.5 | IMPVALL/H-E04140 | 39 | 0.485 | 37.4 | 20.23 |
| 2 | 1987 Superstition Hills (B) | 6.7 | SUPERST/B-ICC000 | 60 | 0.358 | 46.4 | 17.50 |
| 3 | 1989 Loma Prieta | 6.9 | LOMAP/G03000 | 40 | 0.555 | 35.7 | 8.21 |
| 4 | 1992 Cape Mendocino | 6.9 | CAPEMEND/PET000 | 36 | 0.590 | 48.4 | 21.74 |
| 5 | 1994 Northridge | 6.7 | NORTHR/NWH360 | 40 | 0.590 | 97.2 | 38.05 |
| 6 | 1999 Duzce, Turkey | 7.2 | DUZCE/DZC270 | 26 | 0.535 | 83.5 | 51.59 |

## 4.4. PRACTICAL DESIGN METHODOLOGY

One of the main features of the friction energy dissipation devices is their capability to adjust the slip forces ($F_s$) of the friction connections independently at different levels by regulating the clamping forces of the bolts. This offers the opportunity to use more efficient height-wise slip load distributions to improve the seismic performance of friction energy dissipation devices.

### 4.4.1. Performance Parameters

In this study, maximum inter-storey drift and energy dissipation capacity of friction device were used as main performance parameters to obtain the best design solutions. Maximum inter-storey drift has been widely used in seismic design guidelines (e.g. ASCE/SEI 41-13

(2014)) as a simple and practical failure performance criterion to assess the damage in structural and non-structural elements. The energy dissipation capacity of the dampers is also a good measure to assess the efficiency of the passive control systems under seismic loads.

To assess the energy dissipation capacity of the friction devices, $R_w$ is introduced as the ratio between the friction work of the friction device, $W_{sf}$, and the deformation work of the main structural elements (Petkovski and Waldron, 2003; Nabid et al., 2017).

$$R_w = \frac{W_{sf}}{W_{sb} + W_{sc}} \tag{4.1}$$

where $W_{sb}$ and $W_{sc}$ represent the static work of the beam and column elements, respectively.

Fig. 4.4 illustrates the variation of the average maximum inter-storey drift ratio and energy dissipation parameter, $R_w$, versus slip load ratio for the 3, 5, 10, 15 and 20-storey frames under the six selected natural earthquakes. The frames were designed using the conventional uniform height-wise slip load distribution. For better comparison, the maximum inter-storey drift ratios of the frames with friction wall dampers under different earthquakes were scaled to the maximum inter-storey drift ratios of the corresponding bare frames (i.e. no friction damper). The slip load ratio used in the figures also represents the ratio between the average of the slip loads and the average of the storey shear strengths at all storey levels.

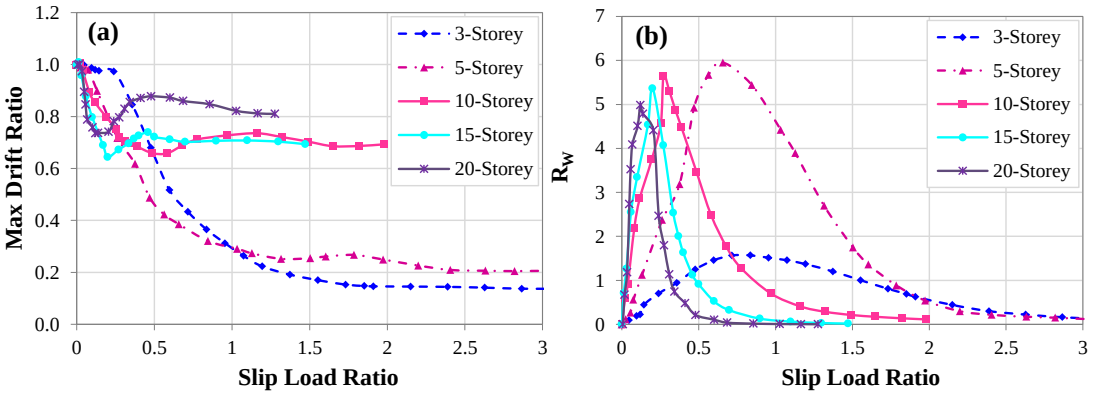


**Fig. 4.4.** Variation of (a) maximum drift ratio and (b) $R_{w2}$ of 3, 5, 10, 15 and 20-storey frames versus slip load ratio (ratio between average of slip loads and average of storey strengths), average of six natural earthquakes

As shown in Fig. 4.4, there is an optimum range of slip load ratios for all the studied frames that on average leads to higher energy dissipation in the friction dampers and lower inter-storey drift ratios. This conclusion is in good agreement with the results reported by

Petkovski and Waldron (2003) and Nabid et al. (2017). It can be noted from Fig. 4.4 (a) that using the friction wall dampers with uniform slip load distribution was more efficient for low to medium-rise frames (i.e. 3 and 5-storey frames) with almost 80% reduction in maximum inter-storey drift compared to the frames with no friction damper (i.e. slip load ratio of zero). This will be discussed in more details in the following sections.

### 4.4.2. Optimum Slip Load Range

In a recent study, Nabid et al. (2017) compared the seismic performance of 3, 5, 10, 15 and 20-storey RC frames with friction-based wall dampers designed based on five different slip load distribution patterns. According to their results, the optimum range of the slip load ratio decreases by increasing the number of storeys, while in general it is not considerably affected by the selected slip load pattern. The following empirical equation was proposed to obtain the optimum slip load ratio for seismic design of multi-storey RC frames with friction-based wall dampers:

$$R = 1.12e^{-0.11n} \tag{4.2}$$

where $R$ is the optimum design slip load ratio and $n$ is the number of storeys. Considering Equation 4.2, the total slip load values can be calculated as follows:

$$\sum_{1}^{n} F_{s,i} = R \times \sum_{1}^{n} F_{y,i} \tag{4.3}$$

Where $F_{s,i}$ and $F_{y,i}$ are the slip load and the storey shear strength of the $i^{th}$ storey. The shear strength of each storey ($F_{y,i}$) can be easily calculated by conducting a non-linear pushover analysis (Hajirasouliha and Doostan, 2010). The total slip load values can be then distributed along the height of the structure using any prescribed distribution pattern. If the uniform height-wise slip load distribution is considered, the slip load values at each storey level ($F_{s,i}$) can be easily calculated using the equation below:

$$F_{s,i} = \frac{R}{n} \times \sum_{1}^{n} F_{y,i} = \frac{1.12e^{-0.11n}}{n} \times \sum_{1}^{n} F_{y,i} \tag{4.4}$$

It should be mentioned that for practical applications a uniform slip load distribution is commonly used for the seismic design of friction dampers. While this distribution pattern can simplify the design process, it does not necessarily lead to the best design solution under different input earthquakes (Nabid et al., 2017). Therefore, in the following section, an

optimum design methodology is proposed to obtain more efficient slip load distribution patterns.

## 4.5. PROPOSED PERFORMANCE-BASED OPTIMISATION METHODOLOGY

In conventionally designed friction wall dampers (i.e. uniform slip load distribution), the deformation demand under strong earthquakes may not utilise the maximum level of seismic capacity in certain storeys while localised damage may be observed in the other storeys. If the slip loads at storeys with large inter-storey drifts are increased incrementally, while the slip loads are decreased at storeys with small drifts, it is expected to eventually obtain a status of uniform displacement demand. In such a case, the maximum capacity of each friction device to dissipate the earthquake input energy is utilised. It should be mentioned that a similar concept has been previously used by other researchers for optimum seismic design of different types of structural systems including shear-buildings (Moghaddam and Hajirasouliha, 2008; Ganjavi et al., 2016), truss-like structures (Hajirasouliha et al., 2011), RC frames (Hajirasouliha et al., 2012), and viscous dampers (Levy and Lavan, 2006). However, this is the first time that this concept is adopted for seismic design of friction based energy dissipation devices to obtain the best height-wise distribution of the slip loads. On the other hand, a new iterative process is suggested for friction-based dampers to provide optimum design solutions at low computational cost. The proposed method can be used to optimise the seismic behaviour of the structures using different performance parameters such as inter-storey drift and energy dissipation capacity of the dampers.

Maximum inter-storey drift is widely accepted as an effective and practical response parameter to estimate the damage to both structural and non-structural components in building structures (e.g. ASCE 41-13 (2014)). By considering the maximum inter-storey drift as the main design parameter, the following optimisation algorithm is adopted in this study:

1) The friction wall dampers are initially designed with uniform slip load distribution using the slip load values obtained from Equation 4.4. It will be shown in the next section that the optimum design solution is independent of the initial slip load distribution.

2) The structure is subjected to the selected design earthquake and the corresponding performance parameters (here maximum inter-storey drift values) are obtained. The slip load values are then redistributed based on the ratio between the maximum inter-storey drift at

each level and the average of the all storey drifts. Using the proposed equation, the slip load is increased in the storeys where the inter-storey drift exceeded the average inter-storey drift, and reduced in the storeys with inter-storey drifts below the average value until a uniform height-wise inter-storey drift distribution is obtained:

$$\left(F_{s,i}\right)_{n+1} = \left(F_{s,i}\right)_n \times \left(\frac{\Delta_i}{\Delta_{ave}}\right)_n^{\alpha} \tag{4.5}$$

where $\Delta_i$ and $\Delta_{ave}$ are the maximum drift at $i^{th}$ storey and the average of all storey drifts, respectively, at $n^{th}$ iteration. $\alpha$ is a convergence parameter ranging from 0 to 1. It will be shown in the following sections that this parameter can significantly affect the convergence and the computational cost of the nonlinear optimisation problem. The value of this factor depends on several parameters such as the type of structure, number of storeys and optimisation algorithm. In this study, $\alpha$ factor was set to be 0.2 for all the optimisation procedures. It should be mentioned that the proposed equation is general and can be applied to any RC frames with friction dampers irrespective of the number of storeys and the type of the friction dampers (i.e. wall or brace-type).

3) To control the additional base shear and column axial forces imposed by the friction wall dampers, the new slip loads obtained from the previous step are scaled so as the average of the slip loads in different storeys remains unchanged compared to the initial step ($F_{s,i}$ in Equation 4.4).

4) The coefficient of variation is defined as the ratio of the standard deviation (the square root of the variance) to the mean value of a population. It shows the extent of variability in relation to the mean of the population. The coefficient of variation (COV) of inter-storey drifts (selected damage index) is calculated for each step using Equation 4.6 to control the dispersion of each storey drift relative to the mean value. The design procedure is then repeated from step 2 until the $COV_\Delta$ is small enough (e.g. less than 10). Based on the concept of Uniform Damage Distribution, the design solution can be considered as practically optimum at this stage.

$$\left(COV_\Delta\right)_n = \left(\frac{\sqrt{(Var_\Delta)_n}}{(Ave_\Delta)_n}\right) \times 100 \tag{4.6}$$

where $Var_\Delta$ and $Ave_\Delta$ are the variance and the average of all storey drifts, respectively.

### 4.5.1. Optimum Design for the Selected Natural Earthquakes

The proposed optimisation algorithm is used to obtain the optimum slip load distribution of the 3, 5, 10, 15 and 20-storey frames for the six selected natural earthquakes given in Table 4.1. Fig. 4.5 compares the height-wise inter-storey drift distribution of optimum design frames and those designed with uniform slip load distribution under each design earthquake. The horizontal axis is the ratio between the maximum drift of the reference frame at each storey to the maximum drift of the corresponding bare frame, denoted as "maximum drift ratio".

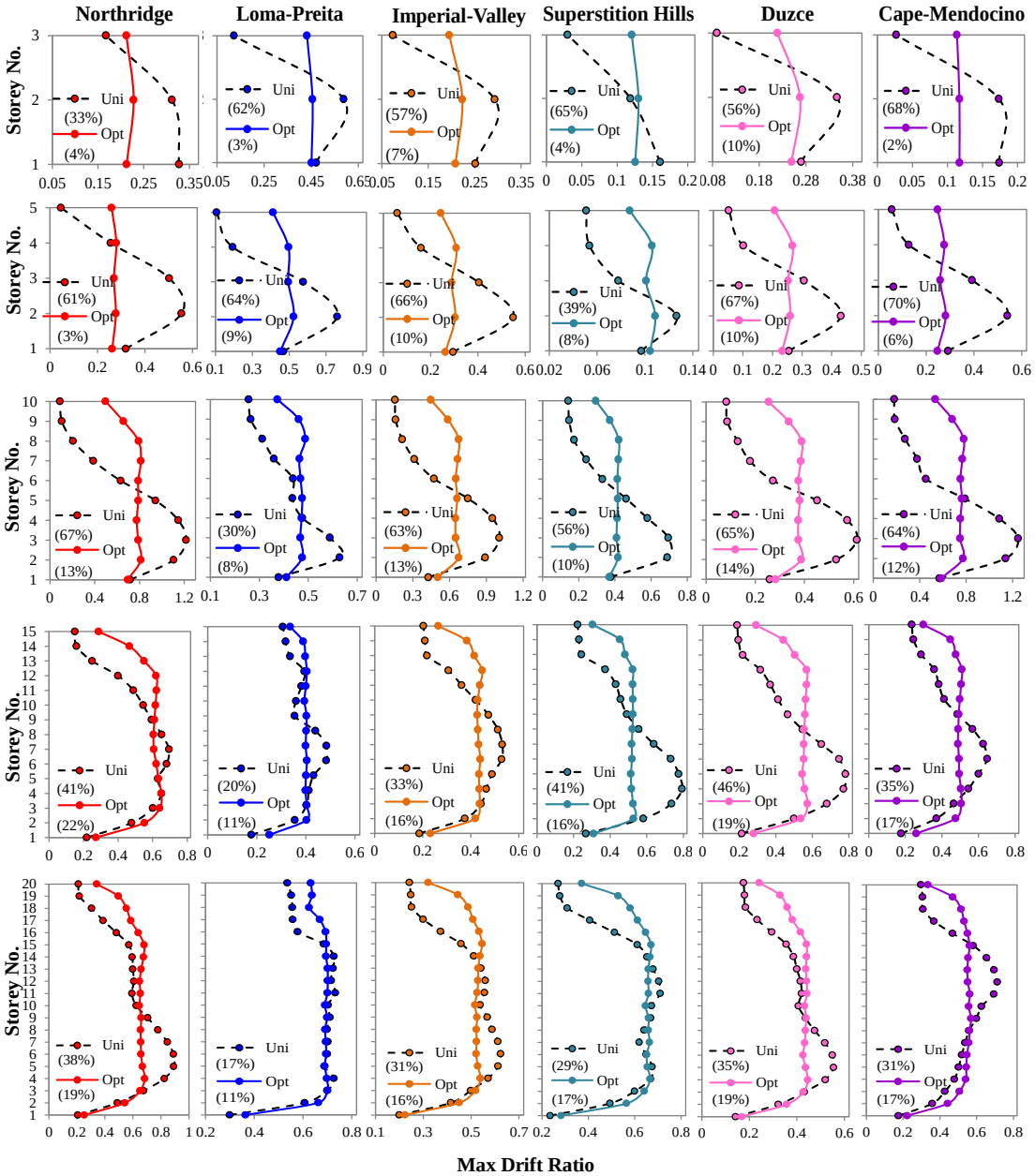


**Fig. 4.5.** Height-wise distribution and COV (%) of maximum inter-storey drift ratios (scaled to the maximum drift of the corresponding bare frame) for 3, 5, 10, 15 and 20-storey frames, six natural earthquakes

The results in Fig. 4.5 indicate that the optimum design frames exhibit a more uniform height-wise distribution of inter-storey drifts and a considerably lower maximum inter-storey drift ratio, which is consistent with the concept of Uniform Damage Distribution. Therefore, the proposed design method can efficiently prevent damage concentration and soft storey failure in multi-storey frames. Table 4.2 summarizes the reductions in the maximum lateral drifts for the reference frames under the six natural earthquakes when designed using the proposed optimum design methodology compared to the conventional design using the uniform slip load distribution. It is shown that using the optimum distribution of the slip loads in the friction energy dissipation devices resulted in up to 33, 50, 39, 34, and 23% reductions in the maximum drift ratios for the 3, 5, 10, 15 and 20-storey frames, respectively.

It should be mentioned that the efficiency of the proposed optimisation method is in general lower for high-rise buildings (i.e. 15 and 20-storey frames), since the uniform slip load distributions led to a relatively more uniform distribution of maximum lateral drifts and therefore lower $COV_{\Delta}$ values as shown in Fig. 4.5.

**Table 4.2.** Reduction of the maximum drift ratios for the optimum design 3, 5, 10, 15 and 20-storey frames compared to conventionally designed frames, six natural earthquakes

| *Earthquake* | *3-Storey* | *5-Storey* | *10-Storey* | *15-Storey* | *20-Storey* |
|---|---|---|---|---|---|
| Northridge | 30.5% | 49.7% | 33.2% | 6.3% | 23.3% |
| Loma Prieta | 22.6% | 31.1% | 22.4% | 16.4% | 4.3% |
| Imperial Valley | 23.9% | 43.9% | 32.9% | 15.8% | 12.5% |
| El Centro | 19.1% | 14.1% | 39.4% | 33.5% | 5.6% |
| Duzce | 22.9% | 38.0% | 36.6% | 26.6% | 19.7% |
| Cape Mendocino | 32.6% | 47.8% | 37.6% | 21.3% | 20.1% |
| *Average* | *25.2%* | *37.4%* | *33.7%* | *20.0%* | *14.3%* |

### 4.5.2. Optimum Design for the Synthetic Spectrum-Compatible Earthquakes

To include the ground motion variability, the accuracy of the proposed optimum design method is also evaluated for the set of six synthetic spectrum-compatible earthquakes having the average acceleration response spectrum close to the IBC-2015 design spectrum. As mentioned before, the obtained synthetic records can be considered as good representatives of the IBC design response spectrum.

Fig. 4.6 (a) shows the variation of the maximum inter-storey drifts for the reference frames as the optimisation iterations proceed. A faster convergence was generally observed for the

low-rise frames (i.e. 3 and 5-storey); however in all cases the optimum solution was obtained in less than 20 steps with almost no oscillation. It should be noted that to obtain the optimum design solutions using heuristic optimisation methods such as Genetic Algorithm (GA) and Particle Swarm Optimisation would require over 50,000 non-linear dynamic analyses (e.g. 100 samples, 500 generations). This clearly highlights the computational efficiency of the proposed optimisation method. As an example, the evolutionary change in the height-wise maximum drift distribution of the 10-storey frame is illustrated in Fig. 4.6 (b). It is shown that the maximum drift distribution is considerably more uniform in the optimum solution (i.e. step 20) compared to the conventional design based on uniform slip load distribution (i.e. step 0), while the maximum drift is also reduced.

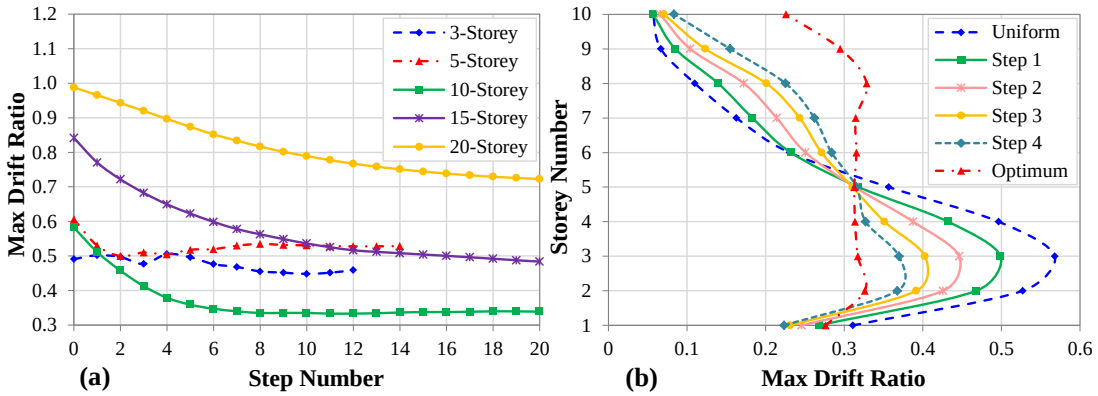


**Fig. 4.6.** Variation of (a) maximum inter-storey drift ratios (scaled to the maximum drift of the corresponding bare frame) for 3, 5, 10, 15 and 20-storey frames, and (b) height-wise distribution of maximum drift ratios for 10-storey frame, average of six synthetic earthquakes, $\alpha$=0.2

Fig. 4.7 shows the height-wise distribution of the maximum inter-storey drift ratios (ratio of the maximum drift in the frame with friction damper to that of the corresponding bare frame) and the slip load ratios (ratio of the slip load to the average of the storey shear strengths) for 3, 5, 10, 15, and 20-storey frames designed based on the conventional uniform and optimum slip load distributions (with the same average) subjected to the synthetic design earthquakes. Similar to the natural earthquake records, the results in Fig. 4.7 (a) indicate that the optimum design models always exhibit a considerably more uniform distribution of inter-storey drifts and a lower maximum inter-storey drift compared to the conventional design solutions. The proposed performance-based optimisation procedure could efficiently identify the storeys in which the friction wall damper is not required. For example, it is shown in Fig. 4.7 (b) that the slip load values at the first and the upper storey levels in medium to high-rise frames (10, 15 and 20-storey frames) tend to zero. This will in turn lead to more economical design solutions with less number of friction dampers.

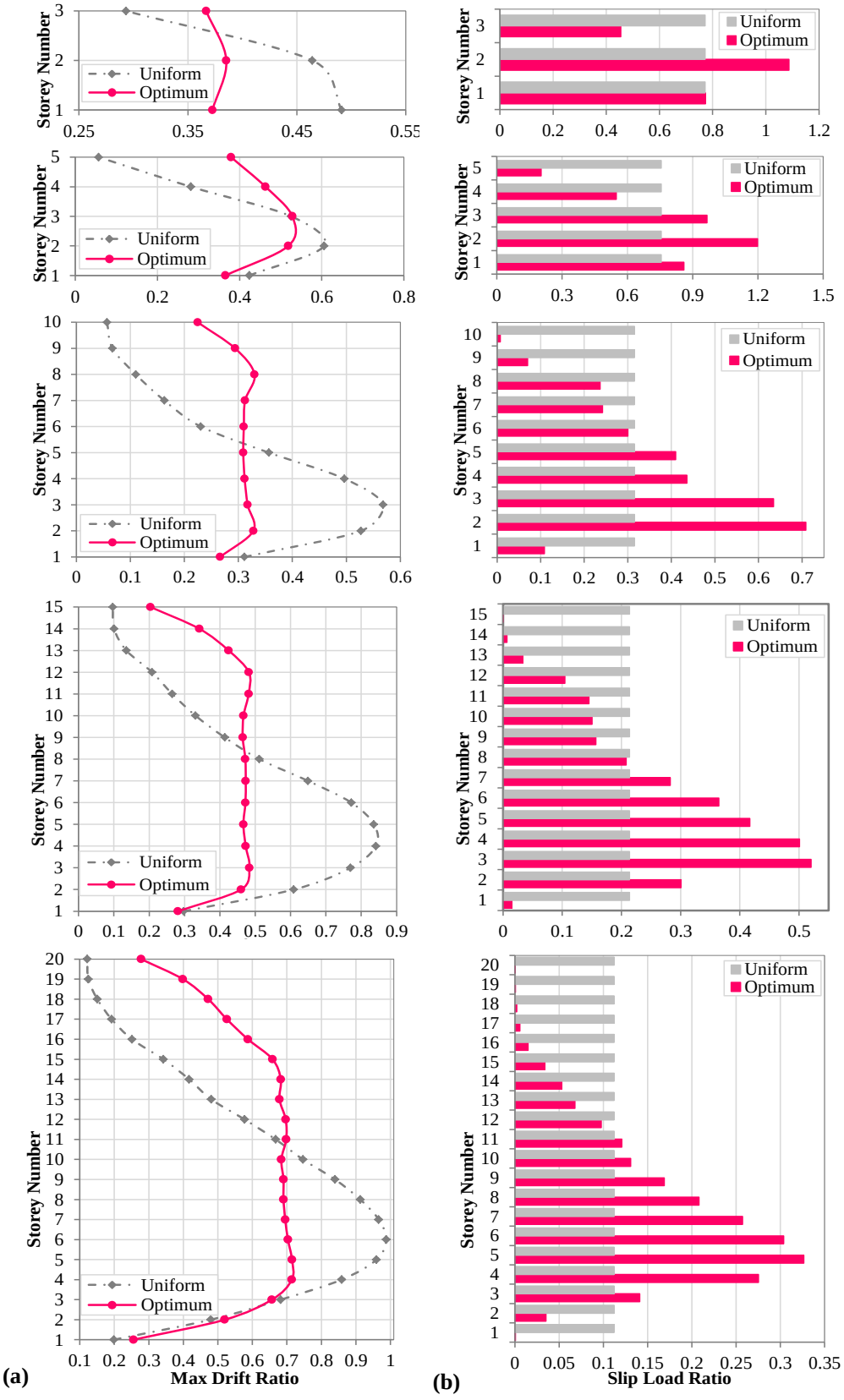


**Fig. 4.7.** Height-wise distribution of (a) maximum drift ratios (scaled to the maximum drift of the corresponding bare frame) and (b) slip load ratios (scaled to the average of storey shear strengths) for 3, 5, 10, 15 and 20-storey frames designed with uniform and optimum slip load distributions, average of six synthetic earthquakes

Fig. 4.8 compares the maximum inter-storey drift, column axial load, base shear and energy dissipation capacity ($R_w$) of the optimum design frames with those designed using uniform slip load distributions. The results in Figs. 4.8 (a) to (c) are the ratio of the response of the optimum frame to that of the corresponding bare frame. The results in general indicate that, compared to conventional design solutions, using the proposed optimisation method could considerably increase the energy dissipation in the friction devices (up to 46%) and reduce the maximum inter-storey drifts (up to 43%) under synthetic spectrum-compatible earthquakes, while the maximum column axial load and the base shear ratios were almost unchanged (less than 4% difference).

It can be noted from Fig. 4.8 (d) that the improvement in the energy dissipation capacity was less pronounced in the 20-storey frame; however, using the optimum slip load distribution could still reduce the maximum inter-storey drifts by 28%. The maximum reduction in the inter-storey drift was observed in the 10 and 15-storey frames, where the optimum design procedure could reduce the maximum inter-storey drifts by more than 40%.

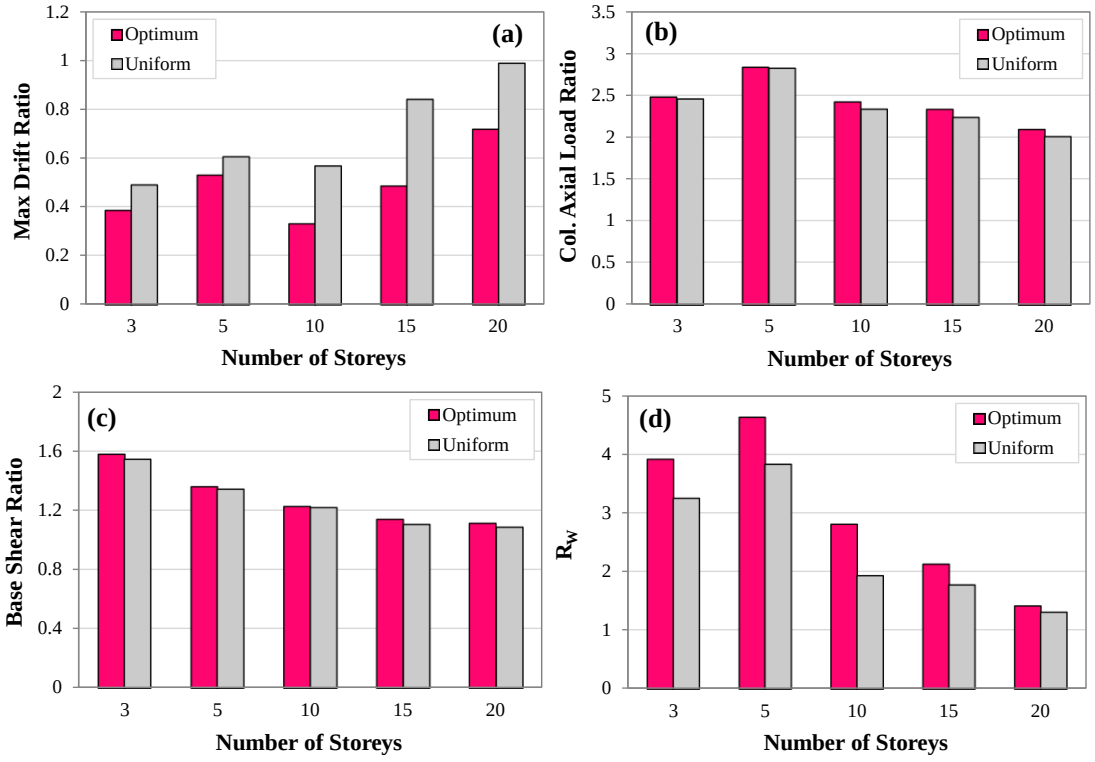


**Fig. 4.8.** (a) Inter-storey drift, (b) axial load and (c) base shear of 3, 5, 10, 15 and 20-storey frames with damper to those of the corresponding bare frames, and (d) energy dissipation capacity of the optimum and conventional design frames, average of six synthetic earthquakes

## 4.6. SENSITIVITY ANALYSES

### 4.6.1. Effect of Initial Slip Load Distribution

The effect of initial slip load distribution was investigated on the proposed optimisation method by considering three different distribution patterns including the conventional uniform, inverted triangular cumulative and uniform cumulative (shown in Fig. 4.9) for preliminarily design of the 5-storey frame under a synthetic earthquake. For better comparison, a similar average slip load was used in all preliminarily designed frames. Fig. 4.9 compares the corresponding variations of the slip load values for each individual storey as the iterations proceed.

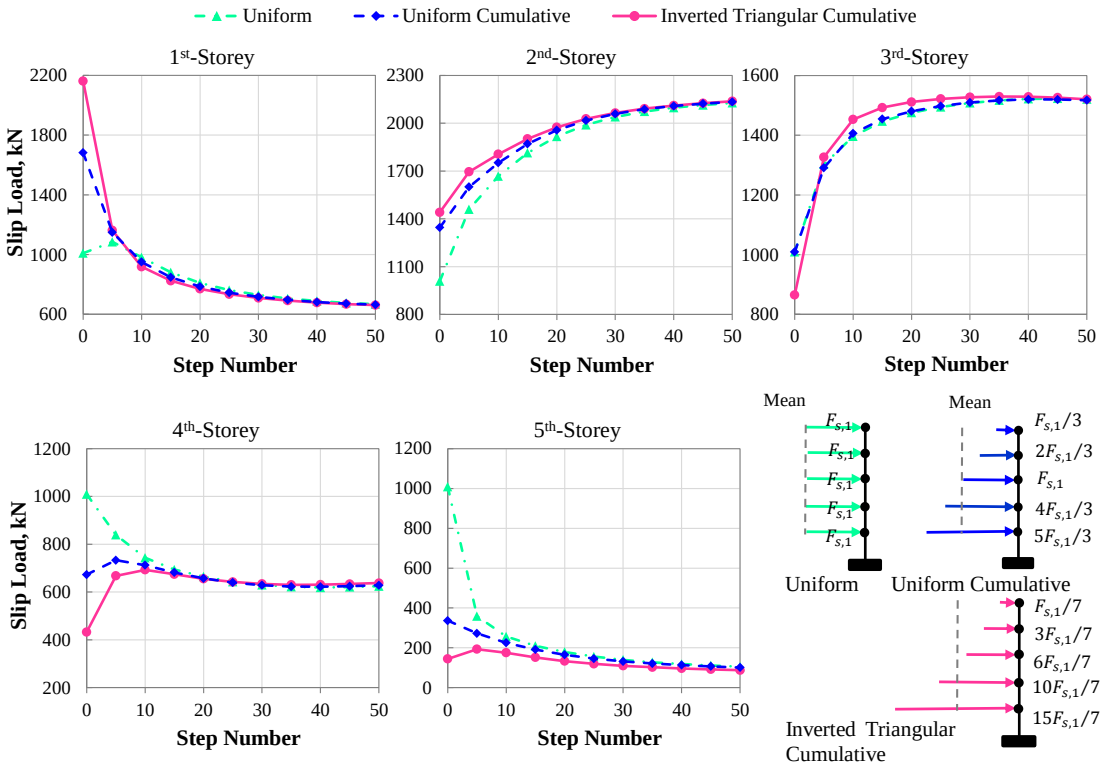


**Fig. 4.9.** Variation of slip load at each individual floor using different initial distribution patterns, 5-storey frame, α=0.2, synthetic earthquake

The graphs show that in the first few steps of the optimisation, there were considerable discrepancies between the slip load values using different initial slip load patterns. However, as the iterations proceed, depending on the floor level and the initial distribution pattern, the slip loads were either decreased or increased to converge to a certain value. This implies that the final optimum solution is independent from the initial slip load distribution considered in the optimisation process. However, using an appropriate initial design can result in a faster convergence to the final optimum solution. In this example, the uniform cumulative pattern

which was previously suggested by Nabid et al. (2017) as a more efficient slip load pattern is shown to converge to the optimum solution in a slightly smaller number of steps.

### 4.6.2. Effect of Convergence Parameter

The convergence parameter α plays an important role in the computational efficiency of the proposed optimisation method. Comprehensive sensitivity analyses were performed to obtain the most appropriate values of α for optimum design of RC frames with friction wall dampers. For example, Fig. 4.10 illustrates the variation of the maximum inter-storey drift ratios in 5 and 10-storey frames during optimisation process under a synthetic earthquake for α values of 0.01, 0.05, 0.1, 0.2, 0.5 and 1, starting from a reference frame designed with uniform cumulative slip load distribution. It is shown that in general as α increases from 0.01 to 0.5, the speed of convergence increases without any significant fluctuation. However, for α values greater than 0.5, the proposed method does not converge to the optimum design solution in both 5 and 10-storey frames. Also it can be noted that the convergence speed for the α values less than 0.2 is very slow, and therefore, a substantially higher number of steps is required to obtain the optimum solution. This indicates that an acceptable convergence is obtained by using α factor between 0.2 and 0.5. A similar conclusion was obtained from other frames and seismic excitations. All analyses in this study were carried out using the convergence factor equal to 0.2.

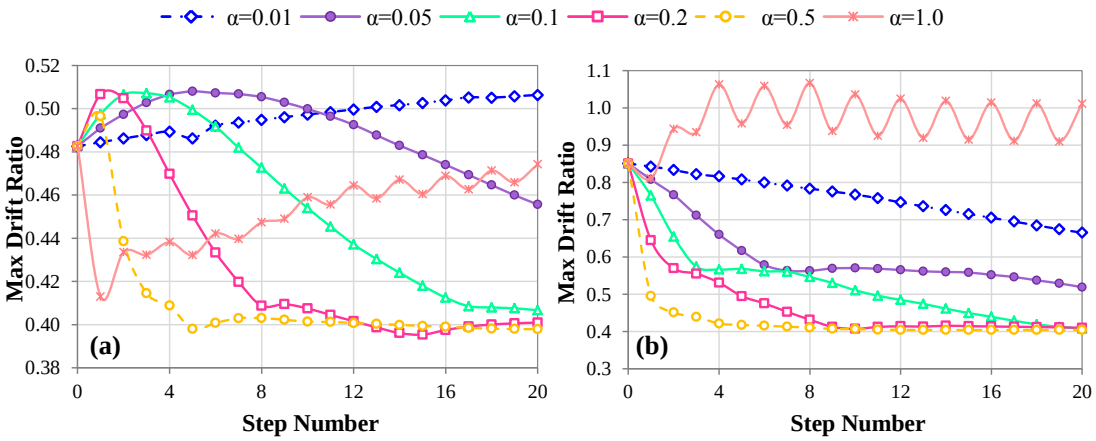


**Fig. 4.10.** Variation of maximum inter-storey drift ratios (scaled to the maximum drift of the corresponding bare frame) for (a) 5-storey and (b) 10-storey frames using different values of convergence parameter α

### 4.6.3. Effect of Design Earthquake

The optimum distribution of the slip load pattern is influenced by the characteristics of the design earthquake and therefore varies from one earthquake to another. To study the effect of the design earthquake on the optimum solution, the reference frames were optimised for

the six natural earthquake records listed in Table 4.1. Fig. 4.11 compares the optimum and uniform distributions of the slip load ratios (ratio of the slip load to the average of the storey shear strengths) under the selected earthquakes for the 5 and 10-storey frames. For better comparison, the results are scaled to the average storey shear strength. It can be seen that while there are some discrepancies between the optimum slip load values at each floor for different earthquakes, the general distribution of the optimum slip loads follow a similar trend. A similar conclusion was also obtained for the other frames. This can be explained as the selected spectrum compatible earthquakes are all strong ground motions recorded on a similar soil class profile, and therefore, have almost similar characteristics.

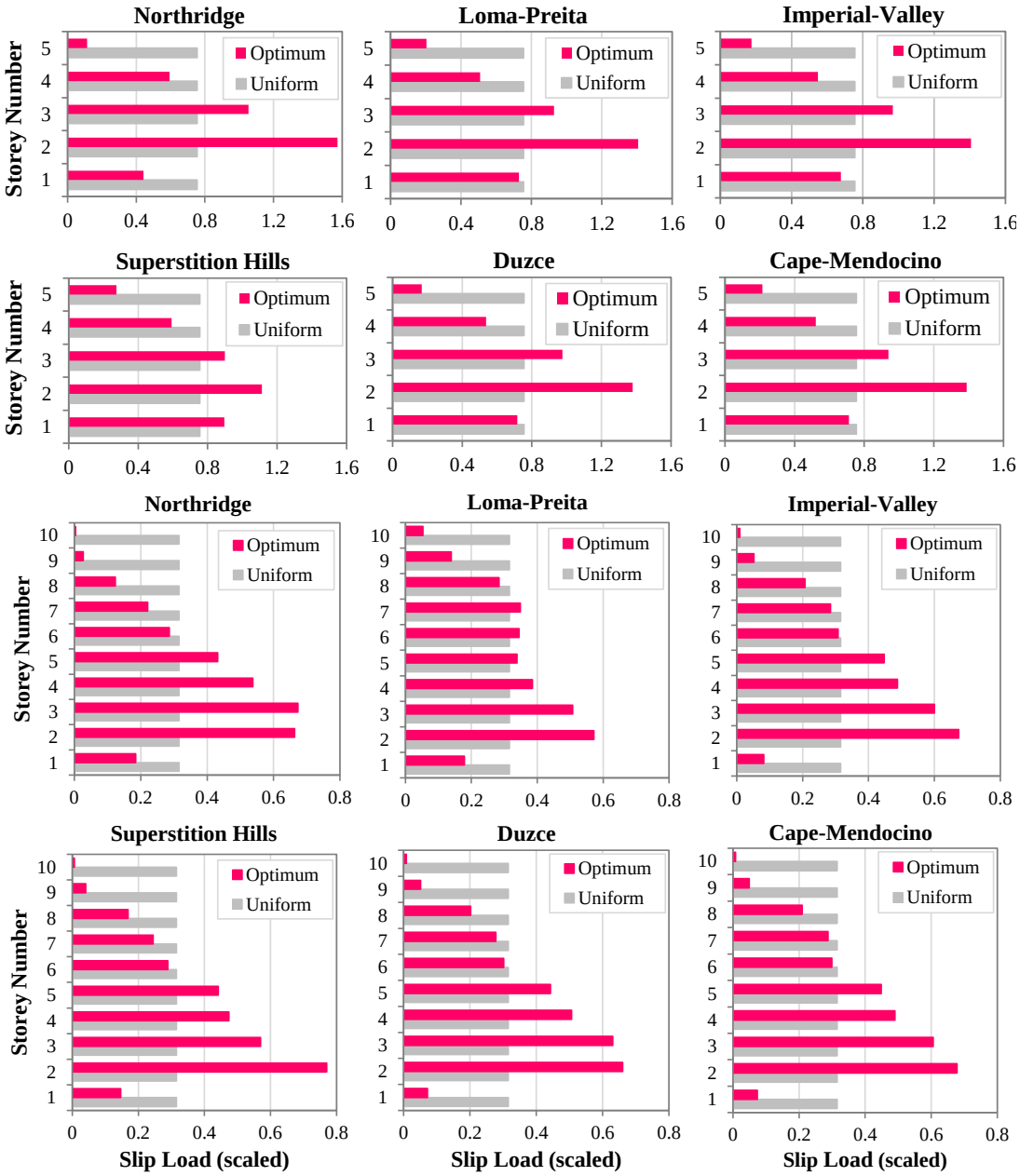


**Fig. 4.11.** Comparison of optimum and uniform distribution of slip load ratios (scaled to the average of storey shear strengths) for 5 and 10-storey frames under six natural earthquakes

## 4.7. GLOBAL DAMAGE INDEX

To assess the efficiency of the adopted optimisation methodology to reduce the overall structural damage under seismic excitations, a cumulative damage index is used based on a classical low-cycle fatigue approach (Krawinkler and Zohrei, 1983). Variations in the energy dissipation capacity of the structure were taken into account as a function of displacement demands in the adopted damage model (Miner, 1945; Teran-Gilmore and Jirsa, 2004). Independent damages are assumed to be caused by different plastic excursions which are identified by using a Rainbow Counting Method (Powell and Allahabadi, 1987). The cumulative damage index is calculated using the following equation:

$$DI_i = \sum_{j=1}^{N} \left( \frac{\Delta\delta_{pj}}{\delta_u} \right)^c \tag{4.7}$$

where $DI_i$ and N are defined as cumulative damage index at $i^{th}$ storey and the total number of plastic excursions, respectively. The cumulative damage index ranges from 0 for intact to 1 for completely damaged storeys. $\Delta\delta_{pj}$ is considered as the plastic displacement of the $j^{th}$ excursion, $\delta_u$ is the ultimate plastic displacement, and the power factor c is the structural parameter accounting for the effect of plastic deformation magnitude. As suggested by Cosenza and Manfredi (1996), *c* is assumed to be 1.5 in this study.

To estimate the level of damage exhibited by the entire structure, the global damage index, $DI_g$, is defined as a weighted average of the damage indices at all storey levels, with the weighting function being the energy dissipated at each storey.

$$DI_g = \frac{\sum_{i=1}^{n} DI_i W_{pi}}{\sum_{i=1}^{n} W_{pi}} \tag{4.8}$$

where $n$ is the number of storey levels, $DI_i$ is the damage index at $i^{th}$ storey and $W_{pi}$ is the dissipated energy at $i^{th}$ storey. Fig. 4.12 (a) compares the average global damage indices of the 3, 5, 10, 15 and 20-storey bare frames with the frames designed using the conventional uniform and the optimum slip load distributions under the spectrum compatible synthetic earthquakes. It is evident that the proposed friction wall dampers with the uniform slip load distribution could considerably reduce the global damage index of low to medium-rise bare frames (i.e. 3 to 10-storey), while they were not very efficient for tall buildings (i.e. 15 and 20-stroey). Using optimum design dampers, however, could efficiently reduce the global damage index in all cases. The results indicate that, compared to the conventionally designed

frames with uniform slip load distribution, the proposed optimum design methodology decreased the global damage index of the 3, 5, 10, 15 and 20-storey frames by 49%, 23%, 75%, 65% and 38%, respectively.

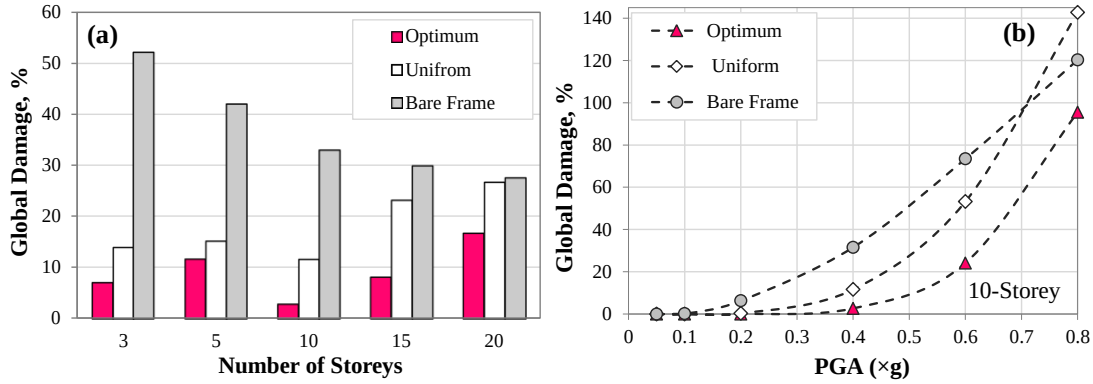


**Fig. 4.12.** Global damage index of the bare frames and the frames with friction dampers designed based on uniform and optimum slip load distributions: (a) 3, 5, 10, 15 and 20-storey frames, (b) Incremental dynamic analysis of 10-storey frames, average of six synthetic earthquakes

The efficiency of the proposed optimisation method is also evaluated for low-to-high earthquake intensity levels. Incremental dynamic analyses were conducted on the 10-storey bare frame and the frames with friction wall dampers designed based on uniform and optimum slip load distributions. Fig. 4.12 (b) compares the average of the global damage indices ($DI_g$) of the frames under the set of six synthetic spectrum-compatible earthquakes. The PGA of the input earthquakes was ranged from 0.05g to 0.8g to cover small to large magnitude earthquakes. The results show that the frames with optimum design friction wall dampers experience considerably less global damage (up to 77%) at all intensity levels compared to those with conventional friction dampers. It is especially evident that the efficiency of the friction dampers with uniform slip load distribution is significantly reduced for earthquakes with PGA levels higher than 0.6 g. The main reason is that using identical slip load values at all storey levels leads to a high concentrated lateral displacement and localised damage at certain storeys, while the optimum slip load distribution obtained from the proposed design methodology results in a more uniform distribution of storey damage.

## 4.8. OPTIMUM DESIGN SOLUTION FOR A CODE DESIGN SPECTRUM

The seismic ground motion is the main source of uncertainty in the seismic design of structures. Therefore, there is a concern that this may influence the efficiency of the optimum structures that are designed based on a single earthquake event. Previous study by

Hajirasouliha et al. (2012) confirmed that, for performance-based design of RC structures, a better seismic design can be obtained by using a synthetic earthquake representing the average spectrum of a set of natural earthquakes. In this study, the efficiency of this concept is evaluated for optimum design of RC frames with friction wall dampers for a specific code design spectrum.

Fig. 4.13 compares the average optimum slip load ratio (ratio of the slip loads to the average of the storey shear strengths) distributions obtained for the 10-storey frames with friction-based wall dampers subjected to the selected natural and synthetic earthquakes. As it was mentioned in Section 3.3, the average spectrum of the six natural ground motions and the average spectrum of the six synthetic earthquakes both have a very good agreement with the selected IBC-2015 design spectrum (see Fig. 4.3). It can be seen from Fig. 4.13 that the optimum slip load distributions corresponding to the natural and synthetic earthquakes are almost identical. This implies that there is a unique optimum design solution for each frame subjected to the design spectrum. Therefore, to manage the uncertainty of the design seismic loads, the frames can be designed based on the average of the optimum slip load distributions corresponding to the set of earthquakes representing the design spectrum.

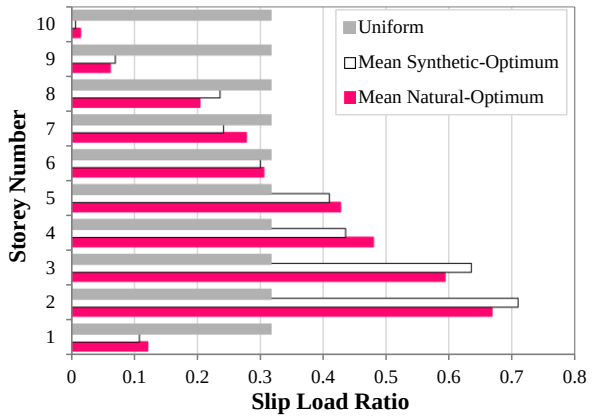


**Fig. 4.13.** Comparison of uniform and average of optimum slip load distributions for the six synthetic and six natural earthquakes (scaled to the average of storey shear strengths).

Fig. 4.14 compares the maximum inter-storey drift ratios and global damage indices of the 10-storey frames designed based on (a) uniform slip load distribution, (b) average of optimum slip load distributions for the six synthetic spectrum compatible earthquakes, and (c) optimum slip load distribution corresponding to each individual natural earthquake. The results indicate that while using the average of the optimum slip loads obtained for the synthetic earthquakes (i.e. Ave Synthetic-Optimum) is not as efficient as using the specific optimum slip load pattern obtained for each earthquake, it is still considerably more efficient than the conventional slip load pattern. For the same average of slip loads, it can be seen

from Fig. 4.14 (a) that the 10-storey frames designed with the Ave Synthetic-Optimum pattern exhibit on average 24% (by up to 34%) less maximum inter-storey drift compared to their conventionally designed counterparts using uniform slip load distribution. Similarly Fig. 4.14 (b) shows that using the average optimum slip load pattern resulted in by up to 72% lower global damage under the selected natural earthquakes. This can confirm the efficiency of using the average of optimum load patterns corresponding to a set of synthetic spectrum-compatible earthquakes (representatives of the design spectrum) to achieve better and more effective seismic design solutions for RC frames with friction-based wall dampers.

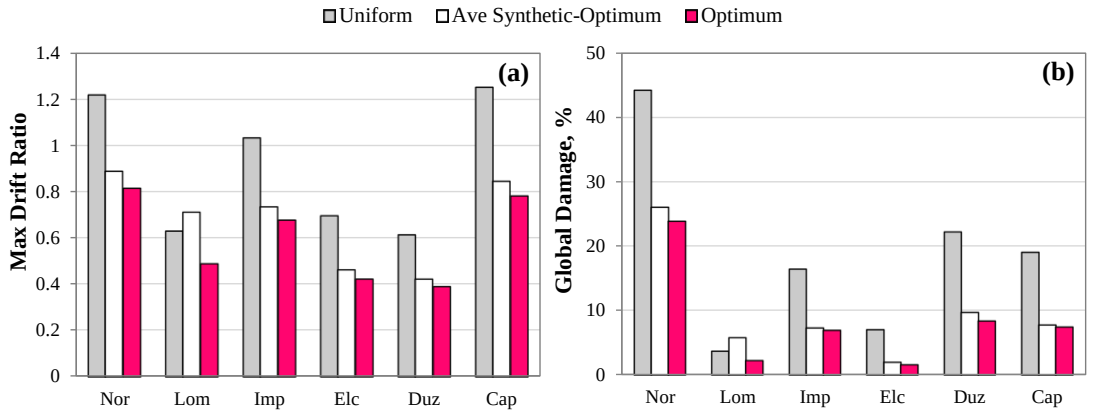


**Fig. 4.14.** (a) Maximum drift ratio (scaled to the maximum drift of the corresponding bare frame) and (b) Global damage index of 10-storey frames designed with uniform slip load distribution, average of the optimum slip loads obtained for the synthetic earthquakes (Ave Synthetic-Optimum), and the optimum load patterns obtained for each individual earthquake (optimum)

Overall, the results of this study demonstrate the efficiency and reliability of the proposed optimisation method, which can provide an efficient tool for optimum seismic design of friction energy dissipation devices for practical purposes. It should be mentioned that the proposed methodology is general and can be adopted for optimum performance-based design of other types of dampers and structural systems.

## 4.9. SUMMARY AND CONCLUSIONS

A low-cost performance-based optimisation method was proposed to enhance the seismic performance of RC frames with friction-based wall dampers using the concept of uniform damage distribution. The efficiency of the method was demonstrated through the optimum design of 3, 5, 10, 15, and 20-storey RC frames with friction wall dampers under six natural and six synthetic spectrum-compatible earthquakes. The proposed method could efficiently converge to the best design solution by obtaining the optimum slip load distribution and

removing less efficient dampers in only a few steps. The proposed method was then further developed to deal with the optimum design of friction dampers for a specific design spectrum. The following conclusions can be drawn based on the results of this study:

- It was shown that the convergence parameter, $\alpha$, has a major effect on the computational cost and convergence of the optimisation process. The $\alpha$ values ranging from 0.2 to 0.5 were shown to be generally more efficient to converge to the optimum design solutions for friction-based wall dampers in only a few steps. The results of sensitivity analyses also indicated that the optimum solution is independent from the initial slip load distribution considered in the optimisation process. However, using a suitable initial design can result in a faster convergence.

- Compared to the conventionally designed friction wall dampers with uniform slip load distribution, the optimum design dampers exhibited up to 43% and 75% lower inter-storey drift ratios and global damage indices, respectively, when subjected to the synthetic spectrum-compatible earthquakes. It was shown that, for the same total friction force, using the proposed optimisation method can increase the energy dissipation capacity of the friction wall dampers by up to 46%. The improvement in the energy dissipation capacity was more pronounced in low to medium-rise buildings. The efficiency of the proposed method was also demonstrated under the set of six natural earthquakes, where using optimum design dampers in 3 to 20-storey frames resulted in up to 50% lower inter-storey drift ratios compared to their conventionally designed counterparts.

- By performing nonlinear incremental dynamic analyses, it was shown that the proposed optimum design method can significantly reduce (up to 77%) the global damage index of the conventionally designed frames over a wide range of earthquake PGA levels. The optimum design systems were shown to be efficient at all intensity levels, while the efficiency of the frames with conventionally designed friction dampers was significantly reduced at higher PGA levels.

- Although the final optimum solution is influenced by the characteristics of the input earthquake excitation, the results indicated that the distribution of the optimum slip loads for the set of spectrum compatible earthquakes follow a similar trend. It was shown that the seismic load uncertainty can be efficiently managed by using the average of optimum load patterns corresponding to the synthetic earthquakes representing the design spectrum. The friction wall dampers designed with average

optimum slip load pattern exhibited up to 34% less maximum inter-storey drift and 72% less cumulative damage.

## REFERENCES

ACI 318-14 (2014). "Building Code Requirements for Structural Concrete and Commentary on Building Code Requirements for Structural Concrete (ACI 318R-14)." *American Concrete Institute*, Farmington Hills, MI.

Adachi, F., Yoshitomi, S., Tsuji, M. and Takewaki, I. (2013). "Nonlinear optimal oil damper design in seismically controlled multi-storey building frame." *Soil Dynamics and Earthquake Engineering*, **44**: 1–13.

Agrawal, A. K. and Yang, J. N. (1999). "Design of passive energy dissipation systems based on LQR control methods." *Journal of Intelligent Material Systems and Structures*, **10**: 933–944.

Aiken, I. (1996). "Passive energy dissipation - hardware and applications." *In Proceedings: Los Angeles County and Seaosc Symposium on Passive Energy Dissipation Systems for New and Existing Buildings*, Los Angeles, CA.

Asahina, D., Bolander, J. E. and Berton, S. (2004). "Design optimisation of passive devices in multi-degree of freedom structures." *In Proceedings: 13th World Conference on Earthquake Engineering*, Vancouver, B.C., Canada.

ASCE/SEI Standard 41-13. (2014). "Seismic Rehabilitation of Existing Buildings." *American Society of Civil Engineers*, 1st Edition, Reston, Reston, Virginia.

ASCE/SEI Standard 7-10 (2010), "Minimum Design Loads for Buildings and Other Structures." *American Society of Civil Engineers*, Reston, Virginia.

Cosenza, E. and Manfredi, G. (1996). "Seismic design based on low cycle fatigue criteria." *In Proceedings: 11th World Conference on Earthquake Engineering*, Acapulco, Mexico. Paper No. 1141

Filiatrault, A. and Cherry, S. (1990). "Seismic design spectra for friction-damped structures." *Journal of Structural Engineering*, **116**(5): 1334–1355.

FitzGerald, T. F., Anagnos, T., Goodson, M. and Zsutty, T. (1989). "Slotted bolted connections in aseismic design for concentrically braced connections." *Earthquake Spectra*, **5**: 383–391.

Fujita, K., Moustafa, A. and Takewaki, I. (2010). "Optimal placement of viscoelastic dampers and supporting members under variable critical excitations." *Earthquakes and Structures*, **1**(1): 43–67.

Ganjavi, B., Hajirasouliha, I. and Bolourchi, A. (2016). "Optimum lateral load distribution for seismic design of nonlinear shear-buildings considering soil-structure interaction." *Soil Dynamics and Earthquake Engineering*, **88**: 356–368.

Gluck, N., Reinhorn, A. M., Gluck, J. and Levy, R. (1996). "Design of supplemental dampers for control of structures." *Journal of Structural Engineering*, **122**: 1394–1399.

Grigorian, C. E., Yang, T. S. and Popov, E. P. (1993). "Slotted bolted connection energy dissipators." *Earthquake Spectra*, **9**(3), 491–504.

Hajirasouliha, I. and Doostan ,A. (2010). "A simplified model for seismic response prediction of concentrically braced frames." *Advances in Engineering Software*, **41**(3): 497–505.

Hajirasouliha, I., Asadi, P. and Pilakoutas, K. (2012). "An efficient performance- based seismic design method for reinforced concrete frames." *Earthquake Engineering and Structural Dynamics*, **41**: 663–679.

Hajirasouliha, I., Pilakoutas, K. and Moghaddam, H. (2011). "Topology optimization for the seismic design of truss-like structures." *Computers and Structures*, **89**: 702–711.

Hejazi, F., Toloue, I., Jaafar, M. S. and Noorzaei, J. (2013). "Optimization of earthquake energy dissipation system by genetic algorithm." *Computer-Aided Civil and Infrastructure Engineering*, **28**: 796–810.

Honarparast, S. and Mehmandoust, S. (2012). "Optimum distribution of slip load of friction dampers using multi- objective genetic algorithm." *In Proceedings: 15$^{th}$ World Conference on Earthquake Engineering*, Lisbon, Portugal.

International Building Code (IBC), (2015). "International Code Council", Country Club Hills, USA.

Krawinkler, H. and Zohrei, M. (1983). "Cumulative damage in steel structures subjected to earthquake ground motions." *Computers and Structures*, **16**: 531–541.

Lavan, O. and Dargush, G. F. (2009). "Multi-objective evolutionary seismic design with passive energy dissipation systems." *Journal of Earthquake Engineering*, **13**: 758–790.

Lavan, O. and Levy, R. (2006). "Optimal peripheral drift control of 3D supplemental viscous dampers." *Journal of Earthquake Engineering*, **10**(6): 903–923.

Levy, R. and Lavan, O. (2006). "Fully stressed design of passive controllers in framed structures for seismic loadings." *Structural and Multidisciplinary Optimization,* **32**(6): 485–498.

Marsh, C. (2000). "Friction dampers to control building motionics." *Architectural Science Review*, **43**: 109–111.

Martinez, C. A., Curadelli, O. and Compagnoni, M. E. (2014). "Optimal placement of nonlinear hysteretic dampers on planar structures under seismic excitation." *Engineering Structures,* **65**: 89–98.

Miguel, L. F. F., Miguel, L. F. F. and Lopez, R. H. (2014). "Robust design optimisation of friction dampers for structural response control." *Structural Control and Health Monitoring,* **21**: 1240–1251.

Miguel, L. F. F., Miguel, L. F. F. and Lopez, R. H. (2016a). "Failure probability minimization of buildings through passive friction dampers." *The Structural Design of Tall and Special Buildings*, **25**: 869–885.

Miguel, L. F. F., Miguel, L. F. F. and Lopez, R. H. (2016b). "Simultaneous optimization of force and placement of friction dampers under seismic loading." *Engineering Optimization,* **48**: 586–602.

Milman, M. H. and Chu, C. C. (1994). "Optimization methods for passive damper placement and tuning." *Journal of Guidance, Control and Dynamics*, **17**(4): 848–856.

Miner, M. A. (1945). "Cumulative damage in fatigue*." Journal of Application Mechanics,* **12**(3), 159–164.

Moghaddam, H. and Hajirasouliha, I. (2008). "Optimum strength distribution for seismic design." *The Structural Design of Tall and Special Buildings*, **17**: 331–349.

Moreschi, L. M., Singh, M. P. (2003). "Design of yielding metallic and friction dampers for optimal seismic performance." *Earthquake Engineering and Structural Dynamics*, **32**: 1291–1311.

Mualla, I. H. (2000). "Experimental evaluation of new friction damper device." *In Proceedings: 12th World Conference on Earthquake Engineering*, Auckland, New Zealand.

Murakami, Y. at al. (2013). "Simultaneous optimal damper placement using oil, hysteretic and inertial mass dampers." *Earthquakes and Structures,* **5**(3): 261–276.

Nabid, N., Hajirasouliha, I. and Petkovski, M. (2017). "A practical method for optimum seismic design of friction wall dampers." *Earthquake Spectra,* **33**(3): 1033–1052.

Nikoukalam, M. T., Mirghaderi, S. R. and Dolatshahi, K. M. (2015). "Analytical study of moment-resisting frames retrofitted with shear slotted bolted connection." *Journal of Structural Engineering (ASCE*), **141**(11): 1–15.

Pall, A. S. and Marsh, C. (1982). "Response of friction damped braced frames." *Journal of Structural Division, Proceedings of the American Society of Civil Engineers, CASCE* **108**: 1313–1323.

Pall, A. S. and Pall, R. T. (2004). "Performance-based design using pall friction dampers - An economical design solution." *In Proceedings: 13th World Conference on Earthquake Engineering*, Vancouver, Canada. Paper No. 1955.

Park, J. H., Kim, J. and Min, K. W. (2004). "Optimal design of added viscoelastic dampers and supporting braces." *Earthquake Engineering and Structural Dynamics,* **33**(4): 465–484.

Patro, S. K. and Sinha, R. (2010). "Seismic performance of dry-friction devices in shear-frame buildings." *Journal of Civil Engineering and Architecture,* **4**(12).

PEER NGA. Online database. Available from: http://peer.berkeley.edu/nga/search.html [23 Feb 2016].

Petkovski, M. and Waldron, P. (2003). "Optimum friction forces for passive control of the seismic response of multi-storey buildings." *In Proceedings: 40 years of European Earthquake Engineering SE40EEE*. Ohrid, Macedonia.

Powell, G. H. and Allahabadi, R. (1987). "Seismic damage prediction by deterministic methods: concepts and procedures." *Earthquake Engineering and Structural Dynamics*, **16**: 719–734.

Prakash, V., Powell, G. H. and Campbell, S. (1993). "DRAIN-2DX base program description and user guide." Version 1.10. University of California, Berkeley, California.

Sadek, F., Mohraz, B., Taylor, A. W. and Chung, R. M. (1996). "Passive energy dissipation devices for seismic applications." *Building and Fire Research Laboratory National Institute of Standards and Technology (NIST) Gaithersburg*, Maryland, USA.

Sasani, M. and Popov, E. P. (1997). "Experimental and analytical studies on the seismic behaviour of lightweight concrete panels with friction energy dissipaters." *Earthquake Engineering Research Centre,* Report No. UBC/EERC-97/17, Berkeley, California.

Sasani, M. and Popov, E. P. (2001). "Seismic energy dissipaters for RC panels; analytical studies." *Journal of Engineering Mechanics*, **127**(8), 835–843.

Shirkhani, A., Mualla, I. H., Shabakhty, N. and Mousavi, S. R. (2015). "Behavior of steel frames with rotational friction dampers by endurance time method." *Journal of Constructional Steel Research,* **107**: 211–222.

Singh, M. P. and Moreschi, L. M. (2001). "Optimal seismic response control with dampers." *Earthquake Engineering and Structural Dynamics,* **30**: 553–572.

Takewaki, I. (2011). "Building control with passive dampers: optimal performance-based design for earthquakes." *John Wiley and Sons (Asia) Books,* Singapore, 51–75.

Teran-Gilmore, A. and Jirsa, J. O. (2004). "The concept of cumulative ductility strength spectra and its use within performance-based seismic design." *ISET Journal of Earthquake Technology,* **41**(1): 183–200.

Uetani, K., Tsuji, M. and Takewaki, I. (2003). "Application of an optimum design method to practical building frames with viscous dampers and hysteretic dampers." *Engineering Structures*, **25**(5): 579–592.

Vanmarke, E. H. (1976). "SIMQKE: A program for artificial motion generation, user's manual and documentation." Department of Civil Engineering, Massachusetts Institute of Technology.

Whittle, J. K., Williams, M. S. and Karavasilis, T. L. (2013). "Optimal placement of viscous dampers for seismic building design." Chapter 2 In: Lagaros ND, Plevris V and Mitropoulou CC (Ed) Design optimization of active and passive structural control systems, edition pp 34-50.

Whittle, J. K., Williams, M. S., Karavasilis, T. L. and Blakeborough, A. (2012). "A comparison of viscous damper placement methods for improving seismic building design." *Journal of Earthquake Engineering,* **16**(4): 540-560.

Wu, B., Zhang, J., Williams, M. S. and Ou, J. (2005). "Hysteretic behavior of improved pall-typed frictional dampers." *Engineering Structures*, **27**: 1258–1267.

# CHAPTER 5

# Multi-Criteria Performance-Based Optimisation of Friction Energy Dissipation Devices in RC Frames

## 5.1. ABSTRACT

A computationally-efficient method for multi-criteria optimisation is developed for performance-based seismic design of friction energy dissipation dampers in RC structures. The proposed method is based on the concept of Uniform Distribution of Deformation (UDD), where the slip-load distribution along the height of the structure is gradually modified to satisfy multiple performance targets while minimising the additional loads imposed on existing structural elements and foundation. The efficiency of the method is demonstrated through optimisation of 3, 5, 10, 15 and 20-storey RC frames with friction wall dampers subjected to design representative earthquakes using single and multi-criteria optimisation scenarios. The optimum design solutions are generally obtained in only a few steps, while they are shown to be independent of the selected initial slip loads and convergence factor. Optimum frames satisfy all predefined design targets and exhibit up to 48% lower imposed loads compared to designs using a previously proposed slip-load distribution. Dampers designed with optimum slip load patterns based on a set of spectrum-compatible synthetic earthquakes, on average, provide acceptable design solutions under multiple natural seismic excitations representing the design spectrum.

*Keywords: Multi-criteria optimisation, Seismic performance, Friction damper, Slip load distribution, Energy dissipation.*

## 5.2. INTRODUCTION

Supplemental passive control devices have been widely utilised as a viable cost-effective approach to enhance the seismic performance of existing and newly designed buildings by modifying the dynamic characteristics and increasing the energy dissipation capacity of the structures. As current design codes do not generally provide guidelines for optimising the configurations of passive control devices, this can be a challenging task due to complexity and high nonlinearity of these systems under earthquake excitations (Whittle et al., 2012 and 2013). Several optimisation methods have been adopted for optimum design of energy dissipation devices such as: Linear Quadratic Regulator (LQR) (Gluck et al., 1996; Agrawal and Yang, 1999), Simulated Annealing (SA) (Milman and Chu, 1994), Gradient-based Optimisation (Singh and Moreschi, 2001; Uetani et al., 2003; Park et al., 2004; Fujita et al., 2010), Genetic Algorithm (GA) techniques (Moreschi and Singh, 2003; Lavan and Dargush, 2009; Apostolakis and Dargush, 2010; Hejazi et al., 2013), Fully Stressed Design Optimisation (Levy and Lavan, 2006) and a procedure using Sensitivity Analysis and Redesign (Takewaki, 2011; Adachi et al., 2013; Murakami et al., 2013). The concept of performance-based seismic design was also adopted for optimisation of structures with supplemental energy dissipation devices. Liu et al. (2005), Lavan and Levy (2010) and Lavan and Amir (2014) developed a performance-based optimal design methodology to obtain the best sizing and allocation of viscous dampers in regular and irregular building structures. Similarly, Kim and Choi (2006) proposed a displacement-based design procedure to obtain an optimum number of velocity-dependent supplemental dampers for existing steel structures to satisfy a given performance limit state. Takewaki (2011) introduced criteria-based and sensitivity-based design algorithms for optimal quantity and placement of passive energy dissipation devices, where displacement, acceleration, and earthquake input energy were regarded as the main performance-based design indices. It should be noted that majority of the above mentioned studies have been limited to the optimum design of velocity dependent passive control systems such as viscous and viscoelastic dampers.

Friction-based dampers are considered as one of the appropriate passive energy dissipative systems due to their high adjustability and high energy dissipation capacity resulting from Coulomb dry friction (Aiken 1996). To avoid high stress concentrations at the connection zones in RC frames, wall-type friction-based wall dampers have been proposed by several researchers (Sasani and Popov, 2001; Petkovski and Waldron, 2003; Cho and Kwon, 2004; Nabid et al., 2017). In general, the efficiency of friction energy dissipation devices is highly sensitive to the dampers' location and height-wise distribution of slip loads (the loads at

which the friction devices start slipping and dissipating energy). In one of the early attempts, Filiatrault and Cherry (1990) developed an optimisation algorithm to obtain the best slip load distribution by minimising an energy performance index. They showed that the optimum slip load values are more dependent on the frequency and amplitude of the earthquake input than the structural features. A Genetic Algorithm (GA) was employed by Moreschi and Singh (2003) for optimum height-wise placement of friction dampers in steel braced frames when satisfying a predefined performance objective. Using a similar approach, Miguel et al. (2014) utilised the GA technique for multi-objective optimisation of friction dampers in shear-buildings subjected to seismic loading. In a follow-up study, Miguel et al. (2016) adopted a Backtracking Search Algorithm (BSA) for simultaneous optimisation of the slip forces and locations of the friction dampers in shear-buildings subjected to earthquake ground motions. More recently, a practical optimisation methodology was developed by Nabid et al. (2018) for seismic design of RC frames with friction dampers. It was shown that the method can increase the energy dissipation capacity of the dampers, while preventing damage concentration and soft storey failure in the frames. However, their proposed method is based on redistributing constant total slip load values (sum of slip loads in all dampers), and hence cannot be directly used to achieve a specific target for performance-based seismic design purposes. Moreover, their optimisation algorithm is not capable of satisfying multiple performance objectives simultaneously.

It should be noted that most of the aforementioned optimisation techniques have at least one of the following limitations: (a) they are only adopted for viscous and viscoelastic dampers and may not be appropriate for optimum design of friction energy dissipation devices; (b) they assume a linear behaviour for the main structural system, and thus, do not capture the damage of the structural elements which is generally unavoidable during strong earthquakes; (c) they use equivalent earthquake static loads or non-linear push over analyses and therefore do not take into account the effects of dynamic loads; (d) they are computationally expensive and/or require complex mathematical calculations and are not suitable for practical applications. Consequently, there is a need for developing a computationally efficient methodology for optimum design of non-linear structural systems with friction-based dampers under seismic excitations.

This paper introduces a completely new multi-criteria performance-based optimisation framework for optimum design of friction-based energy dissipation devices using the concept of uniform distribution of deformation demands. The proposed method is used to obtain the optimum slip load distribution for friction wall dampers in RC frames while

satisfying prescribed performance criteria. The efficiency of the method is then demonstrated for different performance targets and earthquake scenarios.

## 5.3. ANALYTICAL MODELLING AND ASSUMPTIONS

### 5.3.1. RC Frames with Friction Wall Dampers

In this study 3, 5, 10, 15, and 20-storey RC frames were selected with the typical geometry shown in Fig. 5.1 (a). The schematic view of the utilised friction damper (Fig. 5.1 (b)) comprises a reinforced concrete wall panel connected to the frame through a friction device at the top, a horizontal connection at the bottom, and two vertical supports in the sides. The connections are designed to transfer the loads to the beam-column connection, thus avoiding extra shear forces in the middle of the adjacent columns and beams. The friction device is a Slotted Bolted Connection (SBC) using two steel plates over a central T-shape slotted steel plate anchored to the top floor beam (Fig. 5.1 (b)). It should be noted that the bottom of the concrete panels at ground level is fixed to the base to transfer the imposed loads directly to foundation, and therefore, reduce the maximum column axial loads. More detailed information about the adopted friction wall damper can be found in Nabid et al. (2017).

The frames were assumed to be located on a soil type C of Eurocode 8 (EC8; CEN, 2004a) category and were designed for low-to-medium seismicity regions, using PGA of 0.2 g. The uniformly distributed permanent and non-permanent loads were considered to be 5.5 kN⁄m$^2$ and 2.5 kN⁄m$^2$ for interior floors, and 5.3 kN⁄m$^2$ and 1.0 kN⁄m$^2$ for the roof. The reference frames were initially designed to resist the seismic loads based on EC8 (CEN, 2004a) and in accordance with the minimum requirements of Eurocode 2 (EC2; CEN, 2004b) for moment-resisting RC frames with medium ductility (DCM). The concrete compressive strength ($f_c'$) and the yield strength of steel reinforcement bars ($f_y$) were assumed to be 35 and 400 MPa, respectively.

The pushover and nonlinear time-history analyses were conducted using the OpenSees software (McKenna and Fenves 2000). Concrete and reinforcing steel bars were modelled using a uniaxial constitutive material with linear tension softening (Concrete02) and a Giuffre–Menegotto–Pinto model (Steel02) with 1% isotropic strain hardening, respectively. Beam and column members were divided into three elements and modelled using displacement-based nonlinear beam-column elements with fibre sections while four Gauss–Lobatto integration points were considered for each element. P-Delta effects were taken into account and the Rayleigh damping model with a constant damping ratio of 0.05 was

assigned to the first mode and to the modes at which the cumulative mass participation exceeds 95%. In this study, it was assumed that the strength of the concrete wall panels (15 cm thickness) is always higher than the maximum loads transferred from the friction device, and therefore, they were modelled using equivalent elastic elements.

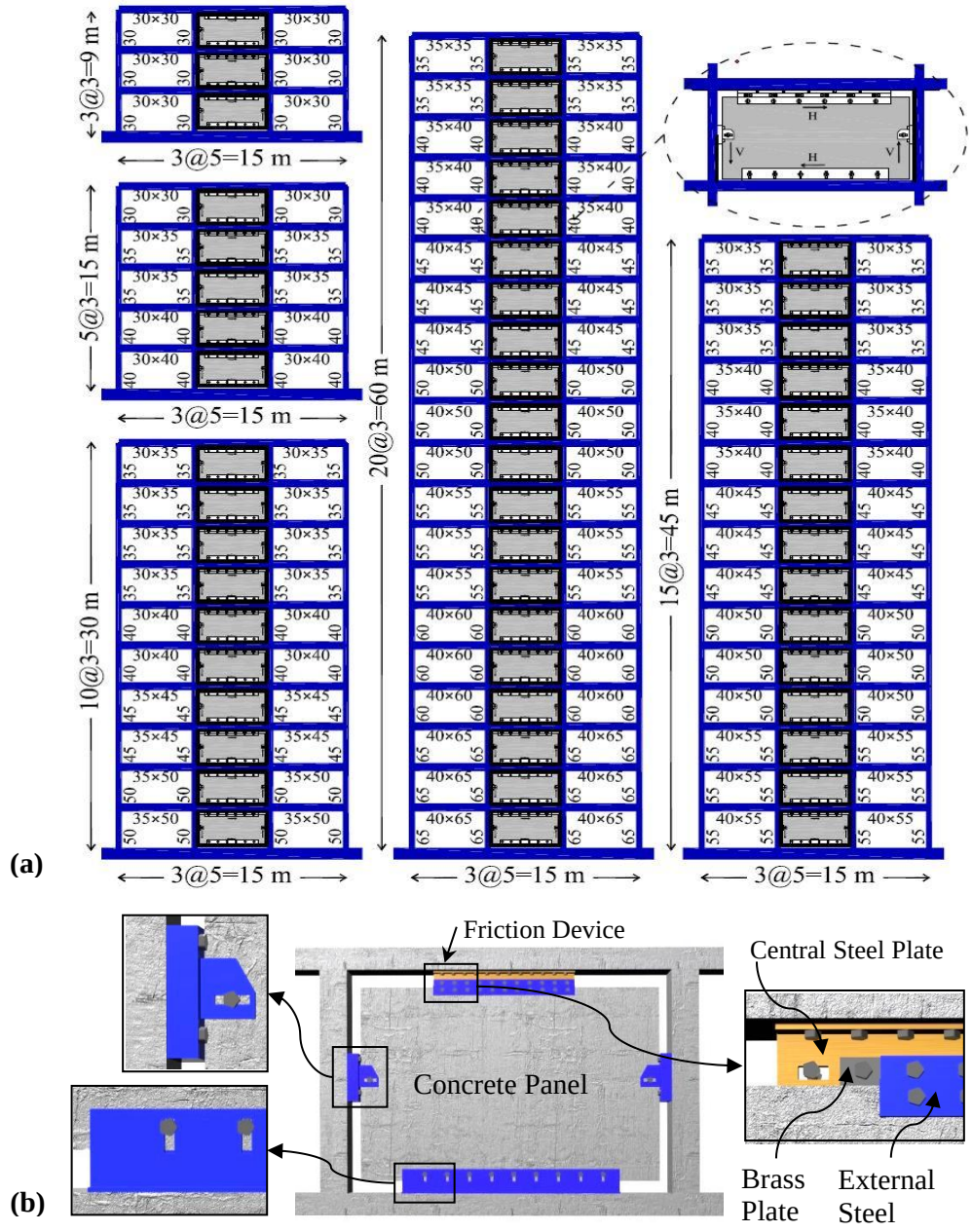


**Fig. 5.1.** (a) Geometry of the reference RC frames equipped with friction wall dampers, (b) schematic view of the friction wall damper (adopted from Nabid et al. (2017))

A nonlinear spring with an elastic-perfectly plastic uniaxial material, representing an ideal Coulomb friction hysteretic behaviour, was used to model the friction device. The beam-to-column connections were assumed to be fully rigid with no shear failure in the panel zones.

A computer code in MATLAB (2014) was developed and linked to the OpenSees (McKenna et al., 2000) program to calculate the energy dissipation in the beam and column elements and friction devices under earthquake loads.

### 5.3.2. Earthquake Ground Motions

To demonstrate the efficiency of the proposed performance-based optimisation framework, a set of six natural ground motions obtained from the Pacific Earthquake Engineering Research Center online database (PEER NGA) was used in the non-linear dynamic analyses in this study. Table 5.1 shows the characteristics of the selected natural ground motions. All earthquake excitations had high local magnitudes (i.e. Ms>6.5) and were recorded on soil class C of EC8 with less than 45 km distance from the epicentre. In addition, the TARSCTHS program (Papageorgiou et al. 2002) was used to generate synthetic earthquakes to be matched with the EC8 design response spectrum for the high seismicity regions (i.e. PGA=0.4g) with soil class C. It should be noted that most seismic performance-based design guidelines (e.g. FEMA 356 (2000) and ASCE/SEI 41-06 (2006)) aim to control the seismic response of the buildings under two different earthquake levels: (a) Design Basis Earthquake (DBE) with 10% probability of exceedance in 50 years, and (b) Maximum Considered Earthquake (MCE) with 2% probability of exceedance in 50 years. In this study, it is assumed that the DBE and MCE design spectra match with the EC8 design response spectrum for soil class C with PGA levels equal to 0.4g and 0.6g, respectively. This means that in this study the MCE events are taken to be 1.5 times of the DBE events.

**Table 5.1.** Properties of the selected natural ground motions

| *No.* | *Earthquake* | *Ms* | *Station/Component* | *Duration (s)* | *PGA (g)* | *PGV (Cm/s)* | *PGD (Cm)* |
|---|---|---|---|---|---|---|---|
| 1 | 1979 Imperial Valley | 6.5 | IMPVALL/H-E04140 | 39 | 0.485 | 37.4 | 20.23 |
| 2 | 1987 Superstition Hills (B) | 6.7 | SUPERST/B-ICC000 | 60 | 0.358 | 46.4 | 17.50 |
| 3 | 1989 Loma Prieta | 6.9 | LOMAP/G03000 | 40 | 0.555 | 35.7 | 8.21 |
| 4 | 1992 Cape Mendocino | 6.9 | CAPEMEND/PET000 | 36 | 0.590 | 48.4 | 21.74 |
| 5 | 1994 Northridge | 6.7 | NORTHR/NWH360 | 40 | 0.590 | 97.2 | 38.05 |
| 6 | 1999 Duzce, Turkey | 7.2 | DUZCE/DZC270 | 26 | 0.535 | 83.5 | 51.59 |

Fig. 5.2 compares the elastic acceleration response spectra of the selected natural earthquake records, the EC8 design spectrum and the spectrum of the generated synthetic earthquake. It is observed that both the average spectrum of the synthetic earthquakes and the average

spectrum of the natural ground motions can represent the EC8 design spectrum with a good accuracy, and therefore, can be efficiently utilised to evaluate the seismic performance of the designed frames.

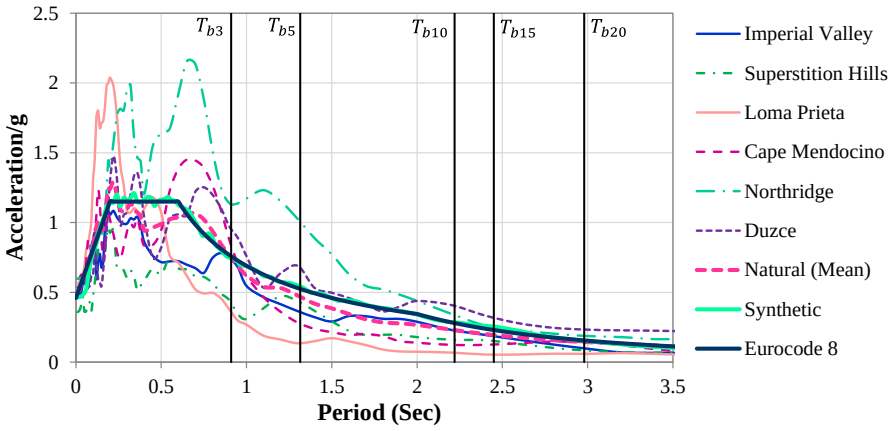


**Fig. 5.2.** Comparison between the elastic acceleration response spectra of the selected natural and synthetic earthquake records and the EC8 design spectrum, 5% damping ratio

## 5.4. OPTIMUM SLIP LOAD RANGE FOR MAXIMUM ENERGY DISSIPATION

One of the main advantages of friction energy dissipation devices in general is the capability to adjust the height-wise distribution of slip forces ($F_s$) to achieve predefined performance targets. Nabid et al. (2017) studied the efficiency of friction wall dampers designed with different slip load distribution patterns in improving the seismic performance of substandard RC structures. Based on the results of their study, the following empirical formula was proposed to obtain an efficient height-wise distribution of slip loads for buildings with different number of storeys:

$$R = 1.12e^{-0.11n} \tag{5.1}$$

where $n$ is the number of storeys, and $R$ is the slip load ratio defined as the ratio between the average of slip loads and the average of storey shear strengths at all storey levels. By considering the uniform cumulative pattern for height-wise slip load distribution (as suggested by Nabid et al. (2017)), the slip load values at each storey level can be calculated using the equation below:

$$F_{s,i} = \frac{\sum_{1}^{n} F_{y,i} \times R}{n(n+1)/2} \times (n+1-i) = \frac{\sum_{1}^{n} F_{y,i} \times 1.12e^{-0.11n}}{n(n+1)/2} \times (n+1-i) \quad (5.2)$$

where $F_{s,i}$ and $F_{y,i}$ are the slip load and the storey shear strength of the $i^{th}$ storey, respectively. The shear strength of each storey ($F_{y,i}$) can be calculated from a non-linear pushover analysis (Hajirasouliha and Doostan, 2010). In this section, the adequacy of this empirical equation in improving the energy dissipation capacity of the friction wall dampers is assessed for the set of RC frames used in this study (see Fig. 5.1).

The seismic performance of the selected RC frames with friction wall dampers is quantified in terms of maximum inter-storey drift, maximum axial load in the columns, base shear, and an energy dissipation parameter ($R_w$) defined as the ratio between the friction work of the dampers and the plastic deformation work of the structural elements (Petkovski and Waldron, 2003; Nabid et al., 2017). While the maximum inter-storey drift and energy dissipation ($R_w$) parameters are used to assess the efficiency of the dampers, the maximum axial load and base shear values are considered to control the additional loads imposed by the friction wall system to the existing structural elements. It should be noted that according to EC8 (CEN, 2004a), the column axial load ratio (defined as $N_e/A_c\, f_c'$) should be limited to 0.55 and 0.65 for ductility classes DCH (high) and DCM (medium), respectively, where $A_c$ is the cross section area of the column and $N_e$ is the column axial load under seismic and concurrent gravity actions. This highlights the importance of reducing the additional axial loads imposed by the utilised friction wall system.

Fig. 5.3 displays the average variations of selected performance parameters versus slip load ratio for the 3, 5, 10, 15 and 20-storey frames under the six selected natural earthquakes. For better comparison, the drift and base shear results in this figure are scaled to those of the corresponding bare frames. Similar to the results reported by Nabid et al. (2017), it is shown in Fig. 5.3 that there is always an optimum range of slip load ratios for each selected frame that in general leads to higher energy dissipation capacity and lower displacement demands. The optimum slip load values were in the range of 0.65-0.95, 0.50-0.80, 0.25-0.45, 0.10-0.30, and 0.05-0.15 for the 3, 5, 10, 15, and 20-storey frames, respectively. These results compare very well with the optimum slip load ratios calculated by Equation 5.1, irrespective of the difference between the frame geometries used in this study and those in Nabid et al. (2017). It can be seen from Figs. 5.3 (c and d) that the base shear and axial loads imposed by the wall dampers increase by increasing the slip load ratio (up to a maximum limit where the friction devices are all locked). This means that while using the optimum slip range can

efficiently increase the energy dissipation capacity of the dampers, it may lead to excessive base shear and column axial load values and, consequently, impart large loads on the foundations. As shown in Fig. 5.3 (d), some higher slip load factors may lead to maximum axial loads which exceed the moderate and high ductility (DCM and DCH) EC8 target limits, and therefore, cannot be used in practical design applications. To address this issue, in the following sections a methodology is proposed for optimum design of friction dampers to satisfy predefined performance targets while minimising the additional imposed loads.

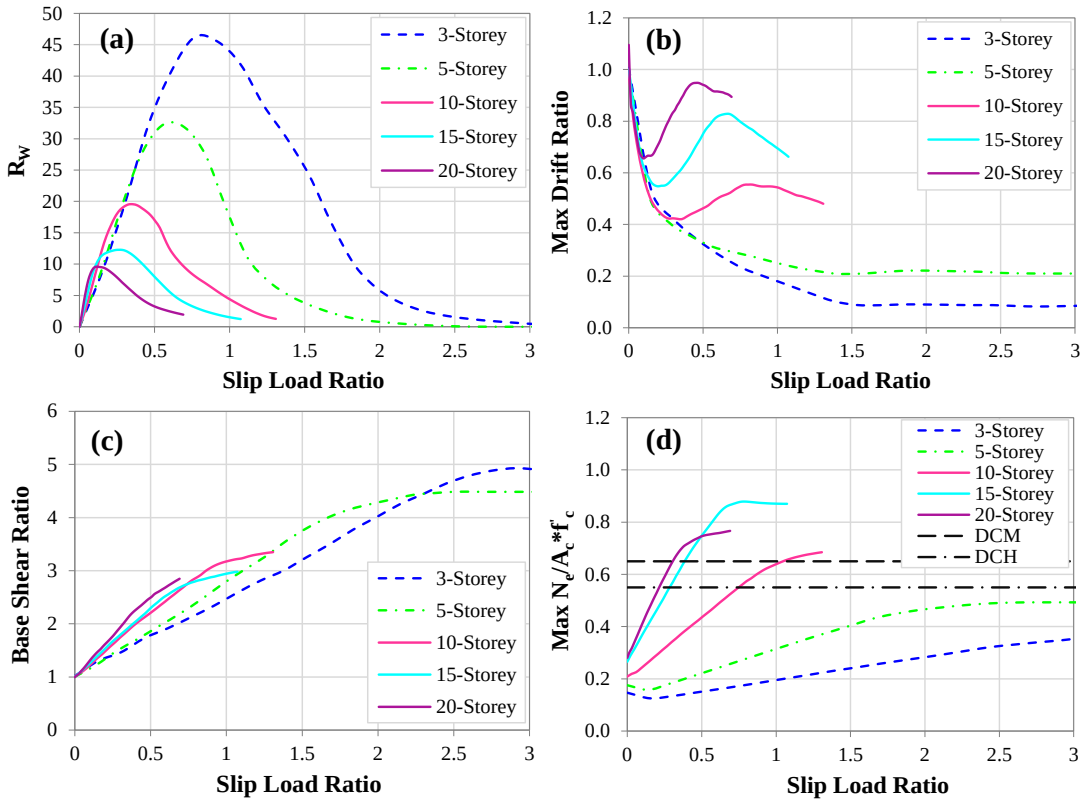


**Fig. 5.3.** Variations of (a) $R_w$, (b) maximum drift ratio, (c) base shear ratio, and (d) maximum $N_e/A_c f_c'$ for the 3, 5, 10, 15 and 20-storey frames as a function of slip load ratio, average of six natural earthquakes

## 5.5. DEVELOPING A PERFORMANCE-BASED OPTIMISATION FRAMEWORK

In this study, an efficient performance-based optimisation framework is developed based on the concept of uniform distribution of deformation demands (or damage) for optimum design of RC frames with friction energy dissipation devices. The objective is to find the best height-wise distribution of slip loads in the friction wall dampers to satisfy a predefined performance level under the design earthquake by using minimum total friction loads. This will reduce the additional loads imposed to the existing structural elements as discussed

before. The slip load values of the friction wall dampers are considered to be the key design variables as they have a dominant effect on controlling the seismic response of the system in the nonlinear response range. In the proposed approach, the slip loads of the friction devices are redistributed using an iterative method until all inter-storey drifts reach the target values. It should be mentioned that a similar optimisation concept was previously used by other researchers for optimum seismic design of different types of structural systems such as RC frames (Hajirasouliha et al., 2012), shear-buildings (Moghaddam and Hajirasouliha, 2008; Ganjavi et al., 2016), truss-like structures (Hajirasouliha et al., 2011), and viscous dampers (Lavan and Levy, 2006). However, this is the first time that the proposed performance-based optimisation method is adopted for seismic design of friction dampers to obtain the best height-wise distribution of the slip loads.

Current performance-based seismic design guidelines such as FEMA 356 (2000), ASCE/SEI 41-06 (2006) and EC8 impose limits on acceptable values of different response parameters (e.g. maximum inter-storey drift, plastic hinge rotation or axial compression stress) to achieve a specific performance level. In this study, maximum inter-storey drift is considered as the performance criterion to assess the efficiency of friction wall dampers in controlling the damage to structural and non-structural elements under earthquake excitations. In FEMA 356 and ASCE/SEI 41-06, maximum inter-storey drift limits of 1%, 2% and 4% are considered for Immediate Occupancy (IO), Life Safety (LS), and Collapse Prevention (CP) performance levels, respectively. In EC8 the inter-storey drifts are limited by the displacement ductility capacity, or indirectly, by the curvature ductility capacity of the structural elements, in accordance with the ductility class of the structure, In the following sections, a practical performance-based optimisation method is developed for optimum seismic design of RC frames with friction wall dampers based on the concept of uniform distribution of deformation demands.

### 5.5.1. Single-Criteria Performance-Based Optimisation Method

As discussed above, in general, increasing the slip loads in the friction wall dampers can reduce the maximum displacement demands during strong earthquakes. However, this may be accompanied by an increase in the based shear and loads imposed to the existing structural elements. This highlights the need for efficient optimum design methods for friction wall dampers that can satisfy the prescribed performance deformation and loading targets under the design earthquake. To this end, the following optimisation algorithm is adopted in this study:

1) A pre-defined slip load distribution is assumed for the initial design of the friction wall dampers. In this study the slip load distribution obtained from Equation 5.2 is used as proposed by Nabid et al. (2017). It should be mentioned that the final optimum design solution is independent of the initial slip load distribution as will be discussed in the following section.

   The RC structure with the designed friction dampers is then subjected to the selected design earthquake and the maximum inter-storey drift at each storey is calculated and compared with the target value. The structure can be considered to be practically optimum if all the inter-storey drifts are close to the performance target within an acceptable tolerance. Otherwise, the design algorithm is continued.

   To satisfy the performance-based design objective, the friction loads in the storeys with inter-storey drift higher than the predefined performance target should be increased. On the other hand, in the storeys with inter-storey drift less than the target value, the slip loads (and hence the additional imposed loads) can be reduced. To achieve this, the following equation is proposed to obtain a more efficient distribution of slip loads:

$$\left(F_{s,i}\right)_{n+1} = \left(F_{s,i}\right)_n \times \left(\frac{\Delta_i}{\Delta_{target}}\right)_n^{\alpha} \tag{5.3}$$

   where $\Delta_i$ and $\Delta_{target}$ are maximum and target inter-storey drifts of $i^{th}$ storey for $n^{th}$ iteration, respectively. $\alpha$ is the convergence parameter ranging from 0 to 1. It will be shown in the following sections that the convergence parameter has a significant effect on the convergence rate of the problem, while it does not affect the final design solution. The results of this study show that α factor of 0.5 always leads to reliable convergence behaviour for the studied frames.

2) The design procedure is then repeated from step 2 until the coefficient of variation of the inter-storey drifts ($COV_{\Delta}$) decreases to an acceptable level (e.g. less than 0.1). Based on the concept of uniform distribution of displacement demands, the structure at this stage is expected to satisfy the design performance target by using minimum amount of total slip loads. This can minimise the adverse effects of using wall dampers on the foundation and the existing structural elements as discussed before. It should be noted that some of the storey levels in the bare frame usually can satisfy the performance target even without using friction wall dampers; and therefore, it is very unlikely to reach a very uniform inter-storey drift distribution in practical applications.

Current performance-based design guidelines (such as FEMA 356 and ASCE/SEI 41-06) usually aim to limit the structural and non-structural damage of ordinary buildings to the LS and CP performance levels during DBE and MCE events, respectively. However, for essential and safety critical facilities (e.g. hospitals) higher performance targets should be satisfied. In this section, the proposed optimisation algorithm is used to obtain the optimum slip load distributions in the 5 and 10-storey frames to satisfy IO performance target under the synthetic earthquake representing the DBE event (see Fig. 5.2). According to FEMA 356 and ASCE/SEI 41-06 seismic design provision, 1% target drift ratio (ratio of the storey drift to the storey height) is considered as the IO performance level.

Figs. 5.4 (a) and (b) illustrate the average distribution of the maximum inter-storey drift ratios for the 5 and 10-storey frames, respectively, without friction walls (i.e. bare frame), with friction walls designed based on Equation 5.2 and those optimised using the proposed optimisation method. It is shown that the proposed optimisation method could efficiently satisfy the predefined performance target while led to a uniform distribution of maximum inter-storey drifts, which in turn prevents damage localisation and soft storey failure mechanism. Using Equation 5.2 for designing the friction wall dampers provided very conservative design solutions with maximum inter-storey drift ratios well below the target value.

Fig. 5.5 compares average of slip load distributions (scaled to the average of storey strengths), column axial load and base shear ratios (scaled to the corresponding bare frame), and the energy dissipation parameters ($R_w$) for the 5 and 10-storey frames with optimised friction walls and those designed based on Equation 5.2. The results indicate that the wall dampers designed based on Equation 5.2 could dissipate significantly higher energy levels compared to the optimised dampers (see Fig. 5.5), which is in agreement with the results reported by Nabid et al. (2017). However, this is accompanied by imposing considerably higher column axial loads and base shear demands (up to 32%) to the structures compared to the optimum design solutions due to using higher slip load values. This implies that the proposed performance-based optimisation methodology fulfils the desired performance objective with the minimum additional imposed loads to the main structure, while it can also reduce the strengthening cost by removing unnecessary friction wall dampers (with zero slip load values).

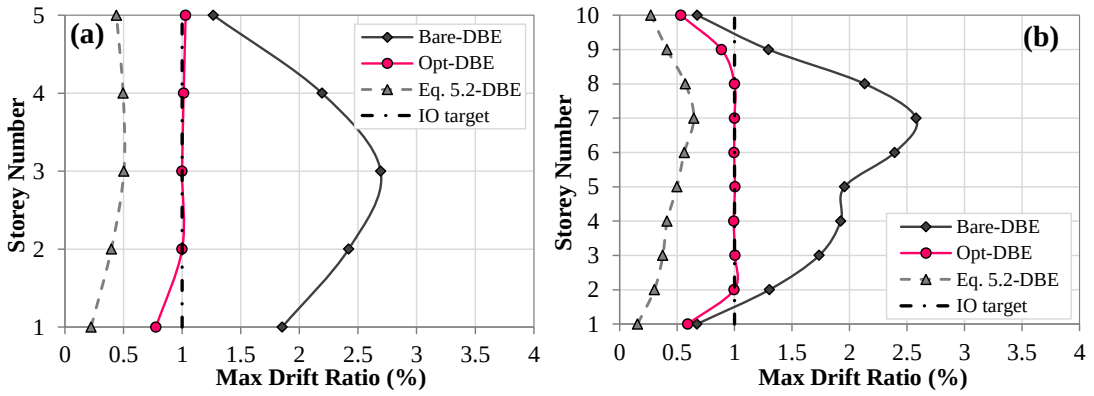


**Fig. 5.4.** Maximum drift ratios for (a) 5-storey and (b) 10-storey frames without friction walls (bare frame), with optimised friction walls and those designed based on Equation 5.2, DBE event

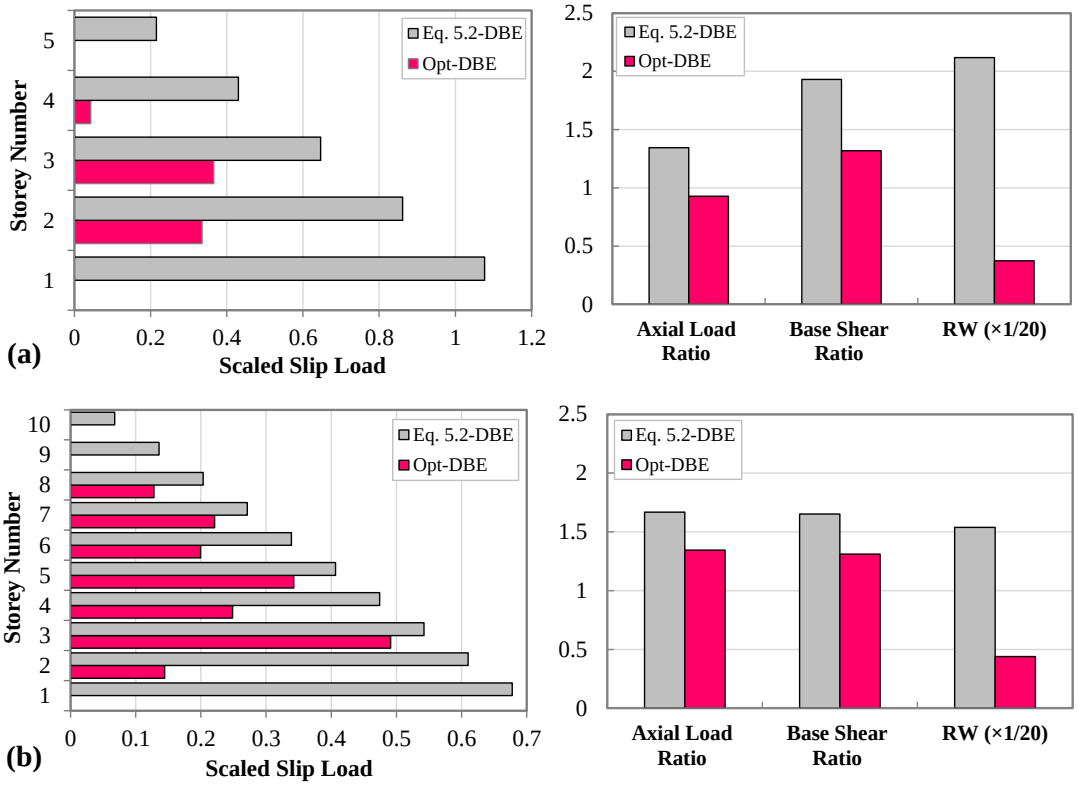


**Fig. 5.5.** Slip load, column axial load and base shear ratios for (a) 5-storey and (b) 10-storey frames with optimised friction walls and those designed based on Equation 5.2, DBE event

### 5.5.2. Multi-Criteria Performance-Based Optimisation Method

The proposed optimum design method can be easily extended to achieve an optimum slip load distribution pattern that satisfies multiple performance objectives. To fulfil this, Equation 5.3 in the proposed optimisation algorithm should be substituted with the following equations:

$$\left(F_{s,i}\right)_{n+1} = \left(F_{s,i}\right)_n \times \left[\Delta R_i\right]^{\alpha} \tag{5.4}$$

$$\Delta R_i = Max\left[\frac{(\Delta_i)_1}{(\Delta_{target})_1}, \frac{(\Delta_i)_2}{(\Delta_{target})_2}, ..., \frac{(\Delta_i)_j}{(\Delta_{target})_j}\right] \tag{5.5}$$

where $(\Delta_i)_j$ and $(\Delta_{target})_j$ are the maximum and target inter-storey drifts of the $i^{th}$ storey for $j^{th}$ performance objective, respectively. To demonstrate the efficiency of the multi-criteria performance-based optimisation algorithm, the 3, 5, 10, 15 and 20-storey RC frames with friction wall dampers were optimised to simultaneously satisfy IO and LS performance limits under DBE and MCE representative spectrum compatible earthquakes, respectively. Figs. 5.6 (a) and (b) show the distributions of the maximum inter-storey drift ratios and slip load ratios for 3, 5, 10, 15 and 20-storey frames without friction walls (bare frames) and with friction wall dampers designed based on Equation 5.2 and the proposed optimum design methodology. The results generally show that while the bare frames clearly violated the performance targets with the damage localised in certain storey levels under the design earthquakes, the optimum solutions could efficiently satisfy the required performance levels with rather more uniform inter-storey drift distributions.

As illustrated in Fig. 5.6 (b), in the case optimum slip load distributions, the slip load values in certain storeys (here mainly at lower and upper storey levels) tend to zero, and consequently, the corresponded supplemental devices can be removed from the structure, which in turn leads to more cost-effective design of friction wall dampers. The results shown in Fig. 5.6 indicate that using the slip load values from Equation 5.2 generally leads to acceptable design solutions; however, the lateral inter-storey drifts may be considerably less than the performance targets. As discussed before, this can impose unnecessary additional column axial loads and base shear demands.

To quantify this effect, Table 5.2 compares the axial load and base shear ratios of 3, 5, 10, 15 and 20-storey frames designed using fixed wall (i.e. very high slip load values), optimised friction walls and those designed using Equation 5.2 under representative DBE and MCE events. According to the results, using fixed walls leads to excessive column axial load values, and hence, exceeding the DCM ductility class in medium to high-rise frames under both DBE and MCE events. Although, using Equation 5.2 resulted in acceptable design solutions, optimum designed wall dampers could reduce the maximum $N_e/A_c f_c'$ and base shear ratio of the studied frames by up to 37% and 48%, respectively. This is in agreement with the results presented in section 5.5.1.

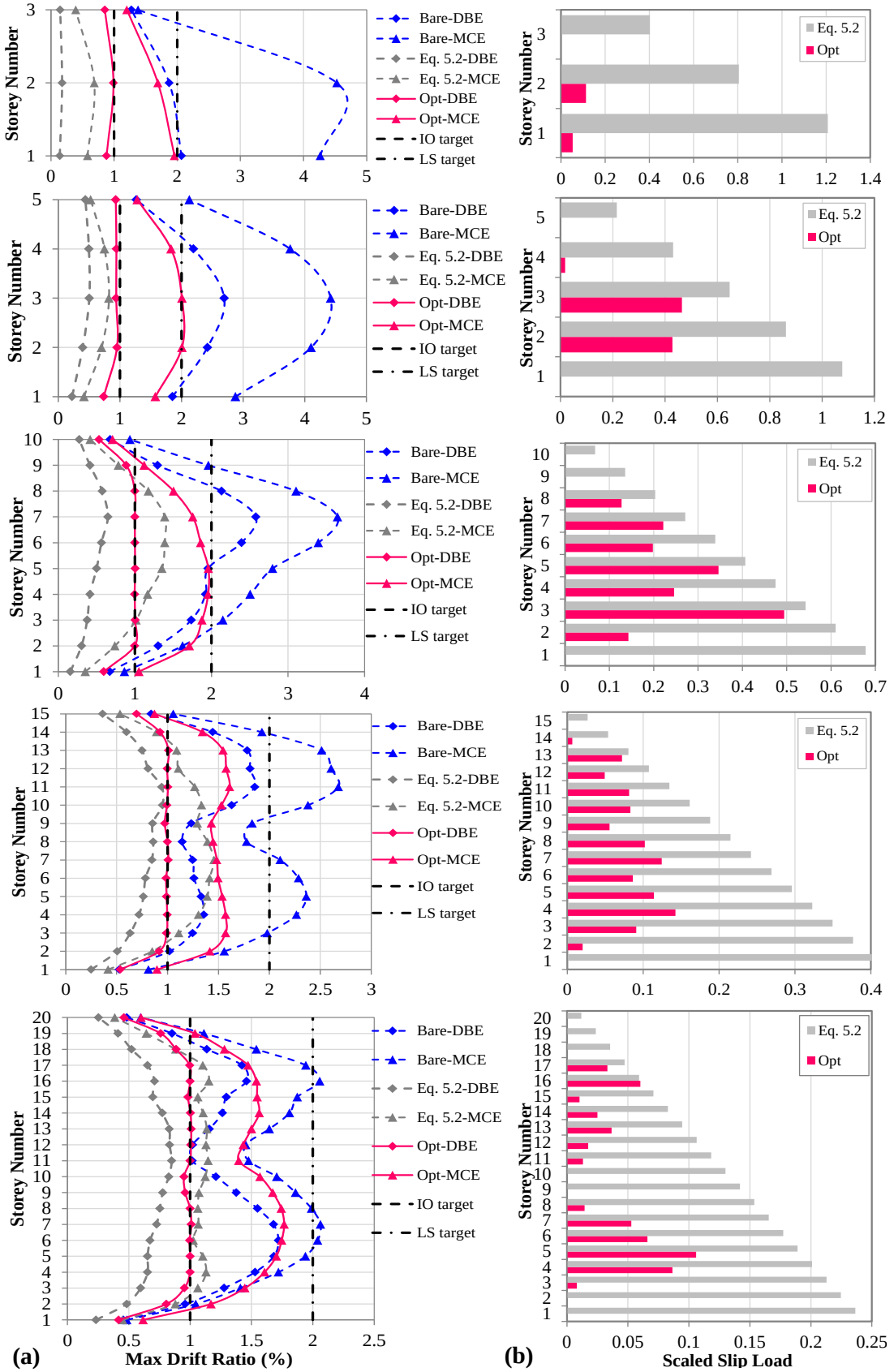


**Fig. 5.6.** (a) Maximum drift ratios and (b) Slip load ratios for 3, 5, 10, 15 and 20-storey frames without wall and with optimised friction walls and those designed based on Equation 5.2, DBE and MCE events

**Table 5.2.** Comparison of maximum $N_e/A_c f_c'$ and base shear ratio (scaled to the corresponding bare frame) for 3, 5, 10, 15 and 20-storey frames designed with fixed walls, optimised friction walls and those designed based on Equation 5.2, DBE and MCE events

| | | *3-Storey* | | *5-Storey* | | *10-Storey* | | *15-Storey* | | *20-Storey* | |
|---|---|---|---|---|---|---|---|---|---|---|---|
| | | $\frac{N_e}{A_c f_c'}$ | *Base Shear* | $\frac{N_e}{A_c f_c'}$ | *Base Shear* | $\frac{N_e}{A_c f_c'}$ | *Base Shear* | $\frac{N_e}{A_c f_c'}$ | *Base Shear* | $\frac{N_e}{A_c f_c'}$ | *Base Shear* |
| *Fixed Wall* | *DBE* | 0.40 | 4.74 | 0.48 | 4.15 | 0.67 | 3.25 | 0.87 | 2.65 | 0.90 | 3.41 |
| | *MCE* | 0.46 | 5.88 | 0.58 | 5.46 | 0.71 | 3.72 | 1.04 | 3.25 | 1.02 | 3.63 |
| *Eq. 5.2* | *DBE* | 0.18 | 1.859 | 0.25 | 1.930 | 0.38 | 1.653 | 0.48 | 1.404 | 0.45 | 1.316 |
| | *MCE* | 0.18 | 2.300 | 0.25 | 2.100 | 0.38 | 1.840 | 0.49 | 1.547 | 0.45 | 1.443 |
| *Optimum* | *DBE* | 0.11 | 1.024 | 0.16 | 1.310 | 0.30 | 1.309 | 0.35 | 1.063 | 0.32 | 1.109 |
| | *MCE* | 0.15 | 1.190 | 0.21 | 1.179 | 0.31 | 1.252 | 0.35 | 1.077 | 0.32 | 1.120 |
| *Reduction (%)* | *DBE* | **36.8** | 44.9 | 34.0 | 32.1 | 19.4 | 20.8 | 28.2 | 24.2 | 29.7 | 15.8 |
| | *MCE* | 17.0 | **48.2** | 16.7 | 43.9 | 20.1 | 32.0 | 29.4 | 30.4 | 29.2 | 22.4 |

Fig. 5.7 compares the distributions of the maximum inter-storey drifts and optimum slip load ratios for the 5-storey frames optimised to satisfy IO performance limit under DBE events (single-criteria optimisation) and the frames optimised to simultaneously satisfy IO and LS performance levels under DBE and MCE events, respectively (multi-criteria optimisation). It is shown that the frames optimised only based on DBE events, did not satisfy the required performance level under MCE events. However, by performing the multi-criteria optimisation, both IO and LS performance targets were satisfied while the total required friction force was increased by 18%.

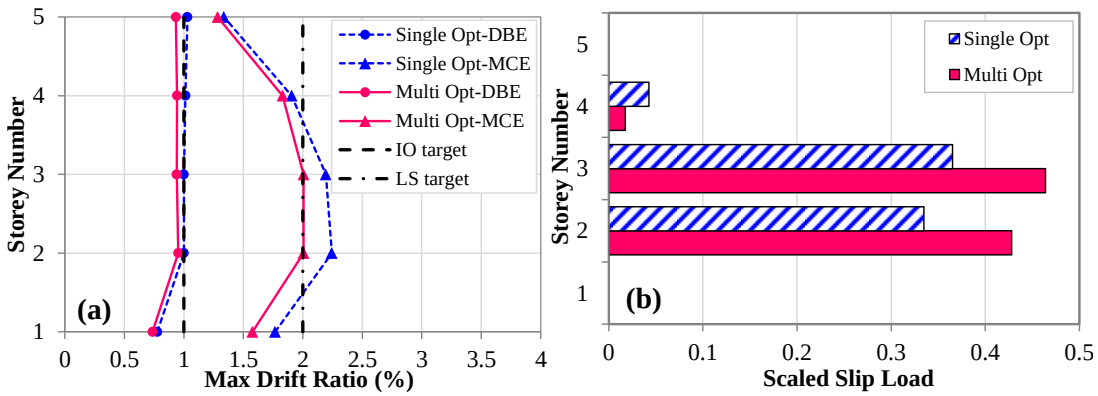


**Fig. 5.7.** Distribution of (a) maximum drift ratios, and (b) optimum slip load ratios for 5-storey frames optimised based on single-criteria and multi-criteria optimisation algorithms, DBE and MCE events

## 5.6. SENSITIVITY OF THE OPTIMISATION METHOD TO THE INITIAL DESIGN AND CONVERGENCE PARAMETER

In previous sections, the slip load values calculated based on Equation 5.2 (uniform cumulative distribution) were used for the initial design of the friction wall dampers in the optimisation process. To investigate the effect of the predefined initial slip loads on the final optimum design solution, the optimisation process was also started with the dampers designed based on a uniform distribution of slip loads with very small slip load values (5 kN) at all storey levels. Fig. 5.8 (a) compares the variation of maximum inter-storey drifts versus iteration steps for the 5-storey frames designed with the two selected slip load distributions under the DBE event. While the maximum drift ratios of the initial structures were considerably different, they both converged to the target value (i.e. IO performance limit) at the end of the optimisation process. However, a faster convergence was achieved by using the distribution pattern obtained based on Equation 5.2 as the starting point. Fig. 5.8 (b) shows that the final distribution of the optimum slip loads was not affected by the initial slip load distribution.

Fig. 5.8 also shows the effects of using convergence parameters α= 0.2 and 0.5 on the convergence rate and the final distribution of slip loads. It can be observed that while the both selected α values can efficiently converge to the same optimum design solution; in general, faster convergence was achieved by using α values of 0.5.

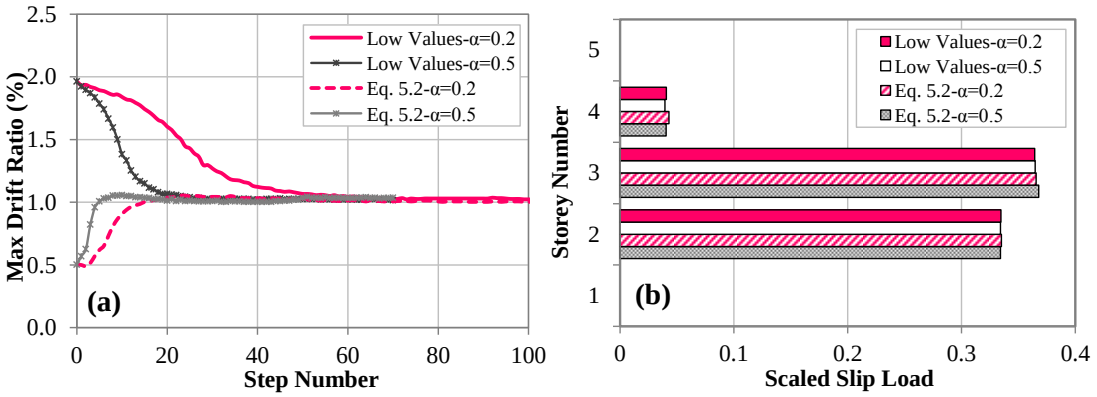


**Fig. 5.8.** (a) Variation of maximum inter-storey drifts versus iteration steps and (b) distributions of optimum slip loads for 5-storey frames initially designed based on Equation 5.2 and very low slip load values at all storey levels, DBE event

## 5.7. OPTIMUM SEISMIC DESIGN FOR AN ENSEMBLE OF EARTHQUAKES

While the seismic excitation is the main source of uncertainty in the seismic design of structures, there is a concern that this may affect the efficiency of the optimum structures designed based on a single earthquake event. One of the most important limitations of the adaptive method is the sensitivity of the optimal frame to the selected design ground motion. Therefore, the optimum design solution under a specific earthquake may not be optimum for a different design earthquake. Previous studies by Hajirasouliha and Pilakoutas (2012) on shear type buildings showed that, to overcome this limitation, a set of synthetic spectrum-compatible earthquakes can be used in the optimisation process. In this section, the efficiency of their proposed design concept is investigated for optimum design of RC structures with friction wall dampers subjected to an ensemble of EC8 spectrum-compatible natural earthquakes.

The 5 and 10-storey frames were optimised for IO and LS performance objectives under the six spectrum-compatible synthetic DBE and MCE events. The average of the optimum slip load values was then used to design the frames (see Fig. 5.9) and their seismic performance was assessed under the six natural earthquakes listed in Table 5.1. As discussed in section 5.3.2, the average response spectrum of these natural earthquake records compares well with the selected EC8 DBE. Similar to the simulated earthquakes, a scale factor of 1.5 was used to obtain MCE natural events used in this section. Fig. 5.10 compares the average height-wise distribution of the maximum drift ratios for the frames without friction walls (bare frames) and those with optimised friction walls subjected to the selected natural earthquakes. Based on the results, the optimum design frames, on average, could satisfy the target performance levels under both DBE and MCE events with a very good accuracy (less than 5% error on average). It can be also noted that the optimum design frames exhibited significantly lower maximum drift ratios (up to 51%) and a relatively more uniform distribution of maximum drift ratios compared to the corresponding bare frames.

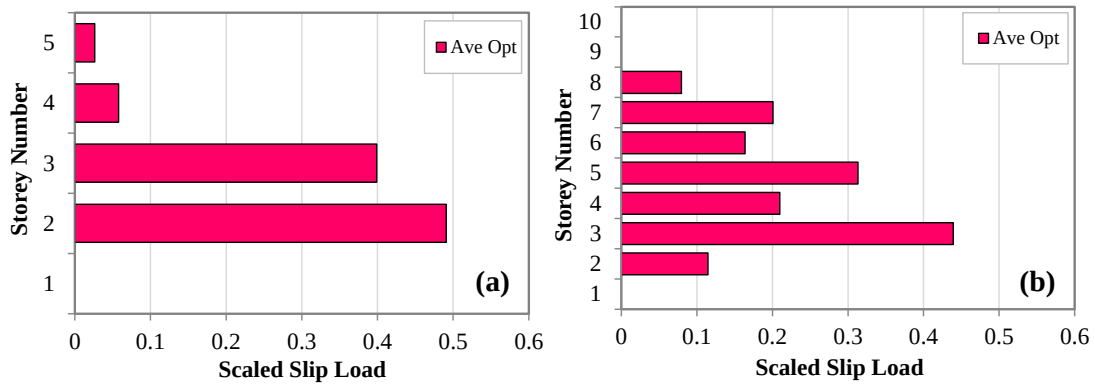


**Fig. 5.9.** Average optimum slip load values for (a) 5-storey and (b) 10-storey frames, Average of six synthetic DBE and MCE events

It should be noted that the proposed approach is general and can be used for any set of earthquake records representing a design spectrum. Considering the low computational costs and simplicity of the proposed performance-based optimisation method, the results of this study should prove useful in practical design of RC frames with friction-based dampers. However, the efficiency of the method should be further investigated for other structural systems and types of dampers.

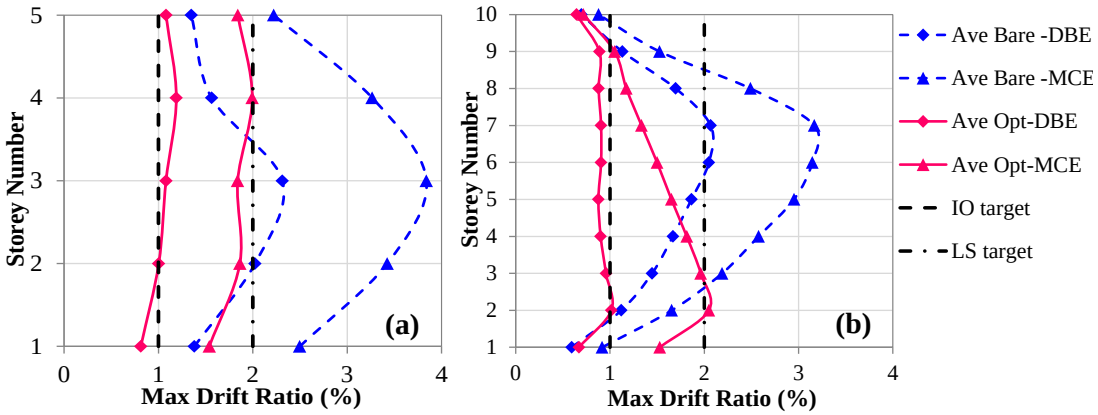


**Fig. 5.10.** Maximum drift ratios of (a) 5-storey and (b) 10-storey frames with optimised friction walls obtained for six synthetic DBE and MCE events, Average of six natural DBE and MCE events

## 5.8. SUMMMARY AND CONCLUSIONS

In this paper is presented a new, computationally efficient (low computational cost) multi-criteria optimisation method developed for performance-based seismic design of RC frames with friction wall dampers. The method is based on the concept of uniform distribution of deformation demands, in which the height-wise distribution of slip loads is modified until multiple predefined performance objectives are simultaneously satisfied with minimum

additional imposed loads to the base structure. The efficiency of the proposed optimisation method was demonstrated through the optimum design of 3, 5, 10, 15, and 20-storey RC frames with friction wall dampers subjected to DBE and MCE representative spectrum-compatible earthquakes using single- and multi-criteria optimisation scenarios. According to the results, the following conclusions can be drawn:

- Using the slip load range suggested by Nabid et al. (2017) could efficiently increase the energy dissipation capacity of friction wall dampers under a set of six natural spectrum-compatible earthquakes. However, it was shown that the designed dampers may lead to excessive base shear and column axial load values.

- The proposed multi-criteria optimisation method was shown to be efficient to satisfy multiple performance objectives under DBE and MCE representative earthquakes, leading to rather uniform distribution of lateral deformations. Compared to the dampers designed to have maximum energy dissipation capacity, the proposed optimisation method resulted in design solutions with less number of required dampers and up to 37% and 48% lower column axial load and base shear demand, respectively.

- Based on the results, the proposed low computational-cost method generally leads to optimum design solutions in only a few steps. It was shown that the final optimum solution is independent of the selected initial slip loads and convergence parameter; however, a considerably faster convergence can be achieved by using an appropriate convergence parameter and slip load distribution pattern as the starting point.

- The uncertainty in the design earthquake excitation was taken into account by optimising the frames based on the average of a set of synthetic spectrum-compatible earthquakes. The results indicated that the optimised frames could satisfy the performance targets under multiple natural seismic excitations representing DBE and MCE design spectra, while exhibited significantly lower maximum drift ratios (up to 51%) compared to their bare frame counterparts.

## REFERENCES

Adachi, F., Yoshitomi, S., Tsuji, M. and Takewaki, I. (2013). "Nonlinear optimal oil damper design in seismically controlled multi-story building frame." *Soil Dynamics and Earthquake Engineering*, **44**: 1–13.

Agrawal, A. K., and Yang, J. N. (1999). "Design of passive energy dissipation systems based on LQR control methods." *Journal of Intelligent Material Systems and Structures,* **10**: 933–944.

Aiken, I. (1996). "Passive energy dissipation - hardware and applications." Proc. of Los Angeles County and SEAOSC symposium on passive energy dissipation systems for new and existing buildings. Los Angeles, California, USA.

Apostolakis, G. and Dargush, G. F. (2010). "Optimal seismic design of moment-resisting steel frames with hysteretic passive devices." Earthquake Engineering and *Structural Dynamics,* **39**: 355–376.

ASCE/SEI Standard 41-06. (2006). "Seismic Rehabilitation of Existing Buildings." American Society of Civil Engineers, Reston, Virginia, USA.

CEN (Comité Européen de Normalization). (2004a). "Eurocode 8: Design of structures for earthquake resistance-Part 1: General rules, seismic actions and rules for buildings." EN 1998–1–1, Brussels.

CEN (Comité Européen de Normalization). (2004b). "Eurocode 2: Design of concrete structures, Part 1–1: General rules and rules for buildings." EN 1992–1–2, Brussels.

Cho, C. G., and Kwon, M. (2004). "Development and modelling of a frictional wall damper and its applications in reinforced concrete frame structures." **33**: 821–838.

FEMA 356, (2000). Pre-standard for the seismic rehabilitation of buildings. Federal Emergency Management Agency.

Filiatrault, A. and Cherry, S. (1990). "Seismic design spectra for friction-damped structures." *Journal of Structural Engineering (ASCE),* **116**(5): 1334–1355.

Fujita, K., Moustafa, A. and Takewaki, I. (2010). "Optimal placement of viscoelastic dampers and supporting members under variable critical excitations." *Earthquakes and Structures,* **1**(1): 43–67.

Ganjavi, B., Hajirasouliha, I. and Bolourchi, A. (2016). "Optimum lateral load distribution for seismic design of nonlinear shear-buildings considering soil-structure interaction." *Soil Dynamics and Earthquake Engineering,* **88**: 356–368.

Gluck, N., Reinhorn, A. M., Gluck, J. and Levy, R. (1996). "Design of supplemental dampers for control of structures." *Journal of Structural Engineering (ASCE,)* **122**: 1394–1399.

Hajirasouliha, I. and Pilakoutas, K. (2012). "General Seismic Load Distribution for Optimum Performance-Based Design of Shear-Buildings." *Journal of Earthquake Engineering,* **16**(4): 443–462.

Hajirasouliha, I., Pilakoutas, K. and Moghaddam, H. (2011). "Topology optimization for the seismic design of truss-like structures." *Computers and Structures,* **89**: 702–711.

Hajirasouliha, I., Asadi, P. and Pilakoutas, K. (2012). "An efficient performance-based seismic design method for reinforced concrete frames." *Earthquake Engineering and Structural Dynamics,* **41**: 663–679.

Hajirasouliha, I. and Doostan, A. (2010). "A simplified model for seismic response prediction of concentrically braced frames." *Advances in Engineering Software,* **41**(3): 497-505.

Hejazi, F., Toloue, I., Jaafar, M. S. and Noorzaei, J. (2013). "Optimization of earthquake energy dissipation system by genetic algorithm." *Computer-Aided Civil and Infrastructure Engineering,* **28**: 796–810.

Kim, J. and Choi, H. (2006). "Displacement-Based Design of supplemental dampers for seismic retrofit of a framed structure." *Journal of Structural Engineering (ASCE),* **132**(6): 873–883.

Lavan, O. and Amir, O. (2014). "Simultaneous topology and sizing optimization of viscous dampers in seismic retrofitting of 3D irregular frame structures." *Earthquake Engineering and Structural Dynamics,* **43**: 1325–1342.

Lavan, O. and Dargush, G. F. (2009). "Multi-objective evolutionary seismic design with passive energy dissipation systems." *Journal of Earthquake Engineering,* **13**: 758–790.

Lavan, O. and Levy, R. (2006). "Optimal peripheral drift control of 3D supplemental viscous dampers." *Journal of Earthquake Engineering,* **10**(6): 903–923.

Lavan, O. and Levy, R. (2010). "Performance based optimal seismic retrofitting of yielding plane frames using added viscous damping." Earthquakes and Structures, **1**: 307–326.

Levy, R. and Lavan, O. (2006). "Fully stressed design of passive controllers in framed structures for seismic loadings." *Structural and Multidisciplinary Optimization,* **32**(6): 485–498.

Liu, W., Tong, M. and Lee, G.C. (2005). "Optimization methodology for damper configuration based on building performance indices." *Journal of Structural Engineering (ASCE),* **131**(11): 1746–1756.

MATLAB. (2014). The MathWorks, Inc.: Natick, Massachusetts, USA.

McKenna, F., Fenves, G. L. and Scott, M. H. (2000). "Open system for earthquake engineering simulation." University of California, Berkeley, California, <http://opensees.berkeley. Edu> (1 August 2016).

Miguel, L. F. F., Miguel, L. F. F. and Lopez, R. H. (2014). "Robust design optimization of friction dampers for structural response control." *Structural Control and Health Monitoring*, **21**: 1240–1251.

Miguel, L. F. F., Miguel, L. F. F. and Lopez, R. H. (2016). "Simultaneous optimization of force and placement of friction dampers under seismic loading." *Engineering Optimization*, **48**: 586–602.

Milman, M. H and Chu, C. C. (1994). "Optimization methods for passive damper placement and tuning." *Journal of guidance, control and dynamics*, **17**(4): 848–856.

Moghaddam, H. and Hajirasouliha, I. (2008). "Optimum strength distribution for seismic design." *The Structural Design of Tall and Special Buildings*, **17**: 331–349.

Moreschi, L. M. and Singh, M. P. (2003). "Design of yielding metallic and friction dampers for optimal seismic performance." *Earthquake Engineering and Structural Dynamics*, **32**: 1291–1311.

Murakami, Y., Noshi, K., Fujita, K., Tsuji, M. et al. (2013). "Simultaneous optimal damper placement using oil, hysteretic and inertial mass dampers." *Earthquakes and Structures*, **5**(3): 261–276.

Nabid, N., Hajirasouliha, I. and Petkovski, M. (2017). "A practical method for optimum seismic design of friction wall dampers." *Earthquake Spectra*, **33**(3): 1033–1052.

Nabid, N., Hajirasouliha, I. and Petkovski, M. (2018), "Performance-based Optimisation of RC Frames with Friction Wall Dampers Using a Low-Cost Optimisation Method." *Bulletin of Earthquake Engineering*, in press.

Papageorgiou, A., Halldorsson, B. and Dong, G. (2002). "TARSCTH (Target Acceleration Spectra Compatible Time Histories)", *Engineering Seismology Laboratory (ESL) at the State University of New York at Buffalo.*

Park, J. H., Kim, J. and Min, K. W. (2004). "Optimal design of added viscoelastic dampers and supporting braces." *Earthquake Engineering and Structural Dynamics*, **33**(4): 465–484.

PEER NGA. Online database. Available from: <http://peer.berkeley.edu/nga/search.html> (23 Feb 2016).

Petkovski, M. and Waldron, P. (2003). "Optimum friction forces for passive control of the seismic response of multi-storey buildings." *Proc., 40 years of European Earthquake Engineering SE40EEE*. Ohrid, Macedonia.

Sasani, M. and Popov, E. P. (2001). "Seismic energy dissipators for RC panels." *Journal of Engineering Mechanics,* **127**(8): 835–843.

Singh, M. P. and Moreschi, L. M. (2001). "Optimal seismic response control with dampers." *Earthquake Engineering and Structural Dynamics,* **30**: 553–572.

Takewaki, I. (2011). "Building control with passive dampers: optimal performance-based design for earthquakes." *John Wiley & Sons (Asia) Books*, Singapore: 51–75.

Uetani, K., Tsuji, M. and Takewaki, I. (2003). "Application of an optimum design method to practical building frames with viscous dampers and hysteretic dampers." *Engineering Structures*, **25**(5): 579–592.

Whittle, J. K., Williams, M. S., Karavasilis, T. L. and Blakeborough, A. (2012). "A comparison of viscous damper placement methods for improving seismic building design." *Journal of Earthquake Engineering*, **16**(4): 540-560.

Whittle, J. K., Williams, M. S. and Karavasilis, T. L. (2013). "Optimal placement of viscous dampers for seismic building design." Chapter 2 In: Lagaros ND, Plevris V and Mitropoulou CC (Ed) Design optimization of active and passive structural control systems, edition pp 34-50.

# CHAPTER 6

# Adaptive Low Computational Cost Optimisation Method for Performance-Based Seismic Design of Friction Dampers

## 6.1. ABSTRACT

This study aims to develop an adaptive low-cost optimisation method for optimum design of friction-based dampers based on the concept of Uniform Distribution of Deformation (UDD). In this approach, the mechanical properties of the dampers are modified according to the maximum displacement demands at different levels until a pre-defined performance target is satisfied for a design earthquake. It is shown that the computational cost can be considerably reduced by using a convergence factor that is modified in proportion to the level of performance violation. To investigate the efficiency of the proposed method, 3, 5 and 10-storey RC frames with friction dampers are optimised using adaptive UDD method, Genetic Algorithm (GA) and a coupled UDD-GA approach. The results indicate that the adaptive UDD method can lead to optimum design solutions with significantly lower computational costs (up to 300 times lower number of non-linear dynamic analyses) compared to both GA and coupled UDD-GA methods. It is shown that frames optimised under a under a single spectrum-compatible earthquake can efficiently satisfy the predefined performance targets under a set of synthetic earthquakes representing the design spectrum. Therefore, the proposed method should provide a reliable approach for more efficient design of friction-based dampers.

*Keywords: Friction damper; Adaptive optimisation; Uniform Distribution of Deformation; Genetic Algorithm.*

## 6.2. INTRODUCTION

Friction and metallic dampers dissipate considerable amounts of seismic input energy through yielding metal and friction between two or more solid bodies, respectively. Both dampers, which are referred as hysteretic dampers, exhibit hysteretic behaviour that can be idealised by an elastic perfectly plastic load-displacement relationship (Filiatrault et al., 2013). Due to their high energy dissipation capacity, the hysteretic dampers are considered as potentially efficient passive control systems to enhance seismic performance of substandard structures. The key task in the design of friction energy dissipation devices is to determine the slip load values (the loads at which the friction devices start slipping and dissipating energy) at each floor leading to best seismic performance in terms of lateral displacement, energy dissipation or imposed forces to the structural elements. Lateral displacements have been considered as appropriate parameter to measure structural damage under earthquake excitations. Displacement control method is one of the main approaches in seismic performance-based design, in which the lateral displacement of each storey level in the structure is restricted using a predefined displacement target value to satisfy a desired performance level under a design earthquake.

The concept of performance-based seismic design was also utilised for optimisation of structures with supplemental dampers. Several performance-based optimal design methodologies were developed by Liu et al. (2005), Lavan and Levy (2010) and Lavan and Amir (2014) to obtain the best sizing and allocation of viscous dampers in regular and irregular building structures. Similarly, a displacement-based design procedure was developed by Kim and Choi (2006) to obtain an optimum number of velocity-dependent dampers for existing steel structures while satisfying a pre-defined performance limit state. Takewaki (2011) proposed criteria-based and sensitivity-based design algorithms for optimal design of passive energy dissipation devices by considering displacement, acceleration, and earthquake input energy as the main performance-based design indices.

In one of the early attempts, Mohammadi et al. (2004) used the concept of uniform deformation of displacement demands to determine the optimal distribution of stiffness in shear-buildings by using a basic iterative procedure. In follow-up studies, Moghaddam and Hajirasouliha (2006; 2008) and Hajirasouliha and Moghaddam (2009) proposed an empirical equation to improve the efficiency of the optimisation process for performance-based design of shear-building structures subjected to seismic excitations.

The concept of UDD has been adopted in several studies for optimum seismic design of passive dampers. For instance, Lavan (2015) used the same concept to present a performance-based approach for optimum design of nonlinear structures with viscous dampers aimed at limiting the maximum drift and acceleration of all the storey levels as well as reducing the seismic forces applied to the structure. In addition, Mohammadi et al. (2018) proposed optimisation design methods based on the theory of UDD for optimum stiffness and distribution design of metallic yielding dampers in concentrically braced steel frames subjected to strong ground motion records. More recently, Nabid et al. (2018) utilised the same concept to develop a practical optimisation methodology for seismic design of friction dampers in RC structures. However, their proposed method is based on redistributing a constant total slip load value (sum of slip loads in all dampers), and hence cannot be directly used to achieve a specific target for performance-based seismic design purposes.

During the optimisation process, the convergence factor is considered as one of the key parameters to determine the speed of the optimisation. The value of this factor depends on the type of structure, number of storeys, optimisation algorithm or, in general, seismic response of structures. It should be mentioned that the majority of the above mentioned researches are either used for the optimum design of velocity dependent passive control systems such as viscous and viscoelastic dampers or are based on a constant predefined convergence parameter which leads to low convergence rate if it is not properly selected. In this study, an adaptive equation is proposed for the selected frames to increase the speed of the optimisation process. The convergence rate of the proposed adaptive UDD optimisation is then compared with those obtained for the previously proposed standard UDD optimisation algorithms using constant values of the convergence factor.

Genetic Algorithm (GA) is a directed population-based random search, based on a biological evolution mechanism and Darwin's survival-of-the-fittest theory for solving complex problems where the number of parameters is large and the analytical solutions are difficult to obtain (Holland, 1975; Goldberg, 1989). Unlike to most classical optimisation methods, GA produces multiple optima, rather than a single local optimum, with no need to gradient information that makes GA a powerful tool for global optimisation (Venter, 2010).

Due to the high accuracy and reliability, standard GA and its improved versions are widely adopted in optimisation of different control systems. In an early attempt, Hadi and Arfiadi (1998) employed the genetic algorithm method to find the optimum mass value of TMD dampers. In a research conducted by Singh and Moreschi (2002), GA was utilised for optimal design of size and location of viscous and viscoelastic dampers by considering a

desired level of reduction in the performance index. Moreschi and Singh (2003) also used GA for optimum height-wise placement of friction dampers in steel braced frames when satisfying a predefined performance objective. A simultaneous optimisation design method using GA was presented by Park et al. (2004) for a visco-elastically damped structural system by considering the structure and the damper as a combined or an integrated system. In their proposed method, the size of structural members, the amount and the location of viscoelastic dampers are considered as design variables while the life-cycle cost is adopted as an objective function to be minimised. Using a similar approach, Miguel et al. (2014) applied the GA technique for multi-objective optimisation of friction dampers in shear-buildings subjected to seismic loading. In this study, a standard GA is adopted to find the global optimum design solutions for selected RC frames with friction dampers as a bench mark for comparison purposes.

In this study a practical performance-based optimisation methodology is developed to find optimal configuration of friction dampers in RC structures under seismic excitations, based on the concept of Uniform Distribution of Deformation (UDD) using an adaptive convergence parameter. The computational efficiency of the proposed method is then demonstrated through optimisation of 3, 5 and 10-storey frames with friction dampers and comparison with the results obtained from standard UDD optimisation with constant convergence factors as well as a Genetic Algorithm (GA) and a coupled UDD-GA approach.

## 6.3. MODELLING AND DESIGN ASSUMPTIONS

### 6.3.1. Design Assumptions

In this study the benchmark structures are 3, 5 and 10-storey RC frames equipped with friction dampers with the typical geometry shown in Fig. 6.1 (a). The details of the friction damper are shown in Fig. 6.1 (b). The employed assembly comprises a concrete wall panel, a friction device at the top, horizontal supports at the bottom, and vertical supports at the sides. A Slotted Bolted Connection (SBC) is used as the friction device, and the friction mechanism is provided by the relative movement between the two external steel plates attached to the wall, and a T-shape central steel plate, attached to the beam; with brass plates inserted at the interfaces. The lateral connections can prevent transferring extra shear forces to the adjacent columns and the floor beams by using appropriate slot direction. More detailed information about the adopted system can be found in Nabid et al. (2017).

The studied RC frames were assumed to be located on a soil type C of Eurocode 8 (EC8) (CEN, 2004a) category and were designed based on the low-to-medium seismicity regions using PGA of 0.2g. The uniformly distributed live and dead loads were considered to be 1.0 kN/m$^2$ and 5.3 kN/m$^2$ for the roof level; and 2.5 kN/m$^2$ and 5.5 kN/m$^2$ for all the other floors. The reference frames were initially designed in accordance with EC8 (CEN, 2004a) and Eurocode 2 (EC2) (CEN, 2004b); for moment-resisting RC frames with medium ductility (DCM). The concrete compressive strength ($f_c'$) and the yield strength of steel reinforcement bars ($f_y$) were assumed to be 35MPa and 400 MPa, respectively.

### 6.3.2. Opensees Modelling

In this study, the OpenSees software (McKenna and Fenves, 2000) was used for modelling and conducting the pushover and nonlinear time-history analyses. To model the concrete and reinforcing steel bars, a uniaxial constitutive material with linear tension softening (Concrete02) and a Giuffre–Menegotto–Pinto model (Steel02) with 1% isotropic strain hardening were used, respectively. Beam and column members were divided into three elements and modelled using displacement-based nonlinear beam-column elements with fibre sections while four Gauss–Lobatto integration points were considered for each element. P-Delta effects were taken into account and the Rayleigh damping model with a constant damping ratio of 0.05 was assigned to the first mode and to the modes at which the cumulative mass participation exceeds 95%. In this study, it was assumed that the strength of the concrete wall panels (15 cm thickness) is always higher than the maximum loads transferred from the friction device, and therefore, they were modelled using equivalent elastic elements. A nonlinear spring with an elastic-perfectly plastic uniaxial material, representing an ideal Coulomb friction hysteretic behaviour, was used to model the friction device. The beam-to-column connections were assumed to be fully rigid with no shear failure in the panel zones. A computer code in MATLAB (2016) platform was developed and linked to the OpenSees program to analyse the output data.

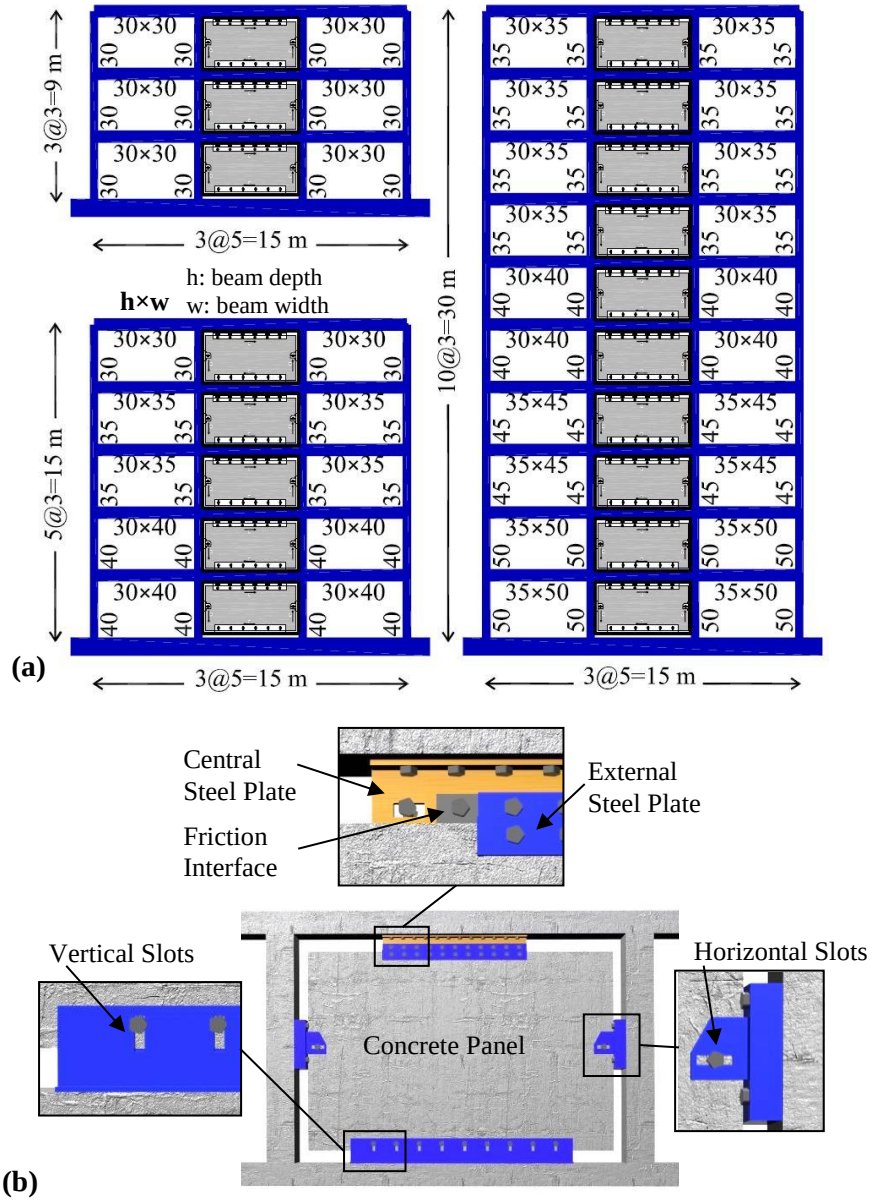


**Fig. 6.1.** (a) Geometry of the reference RC frames equipped with friction wall dampers, (b) schematic view of the friction wall damper (adopted from Nabid et al. (2017))

## 6.4. SYNTHETIC EARTHQUAKE RECORD

Previous research studies (Hajirasouliha et al., 2012; Nabid et al, 2018) have suggested that the earthquake uncertainty, in terms of acceleration response spectra, can be efficiently managed by using the optimum design corresponding to a synthetic earthquake generated to match a response spectrum obtained as an average of the response spectra of a selected set of natural earthquakes. It should be noted that most seismic performance-based design guidelines (e.g. FEMA 356 (2000) and ASCE/SEI 41-06 (2006)) aim to control the seismic response of the buildings under two different earthquake levels: (a) Design Basis Earthquake

(DBE) with 10% probability of exceedance in 50 years, and (b) Maximum Considered Earthquake (MCE) with 2% probability of exceedance in 50 years. In this study, the optimisation process is conducted under DBE level and the results are then controlled to satisfy MCE level requirements. This implies that the structure is optimised under an earthquake event with higher probability of occurrence and then is controlled under a less frequent earthquake scenario. A similar approach has been adopted by Hajirasouliha et al. (2012) for optimum seismic design of RC frames.

Six synthetic DBE level earthquakes compatible with the EC8 design response spectrum were generated using the TARSCTHS (Papageorgiou et al., 2002) software, assuming a high seismicity region (i.e. PGA=0.4g) and soil class C. Fig. 6.2 demonstrates the elastic response spectra of the generated synthetic earthquake records and the EC8 design spectrum. It should be mentioned that although the generated synthetic earthquakes are all compatible with a same design response spectrum, they have random acceleration vibration specifications. In this study, SIM01 is assumed as the DBE event to be used during the performance-based optimisation process, while the other earthquake records are then used to evaluate the sensitivity of the optimum design solutions. The MCE records were obtained by scaling the generated records to have a PGA= 0.6g.

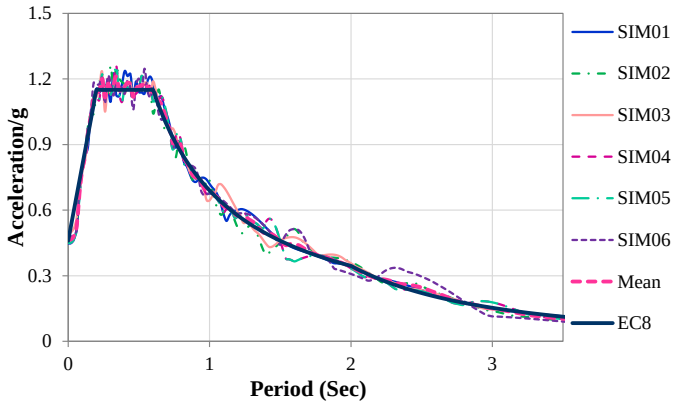


**Fig. 6.2.** Elastic acceleration response spectra of the synthetic earthquake records and the EC8 design spectrum, 5% damping ratio

## 6.5. ADAPTIVE UDD OPTIMISATION ALGORITHM

This section presents the details of the proposed adaptive UDD optimisation algorithm for optimal configuration of friction dampers in RC frame structures under a design earthquake. In this study, the structures are assumed to satisfy the Life Safety (LS) and Collapse Prevention (CP) performance levels under DBE and MCE events, respectively. Therefore, in the proposed iterative optimisation method, the slip load values of the friction devices are

gradually modified until the pre-defined performance targets are satisfied under the representative design earthquakes. Unlike the previously adopted UDD optimisation algorithms with constant values of convergence parameters (e.g. Mohammadi et al., 2004; Hajirasouliha et al., 2012; Lavan, 2015; Mohammadi et al., 2018; Nabid et al., 2018), the proposed method employs an adaptive equation in which the convergence factor is modified in proportion to the level of performance violation. The suggested optimisation algorithm comprises the following iterative steps:

1) A uniform slip load distribution with identical slip load values for all the storey levels is assumed for the initial design of the friction devices. It should be noted that the final optimum design solution is independent of the initial slip load values as shown in a previous study performed by Nabid et al. (2018), however, the optimisation rate can be affected by the initial design.

2) The benchmark structure is then subjected to the selected synthetic spectrum-compatible earthquake and the value of maximum inter-storey drift is obtained at each storey level and compared with the performance target value. For the initial designs with very high or very low slip load values, the maximum drifts may be far below or far above the performance target, which increases the number of iterations in the optimisation procedure.

3) During the optimisation process, the slip loads are changed so that all of the relative displacements reach the predefined performance-based design objective. To satisfy this, the slip load is increased in the storeys where the inter-storey drift exceeded the predefined performance target, and reduced in the storeys with inter-storey drifts below the target value. The process continues until all inter-storey drifts are close to the performance target within a predefined tolerance, when the structure is considered to be practically optimum. The following equation was used to obtain the optimum distribution of slip loads:

$$\left(F_{s,i}\right)_{n+1} = \left(F_{s,i}\right)_{n} \times \left(\frac{\Delta_i}{\Delta_{target}}\right)_{n}^{\alpha} \tag{6.1}$$

where $\Delta_i$ and $\Delta_{target}$ are maximum and target inter-storey drifts of $i^{th}$ storey for $n^{th}$ iteration, respectively; $F_{s,i}$ is defined as the slip load of the friction device at the $i^{th}$storey; $\alpha$ is the convergence parameter, which has a prominent effect on the speed of the optimisation process. Previous studies have proposed different ranges for the convergence parameter

including: 0.1 to 0.2 proposed by Hajirasouliha et al. (2012) for shear-building structures, 0.4 to 0.8 suggested by Mohammadi et al. (2018) for steel frames with metallic-yielding dampers, 0.2 to 0.5 suggested by Nabid et al. (2018) for RC frames with friction dampers, and 0.5 recommended by Lavan (2015) for nonlinear structures with viscous dampers.

To provide the best convergence rates, in this study an adaptive equation (Equation 6.2) is proposed as the convergence factor of the UDD optimisation algorithm. The adaptive convergence factor is determined proportional to the ratio of the relative displacement obtained from the non-linear dynamic analysis in each step and the constant, predefined target displacement. The proposed equation has a power factor obtained based on an extensive parametric study to sufficiently accelerate the convergence of the optimisation process by adapting the α value based on the difference between the maximum drift and the performance target. The power factor increases the α value where the difference between the maximum drift and the performance target is small. On the contrary, to avoid significant changes in the slip loads of the storeys, the selected power factor can reduce the α value where the ratio between the drift and the target displacement is large. However, for faster convergence, there is still more alteration of the slip loads in storeys with higher ratio of drift to target displacement compared to those with smaller ratios. The proposed equation is dimensionless and expected to achieve a good convergence during the optimisation process irrespective to the size of the selected frame.

$$\alpha_i = Abs\left( Ln(\frac{\Delta_i}{\Delta_{target}}) \right)^{-0.25} \tag{6.2}$$

It will be shown in the following sections that the adaptive convergence parameter, in general, leads to the highest convergence rate compared to the optimisation with constant values, while the final design solution is unique. In every optimisation iteration, the coefficient of variation of the inter-storey drifts ($COV_\Delta$) is also calculated. The optimisation algorithm continues from step 2 until an acceptable level of $COV_\Delta$ is achieved (e.g. less than 0.1). The final design solution is then subjected to the MCE record and the maximum inter-storey drifts are controlled to ensure CP level is satisfied. If the performance criteria are violated at any storey level, the corresponding slip load is adjusted using a simple iteration process. Since the initial structure is designed for gravity and seismic loads based on a seismic design code, at some storey levels the target inter-storey drift may be satisfied without using friction dampers. Therefore, it is not usually possible to reach a very uniform inter-storey drift distribution (i.e. very low $COV_\Delta$), especially when the effect of gravity loads

is dominant. However, as will be discussed in the following sections, the proposed algorithm is capable of removing the unnecessary dampers during the optimisation process.

To demonstrate the efficiency of the proposed performance-based adaptive optimisation algorithm, the 3, 5, and 10-storey RC frames with friction dampers were optimised. In this study, LS and CP performance limits were considered to be 2% and 4% maximum inter-storey drift ratio under DBE and MCE representative spectrum compatible earthquakes, respectively. Fig. 6.3 demonstrates the variation of (a) convergence parameters and (b) slip load values in different storey levels of the 3, 5, and 10-storey frames as the iterations proceed.

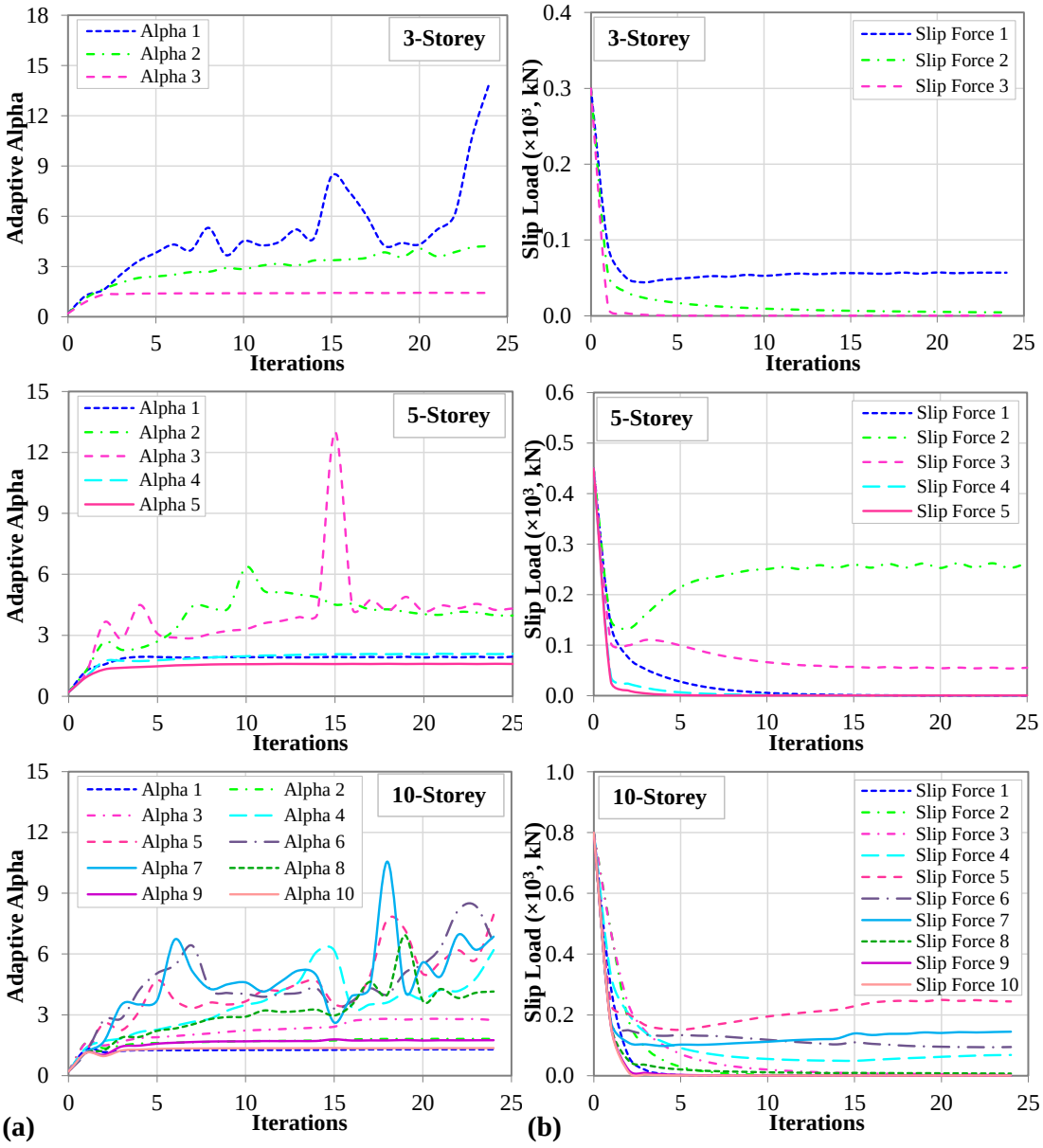


**Fig. 6.3.** Variations of (a) convergence parameter and (b) slip load value at each storey level for 3, 5, and 10-storey frames, DBE event

As expected from Equation 6.2, the storey levels with higher maximum inter-storey drifts, and in turn higher values of slip loads, exhibited more fluctuations in the convergence parameter. According to the results, in general, the slip loads reached their final optimum values in less than 25 steps. As illustrated in Fig. 6.3 (b), the slip loads of the first floor and the top two floors tend to be zero as they have already satisfied the predefined performance levels without using friction dampers. The reason for the low lateral displacement of the first floor is the fixed connections at the base.

## 6.6. COMPARISON BETWEEN ADAPTIVE AND STANDARD UDD OPTIMISATION METHODS

According to previous research (e.g. Hajirasouliha et al., 2012; Nabid, 2018; Mohammadi et al., 2018), the range for the efficient convergence rate varies for different optimisation problems. In addition, while this parameter is affected by the type and size of the structure, it may not be efficient to use a constant value for frame structures with different number of storeys. In this section, the efficiency of the proposed adaptive UDD optimisation algorithm is compared to the standard UDD method with constant values of the convergence factor for the selected 3, 5, and 10-storey frames under the representative DBE event. In case of standard UDD optimisation, the convergence factors are selected between 0 and a value which leads to the fluctuation of the results and divergence of the iterations. Fig. 6.4 compares the convergence rate of the adaptive and standard UDD in terms of maximum drift ratio (drift scaled to storey height) and total slip load value required to satisfy LS performance target under the DBE representative synthetic earthquake.

Figure 6.4 shows that the small values of the convergence factor lead to very slow convergence rates of both maximum drift and slip load, while the higher values of this factor results in divergence of the iterations. The proposed adaptive α factor, however, converges the optimisation in only a few steps (i.e. less than 10 steps). Previous studies conducted by Hajirasouliha et al. (2012) and Nabid et al. (2018) showed that their optimisation iterations did not converge for convergence factors higher than 0.5 and 1, respectively. However, as shown in Fig. 6.4 (a), for the current optimisation problem, α factor greater than 2, 3 and 5 leads to fluctuation of the results for the 3, 5, and 10-storey frames, respectively. Therefore, the efficient range of convergence factor is not limited to a specific domain for all problems.

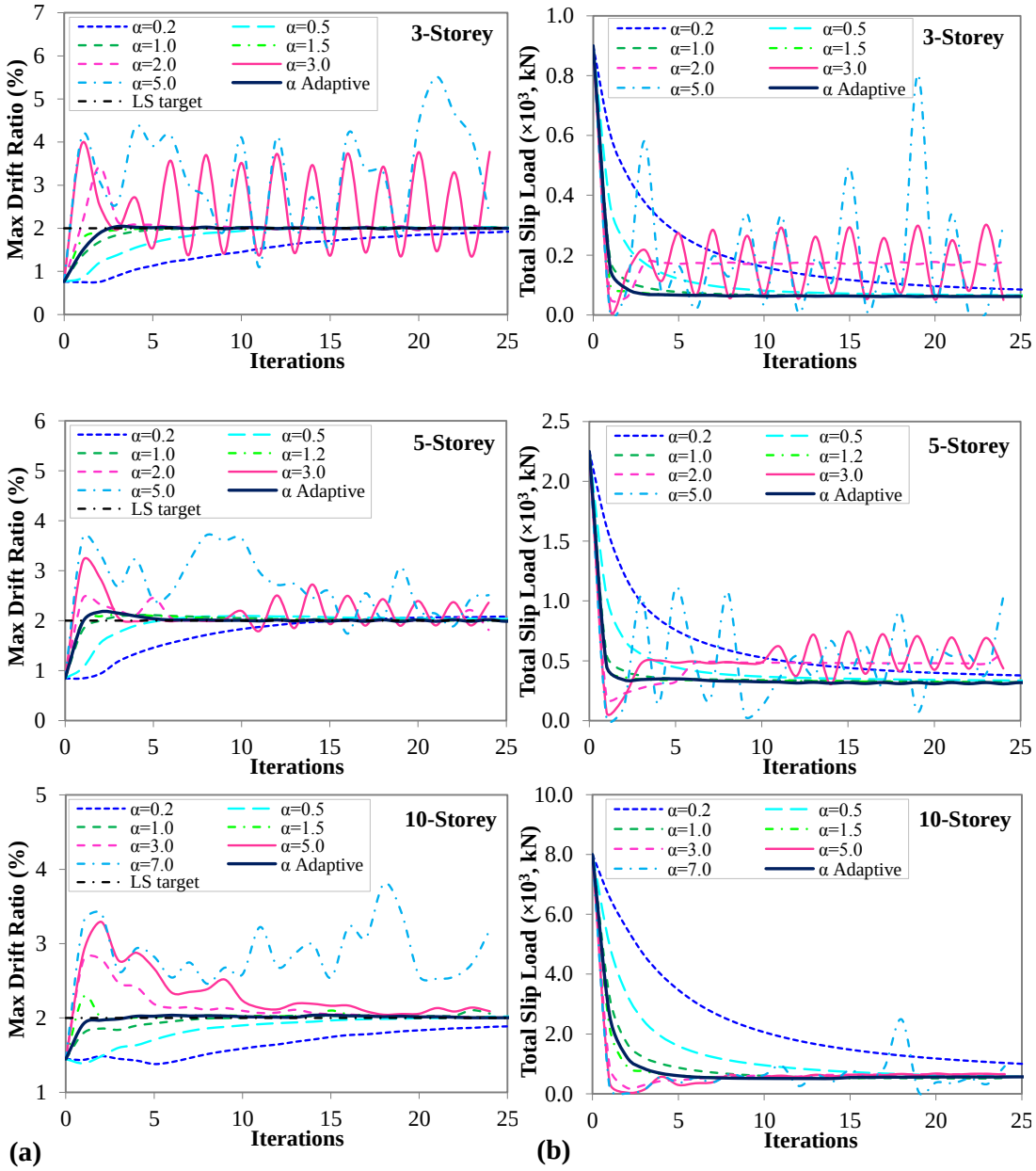


**Fig. 6.4.** Variations of (a) maximum inter-storey drift ratio (scaled to the storey height) and (b) total slip load value for 3, 5, and 10-storey frames, DBE event

## 6.7. OPTIMISATION USING A GENETIC ALGORITHM (GA)

The genetic optimisation algorithm (GA) was first introduced by Holland (1975) to simulate the natural evolutionary process for generating the best or the fittest species. In general, GA aims at increasing the average fitness of the population at each generation by combining the more fit individuals to converge the solution to an optimal point. The evolution (or generation) which is an iterative process, with a population of design solutions at each iteration, is usually initiated from a population of randomly generated individuals. The next

generation of population is produced using three dominant operators including selection, crossover and mutation. Each individual or design solution has a set of properties such as chromosomes which can be mutated. The solutions can be represented in binary as strings of 0s and 1s. In each generation, the fitness (related to the objective function) of every individual is evaluated and the individuals with high fitness have several chances for joining in the reproduction phase. Based on the individual's fitness, a probability is allocated to each individual for being selected as a parent. The next generation is developed from selected parent strings and by using explorative operators such as crossover and mutation. The crossover operator creates variations in the population by dividing the selected parent string into parts and exchanging some of these parts with corresponding parts of another parent string. Mutation operator is usually used as an insurance policy (Goldberg, 1989), and is responsible for reintroducing random changes and diversity in a solution population. Mutation enables children to have features that are non-existing in their parents' strings. Without using the mutation operator, some regions of the search space may never be discovered. The termination criteria of the algorithm are to satisfy either a maximum number of generations or a desired fitness level for the population (Camp et al., 1998).

Conventionally, genetic algorithms are developed to solve unconstrained optimisation problems. For constrained optimisation problems, either GA operations should be modified or the problem should be transformed to an unconstrained problem before the GA can be adopted (Adeli and Cheng, 1994). To handle constrained optimisation problems, several approaches have been proposed. They can be grouped in four major categories (Michalewicz and Schouenauer, 1996): 1) methods based on penalty functions 2) methods based on a search of feasible solutions 3) methods based on preserving feasibility of solutions and 4) hybrid methods.

One of the most popular constraint handling methods is the penalty function method in which infeasible solutions are penalised by reducing their fitness values proportional to the degrees of constraint violation (Smith and Coit, 1997). Different penalty functions have been proposed to solve the constraint problems such as Death Penalty, Static Penalties, Dynamic Penalties, Annealing Penalties and Adaptive Penalties (Yeniay, 2005). In most penalty schemes some coefficients have to be specified at the beginning of the optimisation. It is very challenging to estimate appropriate values as there is no clear physical meaning for these coefficients (Nanakorn and Meesomklin, 2001). When a big value of penalty can prevent a search in an infeasible region, a small penalty will cause the algorithm to spend time on searching an infeasible region. In the first case, GA will converge to a feasible

solution very quickly even if it is far from the optimum, while in the latter case, GA would converge to an infeasible solution (Yeniay, 2005).

In this study, the following GA optimisation procedure is employed for optimum design of the 3, 5 and 10-storey frames with friction dampers, using a Matlab-based (2016) coding developed for this purpose:

1) The initial population of 50 individuals is randomly selected from a wide range of slip loads starting from 0 to a relatively high value (almost equal to the corresponding mean storey shear strength).

2) Non-linear time-history dynamic analysis is performed using the representative DBE event as input, and the maximum inter-storey drift of all the storeys is determined.

3) To consider the optimisation constraints in this study, an effective penalty approach is applied, in which the penalised value for each violated optimisation constraint is gradually decreased as the maximum inter-storey drift gets closer to the predefined performance target (i.e. LS performance level). Therefore, a penalty proportional to the violation of the performance target is applied to the slip loads of the storeys which exceed that value. Then, the objective function *(OF)* which is defined as a summation of the slip loads required for all the friction devices, is calculated. Exploration of the optimal result is then performed according to the fitness of the objective function. Equations 6.3 and 6.4 are used for calculating the penalty function *(PF)* and objective function *(OF)*, respectively:

$$PF = a \times 1e3 \times \left( \frac{\Delta_{\max}}{\Delta_{target}} - 1 \right) \tag{6.3}$$

$$OF = \sum_{i=1}^{N} F_{s,i} + PF \tag{6.4}$$

where $a$ is an empirical scale factor considered to be equal to 1, 1.5 and 3 for the 3, 5 and 10-storey frames, respectively. These numbers were found to be sufficient to scale the penalty value to the same order with the objective function (*i.e. proportional to the number of terms in OF)*. $\Delta_{max}$ and $\Delta_{target}$ are the maximum and target inter-storey drifts, and *N* is the number of storeys. The proposed penalty function which was obtained based on several trial and errors, adds an appropriate (not very large nor very small) expense to the objective function based on the maximum inter-storey displacement and its exceedance of LS performance level. For an analysis with maximum drift less than the target value, penalty

function is considered as 0. In this algorithm, Steps 2 and 3 are repeated for the entire population of samples.

4) Using the GA operators, a new population is generated from the best individuals of the previous generation.

5) The algorithm is then repeated from step 2 to 4 for each generation until the mean value of the objective function converges to the best fitness function in the same generation or the maximum number of generations is achieved. Subsequently, the final design solution is subjected to the MCE representative record and the maximum inter-storey drifts are compared with the predefined CP performance level target. If the inter-storey drift exceeds the target at any storey level, the corresponding slip load is increased using a simple iteration process.

In this study, stochastic uniform approach is chosen as the selection function, and Uniform and Heuristic methods are considered as the mutation and crossover operators, respectively, during the GA optimisation process. In uniform mutation strategy, the value of the chosen gene is replaced with a uniform random value selected between the user-specified upper and lower bounds for that gene (Sivanandam and Deepa, 2007). In heuristic crossover, the fitness values of two parent chromosomes are utilised to ascertain the direction of the search moving from the parent with the worse fitness value to the parent with the better fitness value (Ackora-Prah et al., 2014). Fig. 6.5 illustrates the variation of the mean and best values of the fitness function (objective function, Equation 6.4) for the 3, 5, and 10-storey frames subjected to the representative DBE event as the generations proceed during the GA optimisation. For better comparison, the optimisation was repeated three times for each frame using different sets of random initial populations (slip load values) and the answer with the lowest fitness values was retained as the optimum solution. In all cases, the global optimum answer was reasonably achieved with a small standard deviation. Based on the results, the optimisation procedures converged to the fittest values after about 40 generations for the 3, 5 storey frames and about 60 generations for the 10-storey frame. In this study, the GA optimisation is considered to converge to an optimum design solution when there is no/negligible (i.e. less than 1%) fluctuation in the best fitness values for several consecutive generations (e.g. 10 generations).

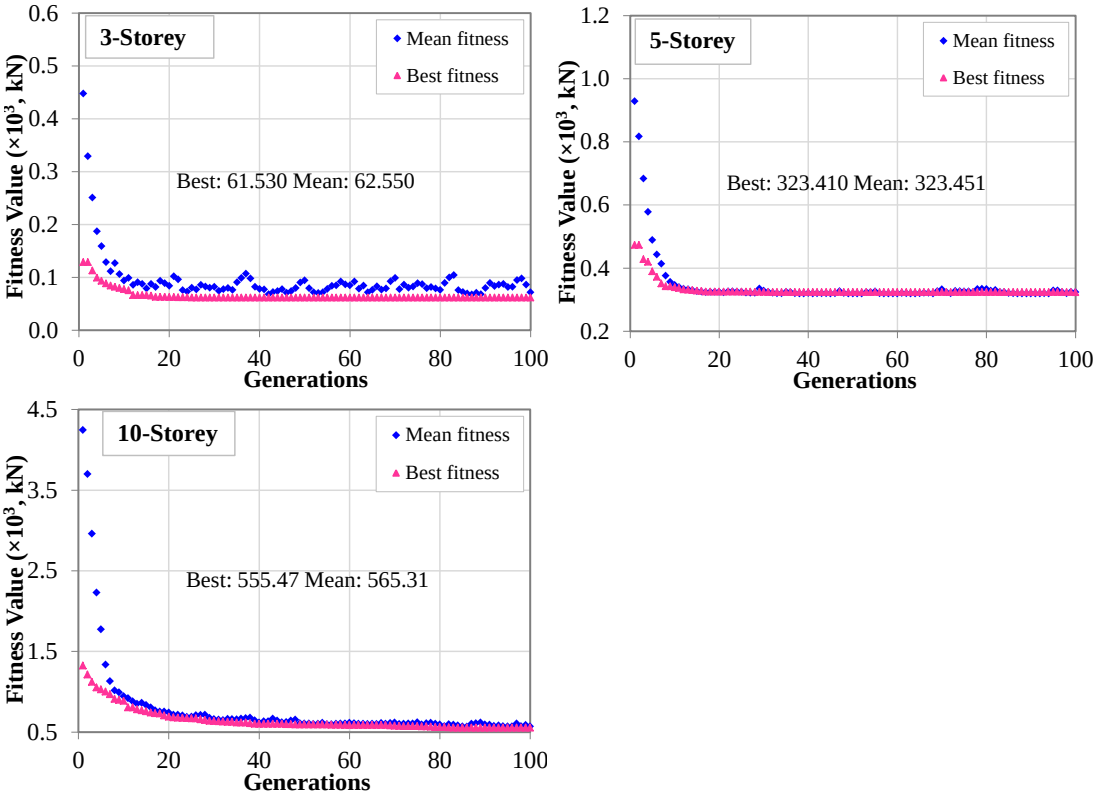


**Fig. 6.5.** Variations of fitness function of 3, 5, and 10-storey frames versus optimisation generation during GA optimisation, DBE event

Fig. 6.6 demonstrates the variations of inter-storey drift and slip load in the friction device at each storey level, the total slip load and the coefficient of variation of the inter-storey drifts ($COV_{\Delta}$) for the 5-storey frame under the representative DBE event as the optimisation proceed. In the evolutionary GA optimisation, the number of nonlinear dynamic response simulations is equal to the population size in each generation (e.g. in this study, one generation is 50 nonlinear dynamic analyses). As can be observed from Fig. 6.6 (a), at the beginning of the optimisation, when a set of slip loads (population) is randomly selected from a wide range of upper and lower bounds of slip loads (scattered points) the resulting inter-storey drifts are considerably higher/lower than the allowable target value (i.e. 6 cm ;see Fig. 6.6 (b)). As the optimisation progresses, successful individuals are mutated to create a new population (a new set of slip loads) while satisfying the performance target level (i.e. LS level) with the minimum value of total slip load (Fig. 6.6 (c)). Fig. 6.6 (d) shows that the GA optimisation converged after about 2000 response simulations (i.e. 40 generations) with $COV_{\Delta}$ decreasing from 105% to around 16%.

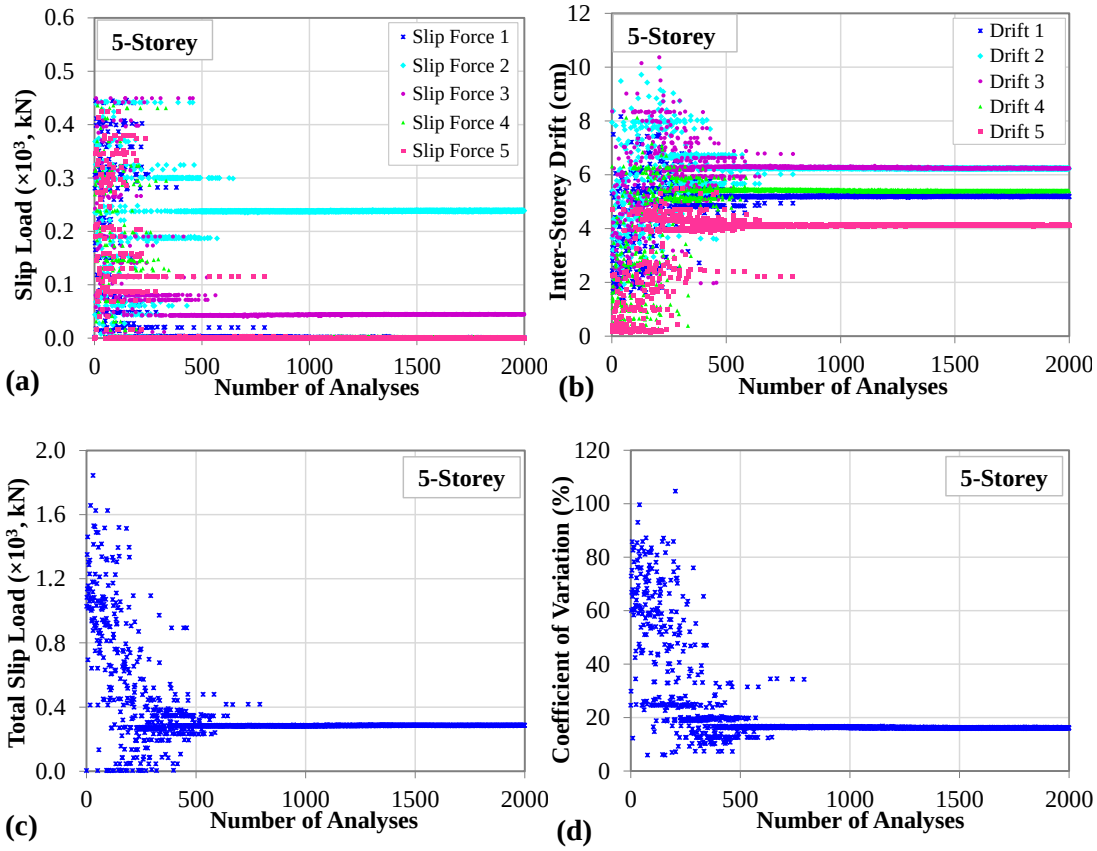


**Fig. 6.6.** Variations of (a) each storey slip load value, (b) each storey lateral drift, (c) total slip load and (d) COV of the drifts for 5-storey frame during GA optimisation, DBE event

## 6.8. COMPUTATIONAL EFFICIENCY OF ADAPTIVE UDD OPTIMISATION METHOD

In order to demonstrate the efficiency of the proposed adaptive optimisation method in terms of convergence speed and optimum design solutions, the results are compared with those obtained from the optimisation using the Genetic Algorithm (GA) technique. In this section, the previous GA optimisations are repeated for the selected frames, starting from predefined slip load values rather than using random selections. The optimum slip load values obtained from the proposed UDD optimisation strategy are considered as the initial slip load values (i.e. initial population) for the GA optimisation.

Table 6.1 compares the objective functions and the total number of non-linear dynamic analyses of the 3, 5 and 10-storey frames optimised using (1) the proposed adaptive UDD method, (2) GA optimisation starting with random values (i.e. GA) and (3) GA optimisation starting with optimum values obtained from the adaptive UDD (i.e. UDD-GA) under the representative DBE event. It can be noted that the number of non-linear dynamic analyses required for the GA optimisation is significantly higher than those needed for the adaptive

UDD (by up to 300 times), while these two methods lead to almost similar objective functions. It is shown that for the 3 and 10-storey frames using the GA method results in a negligible improvement (less than 2%) in the objective function of the final optimum design solutions compared to the adaptive UDD method. For the 5-storey frame, even after 2000 analyses the GA approach has not reached a better design solution than the UDD method.

It is shown in Table 6.1 that using the optimum results from the UDD as the initial population of the GA (i.e. UDD-GA) considerably decreases the number of required analyses (by up to 65%), which means that the UDD-GA combination is a significant improvement in terms of computational costs comparted to the standard GA optimisation. For example, the optimum solution of the coupled UDD-GA method for the 5-storey frame, with a total of 800 simulations, is only slightly better than the one achieved with the adaptive UDD method after only 10 simulations (313.38 kN versus 318.04 kN). This confirms the simplicity and computational efficiency of the proposed adaptive UDD method compared to the global evolutionary optimisation methods such as GA.

Fig. 6.7 illustrates the height-wise distribution of slip load values for the 3, 5 and 10-storey frames optimised using the proposed adaptive UDD, GA and UDD-GA optimisation methods under the representative DBE event. The slip load distributions follow similar patterns for all the selected optimisation approaches. The only exception is the 10-storey frame with higher number of variables, where the slip load distribution obtained from the GA optimisation after 3000 analyses is slightly different with the UDD and UDD-GA results. This implies that there are at least two different slip load distributions that lead to very similar objective functions.

**Table 6.1.** Comparison of GA, adaptive UDD, and UDD-GA methods in terms of total number of non-linear dynamic analyses and objective function (total slip load), DBE event

| | **Adaptive UDD** | | **GA** | | **UDD-GA** | |
|---|---|---|---|---|---|---|
| | No. of analyses | Objective function (kN) | No. of analyses | Objective function (kN) | No. of analyses | Objective function (kN) |
| **3-Storey** | 6 | 61.83 | 2000 | 61.53 | 700 | 61.43 |
| **5-Storey** | 10 | 318.04 | 2000 | 323.41 | 800 | 313.38 |
| **10-Storey** | 14 | 556.92 | 3000 | 556.60 | 1450 | 541.78 |

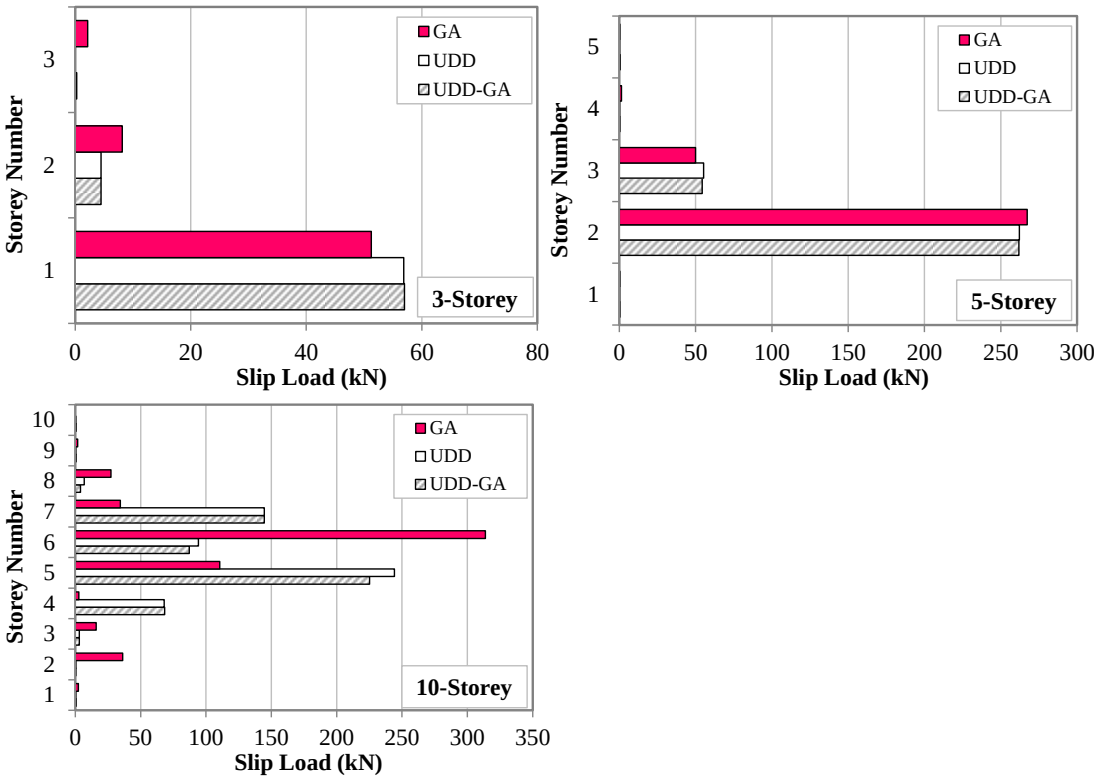


**Fig. 6.7.** Height-wise distribution of optimum slip loads for 3, 5 and 10-storey frames optimised using adaptive UDD, GA and UDD-GA optimisation methods, DBE event

## 6.9. OPTIMUM SEISMIC DESIGN FOR A SET OF SPECTRUM COMPATIBLE EARTHQUAKES

In the previous section specific distributions of slip loads were obtained for the studied frames under a synthetic spectrum compatible earthquake (i.e. SIM01). If the optimum design solution is sensitive to the selected design ground motion, it may not necessarily satisfy the predefined performance target for other earthquakes. To address this issue, based on the previous studies (e.g. Hajirasouliha and Pilakoutas, 2012), spectrum-compatible earthquakes can be used for the optimisation design process. Therefore, a better seismic design can be achieved by using a synthetic earthquake representing a spectrum calculated as an average of the response spectra of several excitation records. In this section, the sensitivity of the optimum design solutions obtained from the adaptive UDD method is evaluated by using five different synthetic earthquakes with random acceleration vibration specifications previously shown in Fig. 6.2 (SIM01 to SIM06). As discussed before, these generated synthetic earthquakes provide a close approximation to the spectrum of the design earthquake.

The frames initially optimised for the SIM01 earthquake are subjected to the synthetic records SIM01 to SIM06 as representative DBE events, and their lateral displacements are compared to the LS performance target level. Fig. 6.8 shows the height-wise distribution of inter-storey drifts for the 3, 5 and 10-storey frames and their mean curves. As expected, the results show that while the optimum design frames have a more uniform distribution of deformation for SIM01 (i.e. optimum distribution), they do not perform optimally under the other synthetic earthquakes. However, the optimum design solutions could satisfy the predefined performance target (i.e. LS level) under all spectrum-compatible earthquakes. The seismic response of the 3, 5 and 10-storey optimum design frames is also investigated under representative MCE events (SIM01 to SIM06 records scaled to have a PGA= 0.6g as explained in Section 6.4). It is shown in Fig. 6.9 that the optimum design solutions could efficiently satisfy the CP performance target under the set of MCE events. It can be noted that, in general, the MCE events were not as critical as the DBE records, which confirms the suitability of the adopted optimisation approach (i.e. optimising the frames under DBE and controlling their response under MCE). Therefore, the optimisation method proposed in this study should prove useful in performance-based design of RC structures with friction dampers for any code based design spectrum.

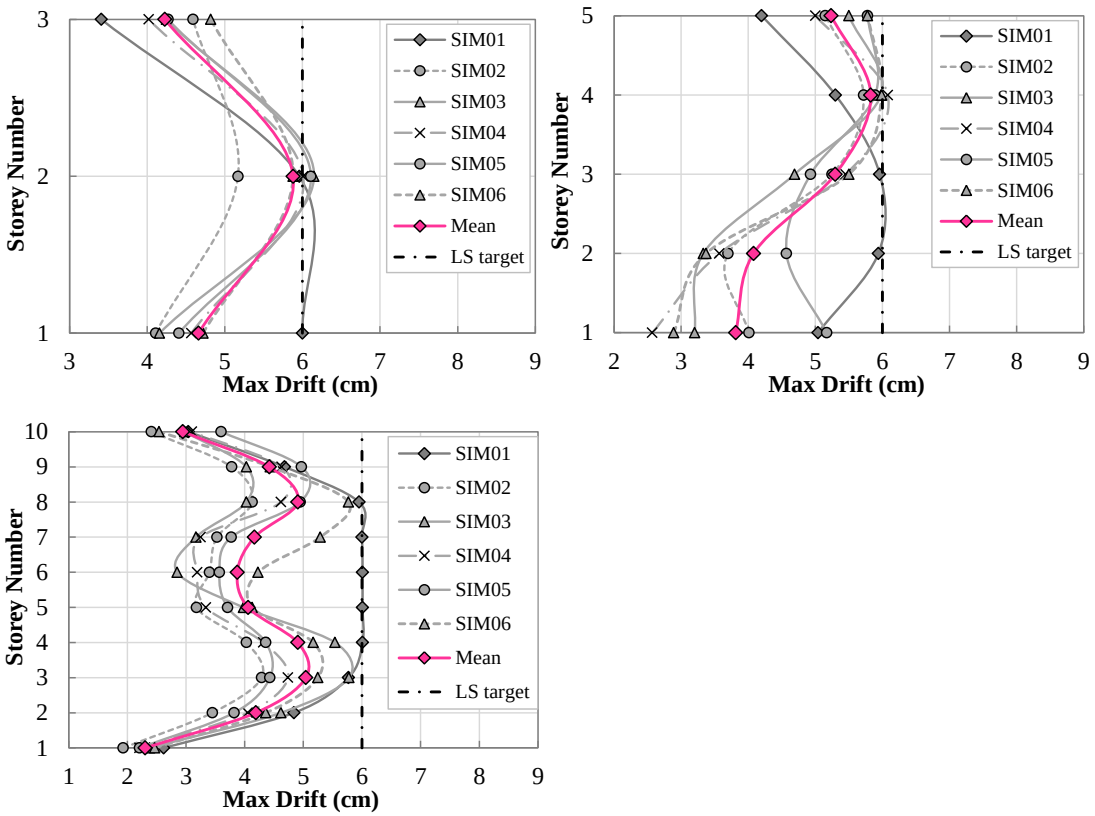


**Fig. 6.8.** Height-wise distribution of inter-storey drifts for 3, 5 and 10-storey optimum design frames, representative DBE events (six synthetic earthquakes)

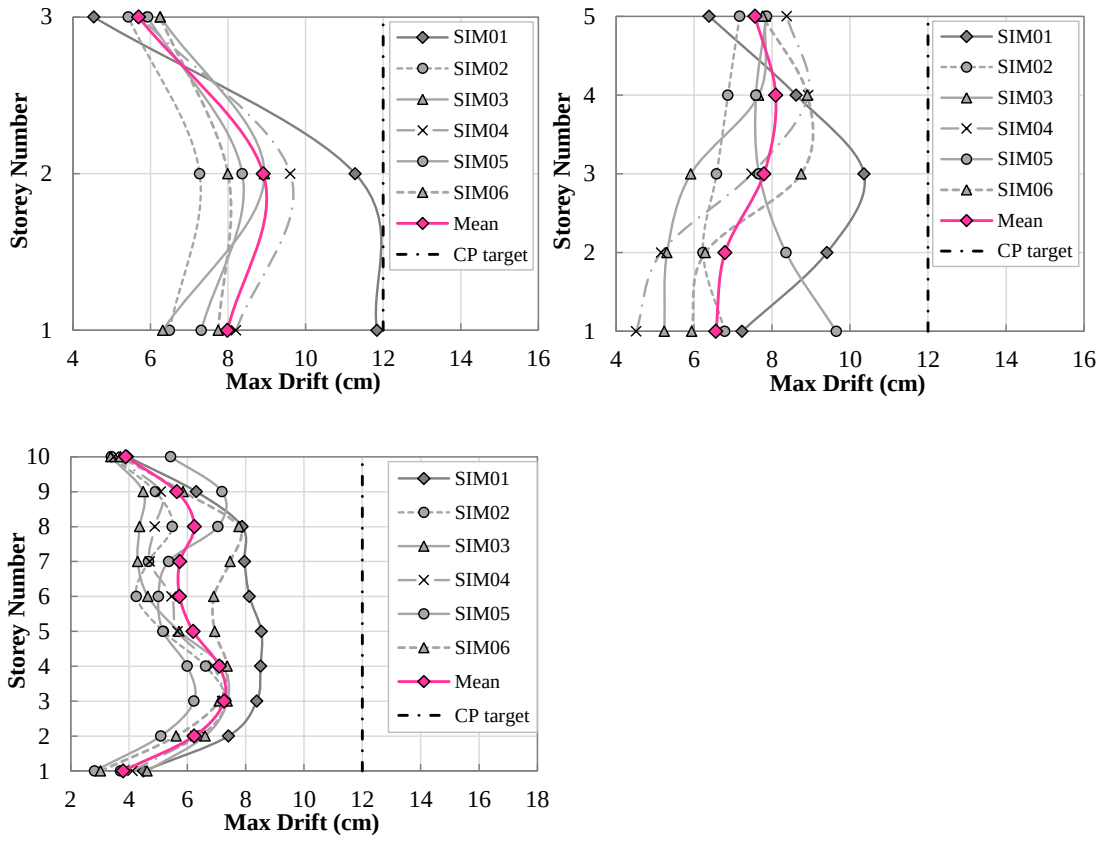


**Fig. 6.9.** Height-wise distribution of inter-storey drifts for 3, 5 and 10-storey optimum design frames, representative MCE events (six synthetic earthquakes)

## 6.10. SUMMMARY AND CONCLUSIONS

An adaptive performance-based optimisation methodology based on the theory of Uniform Distribution of Deformation (UDD) was developed as a tool for finding the optimal configuration of friction-based dampers in RC structures under seismic excitations. The efficiency of the proposed adaptive UDD method is demonstrated through optimisation of 3, 5 and 10-storey frames with friction dampers to satisfy LS and CP performance limits under DBE and MCE representative spectrum compatible earthquakes, respectively. The results are then compared with those obtained from the standard UDD, standard GA and a combination of UDD and GA methods under a synthetic spectrum-compatible earthquake. Based on the results of this study, the following conclusions can be drawn:

- The range of efficient convergence factors for the standard UDD method can be different for different types of structures. The proposed adaptive convergence factor, which was used for three very different multi-storey buildings, was shown to be more

computationally efficient than standard UDD method with constant convergence factors.

- The optimum solutions obtained from the proposed adaptive UDD after a small number of iterations (generally less than 15 nonlinear dynamic analyses) are either very close or even slightly better than those obtained from the GA approach after at least 2000 nonlinear dynamic analyses. This demonstrates a significant advantage of the proposed adaptive UDD over the GA method, in terms of computational efficiency and simplicity.

- Using optimum results obtained from the proposed adaptive UDD as a starting point of the GA considerably increases the optimisation speed (up to 3 times faster) compared to the standard GA using a random initial set. The optimum results obtained from the UDD-GA approach were only slightly better (less than 3%) than those achieved with the proposed adaptive UDD method alone. This indicates that the new adaptive UDD method is sufficiently accurate for most practical applications.

- The sensitivity of the optimisation to earthquake uncertainty was taken into consideration by optimum design of the frames using a synthetic earthquake compatible with a given design spectrum. These structures satisfied all the predefined performance targets under a set of six different synthetic earthquakes generated to represent the design spectrum.

## REFERENCES

Ackora-Prah, J., Gyamerah, S. A. and Andam, P. S. (2014). "A heuristic crossover for portfolio selection." *Journal of Applied Mathematical Sciences*, **8**(65): 3215–3227.

Adeli, H. and Cheng, N. T. (1994). "Augmented Lagrangian genetic algorithm for structural optimisation." *Journal of Aerospace Engineering*, **7**(1): 104–118.

ASCE/SEI Standard 41-06. (2006). "Seismic Rehabilitation of Existing Buildings." *American Society of Civil Engineers*, Reston, Virginia, USA.

Camp, C., Pezeshk, S. and Cao, G. (1998). "Optimised design of two-dimensional structures using a genetic algorithm." *Journal of Structural Engineering*, **124**(5): 551–559.

CEN (Comité Européen de Normalization) (2004a). "Eurocode 8: Design of structures for earthquake resistance-Part 1: General rules, seismic actions and rules for buildings." EN 1998-1-1, Brussels.

CEN (Comité Européen de Normalization) (2004b). "Eurocode 2: Design of concrete structures -Part 1-1: General rules and rules for buildings." EN 1992-1-2, Brussels.

FEMA-356, (2000). Prestandard and Commentary for the Seismic Rehabilitation of Buildings. Report FEMA-356. Federal Emergency Management Agency, Washington DC.

Filiatrault, A., Tremblay, R., Christopoulos, C., Folz, B. et al. (2013). "Elements of earthquake engineering and structural dynamics." 3rd edition, *Published by Presses internationals Polytechnique*.

Goldberg, D. E. (1989). "Genetic algorithms in search, optimisation and machine learning." *Reading MA: Addison-Welsey*.

Hadi, M. N. S. and Arfiadi, Y. (1998). "Optimum design of absorber for MDOF structures." *Journal of Structural Engineering*, **124**(11): 1272–1280.

Hajirasouliha, I., Pilakoutas, K. (2012). "General Seismic Load Distribution for Optimum Performance-Based Design of Shear-Buildings." *Journal of Earthquake Engineering*, **16**(4): 443–462.

Hajirasouliha, I., Asadi, P. and Pilakoutas, K. (2012). "An efficient performance-based seismic design method for reinforced concrete frames." *Earthquake Engineering and Structural Dynamics*, **41**: 663–679.

Holland, J. H. (1975). "Adaptation in natural and artificial systems." *Ann Arbor: The University of Michigan Press.*

Kim, J. and Choi, H. (2006). "Displacement-based design of supplemental dampers for seismic retrofit of a framed structure." *Journal of Structural Engineering*, **132**: 873–883.

Lavan, O. (2015). "A methodology for the integrated seismic design of nonlinear buildings with supplemental damping." *Structural Control and Health Monitoring*, **22**: 484–499.

Lavan, O. and Amir, O. (2014). "Simultaneous topology and sizing optimisation of viscous dampers in seismic retrofitting of 3D irregular frame structures." *Earthquake Engineering and Structural Dynamics*, **43**: 1325–1342.

Lavan, O. and Levy, R. (2010). "Performance based optimal seismic retrofitting of yielding plane frames using added viscous damping." *Earthquakes and Structures*, **1**: 307–326.

Liu, W., Tong, M. and Lee, G. C. (2005). "Optimisation methodology for damper configuration based on building performance indices." *Journal of Structural Engineering*, **131**(11): 1746–1756.

MATLAB (2016). A registered trademark of The Math Works, Inc., Natick, MA.

McKenna, F., Fenves, G. L. and Scott, M. H. (2000). "Open system for earthquake engineering simulation." University of California, Berkeley, California, <http://opensees.berkeley. Edu> [Viewed 1 August 2016].

Michalewicz, Z. and Schouenauer, M. (1996). "Evolutionary algorithms for constrained parameter optimisation problems." *Evolutionary Computation*, **4**: 1–32.

Miguel, L. F. F., Miguel, L. F. F. and Lopez, R. H. (2014). "Robust design optimisation of friction dampers for structural response control." *Structural Control and Health Monitoring*, **21**: 1240–1251.

Moghaddam, H. and Hajirasouliha, I. (2006). "Toward more rational criteria for determination of design earthquake forces." *International Journal of Solids and Structures*, **43**(9), 2631–2645

Moghaddam, H. and Hajirasouliha, I. (2008). "Optimum strength distribution for seismic design of tall buildings." *Structural Design of Tall and Special Buildings*, **17**(2), 331–349.

Mohammadi, R. K. Mirjalaly, M., Mirtaheri, M. and Nazeryan, M. et al. (2018). "Comparison between uniform deformation method and Genetic Algorithm for optimising mechanical properties of dampers." *Earthquakes and Structures*, **1**(14): 1–10.

Mohammadi, R. K., El Naggar, M. H. and Moghaddam, H. (2004). "Optimum strength distribution for seismic resistant shear buildings." *International Journal of Solids and Structures*, **41**: 6597–6612.

Moreschi, L. M. and Singh, M. P. (2003). "Design of yielding metallic and friction dampers for optimal seismic performance." *Earthquake Engineering and Structural Dynamics*, **32**: 1291–1311.

Nabid, N., Hajirasouliha, I. and Petkovski, M. (2017). "A practical method for optimum seismic design of friction wall dampers." *Earthquake Spectra*, **33**(3): 1033–1052.

Nabid, N., Hajirasouliha, I. and Petkovski, M. (2018), "Performance-based optimisation of RC frames with friction wall dampers using a low-cost optimisation method." *Bulletin of Earthquake Engineering*, **16**(10): 5017–5040.

Nanakorn, P. and Meesomklin, K. (2001). "An adaptive penalty function in genetic algorithms for structural design optimisation." *Computers and Structures*, **79**(29): 2527–2539.

Papageorgiou, A., Halldorsson, B. and Dong, G. (2002). "TARSCTH (Target Acceleration Spectra Compatible Time Histories)", *Engineering Seismology Laboratory (ESL) at the State University of New York at Buffalo*

Park, K. S., Koh, H. M. and Hahm, D. (2004). "Integrated optimum design of visco elastically damped structural systems." *Engineering Structures*, **26**(5): 581–591.

Singh, M. P. and Moreschi, L. M. (2002). "Optimal placement of dampers for passive response control." *Earthquake Engineering and Structural Dynamics*, **31**: 955–976.

Sivanandam, S. N. and Deepa, S. N. (2007). "Introduction to Genetic Algorithms," *Springer*, ISBN 9783540731894.

Smith, A. E. and Coit, D. W. (1997). "Constraint handling techniques-penalty functions." In *Handbook of Evolutionary Computation*, Chapter C 5.2. Oxford University Press and Institute of Physics Publishing, Bristol, UK.

Takewaki, I. (2011). "Building control with passive dampers: optimal performance-based design for earthquakes." *John Wiley and Sons (Asia) Books*, Singapore: 51–75.

Venter, G., (2010). "Review of optimisation techniques." *Encyclopaedia of Aerospace Engineering, John Wiley & Sons*, New York, NY.

Yeniay, O. (2005). "Penalty function methods for constrained optimisation with genetic algorithms." *Mathematical and Computational Applications*, **10**(1): 45–56.

# CHAPTER 7

# Application of UDD Optimisation Method in RC Frames with Friction Dampers Using Chevron Bracing System

## 7.1. ABSTRACT

A three-phase performance-based optimisation methodology is introduced based on the concept of Uniform Distribution of Deformation (UDD) for simultaneous optimum design of friction dampers and bracing elements. In the first phase, a discrete optimisation method is adopted for optimal design of the brace elements when unused material is shifted from strong to weak parts of the structure to satisfy Immediate Occupancy (IO) performance level under a Design Basis Earthquake (DBE) event. In the second phase, the mechanical properties of the friction devices are optimised to satisfy Life Safety (LS) performance level under a Maximum Considered Earthquake (MCE) record. In the last phase, the design solution obtained from the second stage is evaluated under the DBE event to modify the slip loads for those storeys in which the IO performance target is violated until the optimum design solution is eventually obtained. The efficiency of the proposed optimisation method is demonstrated through optimum design of a substandard 5-storey RC frame equipped with brace-type friction dampers subjected to a synthetic spectrum compatible earthquake. The results indicate that compared to the code-based design solution with fixed bracings, the optimum frame requires 68% less amount of bracing elements by activating the friction mechanism to satisfy the prescribed performance levels under the representative design earthquakes.

*Keywords: Friction damper; discrete optimisation; Uniform distribution of deformation; Concentrically braced frame.*

## 7.2. INTRODUCTION

Majority of existing buildings stock in developing countries with high seismicity risk were designed based on no or low seismic loading, and therefore, they may not have enough lateral strength and stiffness to resist imposed seismic forces. As one of the solutions, braced steel elements are frequently used in retrofit of existing structures due to their good capability to increase the lateral stiffness and strength of the structural system, and consequently, reduce the lateral displacements under seismic events. Bracing systems equipped with supplemental dampers such as friction, metallic, viscous and viscoelastic energy dissipation devices can be efficiently used to reduce the inelastic energy dissipation demand of structures, and therefore, control the damage during strong earthquakes (Moreschi and Singh, 2003; Lavan and Levy, 2006; Lee et al., 2008; Karavasilis et al., 2012; Kim and An, 2017). The seismic performance of these dual systems generally depends on both the stiffness of the brace elements and the hysteretic behaviour of the adopted energy dissipation mechanism (Uriz and Mahin, 2004). However, in most of the previous studies, the bracing system was assumed to be strong enough to behave in an elastic range without considering the buckling of the braces (e.g. Moreschi and Singh, 2003; Symans et al., 2008; Mohammadi et al., 2018). While the overall buckling of the brace is more relevant to the slenderness ratio of the member, the local buckling is more affected by the width-to-thickness ratio of the cross-section profile (Uriz et al., 2008). In addition, the buckling strength is affected by the initial geometric imperfections, which should be taken into account in the modelling and design of these systems. Previous studies demonstrated that initial geometric imperfections in the brace elements may result in premature buckling, and therefore, different load distributions and inelastic deformation mechanisms in the whole structural system (Uriz and Mahin, 2008; Uriz et al. 2008).

In general, optimum design of non-linear energy dissipation systems for seismic loads is a challenging task due to the high computational costs and complexity of the optimisation problem. In a study conducted by Park et al. (2004), a gradient-based optimisation method was proposed for the simultaneous optimum design of viscoelastic dampers (VEDs) and the brace elements. In addition, the effect of the supporting braces on the control efficiency of VEDs was investigated. Based on their results, the flexibility of the brace should be considered in the optimisation process when sufficient stiffness cannot be provided by the

bracing system. Using their proposed optimisation method led to smaller amount of supporting braces for the same level of safety. Zhu and Zhang (2008) introduced a Self-centring Friction Damping Brace (SFDB) for seismic resistant Concentrically Braced Frame (CBF). Their results indicate that compared to the conventional CBF, their proposed SFDB led to minimum residual drift and was able to withstand different earthquake levels without being damaged. A research was carried out by Chen and Chai (2011) to assess the effects of brace stiffness on seismic performance of structures with supplemental brace-damper systems. They proposed a gradient-based procedure that is capable of determining both the minimum brace stiffness and a set of optimal damper coefficients to meet the target response reduction.

The above mentioned studies either ignored the effect of earthquake dynamic loads for simplification or utilised computationally expensive optimisation procedures which may not be used in practical applications. To address this issue, in the investigation presented in this study, a low cost three-phase performance-based optimisation methodology is proposed based on the theory of Uniform Distribution of Deformation (UDD) for simultaneous optimum design of friction dampers and supporting brace elements in RC structures. The proposed method can satisfy multiple performance targets while the dynamic effects of seismic loads and the effects of initial geometric imperfections on the buckling of the brace elements are taken into account. The efficiency of the proposed algorithm is demonstrated for a 5-storey RC frame, which is designed to satisfy Immediate Occupancy (IO) and Life Safety (LS) performance levels under the Design Basis Earthquake (DBE) and Maximum Considered Earthquake (MCE) events, respectively. It is shown that using the proposed multi-criteria optimisation method can significantly improve the seismic performance of the dual brace-damper system with notably less amount of bracing elements compared to a code-based design braced frame without damping mechanism.

## 7.3. MODELLING AND DESIGN ASSUMPTIONS

### 7.3.1. Design Assumptions

A 5-storey substandard RC frame was considered as the case study example. The dual brace-damper system shown in Fig. 7.1 (a) was then used to improve the seismic performance of the frame to satisfy AISC (2016) design requirements. The bare frame (i.e. frame without braces and friction dampers) was assumed to be located on a soil type D of IBC-2015 (2015) category and was designed based on low seismicity regions using PGA of 0.1g to represent substandard buildings in high seismic regions. The uniformly distributed live and dead loads

were considered to be 2.5 kN/m$^2$ and 5.5 kN/m$^2$ for interior storeys, and 1.0 kN/m$^2$ and 5.3 kN/m$^2$ for the roof level. The reference frame was primarily designed to withstand the seismic loads calculated based on IBC (2015) and ASCE/SEI 7-10 (2010) and in accordance with the minimum requirements of ACI 318 (2014) for RC frames with intermediate ductility. For retrofitting purposes, the bracing elements were then designed based on AISC (2016) so that the structure can withstand the seismic loads of high seismicity region with PGA of 0.65g without using friction devices (i.e. conventional chevron braces).

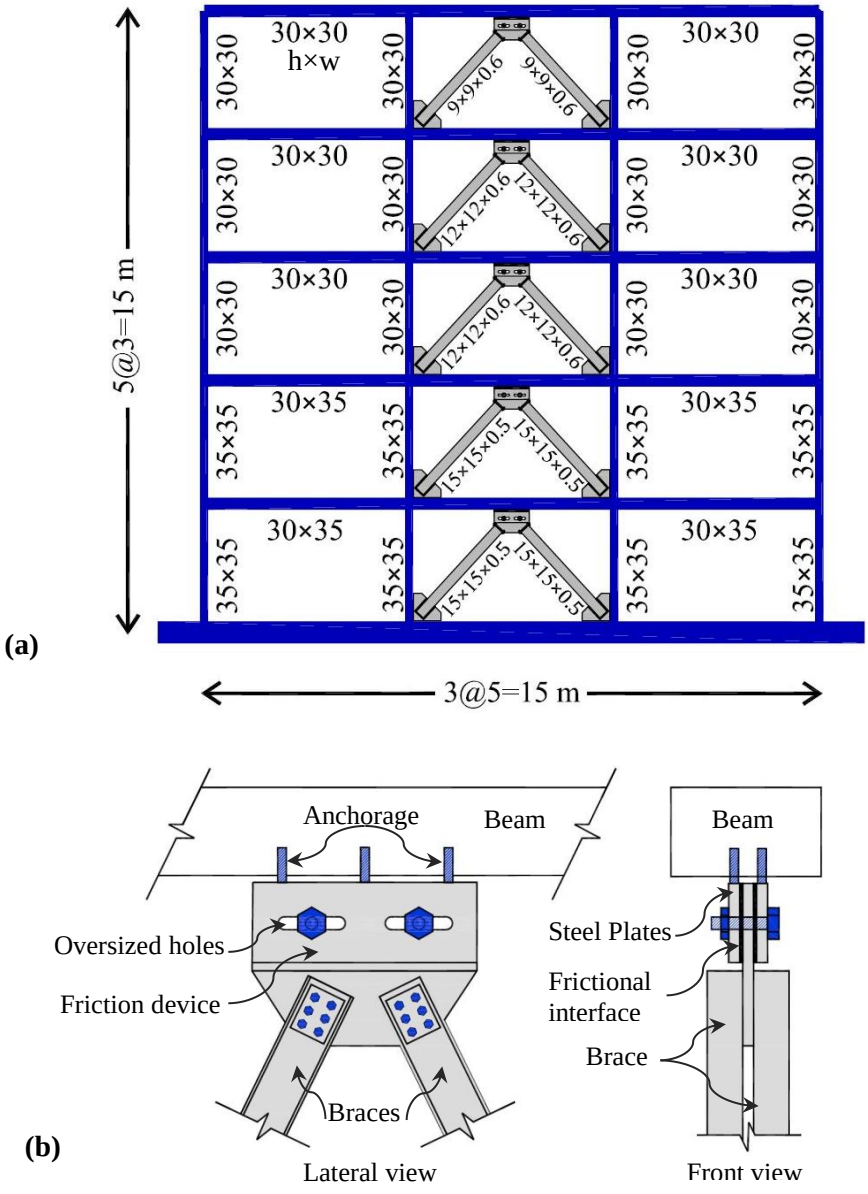


**Fig. 7.1.** (a) Geometry of 5-storey RC frame strengthened with brace-type friction dampers, (b) schematic view of the friction device (adopted from Quintana (2013))

The concrete compressive strength ($f_c'$) and the yield strength ($f_y$) of steel reinforcement bars were assumed to be 25 and 400 Mpa, respectively. Square and rectangular RC sections

were used for beam and column elements, and rectangular Hollow Steel Sections (HSS) were considered for bracing elements. Table 7.1 listed the properties of the selected HSS including the width (a), thickness (t), gross area of the cross section (A), Gyration radius (r), critical buckling load ($F_{cr}$) and the slenderness ratio ($^{kl}/_{r}$). Based on AISC (2016) design code criteria, all compression HSS members were selected to have a slenderness ratio less than 200. For brace elements with pin ends, *k* factor was considered as 1.

Fig. 7.1 (b) illustrates the schematic view of the studied friction damper including a chevron steel bracing connected to the frame using a gusset plate with a friction device at the top, and two gusset plates at the bottom in the beam-column connections. The gusset plate connections are assumed to be rigid and not to buckle under the earthquake excitation loads. The friction device is a Slotted Bolted Connection (SBC) using two steel plates anchored to the top floor beam over a central slotted steel plate attached to the bracings (see Fig. 7.1 (b)). Two brass plates are inserted between the steel plates to ensure more reliable friction behaviour close to the dry Coulomb friction.

**Table 7.1.** Specifications of the selected Hollow Steel Sections (HSS)

| *No.* | *a (mm)* | *t (mm)* | *A ($mm^2$)* | *r (mm)* | *A×r* | *$F_{cr}$ (kN)* | $^{kl}/_{r}$ |
|---|---|---|---|---|---|---|---|
| 1 | 50 | 2.5 | 475 | 19.42 | 9224 | 24.34 | 190.80 |
| 2 | 50 | 3 | 564 | 19.23 | 10844 | 28.34 | 192.71 |
| 3 | 50 | 4 | 736 | 18.85 | 13874 | 35.54 | 196.55 |
| 4 | 50 | 5 | 900 | 18.48 | 16636 | 41.79 | 200.45 |
| 5 | 60 | 5 | 1100 | 22.55 | 24801 | 76.00 | 164.33 |
| 6 | 70 | 5 | 1300 | 26.61 | 34599 | 125.15 | 139.21 |
| 7 | 80 | 5 | 1500 | 30.69 | 46030 | 191.97 | 120.74 |
| 8 | 80 | 6 | 1776 | 30.31 | 53830 | 221.75 | 122.24 |
| 9 | 90 | 6 | 2016 | 34.38 | 69311 | 323.86 | 107.77 |
| 10 | 100 | 6 | 2256 | 38.45 | 86751 | 453.38 | 96.35 |
| 11 | 120 | 5 | 2300 | 46.99 | 108084 | 690.31 | 78.84 |
| 12 | 120 | 6 | 2736 | 46.60 | 127511 | 807.66 | 79.50 |
| 13 | 150 | 5 | 2900 | 59.23 | 171770 | 1382.78 | 62.55 |
| 14 | 150 | 6 | 3456 | 58.84 | 203347 | 1626.13 | 62.97 |
| 15 | 180 | 6 | 4176 | 71.08 | 296819 | 2867.34 | 52.13 |
| 16 | 180 | 8 | 5504 | 70.29 | 386902 | 3696.39 | 52.71 |
| 17 | 180 | 10 | 6800 | 69.52 | 472751 | 4466.94 | 53.29 |
| 18 | 200 | 10 | 7600 | 77.67 | 590326 | 6231.97 | 47.70 |
| 19 | 250 | 10 | 9600 | 98.06 | 941420 | 12547.31 | 37.78 |
| 20 | 300 | 10 | 11600 | 118.46 | 1374164 | 22124.50 | 31.28 |

### 7.3.2. Modelling Assumptions

In this study, OpenSees software (McKenna and Fenves, 2000) was utilised for nonlinear dynamic analyses of the selected RC frame retrofitted by using a chevron bracing system with friction energy dissipation devices. Concrete elements were modelled using a uniaxial constitutive material with linear tension softening (Concrete02) and reinforcing steel bars were modelled using a Giuffre–Menegotto–Pinto model (Steel02) with 1% isotropic strain hardening. Displacement-based nonlinear beam-column elements were used to model RC beams and columns using distributed inelasticity with fiber discretization of the cross sections. The beam and column members were considered to have seven Gauss–Lobatto integration points along the length of each element. Rayleigh damping model was taken into account with a constant damping ratio of 0.05 assigned to the first mode and to the modes at which the cumulative mass participation exceeds 95%.

Rectangular HSS were selected for brace elements which were modelled using displacement-based nonlinear beam-column elements and Steel02 material model wrapped with Fatigue material suggested by Uriz and Mahin (2008). Each brace was divided to the minimum number of two elements with three integration points along the length of each element. To consider the overall buckling in the brace elements, an initial imperfection (camber displacement) of 0.1% of the effective brace length (i.e. excluding the rigid parts attached to the gusset plates) was specified at the brace mid-span as recommended by Uriz et al. (2008). The gusset plate connections were modelled using force-based fiber elements with two integration points and Steel02 material. Figs. 7.2 (a) and (b) illustrate the details of the brace elements and gusset plates modelled in OpenSees. To model the friction device with an ideal Coulomb friction hysteretic behaviour, a nonlinear spring with an elastic-perfectly plastic uniaxial material was adopted.

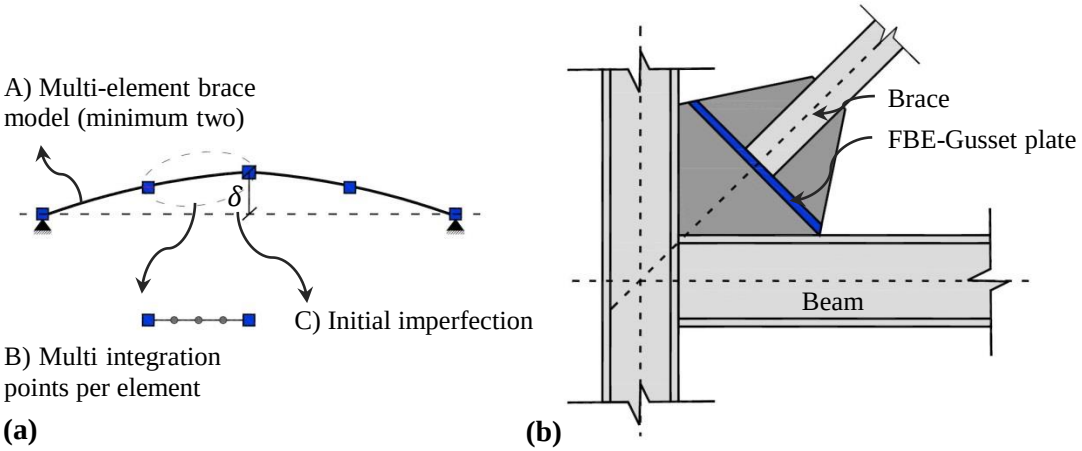


**Fig. 7.2.** Schematic illustration of (a) a multi-element bracing element with initial imperfection and (b) a gusset plate connection used in OpenSees modelling

The beam-to-column connections were assumed to be fully rigid with no shear failure in the panel zones. In order to analyse output data, a MATLAB (2016) script was developed and linked to the OpenSees program.

## 7.4. SYNTHETIC EARTHQUAKE RECORD

Scaled IBC (2015) spectrum-compatible synthetic earthquakes were utilised for optimum performance-based seismic retrofitting of the 5-storey braced frame. A synthetic earthquake record with a PGA of 0.4g was generated using SIMQKE program (Vanmarke, 1976) to be compatible with the soil type D of IBC (2015) elastic design spectrum. Fig. 7.3 demonstrates the 5% damped elastic acceleration response spectrum of the generated synthetic earthquake record and the IBC design spectrum. In this study, the seismic performance of the frame was evaluated under two different earthquake levels: (a) Design Basis Earthquake (DBE) with 10% probability of exceedance in 50 years, and (b) Maximum Considered Earthquake (MCE) with 2% probability of exceedance in 50 years (FEMA 356, 2000; ASCE/SEI 41-06, 2006). The selected synthetic earthquake was scaled to produce excitation records with PGA of 0.3g and 0.65g to represent the DBE and MCE events, respectively, for the performance-based optimisation process.

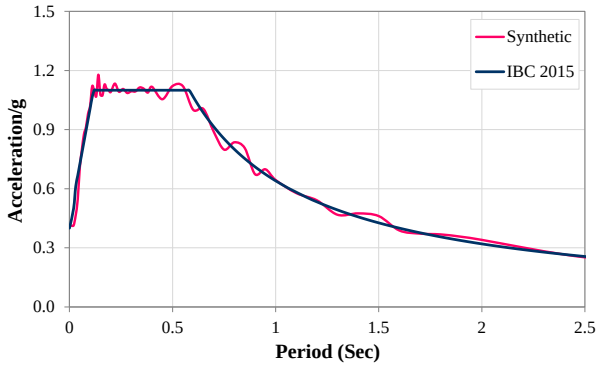


**Fig. 7.3.** Elastic acceleration response spectra of the synthetic earthquake record and the IBC-2015 design spectrum, 5% damping ratio

## 7.5. PROPOSED OPTIMISATION ALGORITHM

In this section, a three-phase performance-based optimisation algorithm is presented based on the concept of Uniform Distribution of Deformation (UDD) for simultaneous optimal design of bracing elements and friction dampers under different design earthquakes. The aim is to satisfy the IO and LS performance targets under the representative DBE and MCE events, respectively while using minimum amount of bracing elements and slip loads at the

friction devices. The following algorithm is suggested for performance-based optimisation of the dual brace-damper systems:

1) In the first phase, the initial code-based design braced frame is considered to satisfy the IO performance level under the representative DBE event. In this stage, a discrete optimisation (using the sections listed in Table 7.1) is utilised to obtain optimum sizes of the braces while the friction dampers are fixed and the slippage is prevented using very high slip load values. The following equation is utilised to modify the brace sections at each iteration until the optimum sections are obtained:

$$\left(A_i\right)_{n+1} = \left(A_i\right)_n \times \left(\frac{\Delta_i}{\Delta_{target}}\right)_n^{\alpha} \tag{7.1}$$

where $\Delta_i$ and $\Delta_{target}$ are maximum and target inter-storey drifts of $i^{th}$storey for $n^{th}$ iteration, respectively. $A_i$ is the area of the bracing elements at the $i^{th}$storey level, and $\alpha$ is the convergence parameter which is considered as 0.1 to avoid rapid changes in the size of the sections and divergence. The optimisation iterations are then continued until the performance target is satisfied and the minimum total area is obtained for the bracing elements. The yielding strengths correspond to the optimum bracing elements are assumed as the initial slip loads of the friction dampers for the next stage.

2) In the second phase, the optimal braced frame obtained from the first stage should satisfy the LS performance target under the representative MCE event. To fulfil this, the slip loads of the friction dampers are modified until the performance target is reached and the minimum amount of total slip load is obtained. The following equation is adopted to calculate the optimum distribution of the slip loads:

$$\left(F_{s,i}\right)_{n+1} = \left(F_{s,i}\right)_n \times \left(\frac{\Delta_i}{\Delta_{target}}\right)_n^{\alpha} \tag{7.2}$$

where $F_{s,i}$ is the slip load of the friction device at the $i^{th}$storey.

3) In the last phase, the brace-damper system with bracing elements obtained from the first phase and the friction dampers achieved from the second phase is evaluated under the DBE event. The slip loads of the friction dampers are then modified using Equation 7.2 only for the storeys in which the IO performance target is violated. This is continued until the IO level is satisfied at all storey levels and the optimisation converge to the optimal design solution.

## 7.6. DISCUSSION OF THE RESULTS

The proposed algorithm was adopted for optimum retrofitting of the 5-storey frame with the dual brace-damper system and the performance of the optimum frame was then compared with that obtained from the code-based design braced frame. Fig 7.4 (a) illustrates the height-wise distribution of lateral inter-storey drifts for the case study frame without bracing, with code-based design bracing elements and with the optimum brace-damper system subjected to the DBE and MCE events. Based on the results, the bare frame was totally collapsed as it violated the Collapse Prevention performance level (i.e. CP Limit) under the MCE event. However, after retrofitting using the AISC design bracing system, not only the CP and LS performance levels were fully satisfied under the DBE and MCE records, respectively; the performance of the retrofitted structure was even upgraded to higher performance levels when the lateral relative displacements of the structure were way below the IO and LS performance limits (as shown in Fig 7.4 (a)).

Using the proposed algorithm, the optimum design braced frame is shown to efficiently fulfil the requirements of the selected performance levels (i.e. IO and LS limits) under the DBE and MCE records, respectively, without unnecessary pressure on the structural system. Fig 7.4 (b) shows the optimum height-wise distribution of the slip loads of the friction devices. It can be seen that the slip loads of the first and last floor tended to be zero, and therefore, by using the friction dampers the number of the required bracing elements was reduced. Fig. 7.5 compares the frame with optimum design dual brace-damper system and its code-based design braced frame counterpart in terms of maximum column axial load, total base shear and total weight of bracing elements under the MCE event. According to the results, the optimum design solution could massively improve the seismic performance of the system by 63%, 65% and 68% reduction in the maximum column axial load, base shear and the total weight of the braces, respectively. This can highlight the efficiency of the proposed methodology for optimum design of the friction-based supplemental energy dissipation devices in concentrically braced frames. However, further investigation is required on wider range of frame geometries, bracing cross sections and earthquake excitations.

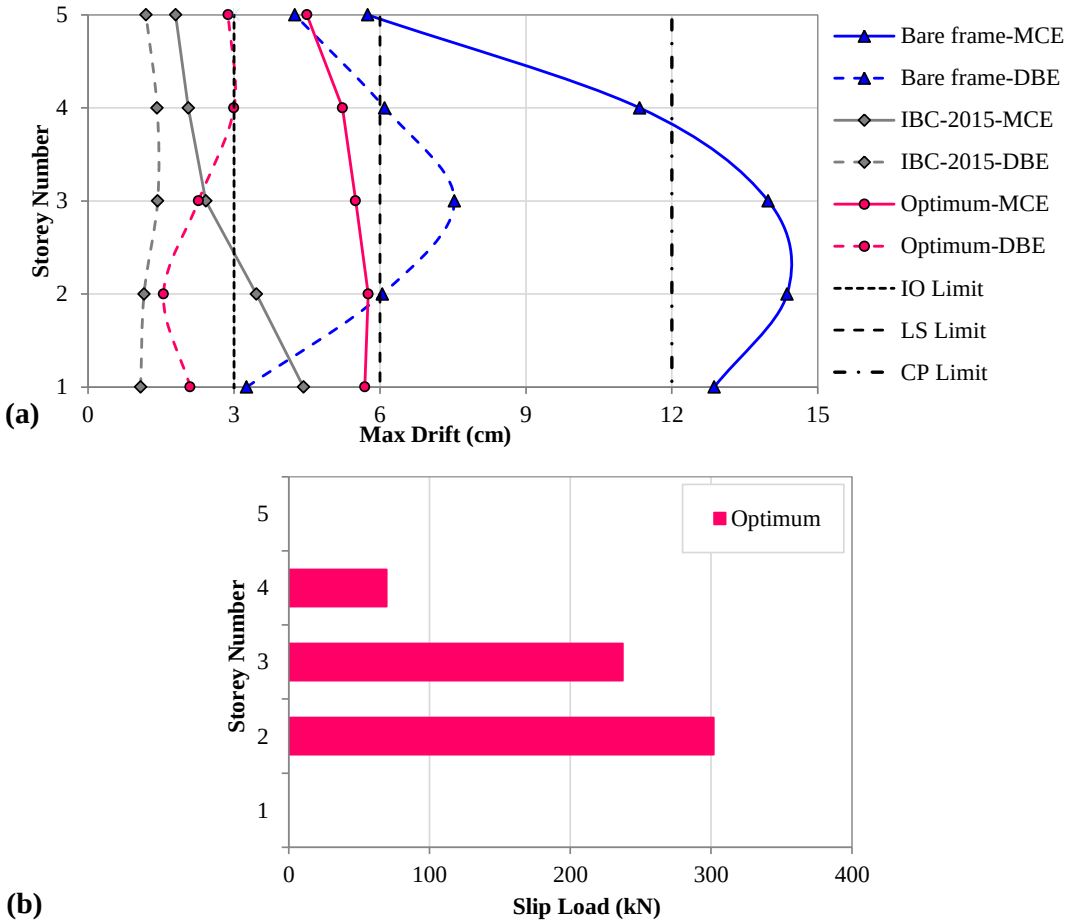


**Fig. 7.4.** Height-wise distribution of (a) lateral inter-storey drifts and (b) slip loads for 5-storey frame with different design scenarios, DBE and MCE events

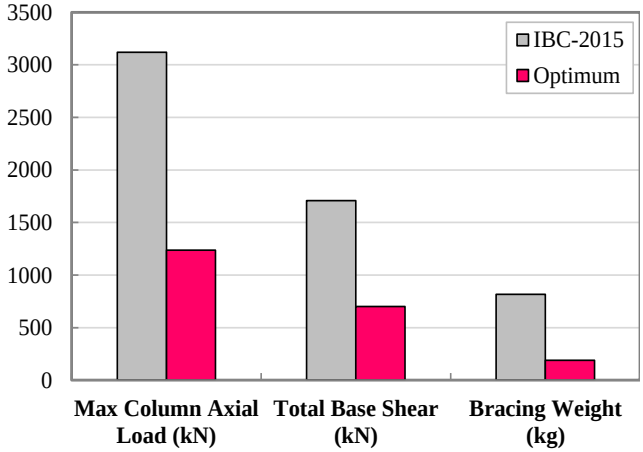


**Fig. 7.5.** Comparison of maximum column axial load, total base shear and total weight of bracing elements for 5-storey optimum design frame and its code-based design counterpart, MCE event

## 7.7. SUMMARY AND CONCLUSIONS

A three-phase performance-based optimisation methodology is developed based on the theory of Uniform Distribution of Deformation (UDD) for simultaneous optimal design of bracing elements and supplemental friction devices in RC structures under seismic excitations. The efficiency of the proposed optimisation method is demonstrated through performance-based optimum design of a 5-storey frame with brace-type friction dampers while satisfying IO and LS performance targets under DBE and MCE events, respectively. Based on the proposed algorithm, in the first phase, a discrete optimisation is used for optimum design of the brace elements while the friction dampers are fixed to satisfy the IO performance level under the representative DBE record. In the second phase, the slip loads of the friction dampers are optimised so as the LS performance target is achieved under the representative MCE event. In the last phase, the design solution obtained from the second phase is evaluated under the DBE event and the slip loads are modified for those storeys in which the IO performance level is violated. According to the results of this study, compared to the code-based design concentrically braced frame, the optimum design frame with friction dampers can efficiently decrease the total weight of the bracing system by 68% while the predefined performance target is fully satisfied. In addition, the optimum design solution results in up to 65% lower imposed column axial load and base shear to the main structure.

## REFERENCES

ACI 318-14 (2014). "Building Code Requirements for Structural Concrete and Commentary on Building Code Requirements for Structural Concrete (ACI 318R-14)." *American Concrete Institute*, Farmington Hills, MI.

AISC (1997), "Seismic Provisions for Structural Steel Buildings." Supplement No.1, *American Institute of Steel Construction*, Chicago, IL.

ANSI/AISC 360-16 (2016). "Specification for Structural Steel Buildings." *American Institute of Steel Construction*, Chicago, IL.

ASCE/SEI Standard 41-06. (2006). "Seismic Rehabilitation of Existing Buildings." *American Society of Civil Engineers*, Reston, Virginia.

ASCE/SEI Standard 7-10 (2010), "Minimum Design Loads for Buildings and Other Structures." *American Society of Civil Engineers*, Reston, Virginia.

Chen, Y. T. and Chai, Y. H., (2011). "Effects of brace stiffness on performance of structures with supplemental Maxwell model-based brace–damper systems." *Earthquake Engineering and Structural Dynamics*, **40**: 75–92.

FEMA 356 (2000). "Prestandard and commentary for the seismic rehabilitation of buildings." *Federal Emergency Management Agency*, Washington, D.C.

IBC (2015). "International Building Code." *International Code Council*, Country Club Hills, IL.

Karavasilis, T. L., Kerawala, S. and Hale, E. (2012). "Hysteretic model for steel energy dissipation devices and evaluation of a minimal-damage seismic design approach for steel buildings." *Journal of Constructional Steel Research*, **70**: 358–367.

Kim, J. and An, S. (2017). "Optimal distribution of friction dampers for seismic retrofit of a reinforced concrete moment frame." *Advances in Structural Engineering*, **20**(10): 1523–1539.

Lavan, O. and Levy, R. (2006). "Optimal design of supplemental viscous dampers for linear framed structures." *Earthquake Engineering and Structural Dynamics*, **35**: 337–356.

Lee, S. H., Park, S. H., Lee, S. K. and Min, K. W. (2008). "Allocation and slip load of friction dampers for a seismically excited building structure based on storey shear force distribution." *Engineering Structures*. **30**: 930–940.

MATLAB 2016. A registered trademark of The Math Works, Inc., Natick, MA.

McKenna, F., Fenves, G. L. and Scott, M. H. (2000). "Open system for earthquake engineering simulation." University of California, Berkeley, California, <http://opensees.berkeley. Edu> [Viewed 1 August 2016].

Mohammadi, R. K., Mirjalaly, M., Mirtaheri, M., and Nazeryan, M. (2018). "Comparison between uniform deformation method and Genetic Algorithm for optimizing mechanical properties of dampers." *Earthquakes and Structures*, **14**(1): 1–10.

Moreschi, L. M. and Singh, M. P. (2003). "Design of yielding metallic and friction dampers for optimal seismic performance." *Earthquake Engineering and Structural Dynamics*, **32**: 1291–1311.

Park, J. H., Kim, J. and Min, K.W. (2004). "Optimal design of added viscoelastic dampers and supporting braces." *Earthquake Engineering and Structural Dynamics*, **33**(4): 465–484.

Quintana, H. C. (2013). "Semiactive friction connections for seismic control of multi-storey buildings." *PhD Thesis*, University of Sheffield, Sheffield, UK.

Symans, M. D., Charney, F. A., Whittaker, A. S., Constantinou, M. C. et al. (2008). "Energy dissipation systems for seismic applications: current practice and recent developments." *Journal of Structural Engineering (ASCE)*, **134**(1): 3–21.

Uriz, P. and Mahin, S. A. (2008). "Toward earthquake-resistant design of concentrically braced steel-frame structures." *Pacific Earthquake Engineering Research (PEER) Centre*, University of California, Berkeley.

Uriz, P., and Mahin, S. A. (2004). "Physical modeling and seismic vulnerability assessment of concentrically braced steel frames." *In Proceedings: SEAOC Convention*, Monterey, CA.

Uriz, P., Filippou, F. C. and Mahin, S. A. (2008). "Model for cyclic inelastic buckling of steel braces." *Journal of Structural Engineering (ASCE)*, **134**(4): 619–628.

Vanmarke, E. H. (1976). "SIMQKE: a program for artificial motion generation, user's manual and documentation." Department of Civil Engineering, Massachusetts Institute of Technology, Cambridge, MA.

Zhu, S. and Zhang, Y. (2008). "Seismic analysis of concentrically braced frame systems with self-centering friction damping braces." *Journal of Structural Engineering (ASCE)*, **134**(1): 121–131.

# CHAPTER 8

# Conclusions and Recommendations for Future Work

## 8.1. SUMMARY AND CONCLUSIONS

The main purpose of this research was to develop a low-computational cost performance-based optimisation methodology for optimum design of frame structures equipped with nonlinear friction-based passive energy dissipation devices under earthquake excitations. Extensive nonlinear dynamic analysis was performed using DRAIN-2DX and OPENSEES software by considering a wide range of frame geometries (i.e. 3, 5, 10, 15 and 20-storey frames with 3 and 5 spans), friction damper configurations (i.e. uniform, uniform cumulative, triangular cumulative, inverted triangular cumulative and a proportional to the storey shear strengths slip load distributions) and ground motion records (i.e. natural and synthetic spectrum compatible earthquakes and two ensembles of near and far-field records). Based on the results of this study the following general conclusions can be drawn:

### 8.1.1. Practical Methods for More Efficient Design of Friction Dampers

- Among all the considered slip load distribution patterns, uniform cumulative slip load distribution is suggested as the most effective pattern in terms of increasing the energy dissipation efficiency of the friction-based energy dissipation devices.

- Irrespective to the slip load distributions, there is always an optimum range for the slip load ratios (normalised to the storey shear strength) that leads to minimum displacement demands and maximum energy dissipation efficiency under spectrum-compatible earthquakes. For slip load ratios lower than the optimum value, the effectiveness of the dampers can be limited due to the small energy dissipation in the friction devices. In addition, for larger slip force ratios leading to connection lock-ups, a linear elastic response is usually resulted with large dynamic magnification and low energy

dissipation. Based on the results, the optimum range of the slip loads exponentially decreases with the increase of the number of storeys.

- A practical empirical equation was proposed to determine a more efficient slip load distribution for seismic design of RC structures with friction dampers by considering different number of storeys subjected to spectrum-compatible natural earthquakes. The friction wall systems designed based on the proposed equation was shown to result in up to 30% lower displacement demands and up to 61% higher energy dissipation efficiencies compared to the conventional systems with a uniform slip load distribution.

- It was shown that friction wall dampers designed with the proposed equation can significantly reduce the displacement demands of the bare frames without a large increase in base shear. While in case of fixed walls (without friction slippage), the maximum axial loads can be well beyond the maximum capacity of the columns, it was shown that by using the proposed design method the total axial loads in the adjacent columns generally remain within the capacity of the columns.

- It was demonstrated that higher PGA (or PGV) levels generally lead to lower energy dissipation efficiency with higher and wider range of optimum slip load ratios. However, the relationship between the PGA and optimum slip load values is not linear and depends on the number of storeys.

- The results indicate that friction wall dampers performed better under far-field earthquakes with, on average, 118% higher energy dissipation efficiency and 24% lower maximum inter-storey drifts compared to the near-field records. In general, the optimum ranges of slip load ratios obtained for the frames under the near-field earthquakes were considerably wider and higher compared to those achieved under the far-field ground motions. For the same PGA level, near-field earthquakes led to about 1.5 times higher optimum slip loads than far-field earthquakes.

- For the same PGV/PGA ratio (or similar frequency content), it was shown that the earthquakes with higher PGA and PGV values resulted in higher optimum slip load ratios. In addition, the earthquakes with relatively high velocities occurring at the periods close to the period of the corresponding bare frames resulted in higher range of optimum slip load values.

- Based on the results of this study, in general, the optimum response of the structures was more sensitive to the PGV than the PGA of the design earthquake. A practical design equation was proposed to estimate the optimum slip load ratios as a function of

PGV and number of storeys and proved to be efficient for both far-field and near-field earthquakes.

### 8.1.2. Low-Cost Performance-Based Optimisation Methods for Optimum Design of Friction Dampers Based on the Concept of Uniform Distribution of Deformation

***Using a constant total friction damper capacity (obtained from the empirical equation):***

- An efficient performance-based optimisation framework was developed based on the concept of uniform distribution of deformation (UDD), in which unused materials are gradually shifted from strong to weak parts of the structure until a state of uniform distribution of deformation (or damage) prevails. The efficiency of the proposed method was demonstrated for the 3, 5, 10, 15 and 20-storey frames used in this study.

- Compared to the conventionally designed friction wall dampers with uniform slip load distribution, the optimum design dampers exhibited up to 43% and 75% lower inter-storey drift ratios and global damage indices, respectively, when subjected to the synthetic spectrum-compatible earthquakes. For the same total friction force, using the proposed optimisation method can increase the energy dissipation efficiency of the friction wall dampers by up to 46%. The improvement in the energy dissipation capacity was more pronounced in low to medium-rise buildings. The efficiency of the proposed method was also demonstrated under a set of six natural earthquakes, where using optimum design dampers in the studied frames resulted in up to 50% lower inter-storey drift ratios compared to their conventionally designed counterparts.

- The results indicated that the convergence parameter, $\alpha$, has a major effect on the computational cost and convergence of the optimisation process. It was observed that the $\alpha$ values ranging from 0.2 to 0.5 is generally more efficient to converge to the optimum design solutions for friction-based wall dampers when the total slip load is constant. The results of sensitivity analyses also indicated that the optimum solution is independent from the initial slip load distribution selected for the optimisation process; however, using a suitable initial design can result in a faster convergence.

- By performing nonlinear incremental dynamic analyses, it was shown that the proposed optimum design method can significantly reduce (up to 77%) the global damage index of the conventionally designed frames over a wide range of earthquake PGA levels. It was concluded that the optimum design systems are efficient at all intensity levels, while the efficacy of the frames with conventionally designed friction dampers is significantly diminished at higher PGA levels.

- The earthquake uncertainty was shown to be efficiently managed by using the average of optimum slip load patterns corresponding to the synthetic earthquakes representing the design spectrum. The friction wall dampers designed with the average optimum pattern exhibited up to 34% less maximum inter-storey drift and 72% less cumulative damage.

***Using variable total friction damper capacity:***

- It was shown that the friction wall dampers designed based on the proposed empirical equation may impose excessive base shear and column axial loads to the main structural elements. The additional imposed loads can be easily controlled by adopting a multi-criteria performance-based optimisation method to satisfy predefined performance targets.

- The suggested multi-criteria optimisation method was shown to be efficient to satisfy multiple performance objectives under the design earthquakes, leading to rather uniform distribution of lateral deformations. Compared to the dampers designed based on the empirical equations, the proposed method resulted in design solutions with considerably lower column axial load (up to 37%) and base shear (up to 48%) demand, respectively. The proposed method was also capable of removing unnecessary (less efficient) friction dampers.

- The uncertainty in the design seismic excitation was taken into consideration by optimising the frames based on a set of synthetic spectrum-compatible earthquakes representing the selected design spectra. Based on the results, the frames designed using the average optimum solutions could satisfy the performance targets under multiple natural seismic excitations representing the same design spectra, while exhibited up to 51% lower maximum drift ratios compared to their bare frame counterparts.

### 8.1.3. Adaptive UDD Performance-Based Optimisation Method against Genetic Algorithm (GA)

- To improve the convergence efficiency of the proposed optimisation method, adaptive equations were developed for the convergence factors used in the optimisation process. The accuracy of the results was also investigated by using a standard Genetic Algorithm (GA) to obtain global optimum design solutions. Based on the results, only after a few iterations (usually less than 30 nonlinear dynamic analyses), the adaptive method led to the solutions that were very close or even slightly better than those attained from the GA approach after at least 3000 nonlinear dynamic analyses.

- It was demonstrated that using optimum results obtained from the adaptive optimisation as the starting point of the GA can noticeably increase the speed of the optimisation procedure (up to 10 times) compared to the standard GA using a random initial population. It was also observed that the optimum results obtained from the combination of the adaptive UDD optimisation and the standard GA (i.e. UDD-GA) were slightly better than those obtained for the proposed adaptive UDD method (less than 6%). This highlights the reliability and efficiency of UDD method for optimum design of nonlinear frames with friction energy dissipation devices.

### 8.1.4. Application of UDD Performance-Based Method for Simultaneous Discrete Optimisation of Bracing Elements and Continuous Optimisation of Friction Devices

- A novel three-phase UDD performance-based optimisation methodology was developed for simultaneous optimal design of bracing elements (discrete size optimisation) and supplemental friction devices (continuous optimisation) for seismic strengthening of RC structures. Compared to the code-based design chevron concentrically braced frame, the optimum design frame with friction dampers could considerably decrease the total weight of the bracing system and the maximum column axial loads and base shear, while the predefined performance targets were satisfied under DBE and MCE records.

## 8.2. RECOMMENDATIONS FOR FUTURE WORK

- In this study, the non-structural concrete wall panel was assumed to be designed strong enough to always have elastic behaviour. Therefore, no limitations were considered for the activation of the friction dampers. However, for practical application, the friction dampers should be activated before the concrete panel is damaged. Further investigation is suggested to be performed on the optimum design of friction dampers restricted by the strength of the concrete panel.

- The financial feasibility and whole life cycle costs of the proposed friction wall damper compared to other conventional systems for seismic strengthening of deficient RC buildings was outside the scope of this research, and therefore, may need to be investigated in more detail before practical applications.

- The proposed multi-criteria optimisation methodology was developed for optimisation of controlled structures to simultaneously satisfy different lateral displacement levels under design earthquakes. However, it can be easily extended for simultaneous

optimisation of different seismic performance parameters such as maximum column axial load, base shear or energy dissipation.

- Further research can be conducted on developing new optimisation framework using the same UDD concept for newly designed structures (e.g. steel structures) equipped with supplemental energy dissipation devices for simultaneous optimisation of structural elements and the added dampers. In addition, the developed performance-based optimisation methodologies can be modified to be used for other types of energy dissipation devices such as viscous dampers by considering the limitations of the design problem.

# APPENDIX A

# Optimum Energy Based Seismic Design of Energy Dissipation Devices in RC Structures

## A.1. ABSTRACT

Energy Dissipation Devices (EDDs) have been widely used for seismic design and strengthening of both new and existing buildings. With designated supplementary EDDs installed in a structure, a considerable portion of the input seismic energy can be dissipated and the damage imparted to the framing system is reduced. However, the energy dissipation of the EDDs depends on the damping characteristic of the employed devices. In general, the efficiency of the friction-based supplemental devices is strongly associated to the design slip load values and their height-wise distribution. In practical implementations, a uniform slip load pattern is usually considered for height-wise distribution of slip loads in multi-storey frames equipped with the friction-based EDDs. However, this conventional design method may result in concentrating and localizing damage in certain storey levels. In this study, a practical performance-based optimisation methodology is developed for seismic design of RC frame buildings with friction-based EDDs. The proposed method aims at redistributing the slip loads of the friction dampers so as more uniform height-wise distribution of energy dissipation capacity is achieved for the dampers. The efficiency of the method is evaluated through the optimum design of 3, 5, 10, 15 and 20-storey RC frames equipped with wall-type friction EDDs under a set of four synthetic spectrum-compatible earthquakes. The results show that the optimum design frames exhibit up to 33% and 72% less maximum

inter-storey drift and global damage, respectively, compared to their conventionally designed counterparts.

*Keywords: Friction damper; Energy dissipation; Slip load distribution; Structural damage; Seismic performance*

## A.2. INTRODUCTION

The past three decades have witnessed significant progress in development of passive Energy Dissipation Devices (EDDs) to improve the seismic performance of new buildings or strengthening of existing substandard structures. Among all the passive EDDs, friction dampers exhibit a good performance characteristic and higher energy dissipation capacity resulted from Coulomb dry friction law. Pall and Marsh (1982, 2004) introduced the first generation of friction-based passive control systems for braced steel frames. An improved model of Pall friction dampers was developed by Wu et al. (2005) using a T-shaped core plate, which was easier to manufacture and assembly. Fitzgerald (1989) used Slotted Bolted Connections (SBC) for the first time to dissipate earthquake input energy and prevent buckling of brace elements in steel braced frames. The energy absorbing mechanism in SBCs is based on the friction between the gusset plates and the sliding channels. In general, the efficiency of friction-based EDDs is strongly associated to the designed slip load values (the lateral shear load in which the steel plates start sliding against each other) and their height-wise distributions. This has motivated many researchers to develop methodologies to optimum design of non-linear dampers for seismic retrofitting purposes. Sasani and Popov (1997) experimentally and analytically investigated the seismic behaviour of a lightweight concrete panel that was anchored to the lower floor beam and connected with three friction EDDs on the top. Petkovski and Waldron (2003) evaluated the effectiveness of a similar concrete wall system in multi-storey RC frames under a set of natural earthquakes. They showed that the slip load values have significant effect on the seismic performance of the structures strengthened or designed with friction EDDs. Cho and Kwon (2004) proposed a new type of wall-type friction damper for RC structures using Teflon sliding sheets in contact with steel plates to guarantee an efficient friction hysteretic behaviour. More recently, Nabid et al. (2017) investigated the efficiency of friction-based wall dampers design with different slip load distribution patterns in improving the seismic performance of substandard RC structures. Based on the results of their extensive analytical study, an empirical formula was proposed to obtain more efficient height-wise distribution of slip loads by considering different seismic performance parameters.

By considering nonlinear dynamic behaviour of structures, employing conventional optimisation techniques based on elastic behaviour of structures may not lead to the optimum solutions in the nonlinear range of behaviour. While most of the existing optimisation techniques for non-linear structural problems are complex and computationally expensive due to high nonlinearity of the systems, there are some efficient methodologies leading to near global optimum solutions by using much less iterations. Moghaddam et al. (2004) proposed a simplified non-linear optimisation methodology using the theory of uniform damage distribution to modify the structural materials for more efficient seismic design of concentrically braced steel frames. In their approach, the structural properties were modified so as inefficient material was gradually shifted from strong to weak areas of the structure. The process was continued until a state of uniform deformation was reached. In a similar study conducted by Lavan and Levy (2006), a methodology was presented for the optimal design of supplemental viscous dampers for framed structures. Their methodology addresses the problem of minimizing the added damping by constraining the maximum drift. Hajirasouliha and Pilakoutas (2012) suggested a general lateral design load distribution for optimum performance-based seismic design of structures using the same theory of uniform damage distribution. More recently, Ganjavi et al. (2016) employed the aforementioned theory to obtain optimum seismic design loads for non-linear shear-buildings on soft soils.

The seismic response of a structure can be described through the relationships between the earthquake input energy and the quantities of different energy dissipation systems in the structure. In the RC frames with friction EDDs, apart from the kinetic, viscous and elastic strain energy, a significant part of the imparted seismic energy is dissipated through the friction mechanism between steel plates. Therefore, the energy dissipation capacity of friction EDDs plays an important role on seismic performance of the entire structure. In this paper, a practical performance-based optimisation framework proposed by Moghaddam et al. (2004) is further developed to achieve more efficient distribution of energy dissipation in the friction EDDs. The optimum design procedure works based on the concept of uniform damage distribution and aims at redistributing the slip loads so as more uniform height-wise distribution of energy dissipation is achieved. To investigate the efficiency of the supplemental friction wall dampers using conventional designs and optimum design solutions, extensive nonlinear dynamic analyses have been conducted on 3, 5, 10, 15, and 20-storey RC frames subjected to a set of four synthetic spectrum compatible earthquakes.

# A.3. MODELLING AND ASSUMPTIONS

## A.3.1. Studied Reference Frames

Friction EDDs are usually used to reduce seismic response of structures for both new buildings and strengthening of the existing structures. In this study, five substandard RC moment resisting frames with 3, 5, 10, 15 and 20 storeys are strengthened with wall-type friction EDDs as shown in Fig. A.1. The frames were considered to be located on a soil type D of the IBC (2015). The distributed dead and live loads were assumed to be 6 kN/m$^2$ and 2 kN/m$^2$, respectively for interior storeys, while the corresponding loads for the roof level were reduced to 5 kN/m$^2$ and 1.5 kN/m$^2$. The frames were designed based on IBC-2015 (and ASCE/SEI 7-10) and in accordance with the minimum requirements of ACI 318-14. Nonlinear dynamic analyses were performed using the program DRAIN-2DX (Prakash et al., 1993).

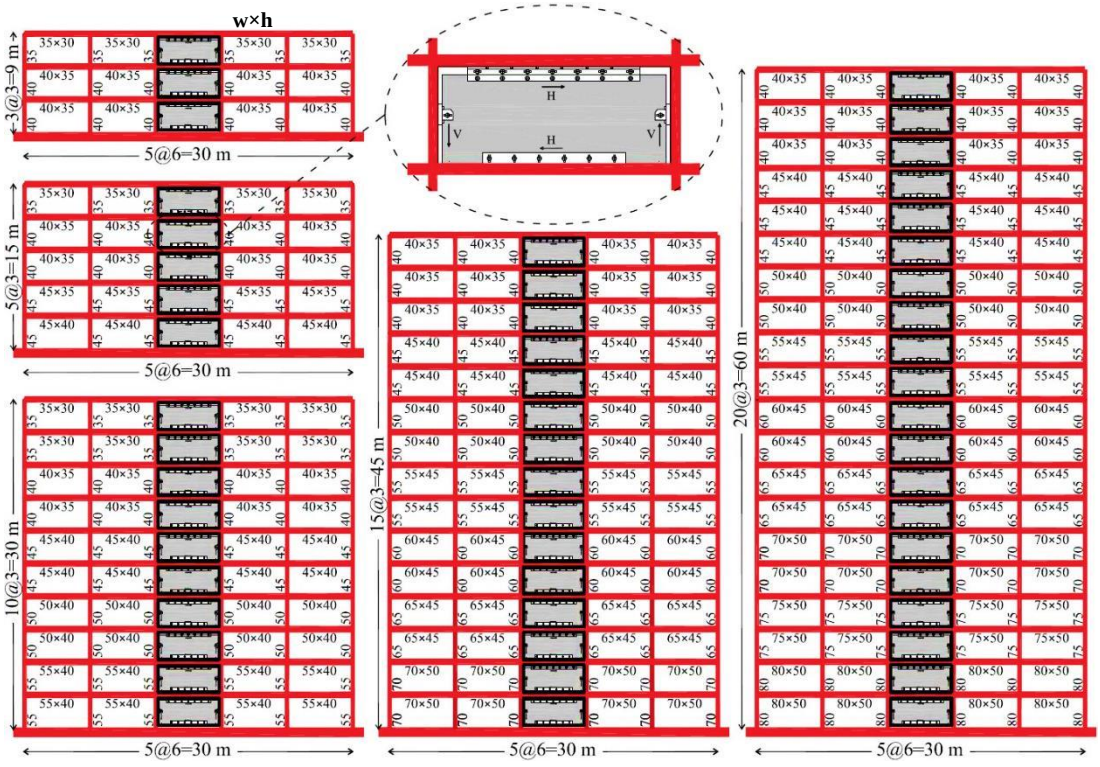


**Fig. A.1.** Geometry of the selected RC frames equipped with friction wall dampers

### A.3.2. Studied Friction Wall Damper

As shown in Fig. A.2, the studied friction wall damper consists of a non-structural concrete wall panel connected to the main beam and column elements by using four supports in the lateral sides (Nabid et al., 2017). Panel-to-column connections with horizontal slots provide the vertical supports which avoid transferring shear forces to the columns. The horizontal support is achieved by using vertical slots in the panel to the lower floor beam connection which prevents transferring shear forces to the connected beam. This configuration guarantees that the displacement of the friction device at the top is equal to the inter-storey drift at each level. The friction device is a simple panel-to-frame Slotted Bolted Connection with two steel plates fixed at the top of the panel and clamped together over a central T-shape stainless steel plate fixed to the top beam. The friction mechanism is achieved through the friction between the central stainless steel plate and the two brass plates. Numerous experimental tests performed by Grigorian et al. (1993) confirm a reliable hysteretic behaviour of this type of friction device under sinusoidal and simulated seismic displacements. The slip force of the friction device in the studied wall damper can be adjusted and tuned independently for each storey by controlling the clamping forces of the bolts. This characteristic provides the possibility of using optimised slip load values with the same connection.

In this study, for the analytical models, an inelastic spring element was used to model the friction device at the top of the panel to provide Coulomb friction behaviour. The concrete wall panel was also assumed as an elastic panel element with larger strength than the maximum slip load of the friction device.

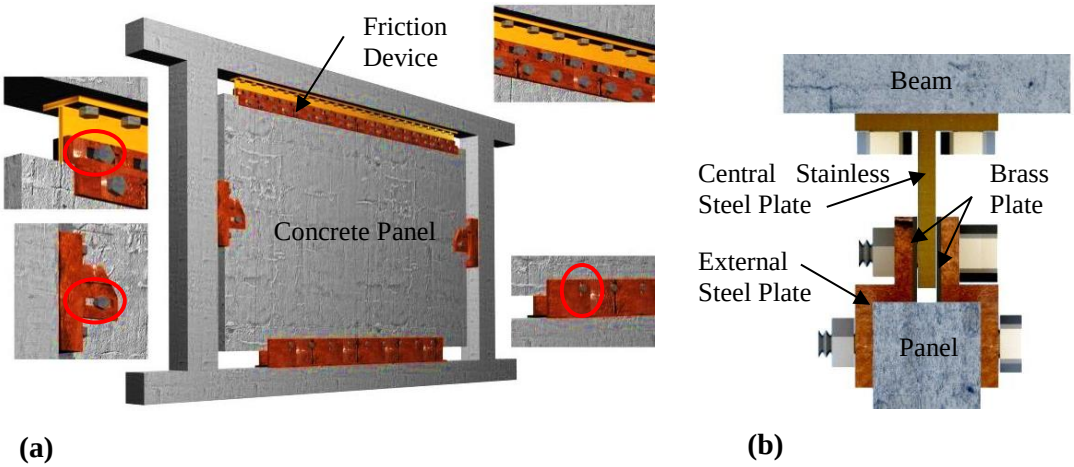


**Fig. A.2.** Details of the (a) proposed friction wall damper, (b) friction device (Nabid et al. (2017))

### A.3.3. Selected Excitation Records

A set of four synthetic earthquakes were generated using SIMQKE program (Vanmarke, 1976) to be compatible with the design response spectra of IBC (2015) for the site class D in high seismic zones (i.e. PGA=0.4g). Fig. A.3 illustrates the elastic acceleration response spectra of the four synthetic earthquakes, the IBC-2015 design spectrum and the average spectrum of the generated synthetic earthquakes. Fundamental periods of the bare frames (i.e. frames without friction dampers) are also overlaid the response spectra in Fig. A.3. It is shown that the average spectrum of the synthetic earthquakes provide a close approximation to the design response spectra. This implies that on average these earthquake records can be considered as good representatives of the selected design spectrum.

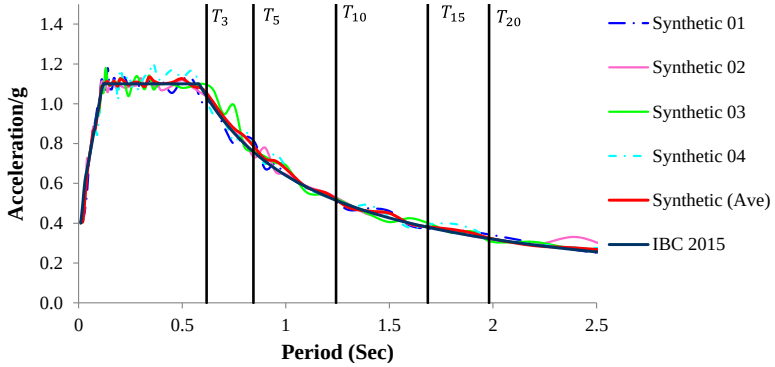


**Fig. A.3.** Elastic spectral acceleration of four synthetic earthquakes and IBC-2015 design spectrum for soil type D, 5% damping ratio.

## A.4. DESIGN METHODOLOGY FOR FRICTION WALL DAMPERS

One of the key properties of the friction EDDs is the possibility of regulating the slip forces ($F_s$) of the friction devices independently for each level by changing the clamping forces of the bolts. Therefore, it is possible to use more efficient height-wise slip load distributions to improve the seismic performance of friction-based energy dissipation devices.

### A.4.1. Energy Dissipation Parameter

Energy dissipation capacity of the friction EDDs is one of the main performance parameter to obtain their best design solution and can be used as a good value measure to evaluate the efficiency of the friction dampers under seismic loads. A weighted energy dissipation parameter, $R_w$ is introduced to evaluate the ratio between the work of the friction device,

$W_{sf}$, and the work of the main structural elements (Petkovski and Waldron 2003, Nabid et al. 2017).

$$R_w = \frac{W_{sf}}{W_{sb} + W_{sc}} \tag{A.1}$$

where $W_{sb}$ and $W_{sc}$ are the static work of the beam and column elements, respectively.

### A.4.2. Optimum Slip Load Range

In a recent study conducted by Nabid et al. (2017), the seismic performance of 3, 5, 10, 15 and 20-storey RC frames with friction-based wall dampers were compared in terms of different slip load distribution patterns. Their result indicates that the optimum range of the slip load ratio has an exponential relationship with the number of storeys. By considering conventional uniform height-wise slip load distribution, the following equation was proposed to obtain the optimum slip load values for each floor of multi-storey RC frames with friction wall dampers:

$$F_{s,i} = \frac{R}{n} \times \sum_{1}^{n} F_{y,i} = \frac{1.12e^{-0.11n}}{n} \times \sum_{1}^{n} F_{y,i} \tag{A.2}$$

where $R$ is the optimum slip load ratio and $n$ is the number of storeys. $F_{s,i}$ and $F_{y,i}$ are the slip load and the storey shear strength of the $i^{th}$ storey. It should be noted that the commonly used uniform slip load pattern for friction may not necessarily lead to the best design solution. The following section will discuss an optimum design methodology to obtain more efficient slip load patterns to improve the efficiency of the friction wall dampers.

## A.5. A METHODOLOGY FOR MORE EFFICCIENT ENERGY DISSIPATION

Under strong earthquakes, if the friction EDDs are designed conventionally with uniform slip load pattern, their maximum seismic capacity may not fully exploited, and therefore, leading to damage localisation in certain storey levels. To address this issue, the slip loads of the underused friction devices should be increased and the unnecessary slip loads should be decreased. In this study, an optimum design methodology was adopted based on the concept of the uniform damage distribution to obtain optimum distribution of slip loads. A similar concept was previously used by Levy & Lavan (2006) for optimum seismic design of

viscous dampers. However, this is the first time that this concept is used for seismic design of friction EDDs to obtain the optimum distribution of the slip loads by considering energy dissipation capacity of the dampers as the main seismic performance parameter.

Energy dissipation capacity of the friction EDDs is one of the main performance parameter to obtain their best design solution and can be used as a good value measure to evaluate the efficiency of the friction dampers under seismic loads. By considering energy dissipation capacity of the friction device as the main design parameter, the following optimisation algorithm is utilised in this study:

1) At the first stage, the RC frames are designed with the conventional friction wall dampers with uniform slip load distribution using the slip load values obtained from Equation A.2.

2) The frames are then subjected to the selected synthetic earthquakes and the performance parameters such as the maximum inter-storey drift and energy dissipation capacity of the friction devices are obtained. Using the following equation, the slip load values need to be redistributed based on the ratio between the energy dissipation of the friction device at each storey and the average of the energy dissipation in all storeys:

$$\left(F_{s,i}\right)_{n+1} = \left(F_{s,i}\right)_{n} \times \left(\frac{E_i}{E_{ave}}\right)_{n}^{\alpha} \tag{A.3}$$

where $E_i$ (or $W_{sf_i}$) and $E_{ave}$ (or $W_{sf_{ave}}$) are the dissipated energy through the friction device at $i^{th}$ storey and the average dissipated energy of the friction devices in all storey levels, respectively, at $n^{th}$ iteration. $\alpha$ is a convergence parameters from the rage between 0 and 1. It was previously shown by the other researchers (Hajirasouliha et al., 2012) that this parameter has a key role in the convergence speed of the problem. The also show that for RC frames, an acceptable convergence is usually obtained by using α value between 0.1 and 0.2. In this study, α factor equal to 0.2 was set as for all the optimisation procedures. More uniform distribution of energy dissipation is eventually resulted by using Equation A.3.

3) For comparison purposes, the new slip load values ($F_{s,i}$ in Equation A.3) obtained from the previous step are scaled such that the average of slip loads in all storeys remains unchanged compared to the initial step.

$$\left[\left(F_{s,i}\right)_{n+1}\right]_{scaled} = \left(\frac{\Sigma\left(F_{s,i}\right)_0}{\Sigma\left(F_{s,i}\right)_{n+1}}\right) \times \left(F_{s,i}\right)_{n+1} \quad \text{(A.4)}$$

4) To control the dispersion of energy dissipation at each storey relative to the mean value, the coefficient of variation of energy dissipation ($COV_E$) is calculated for each step. The optimisation design procedure is then repeated from step 2 until the small value for $COV_E$ is achieved (e.g. less than 10).

The efficiency of the proposed design method is demonstrated by applying the optimisation algorithm on the 3, 5, 10, 15 and 20-storey reference frames. Fig. A.4 shows the average variations of the COVs of the energy dissipations in the friction devices for the 3, 5, 10, 15 and 20-storey frames under the four selected synthetic earthquakes. As displayed by Fig. A.4, the COVs of the energy dissipations are generally decreased, and the maximum reductions of around 97, 75, 54, 33 and 4.5% were observed for the 3, 5, 10, 15 and 20-storey frames, respectively. It should be noted that the optimum design solution is selected based on the minimum values of the COV of the energy dissipation, and therefore, this may not result in the minimum of the maximum inter-storey drift ratios.

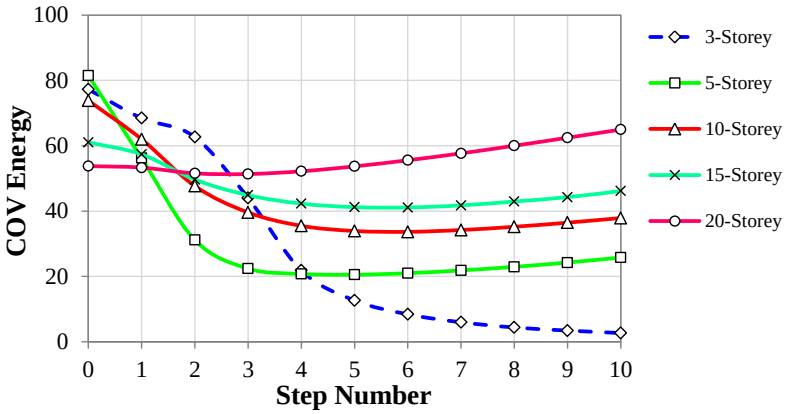


**Fig. A.4.** Average variation of the COV of the energy dissipation for the 3, 5, 10, 15 and 20-storey frames, four synthetic earthquakes, α=0.2

Fig. A.5 compares the average height-wise distribution of the (a) energy dissipation in the friction wall dampers ($W_{sf}$), (b) maximum inter-storey drift and (c) slip load ratios for 3, 5, 10, 15, and 20-storey frames designed based on the conventional uniform and optimum slip load distributions (with the same average) subjected to the selected synthetic design earthquakes. The results indicate that, in general, the proposed optimisation procedure could efficiently reduce the maximum inter-storey drifts by more uniform distribution of the energy dissipation parameter in the friction wall dampers (except for the 3-storey frame).

The maximum reduction of 24, 33, 27 and 8% were obtained for maximum inter-storey drift ratios of the 5, 10, 15 and 20-storey frames, respectively.

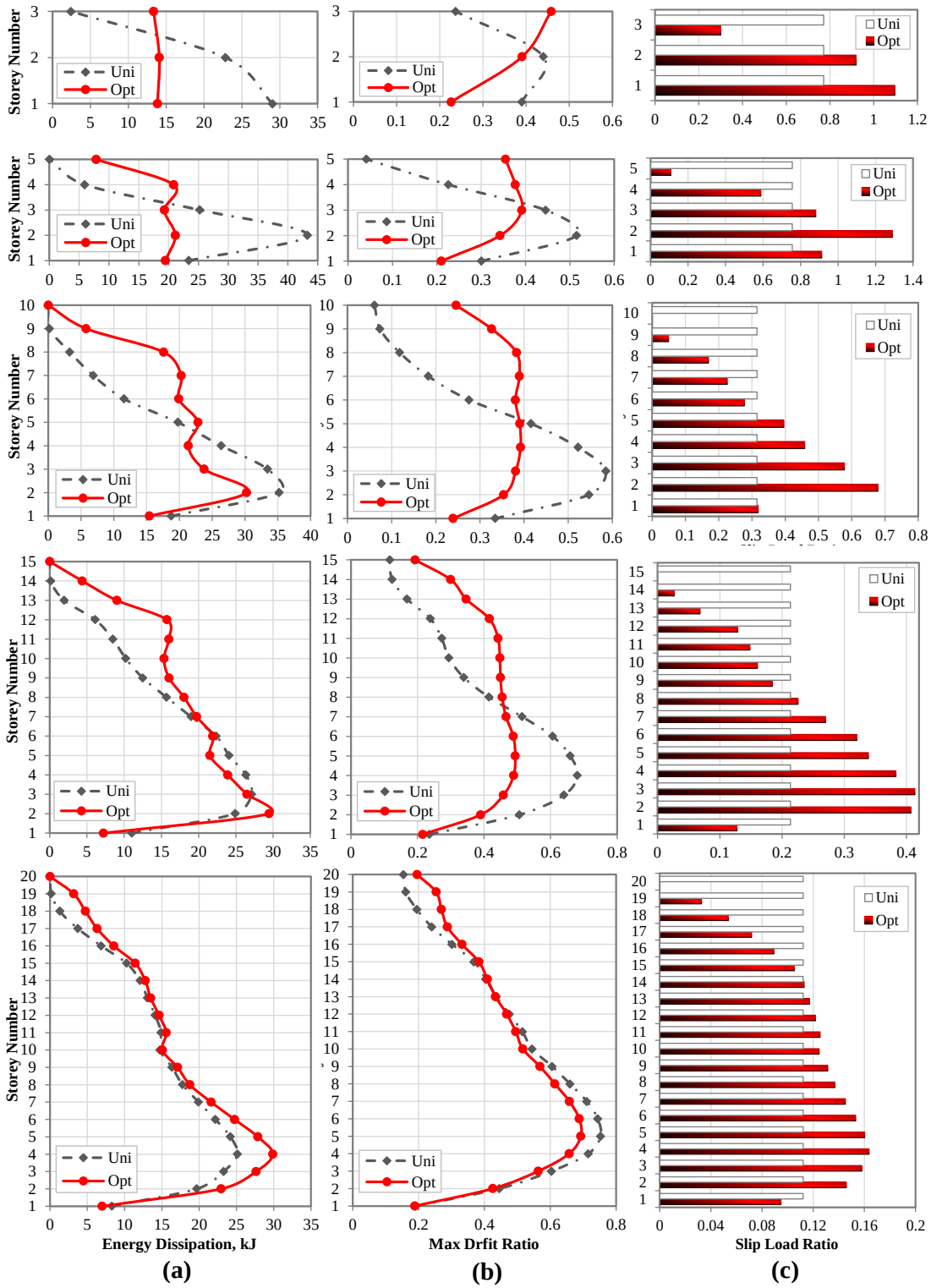


**Fig. A.5.** Average height-wise distribution of (a) energy dissipations in friction devices, (b) maximum drift and (c) slip load ratios for 3, 5, 10, 15 and 20-storey frames designed with uniform and optimum slip load distributions based on maximum energy dissipation capacity, four synthetic earthquakes

Fig. A.5 (c) shows that for the optimum distribution of the slip load ratio, by considering the same total slip load, the uniform pattern need to be modified so that more uniform distribution of energy dissipation is achieved. To satisfy this, some slip load values may be increased and some may tend to zero, and therefore, a number of unnecessary friction wall dampers can be removed from the RC frames (e.g. upper floors in 10, 15 and 20-storey frames), and consequently the cost of the design project can be optimised.

Fig. A.6 compares the average (a) maximum drift (b) column axial load and (c) base shear ratio, and (d) the energy dissipation capacity for the 3, 5, 10, 15 and 20-storey frames with optimum and conventional design dampers under the four synthetic earthquakes. The results show that, in general, using the proposed optimisation method could efficiently reduce the maximum inter-storey drifts by up to 33% and increase the energy dissipation parameter (i.e. RW) in the friction wall dampers by up to 34% under the selected synthetic spectrum-compatible earthquakes. However, the maximum column axial load and the base shear ratios were either remained unchanged or slightly increased (less than 8% and 14% difference, respectively).

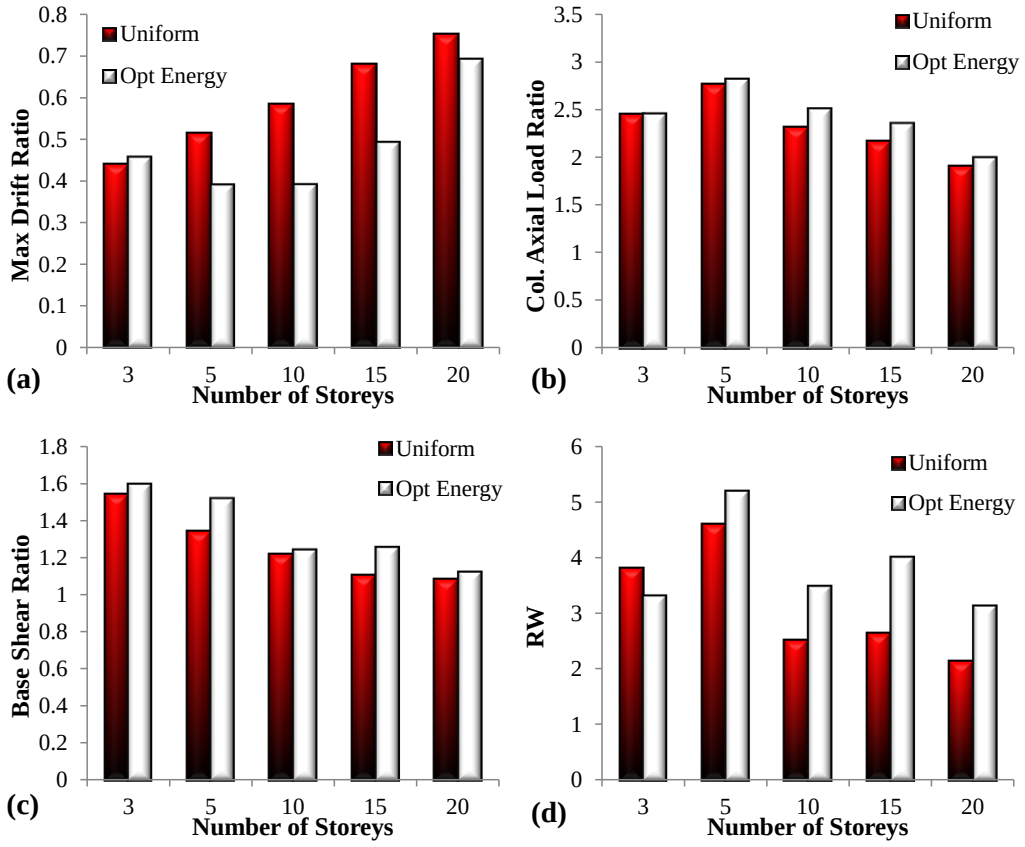


**Fig. A.6.** Average of (a) maximum drift, (b) column axial load and (c) base shear ratio, and (d) energy dissipation capacity of the optimum and conventional design dampers, four synthetic earthquakes

## A.6. CUMULATIVE DAMAGE INDEX

A linear global damage index is used (Krawinkler and Zohrei, 1983) to evaluate the efficiency of the proposed optimisation methodology in terms of overall structural damage under seismic excitations. In this study, the global damage index is obtained as a weighted average of the damage at different storeys by using inter-storey lateral deformation as the weighting function. The following equation is used to calculate the cumulative damage index:

$$DI_i = \sum_{j=1}^{N} \left( \frac{\Delta\delta_{pj}}{\delta_u} \right)^c \tag{A.5}$$

where $DI_i$ is the cumulative damage index at $i^{th}$ storey, from the range between 0 to 1 for undamaged and completely damaged storeys, respectively. N shows the number of plastic excursions, $\Delta\delta_{pj}$ and $\delta_u$ represent the plastic displacement of the $j^{th}$ excursion and the ultimate plastic displacement, respectively; and the c factor is the structural parameter accounting for the effect of plastic deformation magnitude. As suggested by Krawinkler and Zohrei (1983), *c* value is assumed to be 1.5 in this study. The global damage index, $DI_g$, is defined as a weighted average of the damage indices at different storeys to show the damage level of the whole structure. The weighting function is the energy dissipated at each storey.

$$DI_g = \frac{\sum_{i=1}^{n} DI_i W_{pi}}{\sum_{i=1}^{n} W_{pi}} \tag{A.6}$$

where $n$ is the total number of storeys, $DI_i$ and $W_{pi}$ are the damage index and the dissipated energy at the $i^{th}$ storey, respectively. Fig. A.7 represents the average global damage indices of the 3, 5, 10, 15 and 20-storey bare frames and the frames with optimally and conventionally designed friction wall dampers under the four selected synthetic earthquakes. In this study, the optimum slip load distributions were obtained to satisfy more uniform distribution of the energy dissipation capacities of the friction EDDs. It is shown that, in general, using the friction EDDs leads to significant improvements in global damage of the frames compared to the bare frames; however, the efficiency of the proposed optimum design methodology to decrease the level of the global damage was more evident. According to the results, compared to the conventional design friction dampers, the optimum design dampers can lead to maximum reduction of the global damage index by 72%, 13%, 63%, 67% and 14% for the 3, 5, 10, 15 and 20-storey frames, respectively.

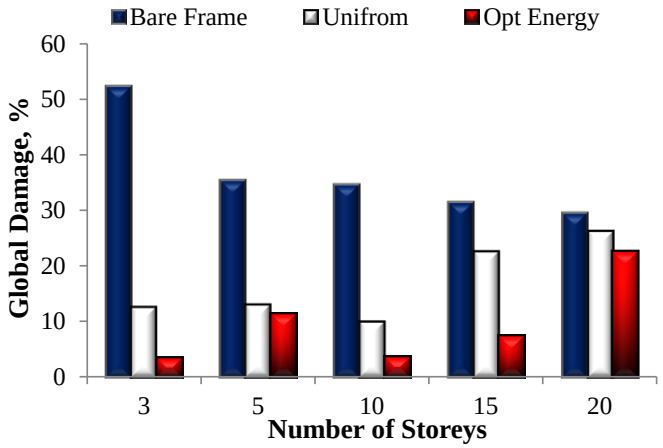


**Fig. A.7.** Average of the global damage index for the 3, 5, 10, 15 and 20-storey bare frames, the frames designed using uniform slip load distribution and optimum slip load distributions, four synthetic earthquakes

## A.7. CONCLUSIONS

An optimisation design methodology was adopted based on the concept of uniform damage distribution to obtain optimum slip load distribution of a wall-type friction Energy Dissipation Device (EDD). Numerous non-linear dynamic analyses were conducted on 3, 5, 10, 15, and 20-storey RC frames with friction wall dampers under a set of four synthetic IBC spectrum-compatible earthquakes. Energy dissipation capacity of the friction device was considered as the main seismic performance parameter to obtain the optimum slip load distribution along the height of the structure. To investigate the efficiency of the proposed optimum design methodology, the results were compared with those of the conventional design friction dampers by considering a uniform slip load distribution pattern. It was shown that the optimum design dampers exhibited by up to 33% and 72% less inter-storey drift ratios and global damage, respectively, under the set of spectrum-compatible earthquakes. It was also shown that for the same total slip load, up to 34% higher energy dissipation capacity in the friction devices was achieved for the optimum friction dampers compared to their conventionally designed counterparts.

## REFERENCES

American Society of Civil Engineers (ASCE), (2010). "Minimum Design Loads for Buildings and Other Structures." *ASCE/SEI Standard 7-10*, Reston, Virginia.

Cho, C. G. and Kwon, M., (2004). "Development and modelling of a frictional wall damper and its applications in reinforced concrete frame structures." *Earthquake Engineering and Structural Dynamics,* **33**: 821–838.

FitzGerald, T. F., Anagnos, T., Goodson, M., Zsutty, T. (1989). "Slotted bolted connections in aseismic design for concentrically braced connections." *Earthquake Spectra* **5**: 383–391.

Ganjavi, B., Hajirasouliha, I. and Bolourchi, A. (2016). "Optimum lateral load distribution for seismic design of nonlinear shear-buildings considering soil-structure interaction." *Soil Dynamics and Earthquake Engineering*; **88**: 356–368.

Grigorian, C.E., Yang, T.S. and Popov, E. P., (1993). "Slotted Bolted Connection Energy Dissipators." *Earthquake Spectra* **9**(3): 491–504.

Hajirasouliha, I., Asadi, P. and Pilakoutas, K., 2012. An efficient performance-based seismic design method for reinforced concrete frames. *Earthquake Engineering and Structural Dynamics* **41**(4), 663-679.

Hajirasouliha, I. and Pilakoutas, K. (2012). "General seismic load distribution for optimum performance- based design of shear-buildings." *Journal of Earthquake Engineering,* **16**(4): 443–462.

International Building Code (IBC). (2015). *International Code Council*, Country Club Hills, USA.

Krawinkler, H., Zohrei, M. (1983). "Cumulative damage in steel structures subjected to earthquake ground motions." *Computers and Structures*; **16**: 531–541.

Levy, R. and Lavan, O. (2006). "Fully stressed design of passive controllers in framed structures for seismic loadings." *Structural and Multidisciplinary Optimization* **32**(6): 485–498.

Moghaddam, H., Hajirasouliha, I. and Doostan, A. (2004). "Optimum seismic design of concentrically braced steel frames: Concepts and design procedures." *Journal of Constructional Steel Research,* **61**: 151–166.

Nabid, N., Hajirasouliha, I. and Petkovski, M. (2017). "A practical method for optimum seismic design of friction wall dampers." *Earthquake Spectra*; **33**(3): 1033-1052.

Pall, A. S. and Marsh, C. (1982). "Response of friction damped braced frames." *ASCE, Journal of Structural Division* **108**: 1313–1323.

Pall, A. S. and Pall, R. T. (2004). "Performance-based design using pall friction dampers; an economical design solution." *In Proceedings: 13th World Conference on Earthquake Engineering*, Vancouver, Canada, Paper No. 1955,

Petkovski, M. and Waldron, P. (2003). "Optimum friction forces for passive control of the seismic response of multi-story Buildings." *In Proceedings: 40 years of European Earthquake Engineering SE40EEE,* Ohrid, Macedonia.

Prakash, V., Powell, G. H. and Campbell, S. (1993). "DRAIN-2DX base program description and user guide." Version 1.10. University of California, Berkeley, California.

Sasani, M. and Popov, E. P. (2001). "Seismic energy dissipaters for RC panels; analytical studies." *Journal of Engineering Mechanics,* **127**(8)**:** 835–843.

Vanmarke, E. H. (1976). "SIMQKE: A program for artificial motion generation, user's manual and documentation." Department of Civil Engineering, Massachusetts Institute of Technology.

Wu, B., Zhang, J., Williams, M. S., Ou, J. (2005). "Hysteretic behaviour of improved pall-typed frictional dampers." *Engineering Structures* **27:** 1258–1267.

# APPENDIX B

# Preliminary Design Calculation for Typical Friction Device

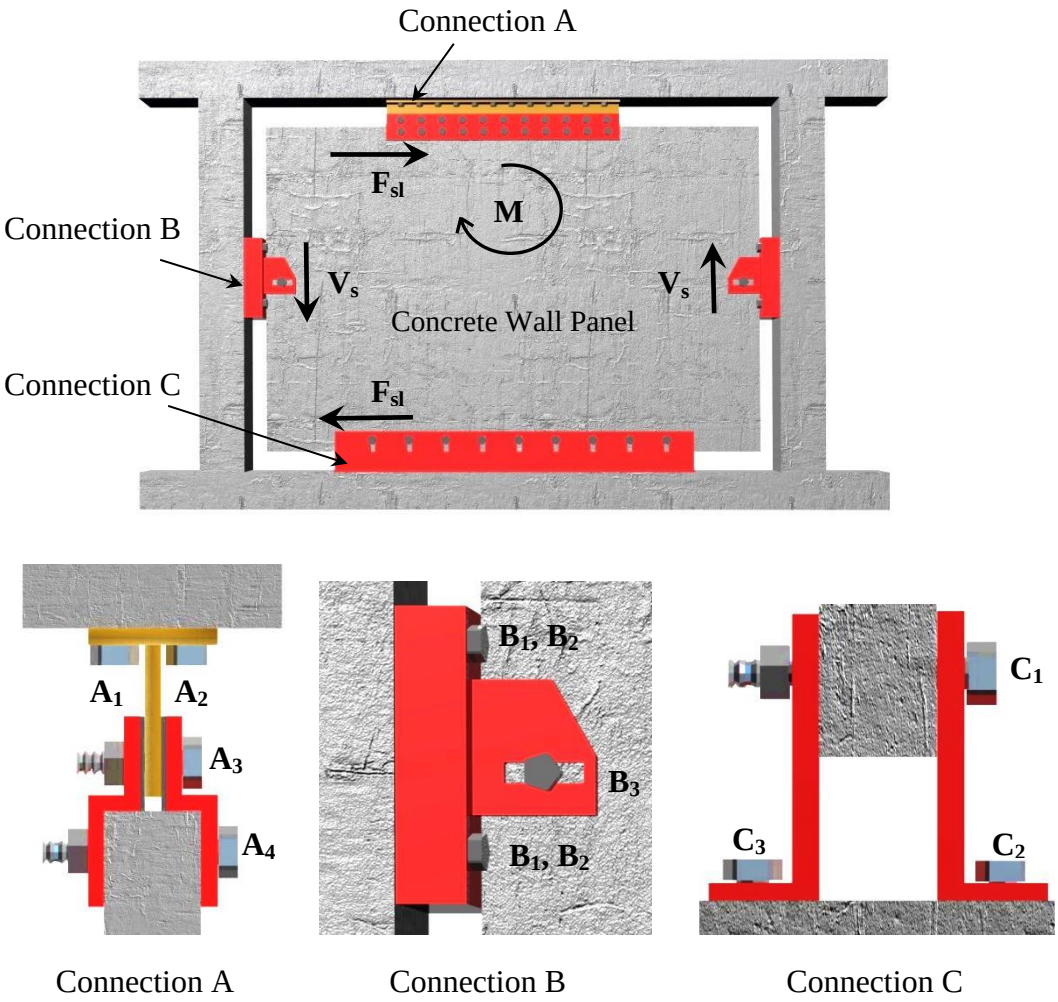


**Fig. B.1.** Proposed friction wall panel and the connection details

**Table B.1.** Definitions and values of the design assumptions

| *Definition* | *Design Assumptions* | |
|---|---|---|
| | *Symbol* | *Value* |
| Slip load (kN) | $F_{sl}$ | - |
| Bending moment of the panel | M | - |
| Panel height (mm) | $h_p$ | 2500 |
| Panel width (mm) | $w_p$ | 4500 |
| Panel thickness (mm) | $t_p$ | 150 |
| Panel weight | $W_p$ | - |
| Concrete density (kg/mm$^3$) | $\rho_c$ | 2.2e-6 |
| Concrete compression strength (N/mm$^2$) | $f'_c$ | 35 |
| Nominal bolt diameter (mm) | $d_b$ | 24 |
| Diameter of the head of the Anchor bolts | $d_h$ | 48 |
| No. of bolt sets to carry pull out stress at connection A/C | $N_p$ | 2 |
| Number of the friction planes | n | 3 |
| Number of bolts | $n_b$ | - |
| Ultimate strength of high strength bolt (N/mm$^2$) | $F_{ub}$ | 800 |
| Yield stress of high strength bolt (N/mm$^2$) | $F_{yb}$ | 640 |
| Preloading force of the bolt (clamping force) | $F_{p,C}$ | - |
| Shear resistance per shear plane | $F_{v,Rd}$ | - |
| Slip resistance of a preloaded bolt | $F_{s,Rd}$ | - |
| Design friction resistance between base plate and grout | $F_{f,Rd}$ | - |
| Design shear resistance of an anchor bolt | $F_{vb,Rd}$ | - |
| Pull-out resistance failure for headed anchor bolts | $N_{Rd,p}$ | - |
| Characteristic resistance in case of pull-out failure | $N_{Rk,p}$ | - |
| Design value of the tension force | $N_{Ed}$ | - |
| Coefficient of friction between base plate and grout layer | $C_{f,d}$ | 0.2 |
| Partial factor for resistance of cross-sections in tension | $\gamma_{M2}$ | 1.25 |
| Partial factor for slip resistance at ultimate limit state | $\gamma_{M3}$ | 1.25 |
| Partial factor for concrete under compression | $\gamma_c$ | 1.5 |
| Partial factor for installation safety of fastening system | $\gamma_{inst}$ | 1.2 |
| Partial factor for concrete break-out failure modes | $\gamma_{Mc}$ | - |
| Partial factor for pull-out resistance | $\gamma_{Mp}$ | - |
| A factor for fasteners in cracked concrete | $\Psi_{ucr,N}$ | 1.0 |
| Slip factor | $\mu$ | 0.20 |
| Tensile stress area of the bolt | $A_s$ | - |
| Gross cross section of the bolt | A | - |
| Bearing area of the anchor head | $A_h$ | - |
| Maximum pull out stress | $R_{max}$ | - |
| Maximum pull out stress per bolt | $R_{max}^{b}$ | - |

# B.1. HOLDING DOWN BOLTS:

## B.1.1. Design for Shear:

There are different anchoring types as shown in Fig. B.2. The cast-in-situ circular headed anchor bolts are considered as the holding down anchor bolts in this design example.

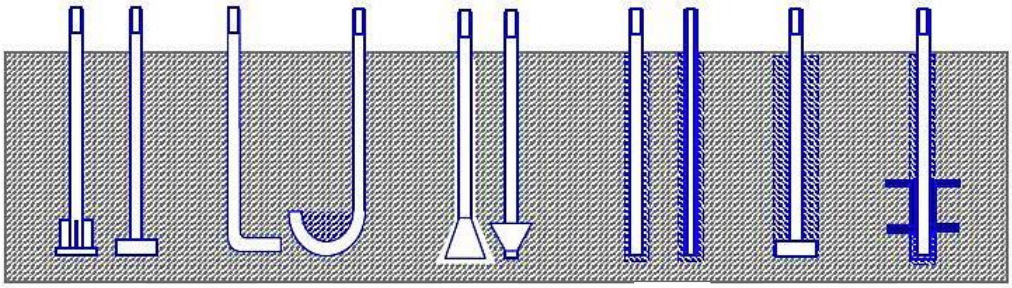

(a) (b) (c) (d) (e) (f)

**Fig. B.2.** Different types of anchor bolts including: a) cast-in-situ headed anchor bolts, b) hooked bars, c) undercut anchor bolts, d) bonded anchor bolts, e) grouted anchor bolts, f) anchoring to grillage beams (Moore and Wald, 2003)

Based on Clause 3.3 of EN 1993-1-8 (2005), the nominal yield strength is less than 640 N/mm$^2$ when acts in shear and not more than 900 N/mm$^2$ otherwise. The bolts are considered to have a circular head with a diameter double the dimeter of the bolts.

It is assumed that all the panel weight is tolerated by the connection C, and therefore, according to Clause 6.2.2 of EN 1993-1-8 (2005), the design shear resistance between a base plate and a grout layer for $C_2$ and $C_3$ is derived as follow:

$$F_{v,Rd} = F_{f,Rd} + n_b F_{vb,Rd}$$

$$F_{f,Rd} = C_{f,d} \times N_{Ed}$$

$$N_{Ed} = W_p = \rho_c w_p h_p t_p = 2.2e-6 \times 4500 \times 2500 \times 150 \times \frac{1}{100} = 37.125\ kN$$

$$F_{f,Rd} = 0.2 \times 37.125 = 7.425\ \ kN$$

$$F_{vb,Rd} = \frac{\alpha_{bc} f_{ub} A_s}{\gamma_{M2}}$$

$$\alpha_{bc} = 0.44 - 0.0003 f_{yb} = 0.44 - 0.0003 \times 640 = 0.248$$

$$F_{vb,Rd} = \frac{0.248 \times 800 \times (\pi \times 24^2)/4}{1.25 \times 1000} = 71.8\ kN$$

By assuming 10 numbers of bolts:

$$F_{v,Rd}{}^{C_2} = F_{v,Rd}{}^{C_3} = F_{f,Rd} + nF_{vb,Rd} = 7.425 + 10 \times 71.8 = 725.425\ \ kN$$

for $A_1$ and $A_2$ with no compression load:

$$F_{v,Rd}{}^{A_1} = F_{v,Rd}{}^{A_2} = nF_{vb,Rd} = 10 \times 71.8 = 718\ \ kN$$

And for $B_1$ and $B_2$:

$$F_{v,Rd}{}^{B_1} = F_{v,Rd}{}^{B_2} = nF_{vb,Rd} = 2 \times 71.8 = 143.6\ \ kN$$

### B.1.2. Design for Pull Out:

Using Clause 6.2.4 of CEN/TS 1992-4-2 (2009) for the cast-in-situ headed anchor bolts:

$$N_{Ed} \le N_{Rd,p} = \frac{N_{Rk,p}}{\gamma_{Mp}}$$

Based on Clause 4 of CEN/TS 1992-4-1(2009):

$$\gamma_{Mp} \simeq \gamma_{Mc} = \gamma_c \times \gamma_{inst} = 1.5 \times 1.2 = 1.8$$

$$N_{Rk,p} = 6 \times A_h \times f_c^{'} \times \Psi_{ucr,N}$$

$$A_h = \pi \frac{(d_h^2 - d^2)}{4} = \pi \frac{(48^2 - 24^2)}{4} = 1851.6\ mm^2$$

$$N_{Rd,p} = \frac{6 \times 1851.6 \times 35 \times 1.0}{1.8 \times 1000} = 216.02\ kN$$

It is assumed that the lengths of the connections A and C are identical to the length of the panel. By considering Fig. B.2 as the bending moment diagram in the connections A and C, the maximum tension force in the anchor bolts can be calculated as follow:

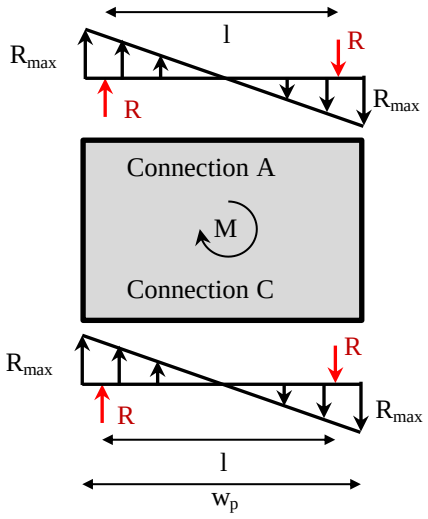


**Fig. B.3.** Bending moment diagram in connections A and C

$$M = F_{sl} \times h_p$$

$$M = R \times l = \frac{R_{\max} \times 2.25}{2} \times (2 \times \frac{2}{3} \times 2.25) = 3.375 \times R_{\max} \rightarrow R_{\max} = \frac{F_{sl} \times 2.5}{3.375} = 0.74 \times F_{sl}$$

$$R^b_{\max} = \frac{R_{\max}}{N_p} = \frac{0.74 \times F_{sl}}{2} = 0.37 \times F_{sl}$$

$$R^b_{\max} \le N_{Rd,p} \rightarrow 0.37 \times F_{sl} \le 216.02 \rightarrow F_{sl} \le 583.84\ kN \quad (1)$$

## B.2. PRE-LOADED FRICTION-TYPE CONNECTION:

To estimate the shear resistant before the slippage, all the bolts can be considered as pre-loaded friction-type connections:

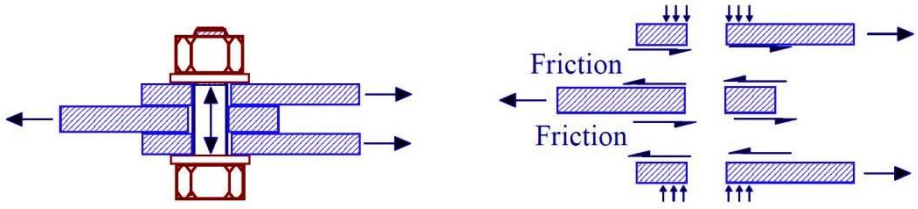


**Fig. B.4.** High-strength bolt in a friction type connection (Moore and Wald, 2003)

According to Clause 3.9.1 of EN 1993-1-8 (2005) and by considering bolt grade 8.8:

$$F_{s,Rd} = \frac{k_s\ n_b\ \mu}{\gamma_{M3}} F_{p,C}$$

Based on the Table 3.6 of EN 1993-1-8 (2005), for $A_3$ bolts in long slotted holes with the axis of the slot parallel to the direction of the load transfer:

$k_s = 0.63$

for $B_3$ and $C_1$ bolts in long slotted holes with the axis of the slot perpendicular to the direction of the load transfer:

$k_s = 0.7$

Using Table 17 of EN 1090-2 (2018):

$\mu = 0.2$

and;

$$F_{p,C} = 0.7 f_{ub} A_s = 0.7 \times 800 \times \frac{\pi \times 24^2}{4} \times \frac{1}{1000} = 253.34\ kN$$

By assuming 10 numbers of bolts for Connection $A_3$:

$$F_{s,Rd}^{A_3} = (10 \times \frac{0.63 \times 3 \times 0.2}{1.25} \times 253.34) = 766.1\ kN$$

For Connection $B_3$:

$$F_{s,Rd}^{B_3} = (1 \times \frac{0.7 \times 3 \times 0.2}{1.25} \times 253.34) = 85.12\ kN$$

And by considering 10 numbers of bolts for Connection $C_1$:

$$F_{s,Rd}^{C_1} = (10 \times \frac{0.7 \times 3 \times 0.2}{1.25} \times 253.34) = 851.22\ kN$$

## B.3. BEARING-TYPE BOLTS:

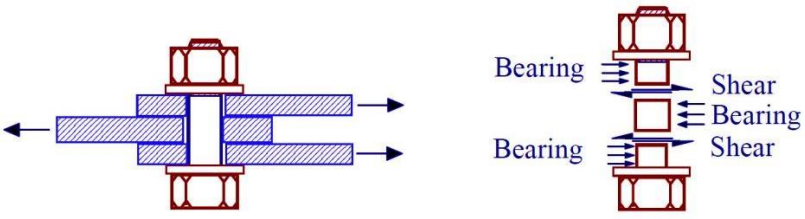


**Fig. B.5.** High-strength bolt in a bearing-type connection (Moore and Wald, 2003)

According to Table 3.4 EN 1993-1-8 (2005) and by considering bolt grade 8.8 for $A_4$:

$$F_{v,Rd} = \frac{\alpha_v f_{ub} A}{\gamma_{M2}} \quad \text{where} \quad \alpha_v = 0.6$$

$$F_{v,Rd}^{A_4} = 10 \times \frac{0.6 \times 800 \times (\pi \times 24^2)/4}{1.25 \times 1000} = 1737.2\ kN$$

Finally the overall bearing resistance for the connections A, B and C can be estimated as follow:

Connection A:

$$F_{v,Rd}{}^{A} = F_{v,Rd}{}^{A_1} + F_{v,Rd}{}^{A_2} + F_{s,Rd}{}^{A_3} + F_{v,Rd}{}^{A_4} = 718 + 718 + 766.1 + 1737.2 = 3939.3\ kN$$
$$\rightarrow F_{sl} \leq 3939.3\ kN \quad (2)$$

Connection B:

$$F_{s,Rd}{}^{B} = F_{s,Rd}{}^{B_1} + F_{s,Rd}{}^{B_2} + F_{s,Rd}{}^{B_3} = 143.6 + 143.6 + 85.12 = 372.32\ kN$$

From Fig B.1:

$$M = F_{sl} \times h_p = V_s \times w_p \rightarrow F_{sl} = 1.8 \times V_s \rightarrow F_{sl} \leq 1.8 \times 372.32 \rightarrow F_{sl} \leq 670.18\ kN \quad (3)$$

Connection C:

$$F_{s,Rd}{}^{C} = F_{s,Rd}{}^{C_1} + F_{s,Rd}{}^{C_2} + F_{s,Rd}{}^{C_3} = 851.22 + 725.425 + 725.425 = 2302.07\ kN$$
$$\rightarrow F_{sl} \leq 2302.07\ kN \quad (4)$$

Results 1-4 show that the shear obtained from the pull out is dominant, and therefore:

$$F_{sl} \leq 583.84\ kN$$

However, if the pull out failure was neglected/controlled, the slip load limit would be:

$$F_{sl} \leq 670.18\ kN$$

## REFERENCES

Moore D.B., Wald F. (2003), "Design of structural connections to Eurocode 3, frequently asked questions." *Building Research Establishment, Ltd.*

EN 1993-1-8, (2005). "Eurocode 3: Design of steel structures - Part 1-8: Design of joints."

EN 1090‑2, (2018). "Execution of steel structures and aluminium structures; Part 2: Technical requirements for steel structures."

DD CEN/TS 1992-4-1, (2009). "Design of Fastenings for use in Concrete, Part 4-1: General."

DD CEN/TS 1992-4-2, (2009). "Design of Fastenings for use in Concrete, Part 4-2: Headed fasteners."